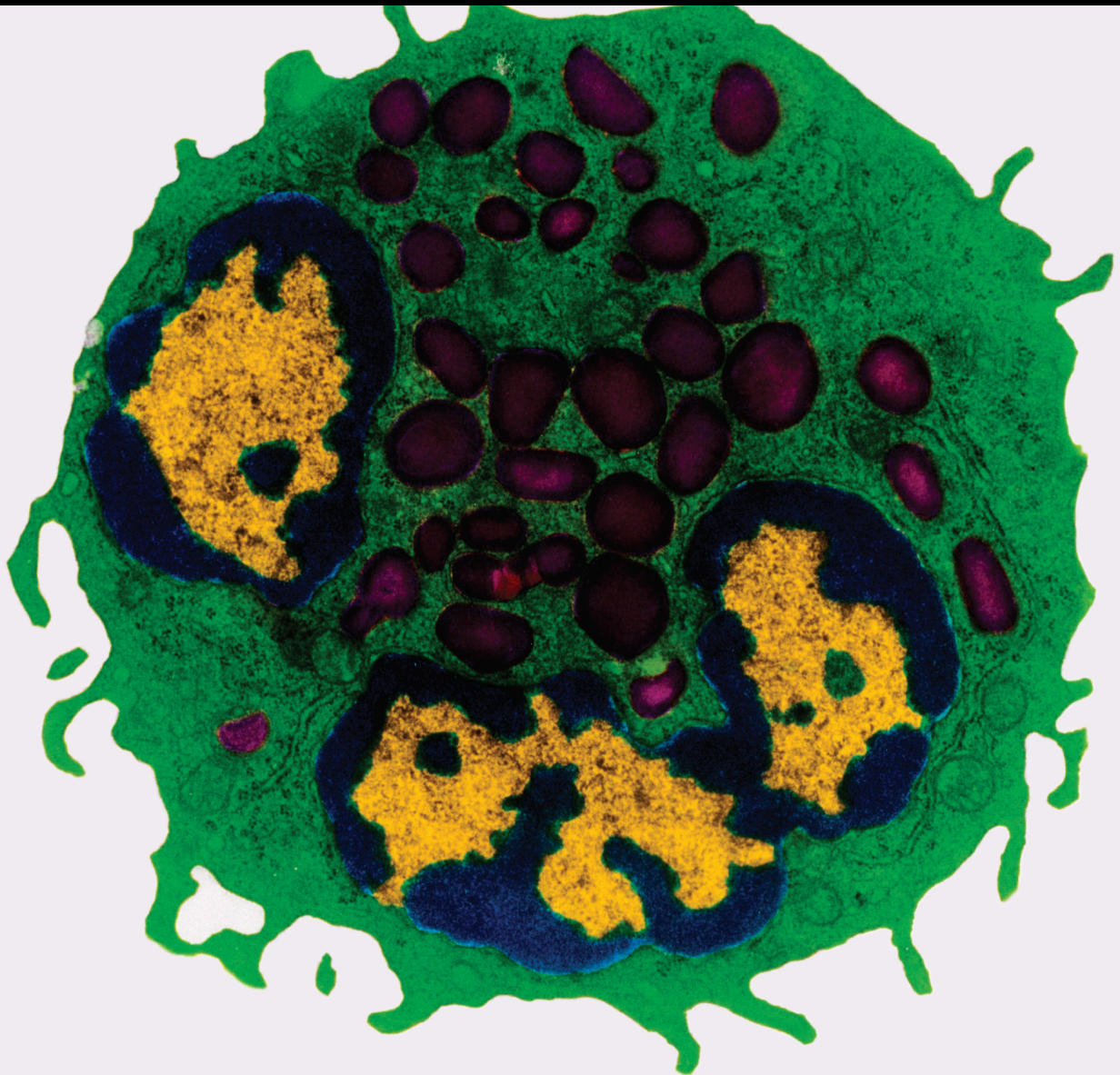


Dendritic Cells: Immune Response in Infectious Diseases and Autoimmunity

Lead Guest Editor: Renata Sesti-Costa

Guest Editors: Luisa Cervantes-Barragan and Pedro M. M. Moraes-Vieira





Dendritic Cells: Immune Response in Infectious Diseases and Autoimmunity

Mediators of Inflammation

Dendritic Cells: Immune Response in Infectious Diseases and Autoimmunity

Lead Guest Editor: Renata Sesti-Costa

Guest Editors: Luisa Cervantes-Barragan and Pedro M. M.
Moraes-Vieira



Copyright © 2020 Hindawi Limited. All rights reserved.

This is a special issue published in "Mediators of Inflammation." All articles are open access articles distributed under the Creative Commons Attribution License, which permits unrestricted use, distribution, and reproduction in any medium, provided the original work is properly cited.

Chief Editor

Anshu Agrawal, USA

Editorial Board

Muzamil Ahmad, India
Maria Jose Alcaraz, Spain
Simi Ali, United Kingdom
Amedeo Amedei, Italy
Oleh Andrukhov, Austria
Emiliano Antiga, Italy
Zsolt J. Balogh, Australia
Adone Baroni, Italy
Jagadeesh Bayry, France
Jürgen Bernhagen, Germany
Tomasz Brzozowski, Poland
Philip Bufler, Germany
Elisabetta Buommino, Italy
Daniela Caccamo, Italy
Luca Cantarini, Italy
Raffaele Capasso, Italy
Calogero Caruso, Italy
Maria Rosaria Catania, Italy
Carlo Cervellati, Italy
Cristina Contreras, Spain
Robson Coutinho-Silva, Brazil
Jose Crispin, Mexico
Fulvio D'Acquisto, United Kingdom
Eduardo Dalmarco, Brazil
Pham My-Chan Dang, France
Wilco de Jager, The Netherlands
Beatriz De las Heras, Spain
Chiara De Luca, Germany
Clara Di Filippo, Italy
Carlos Dieguez, Spain
Agnieszka Dobrzyn, Poland
Elena Dozio, Italy
Emmanuel Economou, Greece
Ulrich Eisel, The Netherlands
Giacomo Emmi, Italy
Fabiola B Filippin Monteiro, Brazil
Antonella Fioravanti, Italy
Stefanie B. Flohé, Germany
Jan Fric, Czech Republic
Tânia Silvia Fröde, Brazil
Julio Galvez, Spain
Mirella Giovarelli, Italy
Denis Girard, Canada
Ronald Gladue, USA

Markus H. Gräler, Germany
Oreste Gualillo, Spain
Qingdong Guan, Canada
Elaine Hatanaka, Brazil
Tommaso Iannitti, United Kingdom
Byeong-Churl Jang, Republic of Korea
Yoshihide Kanaoka, USA
Yasumasa Kato, Japan
Yona Keisari, Israel
Alex Kleinjan, The Netherlands
Marije I. Koenders, The Netherlands
Elzbieta Kolaczowska, Poland
Vladimir A. Kostyuk, Belarus
Dmitri V. Krysko, Belgium
Sergei Kusmartsev, USA
Martha Lappas, Australia
Philipp M. Lepper, Germany
Eduardo López-Collazo, Spain
Andreas Ludwig, Germany
Ariadne Malamitsi-Puchner, Greece
Joilson O. Martins, Brazil
Donna-Marie McCafferty, Canada
Barbro N. Melgert, The Netherlands
Paola Migliorini, Italy
Vinod K. Mishra, USA
Eeva Moilanen, Finland
Alexandre Morrot, Brazil
Jonas Mudter, Germany
Kutty Selva Nandakumar, China
Hannes Neuwirt, Austria
Nadra Nilsen, Norway
Daniela Novick, Israel
Marja Ojaniemi, Finland
Sandra Helena Penha Oliveira, Brazil
Olivia Osborn, USA
Carla Pagliari, Brazil
Martin Pelletier, Canada
Vera L. Petricevich, Mexico
Sonja Pezelj-Ribarić, Croatia
Philenio Pinge-Filho, Brazil
Michele T. Pritchard, USA
Michal A. Rahat, Israel
Zoltan Rakonczay Jr., Hungary
Marcella Reale, Italy





Alexander Riad, Germany
Emanuela Roschetto, Italy
Carlos Rossa, Brazil
Settimio Rossi, Italy
Bernard Ryffel, France
Carla Sipert, Brazil
Helen C. Steel, South Africa
Jacek Cezary Szepietowski, Poland
Dennis D. Taub, USA
Taina Tervahartiala, Finland
Kathy Triantafilou, United Kingdom
Fumio Tsuji, Japan
Giuseppe Valacchi, Italy
Luc Vallières, Canada
Elena Voronov, Israel
Kerstin Wolk, Germany
Suowen Xu, USA
Soh Yamazaki, Japan
Shin-ichi Yokota, Japan
Teresa Zelante, Singapore

Contents









Dendritic Cells: Immune Response in Infectious Diseases and Autoimmunity

Renata Sesti-Costa , Pedro Manoel Mendes de Moraes-Vieira , and Luisa Cervantes-Barragan
Editorial (3 pages), Article ID 2948525, Volume 2020 (2020)







Could Increased Expression of Hsp27, an “Anti-Inflammatory” Chaperone, Contribute to the Monocyte-Derived Dendritic Cell Bias towards Tolerance Induction in Breast Cancer Patients?

Ana Paula Silva de Azevedo-Santos , Mirtes Castelo Branco Rocha, Sulayne Janayna Araujo Guimarães, André Alvares Marques Vale, Fabio Martins Laginha, Flavia Raquel F. Nascimento, Maria Aparecida Nagai, Patrícia C. Bergami-Santos, and José Alexandre Marzagão Barbuto 
Research Article (9 pages), Article ID 8346930, Volume 2019 (2019)



Relationship between Helicobacter pylori Infection and Plasmacytoid and Myeloid Dendritic Cells in Peripheral Blood and Gastric Mucosa of Children

Anna Helmin-Basa , Małgorzata Wiese-Szadkowska , Anna Szaflarska-Popławska , Maciej Kłosowski , Milena Januszewska , Magdalena Bodnar , Andrzej Marszałek , Lidia Gackowska, and Jacek Michalkiewicz 
Research Article (12 pages), Article ID 7190596, Volume 2019 (2019)




Trypanosoma cruzi Mexican Strains Differentially Modulate Surface Markers and Cytokine Production in Bone Marrow-Derived Dendritic Cells from C57BL/6 and BALB/c Mice

Cecilia Gomes Barbosa, Tamires Marielem Carvalho Costa, Chamberttan Souza Desidério, Paula Tatiana Mutão Ferreira, Mariana de Oliveira Silva, César Gómez Hernández , Malú Mateus Santos, Rafael Obata Trevisan, Wesley Guimarães Bovi , Virmondés Rodrigues , Juliana Reis Machado , Luiz Eduardo Ramirez, Carlo José Freire de Oliveira , and Marcos Vinícius da Silva 
Research Article (14 pages), Article ID 7214798, Volume 2019 (2019)

Inhibition of CD83 Alleviates Systemic Inflammation in Herpes Simplex Virus Type 1-Induced Behçet’s Disease Model Mouse

S. M. Shamsul Islam, Hae-Ok Byun, Bunsoon Choi , and Seonghyang Sohn 
Research Article (15 pages), Article ID 5761392, Volume 2019 (2019)

The Important Role of Dendritic Cell (DC) in iNKT-Mediated Modulation of NK Cell Function in Chlamydia pneumoniae Lung Infection

Lei Zhao, Xiaoling Gao , Hong Bai , Antony George Joyee, Shuhe Wang, Jie Yang, Weiming Zhao, and Xi Yang 
Research Article (12 pages), Article ID 4742634, Volume 2019 (2019)

The Inflammatory Response to Enterotoxigenic E. coli and Probiotic E. faecium in a Coculture Model of Porcine Intestinal Epithelial and Dendritic Cells

Henriette Loss , Jörg R. Aschenbach , Karsten Tedin , Friederike Ebner, and Ulrike Lodemann 
Research Article (16 pages), Article ID 9368295, Volume 2018 (2018)

Editorial

Dendritic Cells: Immune Response in Infectious Diseases and Autoimmunity

Renata Sesti-Costa ¹, **Pedro Manoel Mendes de Moraes-Vieira** ²,
and **Luisa Cervantes-Barragan**³

¹Hematology and Hemotherapy Center, UNICAMP, Campinas, SP, Brazil Rua Carlos Chagas, 480. 13083-878

²Department of Genetics, Evolution, Microbiology and Immunology, Institute of Biology, University of Campinas, Campinas, Brazil

³Department of Microbiology and Immunology, Emory University, School of Medicine, Atlanta, GA, USA

Correspondence should be addressed to Renata Sesti-Costa; r227811@dac.unicamp.br

Received 13 February 2020; Accepted 14 February 2020; Published 20 March 2020

Copyright © 2020 Renata Sesti-Costa et al. This is an open access article distributed under the Creative Commons Attribution License, which permits unrestricted use, distribution, and reproduction in any medium, provided the original work is properly cited.

Dendritic cells (DCs) are the sentinels of the immune system. They sense, process, and present antigens to T lymphocytes orchestrating the immune response. The discovery of DCs granted the Nobel Prize for Ralph Steinman, who noticed the presence of rare cells in a culture of mice adherent cells with a distinct stellate morphology [1]. Years later, these cells were shown to express high amounts of major histocompatibility complex class II (MHC-II) molecules, and, even though in very low numbers, they revealed to be the cells responsible for activation and stimulation of naive T lymphocyte [2]. DCs not only activate and subsequently polarize lymphocyte but also can have a tolerogenic role, which is dependent on the factors derived from the surrounded microenvironment [3] and is crucial for the outcome of infectious diseases and autoimmunity by protecting the body from immune-mediated tissue damage. This tolerogenic property is also a target of manipulation by tumor cells to evade the immune response. Thus, understanding the precise regulation of DC function mediated by the different stimulus, such as cytokines and other mediators, remains the goal of numerous studies aiming at skewing T lymphocytes polarization in vaccination protocols for both cancer and infectious diseases.

Since the discovery of DCs, they have been extensively studied in several contexts, from immunity to pathogens and tumors to the induction of tolerance or an immune response to transplants, to self, and more recently to microbi-

ota and dietary antigens, with new discoveries happening constantly. Recent advances in the field have pointed at new DC function as well as new DC subsets with specific transcriptomes [4]. DCs are a heterogeneous group of cells that perform different functions in the immune response. Although the specific phenotype of DCs may differ depending on tissue location and inflammatory context, there are four main groups of DCs identified in both mice and humans, (1) type 1 and (2) type 2 conventional DCs, which have high capacity of processing and presenting antigens to T lymphocytes, (3) plasmacytoid DCs (pDCs), which are the major IFN-I producers, and (4) inflammatory DCs, which are monocyte-derived cells in an inflammatory context that produce inflammatory cytokines [5–7]. Recently, a single-cell RNA-seq study reclassified human DCs into six transcriptionally different subpopulations, two novel types in addition to those aforementioned. One of them is related to pDCs, with the potential to activate T cell, and another subdivision within the class of cDCs1 [8].

The mechanisms of DC development either from progenitors of bone marrow or from circulating monocytes have also gained much knowledge in the past years, enlightening the signaling pathways activated in the rising of the distinct DC subsets. They are either GM-CSF-mediated STAT5 phosphorylation- or FLT3-L-mediated STAT3 phosphorylation-dependent pathways. Moreover, several transcription factors have been identified as subtype specific for the development

of DCs in mouse models [9, 10], such that changes in the cytokine microenvironment and in the transcription factors expressed in dendritic cell progenitors are able to switch DC subset and may influence the outcome of the immune response. Thereby, this complexity makes evident that the study of the development and function of DCs still has much to reveal. The expansion of our understanding of the roles of these unique cells in different scenarios and their underlying mechanisms is crucial for the design of new and specific therapeutic approaches.

This special issue presents a collection of original research articles that unveil the role of dendritic cells, their cellular interactions, and the molecular mechanisms and signaling pathways involved in clinical and experimental models of infections, inflammatory disease, and cancer. First, Azevedo-Santos et al. investigated the mechanisms of the tolerogenic role of DCs from breast tumor patients. In this patients' cohort, they corroborated previous data by demonstrating that monocyte-derived DCs (mo-DCs) from cancer patients are less mature, have a decreased ability to stimulate T lymphocyte proliferation, and produce the anti-inflammatory cytokine IL-10. In addition, they showed that completely differentiated DCs from patients presented the same phenotype as DCs from healthy donors when cocultured with breast cancer-derived cell lines. Nevertheless, monocytes isolated from cancer patients expressed less GM-CSF and IL-4 receptors than monocytes isolated from healthy donors, which may inhibit the differentiation of inflammatory DCs from circulating monocytes. They correlated the presence of the heat shock protein 27 (Hsp27), which is involved in tumor cell proliferation and invasion, with the tolerogenic profile of DCs. In addition to previous data that showed Hsp27 expression in tumor cells, they also revealed that mo-DCs derived from cancer express higher levels of Hsp70. The direct involvement of DC-expressed Hsp27 with the anti-inflammatory response to the tumor still needs clarification.

The maturation state of DCs was the aim of investigation of two articles that show its role in different infectious and inflammatory diseases. In the first article, Islam et al. observed a higher frequency of circulating CD83⁺ DCs in a mouse model of herpes simplex virus-1- (HSV-1-) induced Behçet's disease, when comparing asymptomatic and symptomatic mice. By performing a set of experiments blocking CD83 *in vivo* by different techniques, they revealed an improvement on the severity score associated with reduced frequency of CD83⁺ DCs and downregulation of IL-17 serum levels, which demonstrates the involvement of DCs in the pathology of the disease. Interestingly, ablation of CD83 blockade worsened the symptoms, whereas reestablishment of CD83 inhibition with siRNA treatment, even in the late stage of the disease, restored the beneficial effects and indicates that CD83 is a good candidate for novel therapeutic approaches in Behçet's disease. In the second article, Helmin-Basa et al. detected increased circulating CD83-expressing cDCs in *Helicobacter pylori*-infected children compared to healthy controls, although the percentages and total number of DCs were similar. The induction of circulating cDC maturation was associated with cDC infiltration in

the gastric lamina propria, albeit infiltrating DCs did not express CD83, indicating a more immature profile of DCs in the infected site, which might induce tolerance instead of immunity to local antigens. This set of articles highlighted the importance of DC maturation not only for immunity against HSV-1 and *H. pylori* infections but also for the immune response-driven pathology.

Another article within this special issue by Barbosa et al. emphasized how DC responses can differ depending on the strain of the pathogen involved, even if the strains are closely related, pointing out that DC functions are responsible for the outcome of the infection. They showed that the Mexican *Trypanosoma cruzi* strain Ninoa infected mo-DC more effectively than the Brazilian strain CL-Brener or even another Mexican strain INC5, all three classified as the same genotype subgroup. mo-DCs infected with Ninoa produced more TNF- α and IL-10 than mo-DCs infected with the other strains. The response varied also if the mo-DCs were derived from either BALB/c or C56BL/6 mice, evidencing that phylogenetically close pathogens use different pathways for the modulation of DC function, which affects the course of infection and should be taken into consideration for treatment.

The last set of articles explored the interactions of DCs with other cells and their effects on the immune response to infection in different models. Zhao et al. elegantly showed by both *in vitro* and *in vivo* approaches that DCs play the role of intermediary between invariant natural killer T cells (iNKT) and NK cells during *Chlamydia pneumoniae* infection in mice, which indirectly helps bacterial clearance. They revealed a role for iNKT cells in the regulation of the protective IFN- γ -producing CD27^{high} NK cells by infecting iNKT cell-deficient mice, which displayed changes in NK subsets and an inhibition of NK activation and IFN- γ production. Previous studies demonstrated the role of DCs in NK cell activation and cytokine production; however, *in vitro*, coculture of NK cells with DCs from iNKT deficient mice resulted in reduced expression of CD69 and CD25 and impaired of IFN- γ production by NK cells compared to coculture with WT DCs. Interestingly, adoptive transfer of DCs from either WT or iNKT-deficient mice to infected mice resulted in the same effect observed *in vitro*, demonstrating that iNKT interaction with DCs allows them to modulate NK cell responses. Loss et al. also explored the cellular networks important against bacterial invasion. They studied the crosstalk between porcine mo-DCs and intestinal epithelial cells (IEC). Using *in vitro* assays, they showed that the enteropathogenic bacteria *Escherichia coli* but not the probiotic bacteria *Enterococcus faecium* modulated NLRP3-dependent inflammasome signaling. Contact-dependent communication between mo-DCs and IECs increased inflammasome activation in IECs, whereas it weakened IL-1 β production by DCs. Altogether, these data illustrate the complexity of cellular interactions necessary to orchestrate the precisely effective immune response by different species to fight against a pathogen. We hope you enjoy the reading of this special issue and that it may give you new insights into the biology of DCs, this unique cell with varied functions in diverse context.

Conflicts of Interest

The authors declare no conflict of interest.

Acknowledgments

We thank all the authors for their excellent contribution to this special issue and the reviewers for their efforts and outstanding assistance.

Renata Sesti-Costa
Pedro Manoel Mendes de Moraes-Vieira
Luisa Cervantes-Barragan

References

- [1] R. M. Steinman and Z. A. Cohn, "Identification of a novel cell type in peripheral lymphoid organs of MICE," *The Journal of Experimental Medicine*, vol. 137, no. 5, pp. 1142–1162, 1973.
- [2] M. C. Nussenzweig and R. M. Steinman, "Contribution of dendritic cells to stimulation of the murine syngeneic mixed leukocyte reaction," *The Journal of Experimental Medicine*, vol. 151, no. 5, pp. 1196–1212, 1980.
- [3] K. Mahnke, J. Knop, and A. H. Enk, "Induction of tolerogenic DCs: 'you are what you eat'," *Trends in Immunology*, vol. 24, no. 12, pp. 646–651, 2003.
- [4] C. C. Brown, H. Gudjonson, Y. Pritykin et al., "Transcriptional basis of mouse and human dendritic cell heterogeneity," *Cell*, vol. 179, no. 4, pp. 846–863.e24, 2019.
- [5] M. Guilliams, F. Ginhoux, C. Jakubzick et al., "Dendritic cells, monocytes and macrophages: a unified nomenclature based on ontogeny," *Nature Reviews Immunology*, vol. 14, no. 8, pp. 571–578, 2014.
- [6] A. Mildner and S. Jung, "Development and function of dendritic cell subsets," *Immunity*, vol. 40, no. 5, pp. 642–656, 2014.
- [7] M. Swiecki and M. Colonna, "The multifaceted biology of plasmacytoid dendritic cells," *Nature Reviews Immunology*, vol. 15, no. 8, pp. 471–485, 2015.
- [8] A. C. Villani, R. Satija, G. Reynolds et al., "Single-cell RNA-seq reveals new types of human blood dendritic cells, monocytes, and progenitors," *Science*, vol. 356, no. 6335, 2017.
- [9] A. T. Satpathy, X. Wu, J. C. Albring, and K. M. Murphy, "Re(de)fining the dendritic cell lineage," *Nature Immunology*, vol. 13, no. 12, pp. 1145–1154, 2012.
- [10] P. Bagadia, X. Huang, T. T. Liu et al., "An *Nfil3* - *Zeb2* - *Id2* pathway imposes *Irf8* enhancer switching during cDC1 development," *Nature Immunology*, vol. 20, no. 9, pp. 1174–1185, 2019.

Research Article

Could Increased Expression of Hsp27, an “Anti-Inflammatory” Chaperone, Contribute to the Monocyte-Derived Dendritic Cell Bias towards Tolerance Induction in Breast Cancer Patients?

Ana Paula Silva de Azevedo-Santos ¹, Mirtes Castelo Branco Rocha,¹
Sulayne Janayna Araujo Guimarães,¹ André Alvares Marques Vale,¹ Fabio Martins Laginha,²
Flavia Raquel F. Nascimento,¹ Maria Aparecida Nagai,³ Patrícia C. Bergami-Santos,⁴
and José Alexandre Marzagão Barbuto ⁴

¹Biological and Health Sciences Center, Federal University of Maranhão, Avenida dos Portugueses, 1966, Bacanga, São Luis, Brazil

²Pérola Byington Hospital, Avenida Brigadeiro Luis Antonio, 683 São Paulo, Brazil

³The State of São Paulo Cancer Institute (ICESP), Avenida Dr. Arnaldo, 251 São Paulo, Brazil

⁴Institute of Biomedical Sciences, University of São Paulo, Avenida Prof. Lineu Prestes, 1730 São Paulo, Brazil

Correspondence should be addressed to Ana Paula Silva de Azevedo-Santos; apsazevedo@yahoo.com.br

Received 17 May 2019; Revised 22 August 2019; Accepted 1 October 2019; Published 18 November 2019

Guest Editor: Luisa Cervantes-Barragan

Copyright © 2019 Ana Paula Silva de Azevedo-Santos et al. This is an open access article distributed under the Creative Commons Attribution License, which permits unrestricted use, distribution, and reproduction in any medium, provided the original work is properly cited.

Dendritic cells (DCs) are the most efficient *antigen-presenting cells* and link the innate immune sensing of the environment to the initiation of adaptive immune responses, which may be directed to either acceptance or elimination of the recognized antigen. In cancer patients, though DCs would be expected to present tumor antigens to T lymphocytes and induce tumor-eliminating responses, this is frequently not the case. The complex tumor microenvironment subverts the immune response, blocks some effector mechanisms, and drives others to support tumor growth. Chronic inflammation in a tumor microenvironment is believed to contribute to the induction of such regulatory/tolerogenic response. Among the various mediators of the modulatory switch in chronic inflammation is the “antidanger signal” chaperone, heat shock protein 27 (Hsp27), that has been described, interestingly, to be associated with cell migration and drug resistance of breast cancer cells. Thus, here, we investigated the expression of Hsp27 during the differentiation of monocyte-derived DCs (Mo-DCs) from healthy donors and breast cancer patients and evaluated their surface phenotype, cytokine secretion pattern, and lymphostimulatory activity. Surface phenotype and lymphocyte proliferation were evaluated by flow cytometry, interferon- (IFN-) γ , and interleukin- (IL-) 10 secretion, by ELISA and Hsp27 expression, by quantitative polymerase chain reaction (qPCR). Mo-DCs from cancer patients presented decreased expression of DC maturation markers, decreased ability to induce allogeneic lymphocyte proliferation, and increased IL-10 secretion. In coculture with breast cancer cell lines, healthy donors’ Mo-DCs showed phenotype changes similar to those found in patients’ cells. Interestingly, patients’ monocytes expressed less GM-CSF and IL-4 receptors than healthy donors’ monocytes and Hsp27 expression was significantly *higher* in patients’ Mo-DCs (and in tumor samples). Both phenomena could contribute to the phenotypic bias of breast cancer patients’ Mo-DCs and might prove potential targets for the development of new immunotherapeutic approaches for breast cancer.

1. Introduction

Dendritic cells (DCs) are mononuclear phagocytes, specialized in antigen presentation to naïve T cells and, consequently, to initiation and control of immunity in immunogenic or

tolerogenic response [1–3]. In cancer context, DCs are crucial for the induction of a potent immune response; on the other hand, defects in their differentiation/maturation can be favorable to tumor escape [4]. The complex relationship between tumor cells and the host immune

system is dynamic, and different stimuli can induce heterogeneous DC subsets [5, 6]. A tumor immunoenvironment presents chronic inflammation that contributes to cancer development and progression and increases the accumulation of myeloid-derived suppressor cells [7].

Tumor cells produce several factors that affect DC differentiation. Heat shock proteins (Hsps) are a chaperone protein family induced by cell stress. Hsps have antiapoptotic properties and are actively involved in tumor cell proliferation and invasion [8]. Small heat shock protein 27 (Hsp27) has a role in protection against toxicity mediated by inflammation conditions. Moreover, the expression of Hsp27 induces monocyte to produce IL-10, which is a strong inhibitor of the Th1 response and is constantly found to be elevated in human cancers [9–11].

Breast cancer is the most common invasive cancer in women; in this context, Hsp27 is associated with tumor growth regulation and drug resistance in human breast cancer [11–14]. Banerjee et al. demonstrated that the treatment of monocytes with Hsp27 leads to the differentiation for macrophages with a tolerogenic profile, being these similar to the macrophages found in breast tumors [15]. Laudanski et al. (2007) reported that exogenous inhibition of Hsp27 in monocytes leads to differentiation in immature dendritic cells, and its activation is associated with impaired antitumoral immune responses [10]. Taking into account this theoretical framework, our objective is to evaluate the phenotype and biological function of monocyte-derived DCs from patients with breast cancer as well as the role of Hsp27 in this process.

2. Materials and Methods

2.1. Subjects and Study Design. This was a prospective, single-blind study with convenience sampling, based on researcher availability of breast cancer patients undergoing mastectomy surgery. The protocol was approved by the National Commission of Ethics in Research (CONEP) (695/CEP) and was conducted in the Hospital Pérola Byington (107/06), São Paulo, Brazil. Samples were collected only after obtaining informed consent of donors. Peripheral blood mononuclear cells (PBMCs) were obtained from 18 female healthy volunteers (32 to 50 years) and 20 female patients (33 to 62 years). The histological diagnostics confirmed 14 ductal breast carcinomas, 4 lobular breast carcinomas, and 2 ductal and lobular breast carcinomas (pT₁₋₄, pN₀₋₂ and M₀).

Initially, we obtained DCs derived from monocyte by *in vitro* culture with IL-4 and GM-CSF, adding TNF- α for DC maturation. The patients and healthy donors' Mo-DC phenotypes were characterized by flow cytometry and the functional activity by mixed lymphocyte reaction culture and cytokine secretion. Afterward, the Mo-DCs were cultured with or without breast cancer cell lines for the phenotype and functional characterization. The IL-4 and GM-CSF receptors were investigated in monocytes by flow cytometry. Tumor samples were used to evaluate the Hsp27 expression by quantitative polymerase chain reaction (PCR).

2.2. Mo-DC Culture. We followed the methods of Barbuto et al. [16]. PBMCs were separated over a Ficoll-Paque gradient ($d = 1.076$), resuspended, and seeded in 12-well plates in AIM-V medium. After overnight incubation at 37°C, nonadherent cells were removed, and the adherent cells were cultured in the presence of GM-CSF and IL-4 (50 ng/mL; R&D, Minneapolis, MN, USA) in AIM-V medium. On the 5th day, TNF- α (50 ng/mL; R&D, Minneapolis, MN, USA) was added for DC activation. After 2 further days in culture, the cells were harvested with cold RPMI 1640 and analyzed for flow cytometry. The culture efficiency was calculated for the percentile of cells removed starting from the total of adherent cells by well.

For tumor coculture in transwells, aliquots of tumorigenic (MCF7) and metastatic (SKBR-3) breast cancer cell lines (1×10^5 in 100 μ L of medium) were pipetted (6.5 mm diameter, 0.4 μ m pore size polycarbonate transwell filters) (Corning B.V. Life Sciences, Schiphol-Rijk, The Netherlands) in Mo-DC culture (5th day). After 7 days, the DCs were harvested with cold RPMI 1640 for phenotype and functional characterization.

2.3. Flow Cytometry of Immune Cell Populations. The monocytes and Mo-DCs were analyzed according to their size and granularity. To detect specific surface antigens, the immune cells (5×10^5 cells) were stained with fluorescein isothiocyanate (FITC), phycoerythrin (PE), or PE-Cy5-conjugated mouse monoclonal antibodies (MoAbs) against HLA-DR, CD11c, CD86, CD116, and CD124 or with mouse isotype controls (Caltag Laboratories, Burlingame, CA, USA) and analyzed in a FACSCalibur cytometer (Becton Dickinson, San Jose, CA, USA) with Win MDI2.8 software. At least 10,000 gated events were acquired per antibody analyzed. The expression of the markers was determined for the number and median fluorescence intensity (MFI) of positive cells.

2.4. T lymphocyte Isolation by Rosetting with AET-Treated Sheep Erythrocytes and Allogenic T Cell Proliferation Assay. Nonadherent cells obtained previously after adherent assay of PBMC from healthy donors were incubated for 1 hour with S-(2-aminoethyl) isothiuronium bromide hydrobromide- (AET-) treated sheep red blood cells. T lymphocytes that adhered to red cells (R+), forming rosettes, were submitted a Ficoll gradient 900g for 35 min and isolated from the erythrocyte pellet by disaggregation and lysis of red blood cells with hypotonic saline solution (0.899% NH₄Cl) for 2 min. After that, the cells were washed twice in RPMI 1640 supplemented with 10% heat-inactivated fetal calf serum (FCS) and 2 mM L-glutamine (R10 medium), centrifuged at 250g for 10 min for the removal of red cell debris. T lymphocytes were used in MLR (mix lymphocyte reaction) to evaluate Mo-DC ability to induce lymphoproliferation *in vitro*.

The ability of DCs from healthy donors and breast cancer patients to stimulate allogenic T cells was assessed in this assay. The T cells used in all the experiments were collected from healthy volunteers and breast cancer patients. In this assay, DCs were the stimulator cells and T lymphocytes the responder cells. The latter were added at 5×10^4 cells/well. In each assay, all tests were carried out using two replicates.

Appropriate controls were set up in each 96-well plate (Costar, Cambridge, UK). The stimulator DCs were irradiated with 25 Gy. The T cells were stained with CFSE. DC to T cell ratio (1 : 30) was set up, and the plates were cultured for 7 days at 37°C in a humidified 5% CO₂ incubator. The proliferation index was determined by FlowJo software. The results as a percentage (%) were calculated through the reason of control fluorescence mean/DCs treated to T cell culture fluorescence mean multiplied by 100 and divided by the reason of control fluorescence mean/DCs treated without T cell culture fluorescence mean. The culture supernatants were frozen for cytokine analyses.

2.5. Quantification of IFN- γ and IL-10 by ELISA. IFN- γ and IL-10 concentrations in lymphocyte-DC allogenic culture supernatants were tested using commercially available quantitative enzyme-linked immunosorbent assay (ELISA) kits (Becton Dickinson, San Jose, CA, USA).

2.6. Real-Time Quantitative Polymerase Chain Reaction. Total mRNA from the Mo-DC and tumor breast cancer cells was isolated using Illustra RNAspin Mini Isolation Kit (GE Healthcare, Piscataway, USA). The concentration of total mRNA was determined by measuring the absorbance at 260 nm using a GeneQuant pro (Amersham Biosciences, Cambridge, England). Reverse transcription was carried out with a real-time quantitative polymerase chain reaction, which contains DNase I to avoid DNA contamination (Promega, Madison, EUA). mRNA Hsp27 expression was analyzed using Power SYBR Green master mix (Applied Biosystems, Warrington, UK) according to the manufacturer's instructions. The fold change in target gene expression between the various groups was determined using the comparative Ct ($2^{-\Delta\Delta C_t}$) method, after normalizing to glyceraldehyde-3-phosphate dehydrogenase (GAPDH) and β -actin expression as an internal reference.

2.7. Statistical Analysis. Comparisons of the samples to establish statistical significance were determined by an unpaired *t*-test. Results were considered to be statistically significant when the *p* < 0.05. We used the GraphPad Prism 7 statistical program (OSB Software, São Paulo, Brazil) to analyze the results.

3. Results

Mature DC membrane markers were analyzed by flow cytometry, and Mo-DCs obtained from breast cancer patients showed less HLA-DR, CD11c CD86, CD80, and CCR7 expressions when compared to Mo-DCs from healthy donors (Figure 1(a)). Further, the patient's Mo-DCs had a lower lymphostimulatory capacity and secreted less IFN- γ and more IL-10 (Figures 1(c) and 1(d)) than controls.

Thus, we evaluated the influence of tumor cells upon healthy donors' Mo-DC maturation. Two different human breast cancer cell lines, MCF7 and SKBR-3, when present during the Mo-DC differentiation, caused a decrease in the frequency of mature DCs, even after TNF- α supplementation (Figures 2(a)–2(c)), reduced the Mo-DCs' ability to induce lymphoproliferation (Figure 2(d)), and decreased the IFN- γ

secretion in the cocultures (Figure 2(e)). Contrastingly, Mo-DCs obtained from patients were not affected, neither on their surface (Figures 2(a)–2(c)) nor on their functional phenotype (Figures 2(d)–2(f)) when exposed to the tumor cells.

The combination of granulocyte-macrophage colony stimulating factor (GM-CSF) and interleukin-4 (IL-4) induces the differentiation of Mo-DCs from adherent peripheral blood leukocytes. In accordance with their poorer differentiation into Mo-DCs, peripheral blood mononuclear cells obtained from breast cancer patients showed lower levels of GM-CSF (CD116) and IL-4 receptor (CD124) expression than healthy donors' cells (Figures 3(a) and 3(b)).

Hsp27 is an immunomodulatory protein expressed by breast cancer cells. In this study, the Hsp27 expression was determined in tumors, normal breast tissue, and Mo-DCs from healthy donors and from patients by quantitative RT-PCR, and a significantly higher Hsp27 expression in tumors (Figure 4(a)) and in Mo-DCs (Figure 4(b)) from patients was detected.

4. Discussion

In this study, we investigated the influence of the tumor, *in vivo*, and of tumor cells, *in vitro*, on Mo-DCs. We analyzed their surface phenotype, cytokine secretion, and lymphostimulatory activity and noted that cells from patients or those from healthy donors exposed to tumor cells presented characteristics that could be ascribed to cells with a tolerogenic function. Furthermore, we also noticed the association of these traits with an increased expression of the anti-inflammatory chaperone Hsp27 by Mo-DCs from the patients.

During Mo-DC generation, monocytes were cultured in medium containing GM-CSF and IL-4, cytokines that drive their differentiation into immature DCs, after 5 days. After that, TNF- α was added as a maturation stimulus. Compared to healthy donor Mo-DCs, breast cancer patient Mo-DCs showed a surface phenotype suggestive of a poorer ability to induce T cell activation and a cytokine profile that, likewise, would drive the induction of tolerance rather than response to the antigens they would present. This bias was maintained even after TNF stimulation, which is known to drive DC maturation and enhance their antigen-presenting function [17, 18]. Within the tumor, abnormal differentiation may generate defective DCs which can contribute to the tumor escape from immune system response [19]. Phenotypic and functional impairment of DCs derived from breast cancer patient monocytes was described in previous studies [20, 21]. The relationship between a cancer immunoenvironment and inflammation is widely accepted. Previous studies showed that tumors induce tolerogenic DCs and, consequently, decrease effective immune responses, thus allowing tumor growth [6, 22, 23]. In breast cancer, a deficiency in mature DC in patients was closely associated with the stage and duration of the disease [24].

The interaction between immune cells and tumor has been investigated by several studies, paving the way for new treatments/therapeutic strategies and indicating new targets for therapy. Using breast cancer cell lines in coculture with monocyte-derived dendritic cells, we obtained results

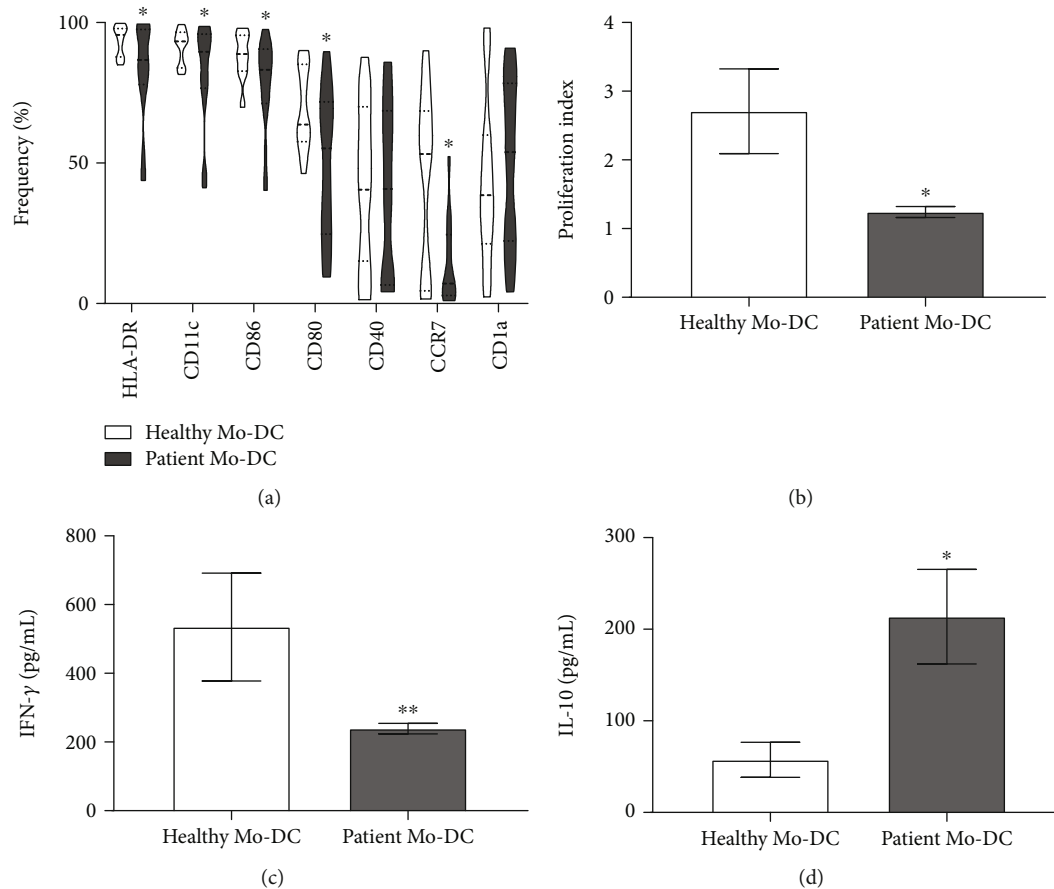


FIGURE 1: Mo-DCs from a breast cancer patient show lower frequency of maturation surface markers than those from healthy donors. (a) Box plots represent the frequency of DC maturation markers. Monocytes were cultivated for 7 days in the presence of GM-CSF and IL-4 (50 ng/ml each) to induce the differentiation of immature Mo-DCs; cell maturation was induced by TNF- α (50 ng/mL) during the last 2 days of culture. On day 7 of culture, Mo-DCs were harvested and labeled with monoclonal antibodies specific to the molecules CD1a, CD11c, CD80, CD86, CD40, HLA-DR, and CCR-7. (b) Allogeneic T lymphocytes previously labeled with CFSE were cocultured with Mo-DCs (from healthy donors or from patients). On day 4 of coculture, the cells were harvested, stained with a viability marker, acquired by flow cytometry, and an index of proliferation was determined by FlowJo software. (c, d) Concentration of IFN- γ and IL-10 in supernatants of cocultures with patients' Mo-DC or healthy donors' Mo-DC, determined by ELISA. The results are expressed as the average concentration (pg/mL) \pm SEM. ($n = 20$ patients and $n = 18$ healthy donors); a t -test was used to compare patients and healthy donor groups. * $p < 0.05$.

suggesting that the tumor microenvironment not only is able to block DC maturation but also appears to have a systemic effect, preventing the normal differentiation of DC, at least from blood monocytes, thus affecting these central antigen-presenting cells, even before any maturation stimulus. The tumor immunoenvironment is complex and dynamic, with various components, among which is a highly heterogeneous population of inflammatory myeloid cells that may support tumor growth and protect the tumor from host immunity [25]. Tumor progression causes tissue remodeling, metabolic alterations, angiogenesis, changes in tissue cytokine milieu, and cell recruitment, leading to a state similar to that of chronic inflammation [26, 27]. In parallel, clinical and experimental reports indicate that such a proinflammatory microenvironment favors myeloid suppressor cell tumor infiltration and progression [27–31].

The frequency of mature DCs obtained from the differentiation of blood monocytes from breast cancer patients, when

compared to healthy donors, was lower. Since GM-CSF and IL-4 are the cytokines used to induce this differentiation [32–34], we investigated the expression of receptors to both cytokines in peripheral blood mononuclear cells from patients and healthy donors. The results showed a loss in both cytokines' receptor expressions in patients' PBMCs. In the inflammatory response, the cytokine signal transduction and the regulation of cytokine gene expression are controlled by heat shock proteins (Hsps) [35]. Hsp27, an important member of the small Hsp family, has been investigated for its elevated intracellular expression and its role as a marker of increased malignancy in human breast tumor cells [13, 36, 37]. Banerjee et al. reported elevated serum Hsp27 levels in breast cancer patients which, in turn, seems to bias the differentiation of monocytes to tolerogenic macrophages, with less tumoricidal activity and with a high proangiogenic capacity that promotes tumor growth [15]. Laudanski et al. demonstrated that Hsp27

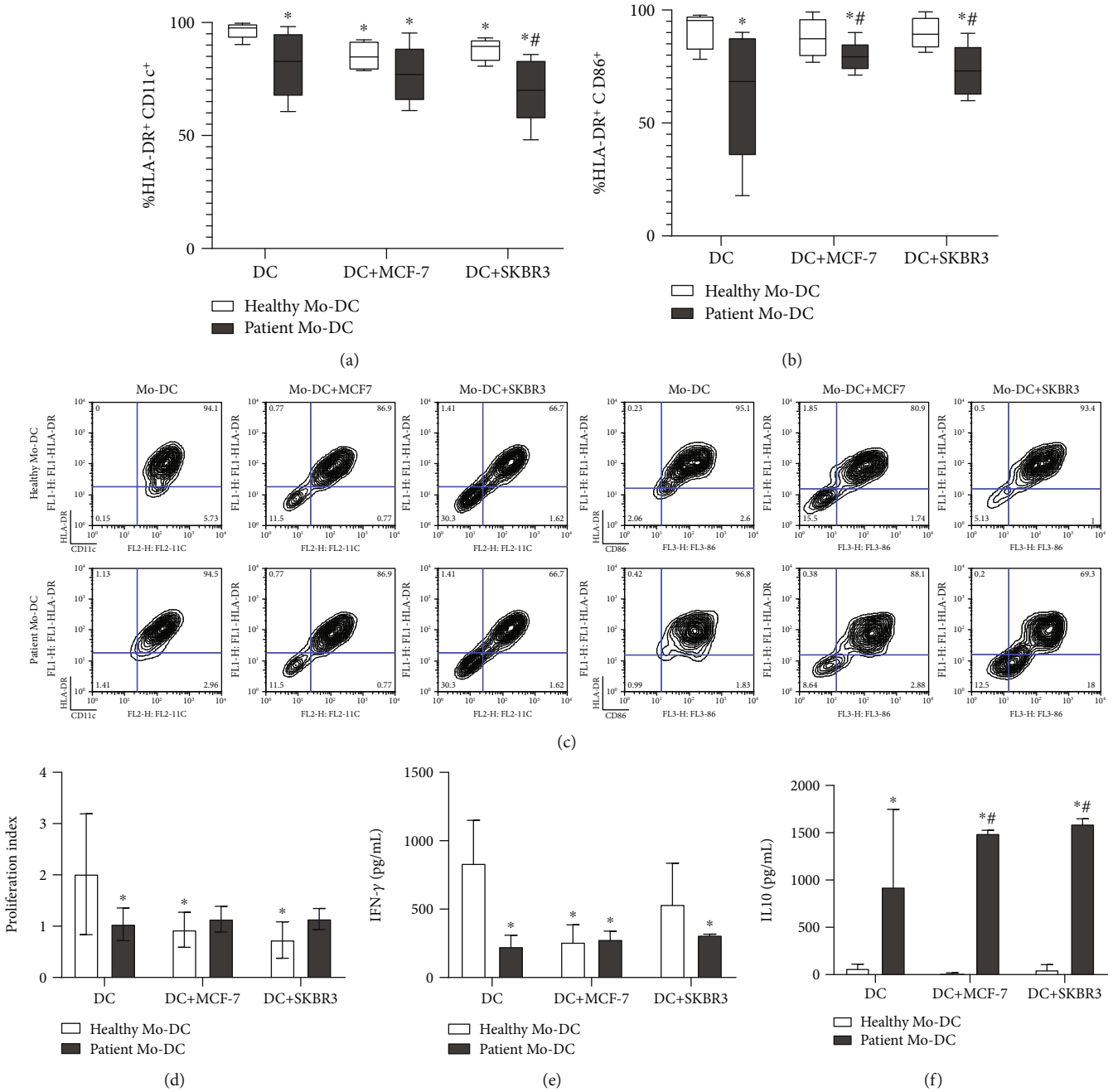


FIGURE 2: Cancer cell lines (MCF-7 and SKBR3) disturbed the maturation of Mo-DCs. (a, b) Box plots represent the frequency of HLA-DR and CD11c or HLA-DR and CD86-expressing Mo-DCs from healthy donors and breast cancer patients. Monocytes were cultivated in the presence of GM-CSF and IL-4, and Mo-DCs maturation was induced by TNF- α . MCF-7 and SKBR3 breast cancer cell lines were cocultured in a transwell system with the Mo-DCs. On day 7 of culture, Mo-DCs were harvested and labelled with monoclonal antibodies for CD11c, CD86, and HLA-DR. (c) Contour plots illustrating HLA – DR \times CD11c or HLA – DR \times CD86 expression under the various conditions. (d) Proliferation index obtained in mixed lymphocyte reaction (MLR) with healthy donors’ or breast cancer patients’ Mo-DC cocultured or not with tumor cell lines, as stimulators. (e, f) IFN- γ and IL-10 concentrations in MLR supernatants. Cytokine concentrations were determined by ELISA. The results are expressed as the average concentration (pg/mL) \pm SEM. ($n = 4$ patients and $n = 4$ healthy donors). A t -test was used to compare different groups. * $p < 0.05$ when compared with Mo-DC obtained from healthy donors and # $p < 0.05$ when compared with Mo-DC from healthy donors in transwell with the respective tumor line cell.

treatment reduced DC differentiation levels in IL-4 and GM-CSF-stimulated monocyte cultures [10]. Hsp27 expression was, therefore, investigated, and the results showed a higher expression in breast cancer tissue when compared to normal breast tissue. As mentioned before, Hsp27 has been shown to

be upregulated in breast cancer [38], associated with drug resistance [36] and described as able to drive immune cells towards tolerance [10, 15]. Our findings are, accordingly, in agreement with these data and suggest that Hsp27 expression not only by tumor cells but also by antigen-presenting cells

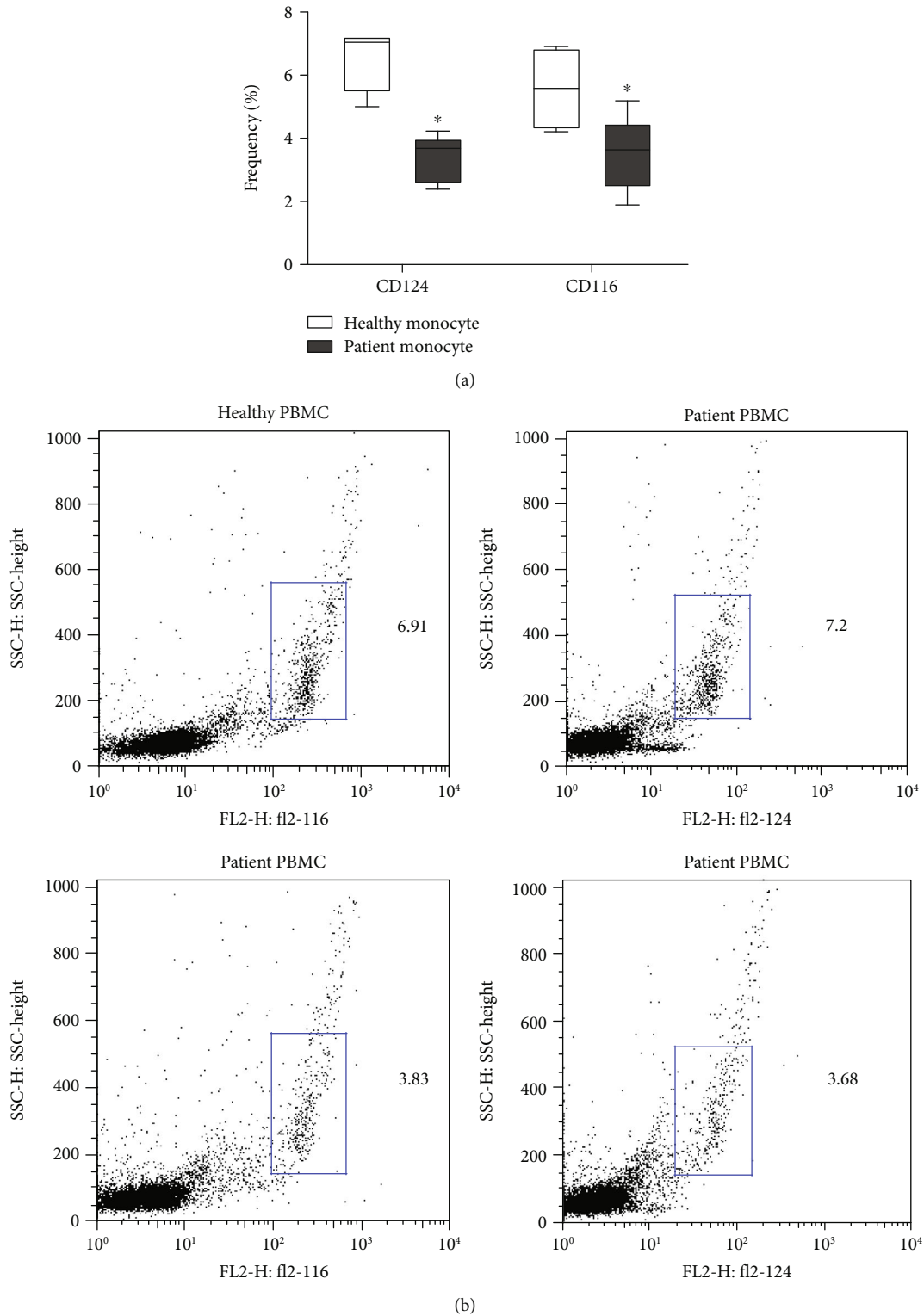


FIGURE 3: Monocytes from breast cancer patients express less IL-4 and GM-CSF receptors. (a) Box plots representing the frequency of CD124 and CD116 expression by peripheral blood mononuclear cells (PBMCs) obtained from healthy donors and breast cancer patients. (b) Dot plots illustrating the expression of CD124 and CD116 by PBMCs from healthy donors and breast cancer patients.

may contribute to the immune escape mechanism in breast cancer, favoring the differentiation of DCs biased to induce tolerance rather than response.

DCs are highly specialized antigen-presentation cells that have an important role in the initiation and control of adaptive immunity, determining the immunogenic or tolerogenic

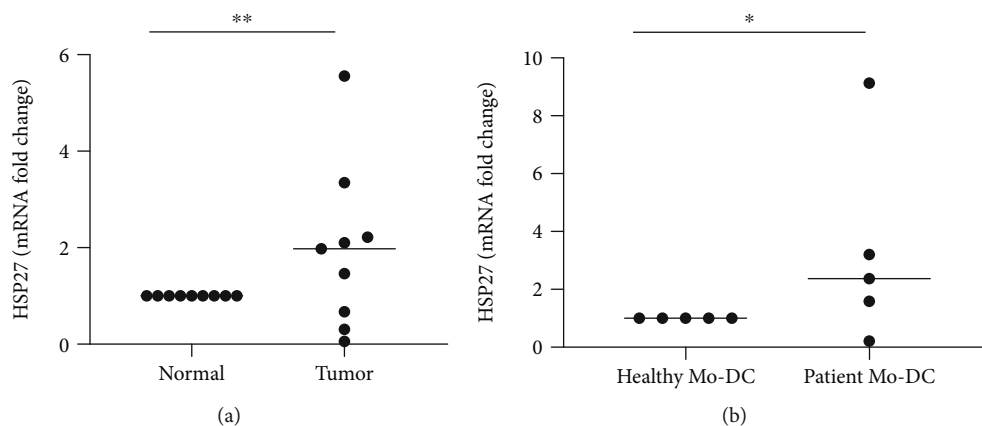


FIGURE 4: Breast cancer and Mo-DCs obtained from patients express higher levels of HSP27 than healthy cells. (a) Comparative real-time PCR Hsp27 gene expression analysis by tumors ($n = 9$) and normal breast (pooled tissues from 5 donors) shows a significantly (1.46-5.45 fold) increased expression of Hsp27 by tumors. (b) The same analysis performed on Mo-DCs from patients and healthy donors detected an increased Hsp27 expression also by patients' Mo-DCs. GAPDH or β -actin were used as internal controls for targeting mRNA expression in tumor and immune cells, respectively. The data were normalized to GAPDH or β -actin mRNA expression level. Individual data are plotted, and the horizontal bar represents the mean. Data were compared using the unpaired t -test; * $p < 0.05$; ** $p < 0.01$.

response [1, 2, 10, 38, 39]. Le Naour et al. described the gene expression and proteomic profiling changes in Mo-DC differentiation/maturation and reported that during DC differentiation the Hsp27 expression was maximal in immature DCs [40]. Furthermore, exogenous human Hsp27 treatment stimulates monocytes to produce IL-10 and reduces the TNF- α levels [41]. Accordingly, we observed that breast cancer and Mo-DCs from breast cancer patients expressed more Hsp27 when compared to non-tumor tissues or healthy donor Mo-DCs. Thus, the immature phenotype and regulatory activity that we observed in Mo-DCs from breast cancer patients could be partially caused by the elevated Hsp27 expression within the tumor microenvironment both by the tumor cells and, possibly, by the local DCs (since, at least the Mo-DCs from patients do show this high expression).

5. Conclusions

Our study shows that an elevated Hsp 27 expression, already described in breast cancer, is also present in Mo-DCs derived from patients' monocytes. These cells have a surface and functional phenotype that may be indicative of a tolerogenic bias, which could favor tumor escape and growth. Furthermore, we identify a lower expression of GM-CSF and IL-4 receptors by patients' monocytes, suggesting that the interaction of these cytokines and the cells may be less than optimal when patients' cells are involved, a phenomenon that could contribute to their affected phenotype and, likewise, to tumor escape. Though we were not able to causally link the lower expression of cytokines' receptors to the higher Hsp27 expression, it is possible to envisage how such interactions within the complex tumor immunoenvironment could lead an immunosuppressive network that would promote tumor growth and which, therefore, could be possible targets for therapeutic modulation.

Data Availability

All data that support the manuscript can be accessed in this article and do not have data restriction.

Conflicts of Interest

The authors declare that there is no conflict of interest regarding the publication of this paper.

Acknowledgments

This work was supported by the Fundação de Amparo à Pesquisa do Estado de São Paulo (FAPESP) and Conselho Nacional de Desenvolvimento Científico e Tecnológico (CNPq). The authors are grateful to Perola Byington Hospital for the clinical assistance and mostly to their patients and volunteers without whom this study would not have been possible.

References









- [1] J. Banchereau and R. M. Steinman, "Dendritic cells and the control of immunity," *Nature*, vol. 392, no. 6673, pp. 245–252, 1998.
- [2] J. Banchereau, F. Briere, C. Caux et al., "Immunobiology of dendritic cells," *Annual Review of Immunology*, vol. 18, no. 1, pp. 767–811, 2000.
- [3] F. Geissmann, M. G. Manz, S. Jung, M. H. Sieweke, M. Merad, and K. Ley, "Development of monocytes, macrophages, and dendritic cells," *Science*, vol. 327, no. 5966, pp. 656–661, 2010.
- [4] D. Gabrilovich, "Mechanisms and functional significance of tumour-induced dendritic-cell defects," *Nature Reviews Immunology*, vol. 4, no. 12, pp. 941–952, 2004.
- [5] M. B. Lutz and G. Schuler, "Immature, semi-mature and fully mature dendritic cells: which signals induce tolerance or immunity?," *Trends in Immunology*, vol. 23, no. 9, pp. 445–449, 2002.

- [6] Y. Ma, G. V. Shurin, Z. Peiyuan, and M. R. Shurin, "Dendritic cells in the cancer microenvironment," *Journal of Cancer*, vol. 4, no. 1, pp. 36–44, 2013.
- [7] S. K. Bunt, L. Yang, P. Sinha, V. K. Clements, J. Leips, and S. Ostrand-Rosenberg, "Reduced inflammation in the tumor microenvironment delays the accumulation of myeloid-derived suppressor cells and limits tumor progression," *Cancer Research*, vol. 67, no. 20, pp. 10019–10026, 2007.
- [8] S. K. Calderwood, M. A. Khaleque, D. B. Sawyer, and D. R. Ciocca, "Heat shock proteins in cancer: chaperones of tumorigenesis," *Trends in Biochemical Sciences*, vol. 31, no. 3, pp. 164–172, 2006.
- [9] M. Sherman and G. Multhoff, "Heat shock proteins in cancer," *Annals of the New York Academy of Sciences*, vol. 1113, no. 1, pp. 192–201, 2007.
- [10] K. Laudanski, A. De, and C. Miller-Graziano, "Exogenous heat shock protein 27 uniquely blocks differentiation of monocytes to dendritic cells," *European journal of immunology*, vol. 37, no. 10, pp. 2812–2824, 2007.
- [11] T. Oya-Ito, Y. Naito, T. Takagi et al., "Heat-shock protein 27 (Hsp27) as a target of methylglyoxal in gastrointestinal cancer," *Biochimica Et Biophysica Acta (BBA)-Molecular Basis of Disease*, vol. 1812, no. 7, pp. 769–781, 2011.
- [12] S. Oesterreich, C. N. Weng, M. Qiu, S. G. Hilsenbeck, C. K. Osborne, and S. A. Fuqua, "The small heat shock protein Hsp27 is correlated with growth and drug resistance in human breast cancer cell lines," *Cancer Research*, vol. 53, no. 19, pp. 4443–4448, 1993.
- [13] D. R. Ciocca, S. Green, R. M. Elledge et al., "Heat shock proteins Hsp27 and Hsp70: lack of correlation with response to tamoxifen and clinical course of disease in estrogen receptor-positive metastatic breast cancer (a Southwest Oncology Group Study)," *Clinical Cancer Research*, vol. 4, no. 5, pp. 1263–1266, 1998.
- [14] P. Shi, M.-m. Wang, L.-y. Jiang, H.-t. Liu, and J.-z. Sun, "Paclitaxel-doxorubicin sequence is more effective in breast cancer cells with heat shock protein 27 overexpression," *Chinese Medical Journal*, vol. 121, no. 20, pp. 1975–1979, 2008.
- [15] S. Banerjee, C.-F. L. Lin, K. A. Skinner et al., "Heat shock protein 27 differentiates tolerogenic macrophages that may support human breast cancer progression," *Cancer Research*, vol. 71, no. 2, pp. 318–327, 2011.
- [16] J. A. M. Barbuto, L. F. C. Ensina, A. R. Neves et al., "Dendritic cell-tumor cell hybrid vaccination for metastatic cancer," *Cancer Immunology, Immunotherapy*, vol. 53, no. 12, pp. 1111–1118, 2004.
- [17] P. Chomarat, C. Dantin, L. Bennett, J. Banchereau, and A. K. Palucka, "TNF skews monocyte differentiation from macrophages to dendritic cells," *The Journal of Immunology*, vol. 171, no. 5, pp. 2262–2269, 2003.
- [18] K. Palucka, L. M. Coussens, and J. O'shaughnessy, "Dendritic cells, inflammation and breast cancer," *Cancer Journal*, vol. 19, no. 6, pp. 511–516, 2013.
- [19] B. Almand, J. I. Clark, E. Nikitina et al., "Increased production of immature myeloid cells in cancer patients: a mechanism of immunosuppression in cancer," *The Journal of Immunology*, vol. 166, no. 1, pp. 678–689, 2001.
- [20] R. N. Ramos, L. S. Chin, A. P. S. A. dos Santos, P. C. Bergami-Santos, F. Laginha, and J. A. M. Barbuto, "Monocyte-derived dendritic cells from breast cancer patients are biased to induce CD4⁺CD25⁺Foxp3⁺ regulatory T cells," *Journal of Leukocyte Biology*, vol. 92, no. 3, pp. 673–682, 2012.
- [21] E. Verronèse, A. Delgado, J. Valladeau-Guilemond et al., "Immune cell dysfunctions in breast cancer patients detected through whole blood multi-parametric flow cytometry assay," *Oncoimmunology*, vol. 5, no. 3, article e1100791, 2016.
- [22] A. Pinzon-Charry, T. Maxwell, and J. Alejandro López, "Dendritic cell dysfunction in cancer: a mechanism for immunosuppression," *Immunology and Cell Biology*, vol. 83, no. 5, pp. 451–461, 2005.
- [23] N. Janikashvili, B. Bonnotte, E. Katsanis, and N. Larmonier, "The Dendritic Cell-Regulatory T Lymphocyte Crosstalk Contributes to Tumor- Induced Tolerance," *Clinical and Developmental Immunology*, vol. 2011, Article ID 430394, 14 pages, 2011.
- [24] H. Hwang, C. Shin, J. Park et al., "Human breast cancer-derived soluble factors facilitate CCL19-induced chemotaxis of human dendritic cells," *Scientific Reports*, vol. 6, no. 1, article 30207, 2016.
- [25] E. Schouppe, P. de Baetselier, J. A. van Ginderachter, and A. Sarukhan, "Instruction of myeloid cells by the tumor microenvironment: open questions on the dynamics and plasticity of different tumor-associated myeloid cell populations," *Oncoimmunology*, vol. 1, no. 7, pp. 1135–1145, 2012.
- [26] A. Mantovani, P. Allavena, A. Sica, and F. Balkwill, "Cancer-related inflammation," *Nature*, vol. 454, no. 7203, pp. 436–444, 2008.
- [27] J. Vakkila and M. T. Lotze, "Inflammation and necrosis promote tumour growth," *Nature Reviews Immunology*, vol. 4, no. 8, pp. 641–648, 2004.
- [28] Y. Saijo, M. Tanaka, M. Miki et al., "Proinflammatory cytokine IL-1 β promotes tumor growth of Lewis lung carcinoma by induction of angiogenic factors: in vivo analysis of tumor-stromal interaction," *The Journal of Immunology*, vol. 169, no. 1, pp. 469–475, 2002.
- [29] V. Bronte, P. Serafini, E. Apolloni, and P. Zanovello, "Tumor-induced immune dysfunctions caused by myeloid suppressor cells," *Journal of Immunotherapy*, vol. 24, no. 6, pp. 431–446, 2001.
- [30] D. I. Gabrilovich, M. P. Velders, E. M. Sotomayor, and W. M. Kast, "Mechanism of immune dysfunction in cancer mediated by immature Gr-1⁺ myeloid cells," *The Journal of Immunology*, vol. 166, no. 9, pp. 5398–5406, 2001.
- [31] S. Ostrand-Rosenberg, M. J. Grusby, and V. K. Clements, "Cutting edge: STAT6-deficient mice have enhanced tumor immunity to primary and metastatic mammary carcinoma," *The Journal of Immunology*, vol. 165, no. 11, pp. 6015–6019, 2000.
- [32] F. Sallusto and A. Lanzavecchia, "Efficient presentation of soluble antigen by cultured human dendritic cells is maintained by granulocyte/macrophage colony-stimulating factor plus interleukin 4 and downregulated by tumor necrosis factor alpha," *Journal of Experimental Medicine*, vol. 179, no. 4, pp. 1109–1118, 1994.
- [33] N. Romani, D. Reider, M. Heuer et al., "Generation of mature dendritic cells from human blood an improved method with special regard to clinical applicability," *Journal of Immunological Methods*, vol. 196, no. 2, pp. 137–151, 1996.
- [34] S. Solano-Gálvez, S. Tovar-Torres, M. Tron-Gómez et al., "Human dendritic cells: ontogeny and their subsets in health and disease," *Medical Sciences*, vol. 6, no. 4, p. 88, 2018.

- [35] P. L. Moseley, "Heat shock proteins and the inflammatory response," *Annals of the New York Academy of Sciences*, vol. 856, pp. 206–213, 1998.
- [36] P. A. O'Neill, A. M. Shaaban, C. R. West et al., "Increased risk of malignant progression in benign proliferating breast lesions defined by expression of heat shock protein 27," *British Journal of Cancer*, vol. 90, no. 1, pp. 182–188, 2004.
- [37] S. H. Kang, K. W. Kang, K.-H. Kim et al., "Upregulated HSP27 in human breast cancer cells reduces Herceptin susceptibility by increasing Her2 protein stability," *BMC Cancer*, vol. 8, no. 1, article 286, 2008.
- [38] J. C. Heinrich, S. Donakonda, V. J. Haupt, P. Lennig, Y. Zhang, and M. Schroeder, "New HSP27 inhibitors efficiently suppress drug resistance development in cancer cells," *Oncotarget*, vol. 7, no. 42, pp. 68156–68169, 2016.
- [39] J. Constantino, C. Gomes, A. Falcão, B. M. Neves, and M. T. Cruz, "Dendritic cell-based immunotherapy: a basic review and recent advances," *Immunologic Research*, vol. 65, no. 4, pp. 798–810, 2017.
- [40] F. Le Naour, L. Hohenkirk, A. Grolleau et al., "Profiling changes in gene expression during differentiation and maturation of monocyte-derived dendritic cells using both oligonucleotide microarrays and proteomics," *Journal of Biological Chemistry*, vol. 276, no. 21, pp. 17920–17931, 2001.
- [41] A. K. De, K. M. Kodys, B. S. Yeh, and C. Miller-Graziano, "Exaggerated human monocyte IL-10 concomitant to minimal TNF- α induction by heat-shock protein 27 (Hsp27) suggests Hsp27 is primarily an antiinflammatory stimulus," *The Journal of Immunology*, vol. 165, no. 7, pp. 3951–3958, 2000.

Research Article

Relationship between *Helicobacter pylori* Infection and Plasmacytoid and Myeloid Dendritic Cells in Peripheral Blood and Gastric Mucosa of Children

Anna Helmin-Basa ¹, Małgorzata Wiese-Szadkowska ¹, Anna Szaflarska-Popławska ²,
Maciej Kłosowski ¹, Milena Januszewska ¹, Magdalena Bodnar ^{3,4},
Andrzej Marszałek ⁵, Lidia Gackowska¹ and Jacek Michalkiewicz ^{1,6}

¹Department of Immunology, Collegium Medicum Nicolaus Copernicus University, Bydgoszcz 85-094, Poland

²Department of Pediatric Endoscopy and Gastrointestinal Function Testing, Collegium Medicum Nicolaus Copernicus University, Bydgoszcz 85-094, Poland

³Department of Clinical Pathomorphology, Collegium Medicum Nicolaus Copernicus University, Bydgoszcz 85-094, Poland

⁴Department of Otolaryngology and Laryngological Oncology, Poznan University of Medical Science, Poznan 61-866, Poland

⁵Chair of Oncologic Pathology and Prophylaxis, Poznan University of Medical Sciences & Greater Poland Cancer Center, Poznan 61-866, Poland

⁶Department of Microbiology and Immunology, The Children's Memorial Health Institute, Warsaw 04-730, Poland

Correspondence should be addressed to Anna Helmin-Basa; a.helminbasa@gmail.com

Received 2 April 2019; Revised 29 August 2019; Accepted 24 September 2019; Published 11 November 2019

Guest Editor: Renata Sesti-Costa

Copyright © 2019 Anna Helmin-Basa et al. This is an open access article distributed under the Creative Commons Attribution License, which permits unrestricted use, distribution, and reproduction in any medium, provided the original work is properly cited.

Purpose. To investigate the frequency and activation status of peripheral plasmacytoid DCs (pDCs) and myeloid DCs (mDCs) as well as gastric mucosa DC subset distribution in *Helicobacter pylori*- (*H. pylori*-) infected and noninfected children. **Materials and Methods.** Thirty-six children were studied; twenty-one had *H. pylori*. The frequencies of circulating pDCs (lineage HLA-DR⁺CD123⁺) and mDCs (lineage HLA-DR⁺CD11c⁺) and their activation status (CD83, CD86, and HLA-DR expression) were assessed by flow cytometry. Additionally, the densities of CD11c⁺, CD123⁺, CD83⁺, CD86⁺, and LAMP3⁺ cells in the gastric mucosa were determined by immunohistochemistry. **Results.** The frequency of circulating CD83⁺ mDCs was higher in *H. pylori*-infected children than in the noninfected controls. The pDCs demonstrated upregulated HLA-DR surface expression, but no change in CD86 expression. Additionally, the densities of gastric lamina propria CD11c⁺ cells and epithelial pDCs were increased. There was a significant association between frequency of circulating CD83⁺ mDCs and gastric lamina propria mDC infiltration. **Conclusion.** This study shows that although *H. pylori*-infected children had an increased population of mature mDCs bearing CD83 in the peripheral blood, they lack mature CD83⁺ mDCs in the gastric mucosa, which may promote tolerance to local antigens rather than immunity. In addition, this may reduce excessive inflammatory activity as reported for children compared to adults.

1. Introduction

Helicobacter pylori (*H. pylori*) colonizes the human stomach. Infection usually starts in early childhood and can persist for decades, sometimes even for the lifetime [1]. *H. pylori*-infected children develop gastric mucosal inflammation [2] but with much lower infiltration of polymorphonuclear and

mononuclear cells and decreased incidence of gastric and duodenal ulceration, gastric adenocarcinoma, and gastric mucosa-associated lymphoid tissue (MALT) lymphoma as compared to adults [3, 4].

Dendritic cells (DCs) are professional antigen-presenting cells (APCs) that induce T cell response against a presented antigen. Their migration from the site of an antigen uptake

to the regional lymph nodes and their subsequent maturation profile decide about the type of the subsequent adaptive immune response profiles against infection (protective or nonprotective responses). The DC maturation process is associated with the expression of several membrane molecules engaged in the DC migration (CCR7), antigen presentation abilities (MHC class II), and their costimulatory activities (CD80, CD83, and CD86) [5, 6].

Human DCs are rare in peripheral blood [7] and consist of two major subsets, myeloid DCs (mDCs) and plasmacytoid DCs (pDCs) [8]. The mDCs express myeloid antigen such as CD11c and can be subdivided into CD1c- and CD141-bearing cells. pDCs lack these markers and instead express CD123, CD303, and CD304 molecules. Both mDC and pDC subsets display APC capacity, but this function is reduced in pDCs, which have relatively low expression of HLA-DR [9]. It is well documented that pDCs promote the generation of regulatory T cells (Tregs) [10].

The circulating DC number and their activation status may change during the course of infection [11, 12] and may alter throughout a lifetime [13]. These cells play an important role in shaping the anti-infection response by constantly completing the population of tissue-residing DCs.

The interaction of DCs with *H. pylori* *in vitro* induces DC maturation and release of proinflammatory cytokines, such as IL-6, IL-8, IL-12, and IL-23 [14–21]. However, the DC cytokine production profile and the T cell response more strongly depend on the *H. pylori* structure [22]. The DCs expressing CD11c⁺ [18, 23, 24], the semi-mature DCs bearing dendritic cell-lysosome-associated membrane glycoprotein (DC-LAMP, or LAMP3), and the DCs with high HLA-DR but little CD80, CD83, and CD86 expression [25, 26] were found in proximity to and in lymphoid follicles, together with FoxP3 T cells, in the *H. pylori*-infected gastric mucosa of adults [26].

In contrast to many studies concerning DC participation in *H. pylori*-induced immune response in adults [23, 24, 26–30], similar ones in children are still rare [31]. Additionally, estimation of the frequencies of mDCs and pDCs and the expression levels of CD83, CD86, and HLA-DR in the peripheral DC subsets have not yet been evaluated in the *H. pylori*-infected children. There is also a paucity of information regarding the expression profile of the human DC maturation markers (LAMP3 and CD83), the myeloid cell marker (CD11c), and the pDC marker (CD123) in the gastric mucosa of *H. pylori*-infected children. Therefore, the aim of this study was (a) to investigate the distribution and activation status of peripheral and gastric mucosa DC subsets (pDCs and mDCs) in the *H. pylori*-infected and noninfected children and (b) to evaluate correlations between the DC subset phenotype characteristics and the activity score on the basis of the updated Sydney gastritis classification system.

2. Materials and Methods

2.1. Ethics Statement. The study was undertaken according to Helsinki declaration with ethics committee approval of Collegium Medicum Nicolaus Copernicus University in

Bydgoszcz, Poland, and informed consent was obtained from all the patients' parents and from the patients older than 16 years prior to blood and antral biopsy collection.

2.2. Patients. In total, thirty-six subjects with dyspeptic symptoms, older than eleven years of age, were included in this study. The exclusion criteria involved the following: (1) a history of antibiotic use during 4 weeks for other reasons than *H. pylori* infection; (2) the presence of other inflammatory diseases, such as celiac disease, inflammatory bowel disease, or allergy; and (3) gastric perforation or hemorrhage, history of surgery, bleeding conditions, or evidence of other clinical conditions or intestinal parasites. Each subject or subject's parents provided the clinical history.

All the children were examined with gastroduodenal endoscopy due to permanent abdominal pain. Based on previous observation that *H. pylori*-associated gastritis of the corpus was present only when antral gastritis was present [32], three antral biopsies were taken from each patient. One biopsy specimen was subjected to a rapid urease test. The second specimen was used for histological analysis. The last specimen was subjected to immunohistochemical staining.

The urease test was performed for every patient. Furthermore, *H. pylori* infection was excluded in every subject by use of the ¹³C urea breath test, performed within one week of undergoing endoscopy. ¹³C concentration was measured with an infrared radiation analyzer (OLYMPUS Fanci2, Tokyo, Japan), assuming 4‰ as the cutoff point.

A patient was considered *H. pylori*-infected when the ¹³C urea breath test and either the rapid urease test or microscopic evaluation were positive for *H. pylori*. A patient was considered noninfected when all three tests were negative. Twenty-one patients were found to be *H. pylori* positive, while fifteen patients satisfied the criteria for a negative *H. pylori* status. None of the patients had ulcer disease or macroscopic lesions of the duodenal mucosa upon endoscopic examination.

The study was conducted in the *H. pylori*-infected and noninfected children and adolescents. The group of noninfected children (controls) consisted of 7 boys and 8 girls (median age 15 years, range 11–18 years). The group of *H. pylori*-infected children comprised 9 boys and 12 girls with recognized gastritis and *H. pylori* infection (median age 15 years, range 12–18 years). None of the patients had a history of other inflammatory diseases or cancer.

2.3. Histological Assessment. The specimen was formalin-fixed and embedded in paraffin, sectioned and stained with hematoxylin and eosin for histological analysis, or Giemsa modified by Gray stain for *H. pylori* detection. Biopsy specimens were graded for gastritis by two independent pathologists based on the updated Sydney system.

Histological variables (presence and density of mononuclear and polymorphonuclear cells, glandular mucosa atrophy, intestinal metaplasia, and *H. pylori*) were scored on a four-point scale: 0, none; 1, mild; 2, moderate; and 3, marked.

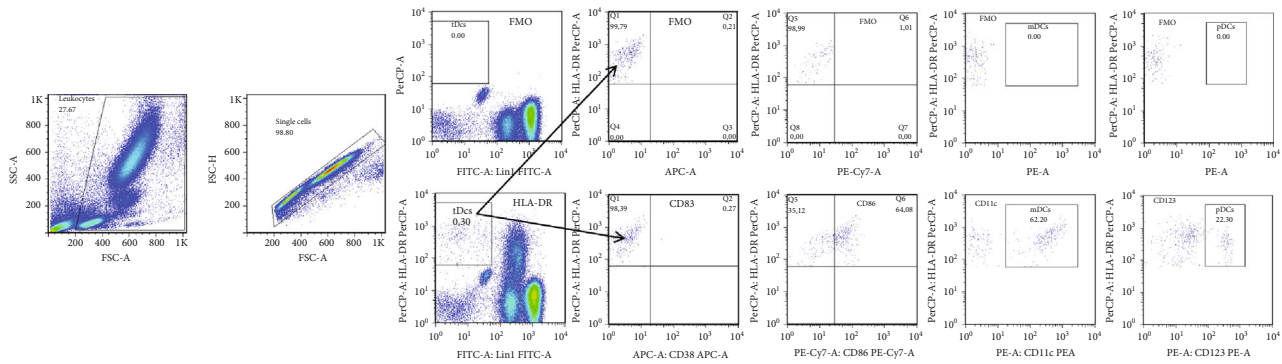


FIGURE 1: Fluorescence minus one controls for the quantification of dendritic cell subsets. Fluorescence minus one (FMO) controls were prepared without adding a particular fluorochrome-conjugated antibody, for instance fluorescence minus fluorescein (FITC), fluorescence minus allophycocyanin (APC), fluorescence minus tandem conjugate of phycoerythrin (PE), and the *cyanine* dye Cy7 (PE-Cy7), and fluorescence minus PE, respectively. The gating for each channel was defined to exclude nearly all backgrounds from the FMO controls on the 2D plots of HLA-DR versus individual fluorescence.

2.4. Flow Cytometry Analyses. During endoscopy, 5 mL of venous blood was taken for immunological testing. The frequencies of total DCs (tDCs), mDCs and pDCs, as well as the expression of CD83, CD86, and HLA-DR were determined in whole blood samples with the use of a five-color flow cytometry method. We followed the methods of Helmin-Basa et al. [33]. First, two tubes containing 200 μ L whole blood were stained with FITC Lin-1 lineage cocktail (antibodies against human CD3, CD14, CD16, CD19, CD20, and CD56), PerCP-anti-human HLA-DR, APC-anti-human CD83, PE-Cy7-anti-human CD86, PE-anti-human CD11c, or PE-anti-human CD123 (BD Biosciences, Franklin Lakes, New Jersey, USA) antibodies for 30 min at room temperature (RT). The erythrocytes were removed with the use of BD Bioscience FACS Lysing Solution (BD Biosciences). The stained leukocytes were suspended in phosphate-buffered saline (PBS) and analyzed immediately with flow cytometry (FACSCanto II, BD Biosciences). The instrument was set up using a BD Cytometer Setup and Tracking beads. Data acquisition was performed using BD FACSDiva software, version 6.1.3 (BD Biosciences) and the analysis with FlowJo 7.5.5 (Tree Star Inc., Ashland, Oregon, USA). Compensation settings were performed with a set of compensation tubes using the BD CompBead antibody-capturing particles and the compensation setup tool with BD FACSDiva software.

Fluorescence minus one (FMO) was used for gating (Figure 1). The gating strategy applied for the DC subset enumeration in two separate tubes is shown in Figure 2. Doublets and aggregates were avoided by selecting singlet cells on a forward scatter: FSC (area)/FSC (height) plot. Logical gating was used to identify tDC, mDC, and pDC populations. tDCs were defined as Lin⁻HLA-DR⁺, mDCs were defined as Lin⁻HLA-DR⁺CD11c⁺ cells, while pDCs were defined as Lin⁻HLA-DR⁺CD123⁺ cells. The geometric mean fluorescence intensity (gMFI) was determined to quantify cell surface expression of activation molecules. Statistical analyses were based on at least 5000 events gated on the mDCs and 2500 events gated on the pDCs.

2.5. Immunohistochemistry. The immunohistochemical studies were performed on archived formalin-fixed paraffin-embedded (FFPE) tissue sections delivered to the Department of Clinical Pathomorphology Collegium Medicum in Bydgoszcz, Nicolaus Copernicus University in Torun.

FFPE tissue sections were cut on a manual rotary microtome (AccuCut, Sakura, Torrance, USA). Paraffin sections (4 μ m) were prepared and mounted onto extra adhesive slides (SuperFrost Plus, Menzel Glasser, Braunschweig, Germany).

The immunohistochemical staining was performed according to previously described procedures [34, 35] and standardized using a series of positive and negative control reactions. The positive control reaction was performed on a model tissue selected according to reference sources (The Human Protein Atlas, <http://www.proteinatlas.org>) [36] and the antibody datasheets. The negative control reactions were performed on additional tissue sections, by substituting the primary antibody with a solution of 1% bovine serum albumin (BSA) diluted in PBS.

Deparaffinization, rehydration, and antigen retrieval were performed by heating sections in Epitope Retrieval Solution high-pH at 95–98°C for 20 min (Dako, Agilent Technologies, Santa Clara, USA) in PT-Link (Dako, Agilent Technologies). Subsequently, endogenous peroxidase activity was blocked with the use of a 3% H₂O₂ solution for 15 min at RT and the nonspecific binding was blocked using 5% solution of BSA for 15 min at RT. Incubation with the primary antibodies, anti-LAMP3 (1:400 dilution, rabbit polyclonal), anti-CD11c (1:1000 dilution, rabbit monoclonal), anti-CD123 (IL-3RA, 1:200 dilution, rabbit polyclonal), anti-CD83 (1:100 dilution, mouse monoclonal), and anti-CD86 (1:50 dilution, rabbit monoclonal) (all from Abcam, Cambridge, England), at 4°C for 16 hours was performed. The antibody complex was detected using EnVision Flex Anti-Mouse/Rabbit HRP-Labeled Polymer (Dako, Agilent Technologies) and localized using 3-3'-diaminobenzidine (DAB) as the chromogen. Finally, tissue sections were counterstained in hematoxylin, subsequently dehydrated, and cleared in a series of

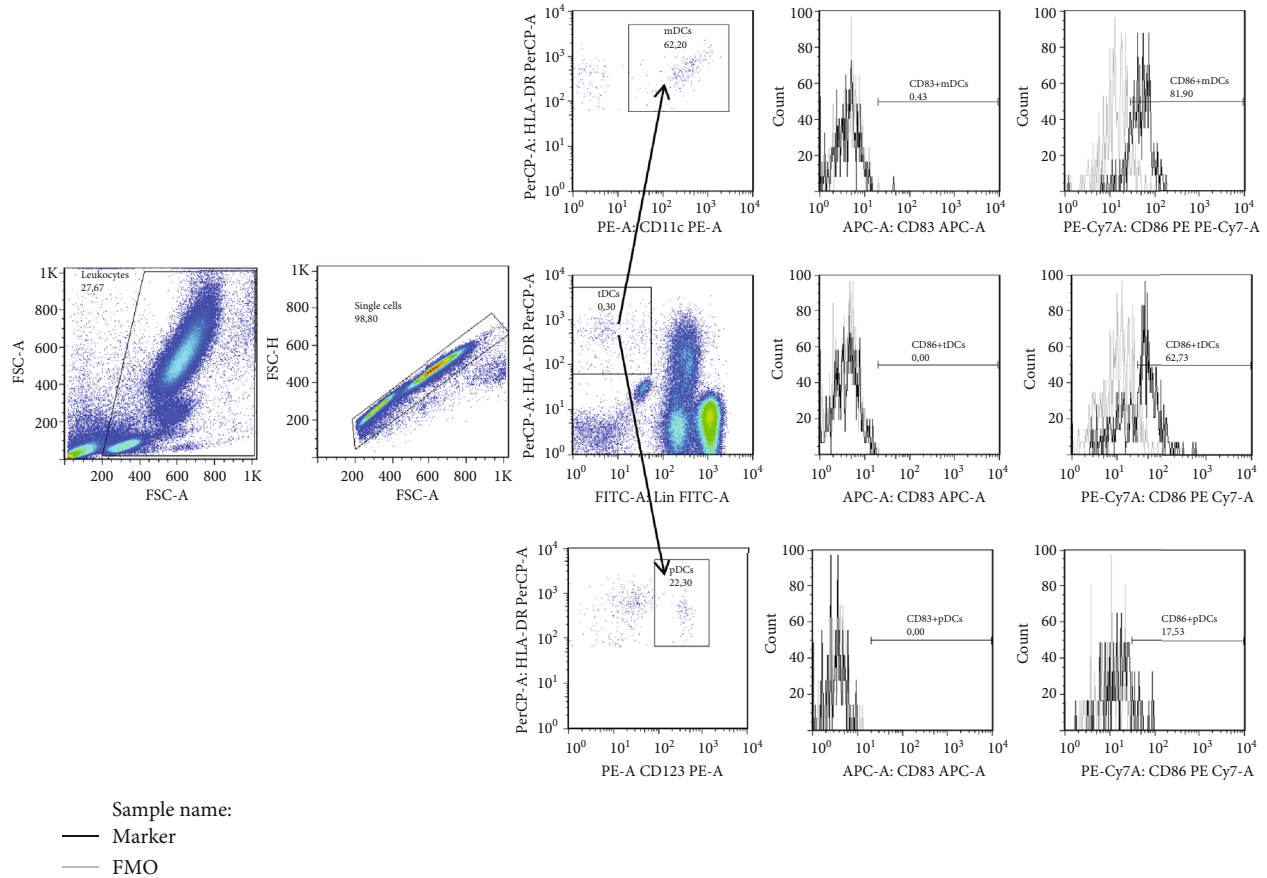


FIGURE 2: Gating strategy for multicolor flow cytometric detection of total dendritic cells and their subsets. At first, leukocytes were gated by forward scatter characteristic (FSC) versus side scatter characteristics (SSC). Next, doublets and aggregates were avoided by selecting singlet cells on a forward scatter: FSC (area)/FSC (height) plot. Then total dendritic cells (tDCs) were gated for fluorescence intensity of HLA-DR peridinin-chlorophyll proteins (PerCP) versus lineage-1 fluorescein (FITC), and using the fluorescence intensity of CD11c phycoerythrin (PE) or CD123 PE, myeloid dendritic cells (mDCs) or plasmacytoid dendritic cells (pDCs) were gated (open histograms). Then in tDCs and their subsets, a percentage of CD83⁺ and CD86⁺ cells was gated (open histograms). The grey line represents the staining profile for fluorescence minus one (FMO) control.

xylene washes, and a cover slip was applied using mounting medium (Dako, Agilent Technologies).

2.5.1. Evaluation of Protein Expression Based on Immunohistochemical Staining. The evaluation of protein expression in the antrum area of obtained FFPE tissue sections was performed at 20x and 40x original objective magnifications, using the ECLIPSE E400 (Nikon Instruments Europe, Amsterdam, Netherlands) light microscope.

For the evaluation of expression, immunohistochemical reactions were scored according to morphometric principles based on a Remmele–Stegner scale (IRS-Index Remmele–Stegner; immunoreactive score) [37], used in our previous publications [34, 38].

The total immunoreactivity score was defined according to the scale obtained from the grade of intensity multiplied by the score of positively stained cells to give a total score from 0 to 12. The intensity of staining was scored as follows: 0, negative; 1, low staining; 2, moderate staining; and 3, strong staining. The number of positive cells was categorized

as follows: (1) in the gastric lamina propria: 0—negative, 1—1 to 5 positive cells, 2—6 to 10 positive cells, 3—11 to 50 positive cells, and 4—51 to 100 positive cells, and (2) in epithelium mucosa: 0—negative, 1—1 to 20 positive cells, 2—21 to 50 positive cells, 3—51 to 80 positive cells, and 4—81 to 100 positive cells.

2.6. Statistical Analyses. All data are expressed as medians with the first and third quartiles. The results were compared using Mann-Whitney *U* test calculated by the STATISTICA 12 software (StatSoft). For normal distribution, variables were analyzed using the Kolmogorov–Smirnov test with Lilliefors correction. The age and gastric inflammation scores were correlated with the frequency of DC and their subsets using the Spearman’s rank correlation. Statistical significance was considered at $p < 0.05$.

3. Results

3.1. Gastric Mucosa Histology. The intensity and activity of antral gastritis were greater in the *H. pylori*-infected children

TABLE 1: Gastric mucosa histology of *H. pylori*-infected and noninfected children (median score (range) according to the updated Sydney system: 0, none; 1, mild; 2, moderate; 3, marked).

	MN cells (intensity)	Antral mucosa			<i>H. pylori</i> [^]
		PMN cells (activity)	Atrophy	Intestinal metaplasia	
Hp+ children	2 (1-3)	1 (0-2)	0 (0-1)	0 (0-0)	1 (1-3)
Hp- children	1 (0-2)	0 (0-1)	0 (0-0)	0 (0-0)	0 (0-0)
<i>p</i>	<0.001*	0.003*	0.703	0.751	<0.001*

Abbreviations: MN: mononuclear cells; PMN: polymorphonuclear cells. Hp+ children: *H. pylori*-infected children; Hp- children: noninfected children. [^]Modified Giemsa staining method. *Statistically significant differences (Mann-Whitney *U* test).

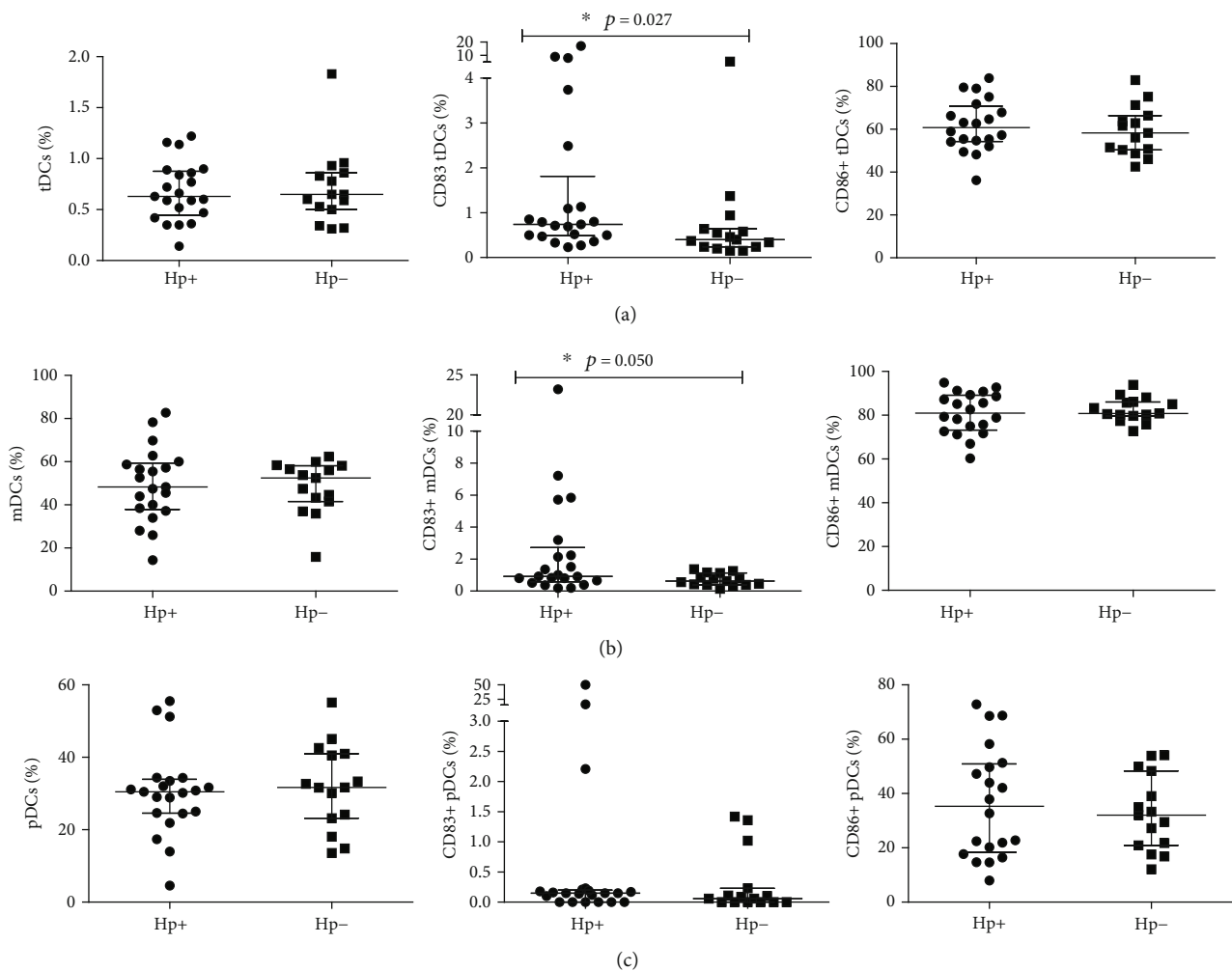


FIGURE 3: Comparison of the distribution of circulating total myeloid and plasmacytoid dendritic cells in *H. pylori*-infected and noninfected children with using individual raw data points. Scatter plots are showing differential percentages of total dendritic cells (tDCs), CD83⁺ tDCs and CD86⁺ tDCs (a), myeloid dendritic cells (mDCs), CD83⁺ mDCs and CD86⁺ mDCs (b), and plasmacytoid dendritic cells (pDCs), CD83⁺ pDCs and CD86⁺ pDCs (c), in *H. pylori*-infected children (Hp+: *n* = 21) compared to noninfected children (Hp-: *n* = 15). Data shown as individual raw data points, medians (horizontal line), and interquartile ranges (upper and lower whiskers). *Statistically significant differences (Mann-Whitney *U* test).

($p < 0.001$ and $p = 0.003$, respectively) when compared to the *H. pylori* noninfected ones (Table 1). Interestingly, three children with *H. pylori* infection had mild gastric mucosal atrophy in the antrum. However, no intestinal metaplasia was seen in the children's gastric mucosa.

3.2. The Distribution of Circulating tDCs, mDCs, and pDCs and Their Activation Status in *H. pylori*-Infected and Noninfected Children. The percentages of tDCs, mDCs, and pDCs were similar between the two groups (Figures 3(a)–3(c)). While the percentages of CD83 expressing tDCs and

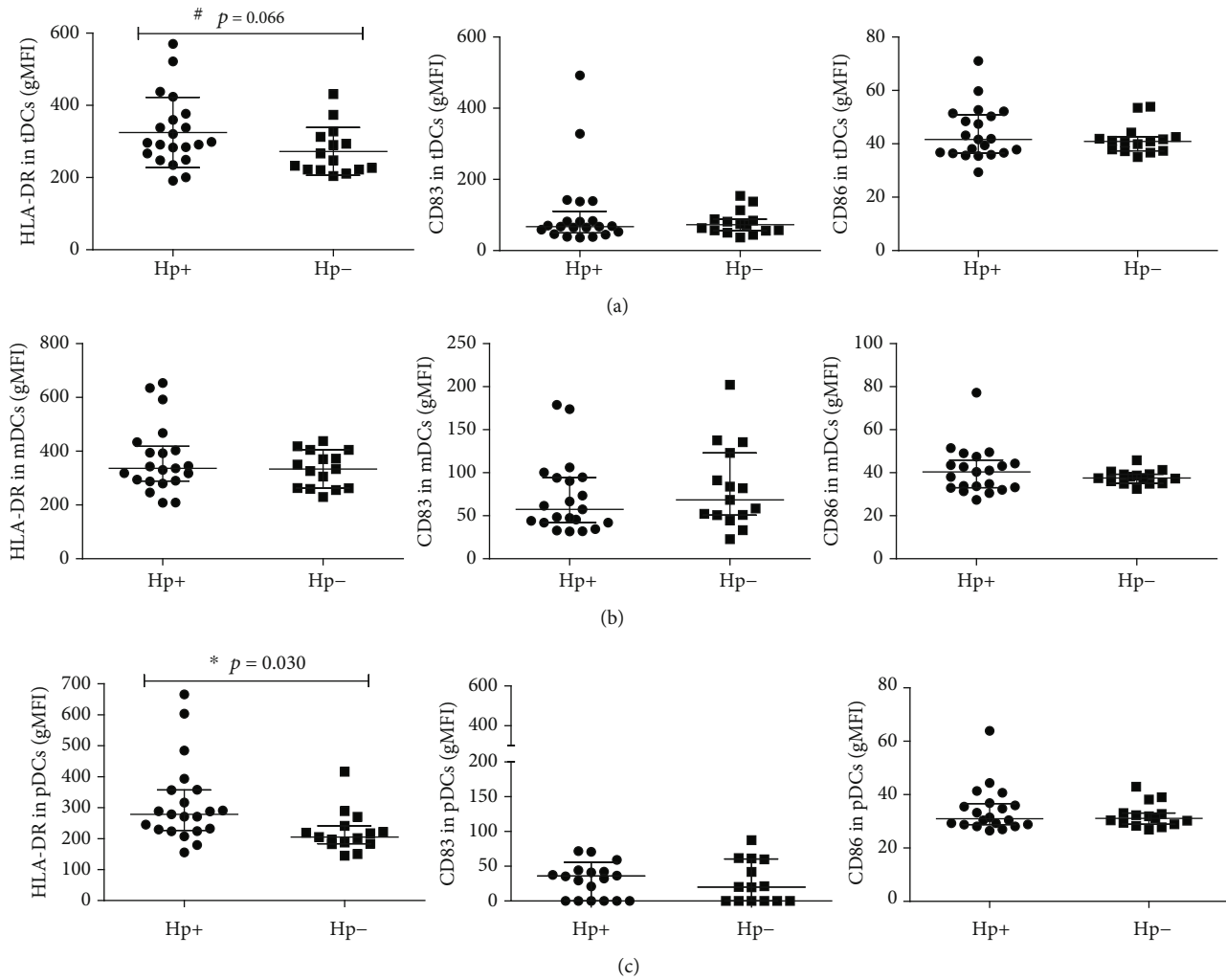


FIGURE 4: Comparison of activation status of total myeloid and plasmacytoid dendritic cells in *H. pylori*-infected and noninfected children with using individual raw data points. Scatter plots are showing differential densities (gMFI (geometric mean fluorescence)) of HLA-DR, CD83, and CD86 markers on the surface of total dendritic cells (tDCs) (a), myeloid dendritic cells (mDCs) (b) and plasmacytoid dendritic cells (pDCs) (c) in *H. pylori*-infected children (Hp+: $n = 21$) compared to noninfected children (Hp-: $n = 15$). Data shown as individual raw data points, medians (horizontal line), and interquartile ranges (upper and lower whiskers). *Statistically significant differences (Mann-Whitney U test).

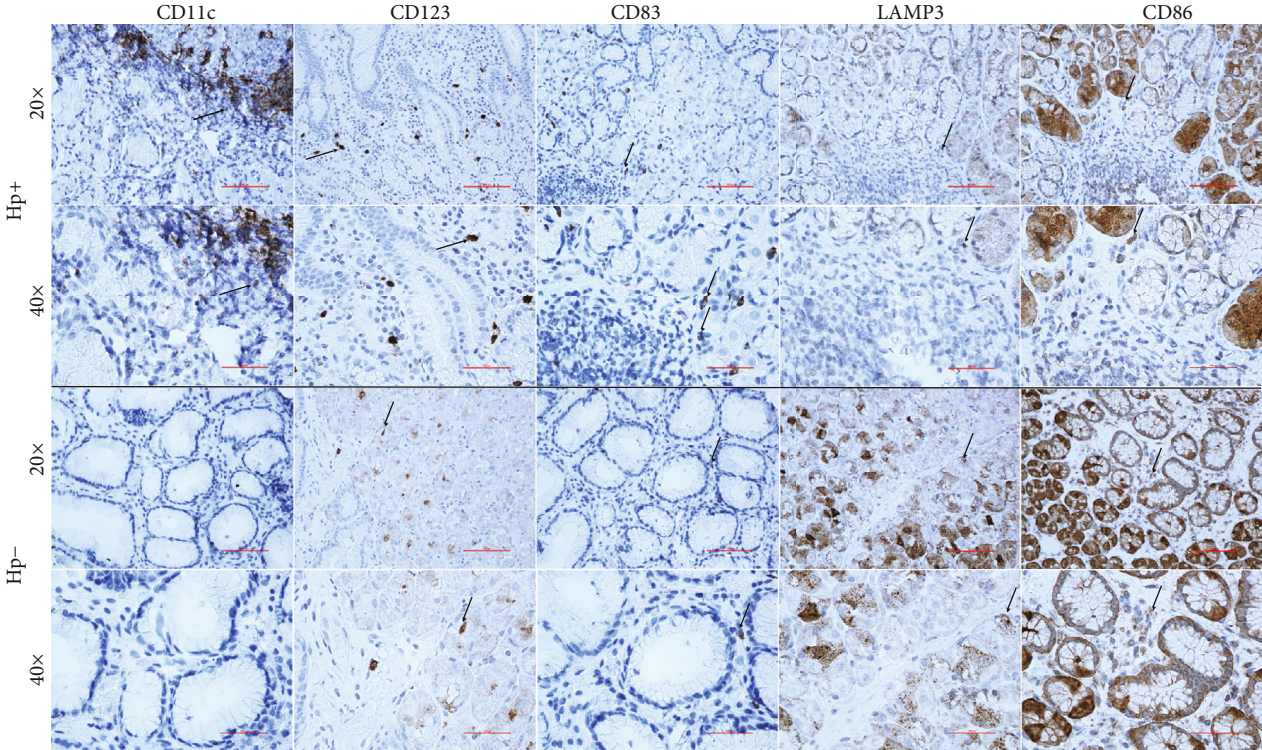
mDCs were markedly higher in *H. pylori*-infected children (0.74% versus 0.40%, $p = 0.027$ and 0.92% versus 0.62%, $p = 0.050$), there was no significant difference in the percentage of CD83-positive pDCs between these two groups. The percentages of CD86 expressing tDCs, mDCs and pDCs were similar between *H. pylori*-infected and noninfected children (Figures 3(a)–3(c)) ($p > 0.05$).

Increased densities of HLA-DR on the surface of tDCs and pDCs were noted in *H. pylori*-infected children compared with noninfected controls (296.10 versus 247.51, $p = 0.066$ and 278.28 versus 204.89, $p = 0.030$, respectively) (Figures 4(a) and 4(c)). There were no statistically significant differences in CD83 and CD86 expression between the two groups ($p > 0.05$) (Figures 4(a)–4(c)).

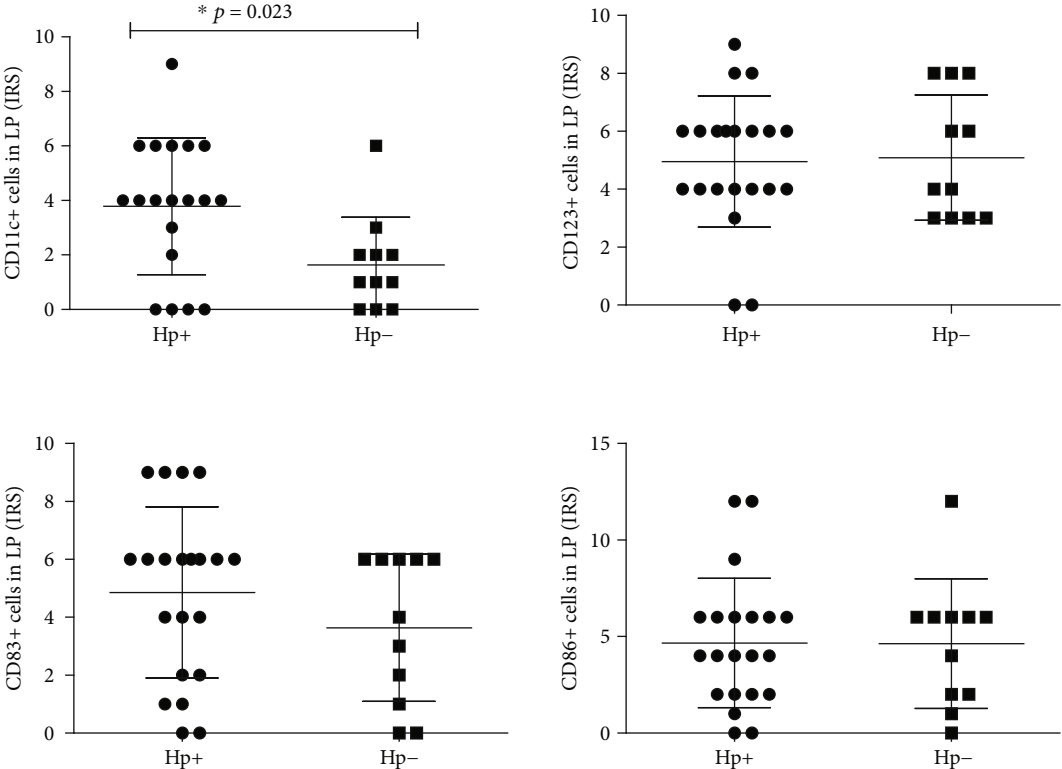
3.3. The Densities of $CD11c^+$, $CD123^+$, $CD83^+$, $CD86^+$, and $LAMP3^+$ Cells in the Gastric Mucosa of *H. pylori*-Infected and Noninfected Children. To determine the effect of *H.*

pylori infection on the local immune system, the gastric mucosa sections were labeled with the following antibodies: anti-CD11c (high expression on mDCs, but low on granulocytes, macrophages, and a subset of B cells), CD123 (a marker of pDCs), CD83 and LAMP3 (markers of mature DCs), and CD86 (costimulatory molecule upregulated on activated DCs and other APCs).

A statistically significant increase in the accumulation of CD11c-positive cells was noted in the gastric lamina propria mucosa of *H. pylori*-infected children ($p = 0.023$) (Figures 5(a) and 5(b)). There was no significant difference between $CD83^+$, $CD86^+$, and $CD123^+$ cells in *H. pylori*-infected and noninfected children ($p > 0.05$). However, the data display a tendency toward an increased density of $CD123^+$ DCs in the gastric epithelium mucosa of *H. pylori*-infected children (Figures 5(a)–5(c)) ($p > 0.05$). Moreover, we used immunohistochemistry to detect $LAMP3^+$ cells in an antrum. We observed these cells but



(a)



(b)

FIGURE 5: Continued.

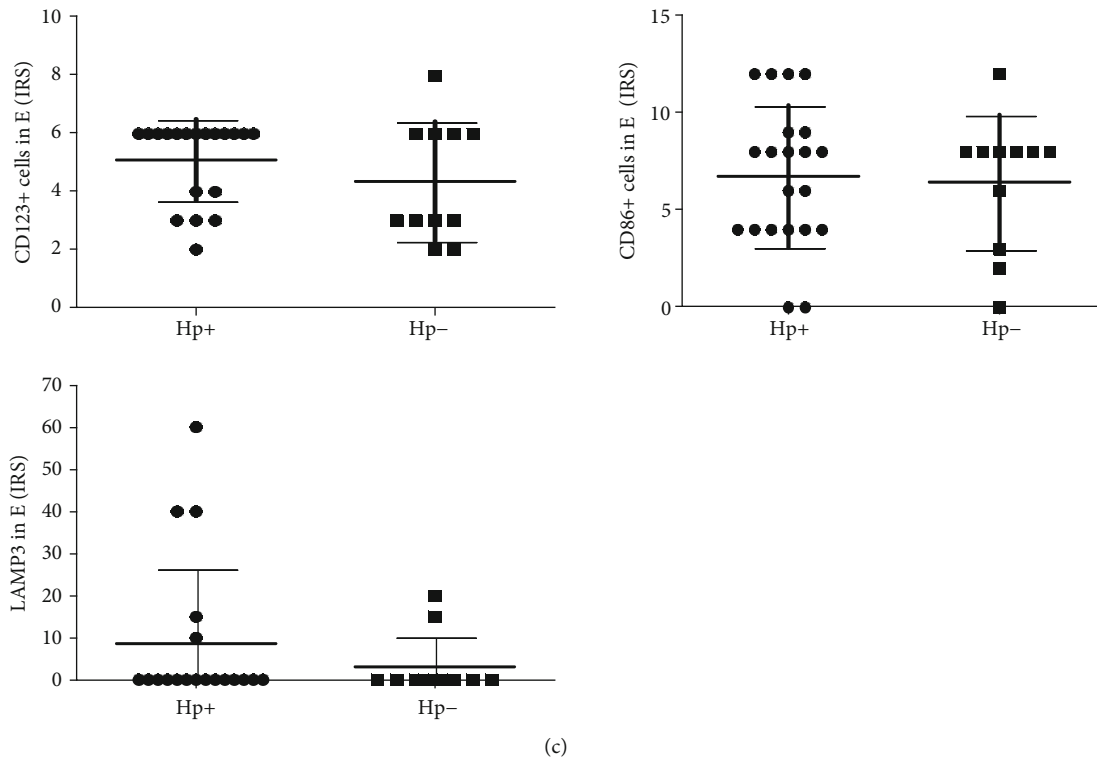


FIGURE 5: Infiltration of dendritic cells into the gastric mucosa in *H. pylori*-infected and noninfected children. Representative images of CD11c, CD123, CD83, LAMP3, and CD86 staining in the lamina propria and epithelium in antral gastric mucosa biopsies from *H. pylori*-infected (Hp+) and noninfected (Hp-) children. Specific staining appears in brown, and the cell nuclei are counterstained with hematoxylin in blue. The arrows indicate positive staining. Visualization was performed by immunohistochemistry. Primary objectives, 20x and 40x (a). Scatter plots are showing differential densities (IRS (immunoreactive score)) of CD11c⁺, CD123⁺, CD83⁺, and CD86⁺ cells in gastric lamina propria mucosa (b) and CD123⁺, CD86⁺, and LAMP3⁺ cells in gastric epithelium (c) in *H. pylori*-infected children (Hp+: $n = 21$) compared to noninfected children (Hp-: $n = 11$). Data shown as individual raw data points, medians (horizontal line), and interquartile ranges (upper and lower whiskers). *Statistically significant differences (Mann-Whitney U test).

only in mucosal epithelium of six children with *H. pylori* infection and 2 noninfected children (Figures 5(a) and 5(c)).

3.4. Correlation Analysis. To evaluate whether *H. pylori*-associated gastritis influences DC frequency or whether these values depend more on age, we correlated age, gastric inflammation, and *H. pylori* density scores with the circulating and gastric DC frequencies.

There was a weak inverse association between age and tDC frequency ($r = -0.32$, $p = 0.05$), but no effect of age on frequencies of mDC ($r = 0.01$, $p > 0.05$) and pDC ($r = 0.08$, $p > 0.05$) subsets was observed (Figure 6(a)). However, we did not observe any correlation between age and density of gastric DCs ($p > 0.05$).

There was no significant association between frequencies of circulating tDCs, their subsets (mDCs and pDCs), gastritis intensity (mononuclear cell infiltrate), its activity (polymorphonuclear cell infiltrate), and *H. pylori* density ($p > 0.05$). Additionally, no correlation was noted between gastric DCs frequencies, gastric inflammation scores, and *H. pylori* density ($p > 0.05$).

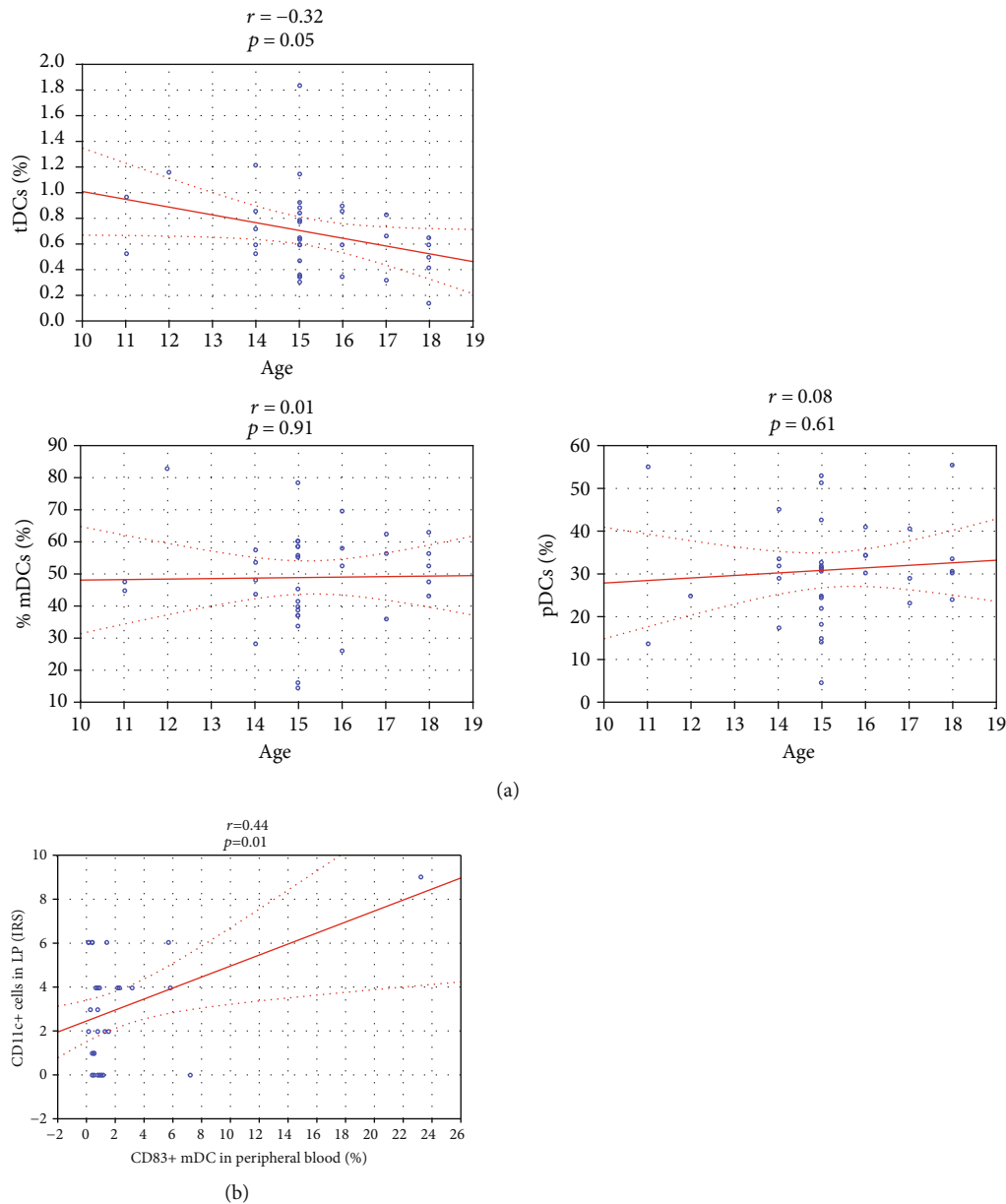
There was only a moderate positive correlation between frequency of circulating CD83⁺ mDCs and density of gastric lamina propria CD11c⁺ cells ($r = 0.44$ and $p = 0.01$, respectively) (Figure 6(b)).

4. Discussion

We described here peripheral DC subset distribution (mDCs and pDCs) and their maturation status (expression of CD83, CD86, and HLA-DR) in the *H. pylori*-infected and noninfected children. Additionally, the densities of CD11c⁺ (mDCs), CD123⁺ (pDCs), CD83⁺ or LAMP3⁺ (mature DCs), and CD86⁺ (activated) cells in the gastric mucosa were determined by immunohistochemistry. Similar to the other studies on *H. pylori* infection, our control group consisted of dyspeptic, noninfected patients [39, 40], because gastroendoscopy is not considered an ethical procedure in the noncomplaining subjects.

H. pylori-infected children exhibited (1) an increased percentage of circulating CD83⁺ mDCs, but with normal expression of CD86 and HLA-DR, (2) upregulation of HLA-DR expression but unchanged expression of CD83 and CD86 on pDCs subset, (3) increased densities of CD11c⁺ cells in the lamina propria and CD123⁺ cells in the epithelium, and (4) a significant association between frequency of circulating CD83⁺ mDCs and lamina propria infiltrating CD11c⁺ DCs.

The gastric mucosa, which does not initially have organized and diffuse lymphoid tissue, acquires MALT-like structures with follicles and germinal centers following contact



(a)

(b)

FIGURE 6: The relationship between the age and frequencies of dendritic cells and their subsets in *H. pylori*-infected and noninfected children. The relationships between the age and the frequencies of circulating total dendritic cells (tDCs), myeloid dendritic cells (mDCs), and plasmacytoid dendritic cells (pDCs) in *H. pylori*-infected and noninfected children were correlated by Spearman's correlation test ($p < 0.05$) (a). The relationship between the frequency of CD83⁺ myeloid dendritic cells (CD83⁺ mDCs) in peripheral blood and the density of CD11c⁺ dendritic cells (CD11c⁺ cells) in lamina propria (LP) in *H. pylori*-infected and noninfected children was correlated by Spearman's correlation test ($p < 0.05$) (b). IRS: immunoreactive score.

with *H. pylori* [41]. *H. pylori* infection in children is associated with a higher accumulation of lymphoid follicles containing CD4⁺ T cells, B cells, and DCs [42] in the lamina propria of the gastric mucosa, identified by macroscopically evident nodularity.

H. pylori bacteria attach to the gastric epithelium and contact the gastric epithelium and subepithelial lamina propria DCs (direct or indirect), which rapidly increase in the *H. pylori*-infected mucosa compared with an uninfected mucosa [18, 23, 24]. DCs loaded with *H. pylori* likely migrate to gastric lymphoid follicles or draining paragastric lymph

nodes to present *H. pylori* antigens to naive CD4⁺ T cells [43, 44], thus initiating and regulating the host *H. pylori*-specific immune response.

Three subsets of circulating DCs exist: the CD123⁺ pDCs and the two types of CD11c⁺ mDCs: CD11c⁺ mDCs with CD11c^{low} and CD141⁺ mDCs with CD11c^{high} [8]. Since DCs are rare in human peripheral blood [7], we focused on (a) the enumeration of the two major DC subsets (CD11c⁺ mDCs and CD123⁺ pDCs) and (b) the estimation of the correlation between these DC phenotypes, *H. pylori*-induced inflammation and *H. pylori* density scores, according to the

updated Sydney system of gastritis classification. Additionally, we used immunohistochemistry to assess DC subset distribution in antral biopsy specimens.

The distribution of circulating DC subsets in *H. pylori*-infected patients has not yet been previously evaluated, and to our knowledge, this is the first study to demonstrate an increased percentage of CD83⁺ mDCs, but with no significant differences in surface expression of activation markers (CD86 and HLA-DR). Terminally differentiated DCs should induce CD83-specific maturation markers and increase the expression of CD86 costimulatory molecule and HLA-DR. Thus, an increase in the frequency of CD83-expressing mDCs along with the absence of upregulation of CD86 and HLA-DR molecules on mDCs might suggest that the maturation status of circulating mDCs in *H. pylori*-infected children was changed but only within the small part of mDCs. However, the rest of circulating mDCs still expressed immature/tolerogenic phenotype (HLA-DR^{low}CD86^{low}).

The peripheral blood is not the best source for the studying of DC maturation status in the course of *H. pylori* infection; hence, we studied also the gastric epithelial and lamina propria DC subset distribution and its maturation markers.

We observed high levels of CD11c-positive cells and a tendency toward increased density of CD83-positive cells in the gastric lamina propria of *H. pylori*-infected children. CD11c is a marker for DCs of myeloid origin (mDCs) which are potent APCs and can activate T cells. CD83 is a more selective marker, present on mature DCs. Hence, we used CD11c and CD83 antigens for detecting mDCs and mature DCs in a gastric mucosa.

CD11c⁺ mDCs could be recruited from the blood in response to *H. pylori* infection, but we could not observe any association between frequency of circulating mDCs and gastric mucosa mDC density. However, we noted association between frequency of circulating mature CD83-bearing mDCs and gastric mDC density. The accumulation of mDCs in the gastric lamina propria of *H. pylori*-infected patients is necessary for mounting adaptive immune response needed for efficient bacterial clearance. The increased number of mDCs but not CD83-positive DCs in the *H. pylori*-infected gastric lamina propria mucosa could indicate that *H. pylori* infection in children may be associated with local accumulation of immature mDCs (lack of CD83-expressing DCs). The presence of these cells might initiate low protective immune response to *H. pylori*.

We had too small biopsy sections to evaluate other activation marker expressions (HLA-DR and CD80). Instead, we studied the expression of more specific DC maturation markers like LAMP3. We could not detect LAMP3⁺ cells in the gastric lamina propria by immunohistochemistry. However, in six *H. pylori*-infected children, we observed these cells in mucosal epithelium. This marker is absent on immature DCs but rapidly increase upon DCs activation [45], so our results might suggest that some *H. pylori*-infected children have small numbers of activated DCs in gastric epithelium. In *H. pylori*-infected adults, DC-LAMP⁺ cells were also observed but they were located only in the gastric lamina propria [26].

Immature human DCs constitutively express intermediate amounts of CD86 and lack of CD80, CD83, and DC-LAMP [45]. CD80 is exclusively induced on mature DCs while CD86 is already present on immature cells and further upregulated upon stimulation [46]. Terminally differentiated DCs induce specific maturation markers including CD83 and DC-LAMP. Recent studies in adults also showed an increased population of HLA-DR-positive [23], DC-SIGN-positive [26], or DC-LAMP-positive DCs with a semimature phenotype (CD83⁺, CD80⁺CD86^{low}) [23, 26] in lymphoid follicles of the gastric lamina propria in the *H. pylori*-infected human gastric mucosa, and these cells were in the same location as follicular FoxP3⁺ Tregs [26]. The presence of CD11c-bearing mDCs but not mature DCs expressing CD83 or LAMP3 molecules in gastric lamina propria in pediatric may promote tolerance to local antigens rather than immunity. The presence of immature DCs and other immature APCs could increase *H. pylori* density in the gastric mucosa. On the other hand, it can also be beneficial, as it may reduce excessive inflammatory activities responsible for gastric ulcers and pre-malignant gastric lesions in some individuals. The absence of mature DCs in a pediatric gastric mucosa might also explain the lower local proinflammatory responses to *H. pylori* infection in children than in adults [47].

Our study also demonstrated a tendency to increase the density of CD123- (marker of pDCs) positive cells in gastric epithelium as compared to normal controls. This pDC subset may mount both protective and tolerogenic immune responses [48] and can induce Treg differentiation [49]. A previous study in adults showed that gastric CD303-expressing DC (other marker of pDCs) cells were present in a very low number in both *H. pylori*-infected and uninfected individuals however with no significant difference between the groups. Thus, the presence of pDCs in the site of *H. pylori* infection (gastric epithelium) may initiate low protective immune response to *H. pylori* often observed.

5. Conclusion

This study shows that although *H. pylori*-infected children had an increased population of mature mDCs bearing CD83 in the peripheral blood, they lack mature CD83⁺ mDCs in the gastric mucosa, which may promote tolerance to local antigens rather than immunity. In addition, this may reduce excessive inflammatory activity as reported for children compared to adults.

Data Availability

The all data used to support the findings of this study are included within the article.

Disclosure

No company had any input or influence into the design, analyses, interpretation, or content of this manuscript.

Conflicts of Interest

There are no conflicts of interest for any author.

References

- [1] N. R. Salama, M. L. Hartung, and A. Muller, "Life in the human stomach: persistence strategies of the bacterial pathogen *Helicobacter pylori*," *Nature Reviews Microbiology*, vol. 11, no. 6, pp. 385–399, 2013.
- [2] B. D. Gold, L. J. van Doorn, J. Guarner et al., "Genotypic, clinical, and demographic characteristics of children infected with *Helicobacter pylori*," *Journal of Clinical Microbiology*, vol. 39, no. 4, pp. 1348–1352, 2001.
- [3] P. R. Harris, S. W. Wright, C. Serrano et al., "*Helicobacter pylori* Gastritis in Children Is Associated With a Regulatory T-Cell Response," *Gastroenterology*, vol. 134, no. 2, pp. 491–499, 2008.
- [4] C. Serrano, S. W. Wright, D. Bimczok et al., "Downregulated Th17 responses are associated with reduced gastritis in *Helicobacter pylori*-infected children," *Mucosal Immunology*, vol. 6, no. 5, pp. 950–959, 2013.
- [5] R. M. Steinman, "Decisions about dendritic cells: past, present, and future," *Annual Review of Immunology*, vol. 30, no. 1, pp. 1–22, 2012.
- [6] L. Bar-On and S. Jung, "Defining dendritic cells by conditional and constitutive cell ablation," *Immunological Reviews*, vol. 234, no. 1, pp. 76–89, 2010.
- [7] F. Geissmann, M. G. Manz, S. Jung, M. H. Sieweke, M. Merad, and K. Ley, "Development of monocytes, macrophages, and dendritic cells," *Science*, vol. 327, no. 5966, pp. 656–661, 2010.
- [8] L. Ziegler-Heitbrock, P. Ancuta, S. Crowe et al., "Nomenclature of monocytes and dendritic cells in blood," *Blood*, vol. 116, no. 16, pp. e74–e80, 2010.
- [9] M. Merad, P. Sathe, J. Helft, J. Miller, and A. Mortha, "The dendritic cell lineage: ontogeny and function of dendritic cells and their subsets in the steady state and the inflamed setting," *Annual Review of Immunology*, vol. 31, no. 1, pp. 563–604, 2013.
- [10] E. Martin-Gayo, E. Sierra-Filardi, A. L. Corbi, and M. L. Toribio, "Plasmacytoid dendritic cells resident in human thymus drive natural Treg cell development," *Blood*, vol. 115, no. 26, pp. 5366–5375, 2010.
- [11] R. S. Hotchkiss, K. W. Tinsley, P. E. Swanson et al., "Depletion of dendritic cells, but not macrophages, in patients with sepsis," *The Journal of Immunology*, vol. 168, no. 5, pp. 2493–2500, 2002.
- [12] M. Lichtner, R. Rossi, F. Mengoni et al., "Circulating dendritic cells and interferon- α production in patients with tuberculosis: correlation with clinical outcome and treatment response," *Clinical and Experimental Immunology*, vol. 143, no. 2, pp. 329–337, 2006.
- [13] G. Orsini, A. Legitimo, A. Failli, F. Massei, P. Biver, and R. Consolini, "Enumeration of human peripheral blood dendritic cells throughout the life," *International Immunology*, vol. 24, no. 6, pp. 347–356, 2012.
- [14] K. Kranzer, A. Eckhardt, M. Aigner et al., "Induction of maturation and cytokine release of human dendritic cells by *Helicobacter pylori*," *Infection and Immunity*, vol. 72, no. 8, pp. 4416–4423, 2004.
- [15] N. Hafsi, P. Voland, S. Schwendy et al., "Human dendritic cells respond to *Helicobacter pylori*, promoting NK cell and Th1-effector responses in vitro," *The Journal of Immunology*, vol. 173, no. 2, pp. 1249–1257, 2004.
- [16] D. G. Guiney, P. Hasegawa, and S. P. Cole, "*Helicobacter pylori* preferentially induces interleukin 12 (IL-12) rather than IL-6 or IL-10 in human dendritic cells," *Infection and Immunity*, vol. 71, no. 7, pp. 4163–4166, 2003.
- [17] M. Hansson, A. Lundgren, K. Elgbratt, M. Quiding-Jarbrink, A. M. Svennerholm, and E. L. Johansson, "Dendritic cells express CCR7 and migrate in response to CCL19 (MIP-3 β) after exposure to *Helicobacter pylori*," *Microbes and Infection*, vol. 8, no. 3, pp. 841–850, 2006.
- [18] W. Khamri, M. M. Walker, P. Clark et al., "*Helicobacter pylori* stimulates dendritic cells to induce interleukin-17 expression from CD4⁺ T lymphocytes," *Infection and Immunity*, vol. 78, no. 2, pp. 845–853, 2010.
- [19] S. Andres, H.-M. A. Schmidt, H. Mitchell, M. Rhen, M. Maeurer, and L. Engstrand, "*Helicobacter pylori* defines local immune response through interaction with dendritic cells," *FEMS Immunology and Medical Microbiology*, vol. 61, no. 2, pp. 168–178, 2011.
- [20] M. Fehlings, L. Drobbe, V. Moos et al., "Comparative analysis of the interaction of *Helicobacter pylori* with human dendritic cells, macrophages, and monocytes," *Infection and Immunity*, vol. 80, no. 8, pp. 2724–2734, 2012.
- [21] M. Wiese, A. Eljaszewicz, A. Helmin-Basa et al., "Lactic Acid Bacteria Strains Exert Immunostimulatory Effect on *H. pylori*-Induced Dendritic Cells," *Journal of Immunology Research*, vol. 2015, Article ID 106743, 10 pages, 2015.
- [22] A. Shimoyama, A. Saeki, N. Tanimura et al., "Chemical synthesis of *Helicobacter pylori* lipopolysaccharide partial structures and their selective proinflammatory responses," *Chemistry - A European Journal*, vol. 17, no. 51, pp. 14464–14474, 2011.
- [23] D. Bimczok, R. H. Clements, K. B. Waites et al., "Human primary gastric dendritic cells induce a Th1 response to *H. pylori*," *Mucosal Immunology*, vol. 3, no. 3, pp. 260–269, 2010.
- [24] V. Necchi, R. Manca, V. Ricci, and E. Solcia, "Evidence for transepithelial dendritic cells in human *H. pylori* active gastritis," *Helicobacter*, vol. 14, no. 3, pp. 208–222, 2009.
- [25] M. Oertli, M. Sundquist, I. Hitzler et al., "DC-derived IL-18 drives Treg differentiation, murine *Helicobacter pylori*-specific immune tolerance, and asthma protection," *The Journal of Clinical Investigation*, vol. 122, no. 3, pp. 1082–1096, 2012.
- [26] M. Hansson, M. Sundquist, S. Hering, B. S. Lundin, M. Hermansson, and M. Quiding-Jarbrink, "DC-LAMP⁺ dendritic cells are recruited to gastric lymphoid follicles in *Helicobacter pylori*-infected individuals," *Infection and Immunity*, vol. 81, no. 10, pp. 3684–3692, 2013.
- [27] A. Saito, A. Yokohama, Y. Osaki et al., "Circulating plasmacytoid dendritic cells in patients with primary and *Helicobacter pylori*-associated immune thrombocytopenia," *European Journal of Haematology*, vol. 88, no. 4, pp. 340–349, 2012.
- [28] M. Kido, J. Tanaka, N. Aoki et al., "*Helicobacter pylori* promotes the production of thymic stromal lymphopoietin by gastric epithelial cells and induces dendritic cell-mediated inflammatory Th2 responses," *Infection and Immunity*, vol. 78, no. 1, pp. 108–114, 2010.
- [29] Y. Yu, S. Zhu, P. Li, L. Min, and S. Zhang, "*Helicobacter pylori* infection and inflammatory bowel disease: a crosstalk between

- upper and lower digestive tract," *Cell Death & Disease*, vol. 9, no. 10, article 961, 2018.
- [30] H. B. Ning, Y. H. Wang, L. F. Zhang, and J. C. Li, "Relation between gastric dendritic cells and *H. pylori*-associated gastritis," *Xi Bao Yu Fen Zi Mian Yi Xue Za Zhi*, vol. 27, no. 8, pp. 899-900, 2011.
- [31] P. R. Harris, L. E. Smythies, P. D. Smith, and G. I. Perez-Perez, "Role of childhood infection in the sequelae of *H. pylori* disease," *Gut Microbes*, vol. 4, no. 6, pp. 426-438, 2013.
- [32] C. M. Pathak, D. K. Bhasin, R. Nada, A. Bhattacharya, and K. L. Khanduja, "Changes in gastric environment with test meals affect the performance of 14C-urea breath test," *Journal of Gastroenterology and Hepatology*, vol. 20, no. 8, pp. 1260-1265, 2005.
- [33] A. Helmin-Basa, M. Czerwionka-Szaflarska, G. Bala et al., "Expression of adhesion and activation molecules on circulating monocytes in children with *Helicobacter pylori* infection," *Helicobacter*, vol. 17, no. 3, pp. 181-186, 2012.
- [34] M. Bodnar, M. Luczak, K. Bednarek et al., "Proteomic profiling identifies the inorganic pyrophosphatase (PPA1) protein as a potential biomarker of metastasis in laryngeal squamous cell carcinoma," *Amino Acids*, vol. 48, no. 6, pp. 1469-1476, 2016.
- [35] M. Bodnar, P. Burduk, P. Antosik, M. Jarmuz-Szymczak, M. Wierzbicka, and A. Marszalek, "Assessment of BRAF V600E (VE1) protein expression and BRAF gene mutation status in codon 600 in benign and malignant salivary gland neoplasms," *Journal of Oral Pathology & Medicine*, vol. 46, no. 5, pp. 340-345, 2017.
- [36] M. Uhlen, P. Oksvold, L. Fagerberg et al., "Towards a knowledge-based Human Protein Atlas," *Nature Biotechnology*, vol. 28, no. 12, pp. 1248-1250, 2010.
- [37] W. Remmele and H. E. Stegner, "Recommendation for uniform definition of an immunoreactive score (IRS) for immunohistochemical estrogen receptor detection (ER-ICA) in breast cancer tissue," *Pathologie*, vol. 8, no. 3, pp. 138-140, 1987.
- [38] M. Bodnar, L. Szyberg, W. Kazmierczak, and A. Marszalek, "Tumor progression driven by pathways activating matrix metalloproteinases and their inhibitors," *Journal of Oral Pathology & Medicine*, vol. 44, no. 6, pp. 437-443, 2015.
- [39] T. F. Soares, G. A. Rocha, A. M. C. Rocha et al., "Phenotypic study of peripheral blood lymphocytes and humoral immune response in *Helicobacter pylori* infection according to age," *Scandinavian Journal of Immunology*, vol. 62, no. 1, pp. 63-70, 2005.
- [40] O. D. Suoglu, S. Gokce, A. T. Saglam, S. Sokucu, and G. Saner, "Association of *Helicobacter pylori* infection with gastroduodenal disease, epidemiologic factors and iron-deficiency anemia in Turkish children undergoing endoscopy, and impact on growth," *Pediatrics International*, vol. 49, no. 6, pp. 858-863, 2007.
- [41] C. Hauke, W. Grabner, M. Grosse, and M. Stolte, "Lymph follicle formation and development of intestinal metaplasia in antrum mucosa as a reaction to *Helicobacter pylori* infection," *Leber, Magen, Darm*, vol. 21, no. 4, pp. 156-160, 1991.
- [42] A. M. Terres and J. M. Pajares, "An increased number of follicles containing activated CD69+ helper T cells and proliferating CD71+ B cells are found in *H. pylori*-infected gastric mucosa," *The American Journal of Gastroenterology*, vol. 93, no. 4, pp. 579-583, 1998.
- [43] L.-A. H. Allen, "Modulating phagocyte Activation," *The Journal of Experimental Medicine*, vol. 191, no. 9, pp. 1451-1454, 2000.
- [44] S. Nagai, H. Mimuro, T. Yamada et al., "Role of Peyer's patches in the induction of *Helicobacter pylori*-induced gastritis," *Proceedings of the National Academy of Sciences*, vol. 104, no. 21, pp. 8971-8976, 2007.
- [45] B. de Saint-Vis, J. Vincent, S. Vandenabeele et al., "A novel lysosome-associated membrane glycoprotein, DC-LAMP, induced upon DC maturation, is transiently expressed in MHC class II compartment," *Immunity*, vol. 9, no. 3, pp. 325-336, 1998.
- [46] M. Hubo, B. Trinschek, F. Kryczanowsky, A. Tuettgenberg, K. Steinbrink, and H. Jonuleit, "Costimulatory molecules on immunogenic versus tolerogenic human dendritic cells," *Frontiers in Immunology*, vol. 4, p. 82, 2013.
- [47] F. Freire de Melo, G. A. Rocha, A. M. C. Rocha et al., "Th1 immune response to *H. pylori* infection varies according to the age of the patients and influences the gastric inflammatory patterns," *International Journal of Medical Microbiology*, vol. 304, no. 3-4, pp. 300-306, 2014.
- [48] M. Colonna, G. Trinchieri, and Y. J. Liu, "Plasmacytoid dendritic cells in immunity," *Nature Immunology*, vol. 5, no. 12, pp. 1219-1226, 2004.
- [49] H. Hadeiba, T. Sato, A. Habtezion, C. Oderup, J. Pan, and E. C. Butcher, "CCR9 expression defines tolerogenic plasmacytoid dendritic cells able to suppress acute graft-versus-host disease," *Nature Immunology*, vol. 9, no. 11, pp. 1253-1260, 2008.

Research Article

***Trypanosoma cruzi* Mexican Strains Differentially Modulate Surface Markers and Cytokine Production in Bone Marrow-Derived Dendritic Cells from C57BL/6 and BALB/c Mice**

Cecilia Gomes Barbosa,¹ Tamires Marielem Carvalho Costa,² Chamberttan Souza Desidério,² Paula Tatiana Mutão Ferreira,² Mariana de Oliveira Silva,¹ César Gómez Hernández ,² Malú Mateus Santos,² Rafael Obata Trevisan,² Wesley Guimarães Bovi ,² Virmondes Rodrigues ,² Juliana Reis Machado ,³ Luiz Eduardo Ramirez,¹ Carlo José Freire de Oliveira ,² and Marcos Vinícius da Silva ¹

¹Laboratory of Parasitology, Department of Immunology, Microbiology and Parasitology, Federal University of Triângulo Mineiro, Uberaba, MG, Brazil

²Laboratory of Immunology, Department of Immunology, Microbiology and Parasitology, Federal University of Triângulo Mineiro, Uberaba, MG, Brazil

³Department of General Pathology, Federal University of Triângulo Mineiro, Uberaba, MG, Brazil

Correspondence should be addressed to Marcos Vinícius da Silva; marcosuftm@gmail.com

Received 16 March 2019; Revised 8 June 2019; Accepted 29 July 2019; Published 15 September 2019

Guest Editor: Luisa Cervantes-Barragan

Copyright © 2019 Cecilia Gomes Barbosa et al. This is an open access article distributed under the Creative Commons Attribution License, which permits unrestricted use, distribution, and reproduction in any medium, provided the original work is properly cited.

Dendritic cells (DCs) are a type of antigen-presenting cells that play an important role in the immune response against *Trypanosoma cruzi*, the causative agent of Chagas disease. *In vitro* and *in vivo* studies have shown that the modulation of these cells by this parasite can directly affect the innate and acquired immune response of the host in order to facilitate its biological cycle and the spreading of the species. Many studies show the mechanisms by which *T. cruzi* modulates DCs, but the interaction of these cells with the Mexican strains of *T. cruzi* such as Ninoa and INC5 has not yet been properly investigated. Here, we evaluated whether Ninoa and INC5 strains evaded the immunity of their hosts by modulating the biology and function of murine DCs. The CL-Brener strain was used as the reference strain. Herein, it was demonstrated that Ninoa was more infective toward bone marrow-derived dendritic cells (BMDCs) than INC5 and CL-Brener strains in both BMDCs of BALB/c and C57BL/6 mice. Mexican strains of *T. cruzi* induced different cytokine patterns. In BMDCs obtained from BALB/c mice, Ninoa strain led to the reduction in IL-6 and increased IL-10 production, while in C57BL/6 mice Ninoa strain considerably increased the productions of TNF- α and IL-10. Also, Ninoa and INC5 differentially modulated BMDC expressions of MHC-II, TLR2, and TLR4 in both BALB/c and C57BL/6 mice compared to Brazilian strain CL-Brener. These results indicate that *T. cruzi* Mexican strains differentially infect and modulate MHC-II, toll-like receptors, and cytokine production in DCs obtained from C57BL/6 and BALB/c mice, suggesting that these strains have developed particular modulatory strategies to disrupt DCs and, consequently, the host immune responses.

1. Introduction

Chagas disease, an illness identified 110 years ago by the physician and researcher Carlos Chagas, is a serious public health problem, affecting approximately 8 million people worldwide

[1, 2]. *Trypanosoma cruzi*, the etiological agent of the disease, presents intraspecific genetic and phenotypic heterogeneity. Based on phylogenetic, molecular, biochemical, and biological markers, the causative agent of the disease is grouped into six discrete typing units (DTUs) ranging from TcI to TcVI

[3–5]. The genetic diversity of *T. cruzi* exerts influence on the biological, clinical, immunological, and epidemiological variation of the disease, and it is also directly related to the establishment of the infection [6, 7]. For example, the TcVI genotype is associated with human Chagas disease in countries of South America, especially north of the equator where several cases of human infection have been reported [4]. Specifically, the CL-Brener strain [8] belongs to the TcVI genotype, and the metacyclic forms derived from this strain are highly invasive *in vitro* and *in vivo* [9–11]. TcI is considered a homogeneous group but contains the largest distribution among the described genotypes and is subdivided into five subgroups (TcIa–TcIe) [5, 12–15]. TcI is the genotype that predominates in Mexico and is responsible for causing most of the clinical manifestations of Chagas disease. The Mexican strain of this genotype has different biological characteristics such as growth, metacyclogenesis, and infectivity *in vitro* and can cause patent and subpatent parasitemia. However, the strains belonging to the same TcI genotype differ in their ability to invade cells and cause infection [16–21]. Experimental studies have shown that although the Mexican strains belong to the same TcI genotype, they present differences in the induction of mortality (0–100%), muscle cell tropism (mainly skeletal and cardiac), and in the inflammatory process generated by the infection. This indicates that biological behavior varies between these strains in the same DTU [16, 17, 19, 20]. Thus, elucidating the underlying mechanisms that generate so many differences even in strains of the same genotype and in the same geographical region is essential for understanding the disease in Mexico.

The *T. cruzi* parasite presents three morphological forms in its biological cycle, and of these, metacyclic trypomastigotes are the infective forms eliminated by triatomines during blood feeding [9, 16, 22–24]. The surface molecules presented by the metacyclic trypomastigotes are fundamental for the interaction of the parasite with the host, and through these surface molecules, the protozoan can be recognized by host defense cells. In this context, dendritic cells (DCs) are one of the preferred targets of the infecting forms of *T. cruzi* [25]. Because of their efficient antigen presentation ability, DCs can detect pathogens and initiate an effective response through a cascade of triggered events that culminates in the presentation of antigen to lymphocytes and activation of a specific and protective immune response [26]. In this process, these cells are activated and direct the host immune response depending on the production of cytokines and the presence and intensity of surface markers that characterize their maturation [27–29]. During antigen presentation, these cells have high expression of molecular markers such as CD80, CD86, and MHC [27, 30–32]. Additionally, cellular migration markers such as CCR7, which are fundamental in the migration process of these cells to the presentation sites, are expressed [27, 33]. Furthermore, various proinflammatory cytokines such as IL-1 β , IL-12, IL-8, TNF- α , and IL-6 are synthesized and assist in the formation of a specific pattern of immune response [27, 34, 35].

The interaction with *T. cruzi* induces inhibition of the expression of important cell activation and cellular maturation

markers such as CD80, CD86, MHC, and CD40 [36]. In addition, *T. cruzi* induces a DC death marker called PDL-1 that inhibits the production of proinflammatory cytokines such as IL-12, TNF- α , and IL-6 and stimulates the synthesis of anti-inflammatory cytokines such as IL-10 and TGF- β targeting a tolerogenic profile where there is less activation of *T. cruzi*-specific T lymphocytes [6, 25, 28, 37, 38]. These immunomodulations by the parasite can vary depending on the *T. cruzi* strain and how they interact with these cells, highlighting the key role of DCs in the development of clinical forms of the disease [6, 7, 37, 39–43]. Although many studies have elucidated the mechanisms by which *T. cruzi* modulates DCs, the interaction of these cells with Mexican strains has not yet been properly investigated. The present study is aimed at investigating the infectivity, expressions of standard recognition receptors and costimulatory molecules, and the production of cytokines in DCs cultured with Mexican strains to understand how they evade the immune responses of their hosts by modulating these cells.

2. Material and Methods

2.1. Parasites. Two strains of *T. cruzi* from Mexico were used. They were maintained in the laboratory of parasitology of the Federal University of the Triângulo Mineiro, UFTM. Ninoa strain (MHOM/MX/1994) [44] was obtained from xenodiagnosis of a patient with acute Chagas disease, while the INC5 strain (MHOM/MX/1994) [45] was isolated from a patient with Chagasic cardiomyopathy [19, 20]. CL-Brener is a Brazilian strain and was used as a reference for the study. This strain was isolated from a *Triatoma infestans*, belonging to the Department of Parasitology of the Federal University of São Paulo, UNIFESP, and was kindly provided by Dra. Nobuko Yoshida. The parasites were cultured at 28°C in liver infusion tryptose (LIT) medium supplemented with 10% fetal bovine serum. Metacyclic forms of cultures in stationary growth phase were purified by column passing DEAE-cellulose as previously described [46].

2.2. Animals and Differentiation of Bone Marrow-Derived DCs (BMDCs). Male BALB/c and C57BL/6 (6–8 weeks old) wild-type mice were bred and maintained in experimental animal facilities of the Federal University of Triângulo Mineiro, UFTM, Uberaba, MG, Brazil, according to the guidelines of the Ethics Committee on Animal Use (CEUA). All the experiments were conducted according to the Ethics Committee on the Use of Animals of the Federal University of Triângulo Mineiro. Bone marrow cells from the femurs and tibiae removed from mice were centrifuged at 400 $\times g$ for 10 min at 8°C in RPMI 1640 medium (GE Healthcare, Uppsala, Sweden). Subsequently, 2 mL of lysis buffer was added for lysing the red cells, and the cells were washed thrice for counting. Cells were counted in a Neubauer chamber and resuspended to 5 $\times 10^6$ cells/mL in RPMI 1640 medium with the addition of 50 mM Hepes (Gibco, Grand Island, NY, USA), 10% of inactivated fetal bovine serum (Gibco, USA), 2 mM L-glutamine (Gibco, USA), 40 mg/mL gentamicin, and 12.5 mg/mL murine GM-CSF (BD) at 37°C

in a humidified atmosphere with 5% CO₂. On day 3, 10 mL of RPMI medium containing 12.5 ng/mL GM-CSF was added. Cells were further differentiated for additional 4 days with GM-CSF containing complete medium. After 7 days of culture, the cells were collected and analyzed by flow cytometry to determine the percentage of CD11b and CD11c, and further experiments were performed only after evaluating this percentage. All cultures presented at least 80% of CD11b⁺CD11c⁺ DCs, and bone marrow-derived dendritic cells (BMDCs) were harvested and cultured in 96-well plates.

2.3. *In Vitro* Infection of DCs. After 7 days of differentiation, BMDCs at a concentration of 1.5×10^5 cells per well (96-well plate) in 250 μ L of 10% RPMI 1640 medium were incubated for 18 h with the three different *T. cruzi* strains (CL-Brener, Ninoa, or INC5 at MOI 2:1) with or without LPS (5 μ g/mL). Cells were then evaluated for parasite infection using 4',6-diamidino-2-phenylindole dihydrochloride (DAPI; Molecular Probes, Eugene, Oregon, US). Expression of MHC-II, CD80, CD86, TLR2, and TLR4 surface markers was evaluated by flow cytometry, and the production of TNF- α , IL-10, IL-12p70, CCL-2, and IL-6 was measured by cytometric bead array. A MOI of 2:1 was chosen because this ratio of cell and parasite was sufficient to affect the different steps of the DC biology or to assess parasitic infectivity.

2.4. Determination of *T. cruzi*-Infected DCs. BMDCs in 96-well plates were analyzed by fluorescence microscopy using DAPI. BMDCs differentiated from both the mouse strains were cultured with different strains of *T. cruzi*, harvested, and incubated at 4°C for 30 min with 10 μ M DAPI. Cells were washed twice with PBS and centrifuged at $400 \times g$ at 4°C for 10 min and immediately analyzed by EVOS Cell Imaging System (Thermo Scientific, USA) at $\times 400$ magnification. The number of intracellular parasites was counted in a total of 100 cells, and percentage of infected cells, parasites per 100 cells, and mean parasite load in infected cells were determined.

2.5. Flow Cytometry Analysis. BMDCs differentiated from both mouse strains were analyzed by flow cytometry using the following monoclonal antibodies: anti-CD11c, anti-MHC-II, anti-CD80, anti-CD86, anti-TLR2, or anti-TLR4, labeled with APC, FITC, PE, or PECy7 according to the intended purpose. The acquisition was obtained using an Accuri flow cytometer (BD Immunocytometry Systems), and the analyses were performed using the FlowJo software.

2.6. Cytometric Bead Array. Cytometric bead array was performed using the CBA Mouse Inflammation Kit (BD Biosciences) according to the manufacturer's instructions, and the following cytokines were measured: TNF- α , IL-10, IL-12p70, IL-6, and chemokine CCL-2. Briefly, supernatants of BMDCs from C57BL/6 and BALB/c mice cultured with *T. cruzi*, with or without LPS, were incubated with beads coupled with specific monoclonal antibodies and PE-conjugated secondary antibodies for 4 h at room temperature. Beads were washed and the acquisition was performed using the Accuri flow cytometer (BD Immunocytometry Systems). The concentration of the samples was estimated by

comparing the PE fluorescence obtained from the standard curve obtained by serial dilution of recombinant murine cytokines. Results were analyzed by 5-parameter logistic regression with FCAP array software and expressed in pg/mL.

2.7. Statistical Analysis. The results were analyzed by GraphPad Prism 7.0 (GraphPad Software, San Diego, CA, USA). The Kruskal-Wallis test with a Dunn's post hoc test was performed for data with a non-Gaussian distribution. Bar graphs show mean and standard error of the mean. The results were considered significant when the *p* value was lower than 0.05 (5%).

3. Results

3.1. Evaluation of the Infectivity of Different Strains of *T. cruzi* in DCs Derived from BALB/c and C57BL/6 Mice. In general, the different *T. cruzi* strains were able to infect DCs. However, the percentage of infection varied depending on the strain and the origin of DCs [6, 7, 37, 47]. In BMDCs derived from BALB/c mice, the percentage of cells infected with the different strains did not show a significant difference despite experiencing a slight increase when these cells were cultured with LPS (Figure 1(a)). Contrastingly, when evaluating the amount of parasites present in a total of 100 BMDCs, we found that cells cultured with *T. cruzi* from the Ninoa strain previously stimulated with LPS exhibited a significant increase in the number of parasites compared to the INC5 strain plus LPS ($p = 0.0427$) (Figure 1(b)). The same profile in relation to the Ninoa and INC5 strains plus LPS was found by analyzing the amount of parasites present in each infected cell ($p = 0.0219$) (Figure 1(c)). In the CL-Brener strain without LPS treatment, the number of parasites per infected cell was significantly higher compared to the INC5 strain also without LPS treatment ($p = 0.0427$) (Figure 1(c)). When the BMDCs derived from C57BL/6 mice were evaluated, the percentage of infected cells after culture with CL-Brener strain plus LPS presented a significant variation ($p = 0.0234$) compared to BMDCs cultured with INC5 strain plus LPS (Figure 1(d)). The amount of parasites per 100 cells showed a significant increase when the CL-Brener strain was compared to the INC5 strain ($p = 0.0422$). The same difference in infectivity was found when the number of parasites in BMDCs cultured with the CL-Brener strain plus LPS was compared to BMDCs cultured with the Ninoa strain plus LPS ($p = 0.0230$) (Figure 1(e)). The same pattern was observed in the amount of parasites per infected cell comparing the effects of the Ninoa and CL-Brener strains ($p = 0.0181$) (Figure 1(f)). In Figure 1(g), we show a representative picture of DAPI labeling evidencing the infectivity of different strains of *T. cruzi* in BMDCs *in vitro*.

3.2. Production of Cytokines and Chemokine CCL-2 in DCs Cultured with Different Strains of *T. cruzi*. The concentration of cytokines in BMDCs from BALB/c mice did not show statistically significant differences in any of the analyses, regardless of whether they were infected only with the strains or in the presence of LPS. The following cytokine levels were

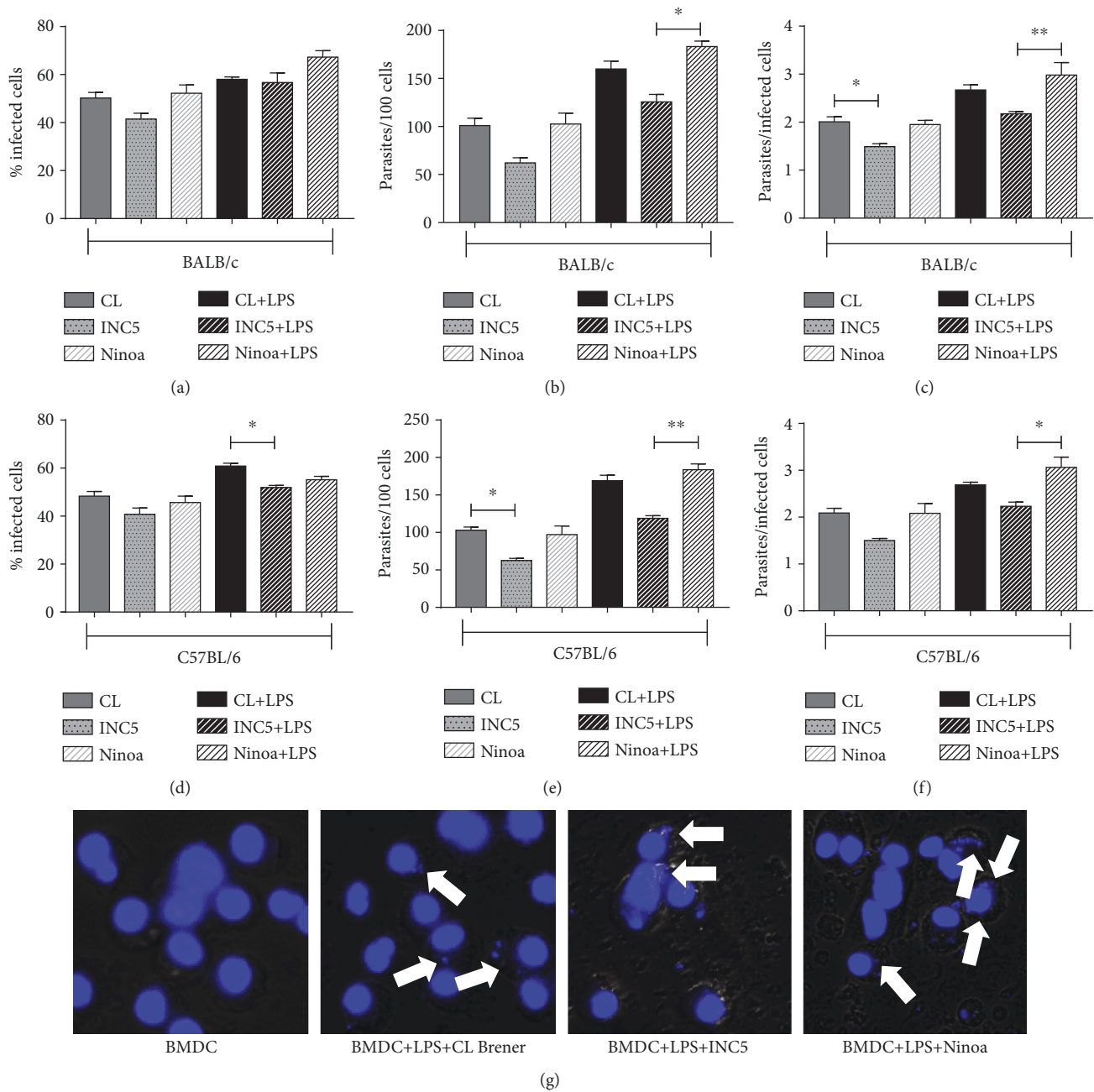


FIGURE 1: *Trypanosoma cruzi* infectivity in murine BMDCs from BALB/c and C57BL/6 mice. BMDCs with or without LPS stimulation (5 $\mu\text{g}/\text{mL}$) were incubated for 18 h with different *T. cruzi* strains (MOI 2:1) and stained with DAPI. (a) and (d) show the percentage of infected cells; in (b) and (e) the number of parasites per 100 cells and in (c) and (f) the ratio of parasites per infected cell are shown. (g) Representative images of BMDCs infected with *T. cruzi* after stimulation with LPS (5 $\mu\text{g}/\text{mL}$) and stained with DAPI. Statistical analysis, when applicable, was performed with the Kruskal-Wallis test with Dunn's posttest, where *** $p < 0.05$.

measured: TNF- α , IL-6, IL-12p70, CCL-2, and IL-10 (Figures 2(a)–2(e)). When we analyzed the cytokines present in the culture supernatant of BMDCs derived from C57BL/6 mice, a significant increase was observed in the production of TNF- α in BMDCs cultured with the Ninoa strain without or plus LPS compared to cultures without *T. cruzi* infection ($p = 0.0094$) (Figure 3(a)). Also, the Ninoa strain induced a significant increment of IL-10 production in LPS-treated cultures compared to LPS alone and all other strains plus LPS ($p = 0.00001$ for LPS, $p = 0.023$ for CL-Brener, and

$p = 0.0331$ for INC5) (Figure 3(e)). We did not find significant differences in the production of IL-6 (Figure 3(b)), IL-12p70 (Figure 3(c)), and CCL-2 (Figure 3(d)).

3.3. Percentage of Cytokine and Chemokine CCL-2 Variation in DCs Cultured with Different Strains of *T. cruzi*. In order to demonstrate how the different *T. cruzi* strains could modulate the ability of dendritic cells to produce cytokines, we calculated the variation of cytokines by determination of percentage of increment or reduction in cytokines produced

by *T. cruzi*-infected BMDCs previously treated with LPS and those maintained only with LPS (5 $\mu\text{g}/\text{mL}$). Globally, the interaction of BMDCs with *T. cruzi* induced TNF- α , IL-6, CCL-2, and IL-10 increment and IL-12p70 reduction. The cytokine IL-6 (Figure 4(b)) showed significant alteration only in the BMDCs derived from BALB/c mice, showing a reduction in cells stimulated with the Ninoa strain compared to cells stimulated with the CL-Brener strain ($p = 0.0387$). On the other hand, the Ninoa strain induced significant increment in CCL-2 compared to CL-Brener in BALB/c mice ($p = 0.01$). IL-10 also showed significant variation for both mice strains, as BMDCs cultured with the Ninoa strain had an increase in IL-10 compared to BMDCs cultured with the INC5 strain in BALB/c mice ($p = 0.0219$) and compared to INC5 and CL-Brener in C57BL/6 mice ($p < 0.0001$). We did not observe any significant changes in the variation of TNF- α (Figure 4(a)) and IL-12p70 among strains (Figure 4(c)). In Figures 4(f)–4(i), it is possible to observe the variation in the production of the cytokines according to the different strains with or without the addition of LPS.

3.4. Evaluation of MHC-II, CD80, CD86, TLR2, and TLR4 Expression in DCs Cultured with Different Strains of *T. cruzi*. Data related to flow cytometry were analyzed by ascertaining the variation of the percentage of positive cells and the variation of the expression per cell (mean fluorescence intensity). Our results point that *T. cruzi* Mexican strains significantly reduce cells expressing MHC-II, TLR2, and TLR4 compared to the Brazilian strain CL-Brener. Specifically, the interaction with INC-5 and Ninoa led to a lower MHC-II⁺ BMDC in both BALB/c ($p = 0.0011$) and C57BL/6 ($p = 0.0004$) mice (Figure 5(a)). The costimulatory molecules CD80 and CD86 presented a negative variation in BMDCs cultured with all evaluated (Figures 5(b) and 5(c)). For both BALB/c and C57BL/6, the CL-Brener strain induced higher percentage of TLR2⁺ BMDCs compared to the INC5 strain ($p = 0.0051$ and $p = 0.0001$, respectively) and to Ninoa ($p = 0.0051$ and $p = 0.0001$, respectively, Figure 5(d)). In a similar way, the CL-Brener strain interaction induced a higher percentage of TLR4⁺ BMDCs in both mice strains compared to the INC5 ($p = 0.0001$ for BALB/c and C57BL/6) and Ninoa strains ($p = 0.0001$ for BALB/c and C57BL/6) (Figure 5(e)).

In both mouse strains, the INC5 strain led to a significant increment in BMDC MHC-II expression compared to the CL-Brener strain ($p = 0.0319$) and Ninoa ($p = 0.0004$) in BALB/c. Interestingly, while in BALB/c mice the CL-Brener strain induced a slight increment in MHC-II, in C57BL/6 mice, this expression was inhibited and significantly different from INC5 and Ninoa ($p = 0.0427$, Figure 6(a)). All *T. cruzi* strains induced an inhibition in CD80 expression for both mouse strains (Figure 6(b)). For CD86, only Ninoa induced a slight increment in expression but without statistical significance (Figure 6(c)). The CL-Brener strain also induced a considerable increment in TLR2 expression in both mouse strains compared to the INC5 and Ninoa strains ($p = 0.0002$ for BALB/c and $p = 0.0001$ for C57BL/6, Figure 6(d)). On the other hand, the CL-Brener strain infec-

tion induced a lower expression of TLR4⁺ BMDCs compared to the INC5 and Ninoa strains ($p = 0.0004$ for BALB/c and $p = 0.01$ for C57BL/6, Figure 6(d)). Radar plots present a summary of the impact of the interaction with different *T. cruzi* strains in LPS-stimulated BMDCs from BALB/c (Figure 6(f)) and C57BL/6 (Figure 6(g)) mice.

4. Discussion

Our study is aimed at evaluating the infectivity and immunomodulatory capacity of different Mexican strains of *T. cruzi* on DCs derived from BALB/c and C57BL/6 mice. Our results point to the fundamental role of these strains in the interaction with these DCs during the *in vitro* coculture, depending on the mouse lineage.

The biological behavior, anatomical route of invasion, inoculum, surface molecules expressed in the metacyclic forms of *T. cruzi*, and host immune response are factors that are closely related to the establishment of the infection [6, 9, 48–50]. Our data showed that all three strains infected DCs efficiently. However, strains belonging to the TcI genotype (AQ1.7, Mutum, and G) presented a profile with low infectivity in BMDCs [6, 51]. This can be explained by the fact that *T. cruzi* presents a high intraspecific genetic and phenotypic diversity, especially for the TcI genotype. Thus, different genetic markers indicate that there is an intra-DTU genetic variation, and the TcI is the genotype that presents high genetic heterogeneity. This may be related to the different epidemiological characteristics and generate controversies regarding the infectivity and pathogenicity of the strains belonging to this genetic group [4, 13, 19, 52].

When inoculated in Swiss mice, the parasites of the INC5 and Ninoa strains presented patent parasitemia, high infectivity, and mortality. Intense tissue parasitism was observed in several organs of the experimental animals, increasing the virulence of these strains [20, 52]. However, trypomastigote forms were used in these other studies [17, 20, 21]. Notably, the different evolutionary forms of *T. cruzi* use different strategies in adhesion or invasion of cells because of the specific stage molecules, which affect the infectivity and pathogenicity, even in the same strain [53, 54]. The parasite inoculation pathway can also influence the biological behavior of the strain because of the different biological barriers that the parasite needs to overcome to establish the infection, directly impacting the immune response and host resistance [50]. One factor that needs to be considered is the type of cell or tissue that the metacyclic form infects. The Ninoa strain showed low parasitemia and mortality and a mild inflammatory process when inoculated orally in mice of this same strain. In oral infection, the parasites enter into the epithelial cells of the stomach and can undergo pepsin action, and the metacyclic trypomastigote forms express on their surface molecules that can facilitate or inhibit this invasion process. Recent studies have shown that the TcI genotype has a poor infective oral profile, as they express gp90 on their surface, and this molecule negatively regulates invasion to the target cell [16, 55].

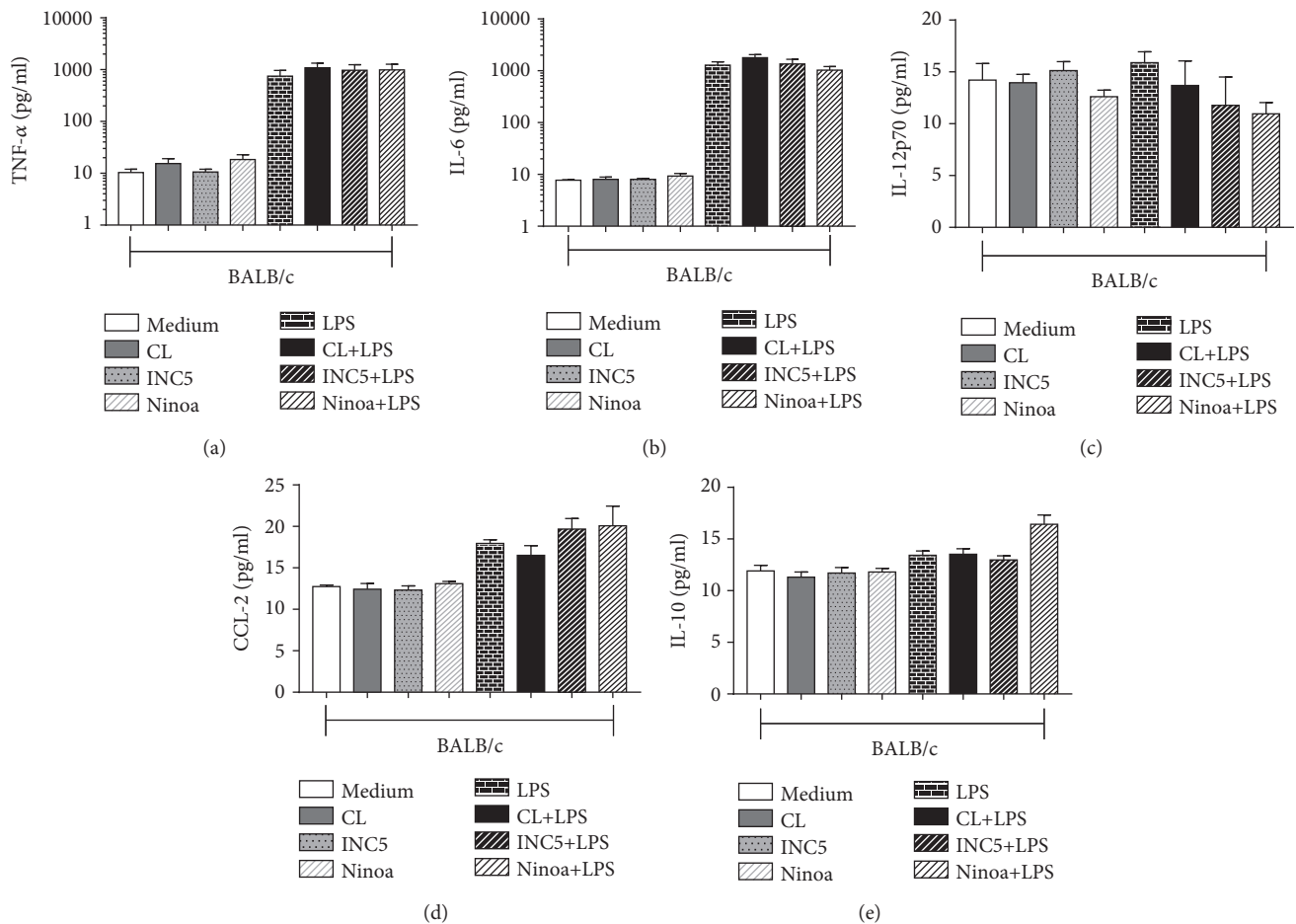


FIGURE 2: Cytokine and chemokine production by BALB/c-derived BMDCs infected with CL-Brener, Ninoa, and INC5 strains of *T. cruzi*. BMDCs with or without LPS stimulation ($5 \mu\text{g}/\text{mL}$) were incubated for 18 h with different *T. cruzi* strains (MOI 2 : 1), and the production of cytokines and chemokine was evaluated by CBA: (a) TNF- α , (b) IL-6, (c) IL-12p70, (d) CCL-2, and (e) IL-10. Statistical analysis, when applicable, was performed with the Kruskal-Wallis test with Dunn's posttest, where $***p < 0.05$.

On the other hand and consistent with our present study, the CL-Brener strain presents a highly infectious profile in *in vitro* studies, and its profile is well studied in oral infection. An explanation for the increased infectivity may be the glycoprotein gp82 expressed on its surface that facilitates the entry of the parasite into the cell through the mobilization of intracellular calcium [9, 11]. These different results using the same strains show that in addition to the parasite genetics, the infected cell line and the immune response caused by the contact of the parasite with the cell are associated with the infection. Additionally, the cells derived from the C57B/6 and BALB/c mice present different degrees of susceptibility and/or resistance [51]. Our results show that the Ninoa strain has a higher infectivity potential when the BMDCs are activated with LPS, while the CL-Brener strain is more infective in BMDCs not yet activated. Different strains have shown distinct infectivity potentials [6], and this can be related to the ability of these cells to recognize the molecules presented on the surface of the parasite [56]. In addition, in BALB/c mice, we observed a similar cell interaction for all strains, while in C57BL/6 the CL-Brener strain had a better perfor-

mance. This suggests that a strain can have different behaviors depending on the mice used, as shown in experiments with Y strain [57].

Once the ability of infection in cells derived from the two strains was confirmed, we analyzed the ability of these strains to modulate surface markers and stimulate the production of cytokines. We observed that both strains of *T. cruzi* and lineage of mice presented different patterns for the parameters evaluated. In BMDC from BALB/c mice, the Ninoa strain lead to a reduction in IL-6 and an increase in IL-10 production, while in C57BL/6 mice the cytokine production was associated with a huge increment in TNF- α and IL-10. Cytokines are one of the most relevant factors in determining the course of infection [17, 51, 58]. During the process of infection by *T. cruzi*, a modulating response associated with susceptibility to the disease can be triggered by the parasite. For instance, in macrophages infected with *T. cruzi*, the activation of TLR is weak, leading to a decrease in the production of proinflammatory cytokines such as IL-12 [59]. In addition, the production of IL-10 and TGF- β is stimulated in infected macrophages, and this causes a favorable response to the

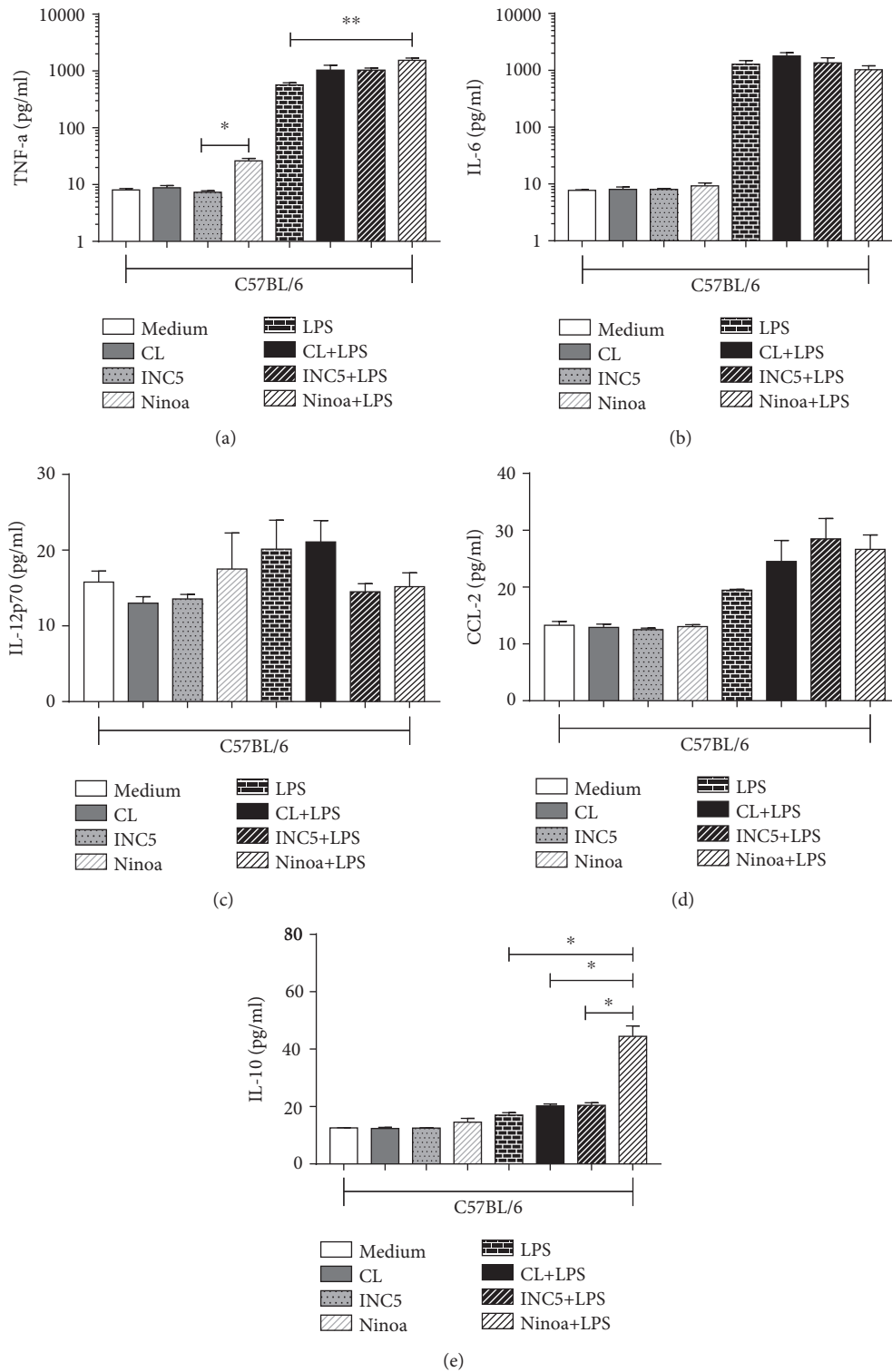


FIGURE 3: Cytokine and chemokine production by C57BL/6-derived BMDC infected with CL-Brener, Ninoa, and INC5 strains of *T. cruzi*. BMDCs with or without LPS stimulation (5 μ g/mL) were incubated for 18 h with different *T. cruzi* strains (MOI 2:1), and the production of cytokines and chemokine was evaluated by CBA: (a) TNF- α , (b) IL-6, (c) IL-12p70, (d) CCL-2, and (e) IL-10. Statistical analysis, when applicable, was performed with the Kruskal-Wallis test with Dunn's posttest, where ***,** $p < 0.05$.

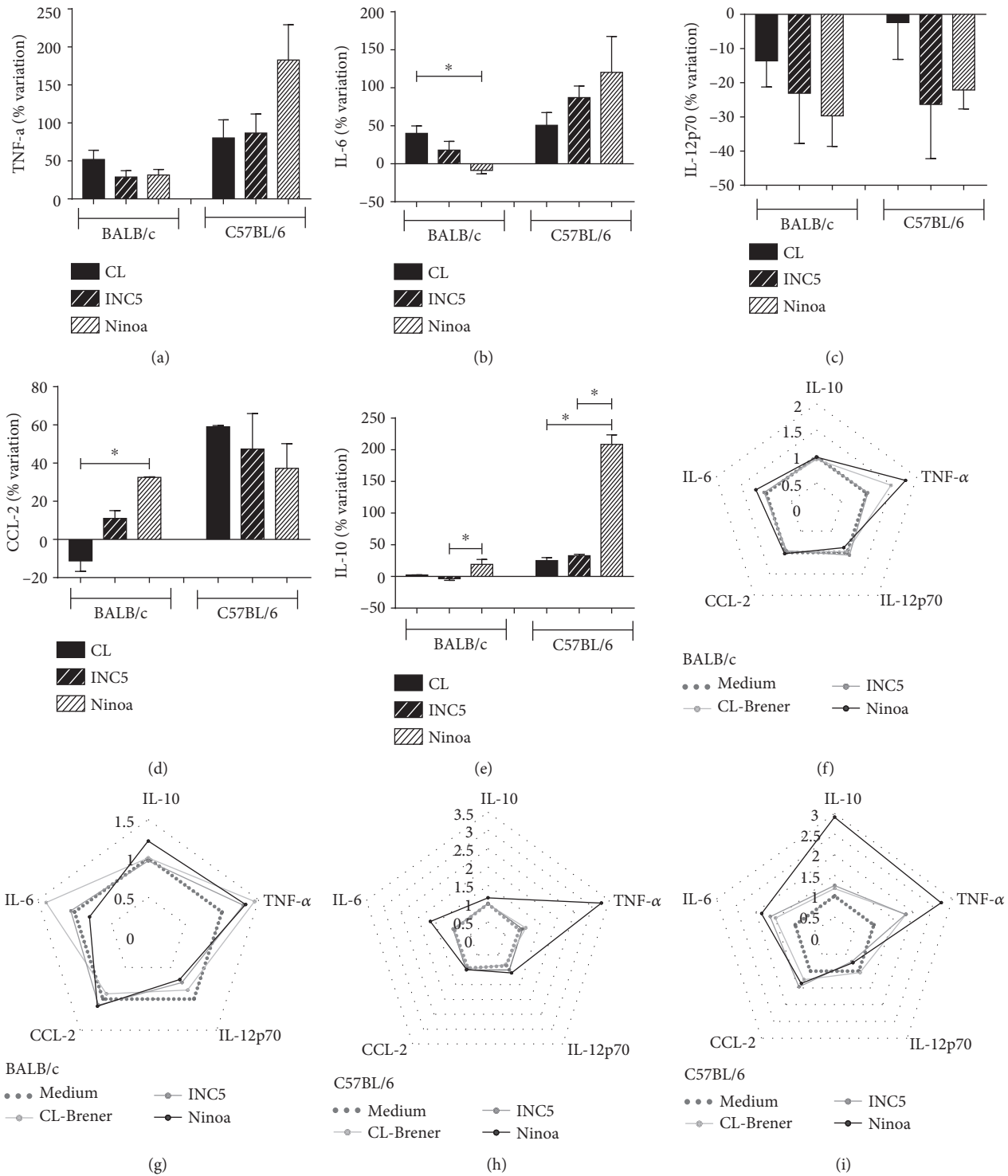


FIGURE 4: Percentage of variation in the levels of pro- and anti-inflammatory cytokines and CCL-2 chemokine in the supernatant of BMDCs of BALB/c and C57BL/6 mice. The variation of cytokines was calculated by determination of percentage of increment or reduction in cytokines produced by *T. cruzi*-infected BMDCs previously stimulated with LPS and those maintained only with LPS (5 μg/mL). (f, h) Representation of the radar graph of the cytokine pattern in the dendritic cell culture supernatant. The lines highlight the change in cytokine levels in dendritic cells infected with different strains (MOI 2:1) in relation to the medium only with dendritic cells. (g, i) The pattern of cytokines in the dendritic cell culture supernatant previously stimulated with LPS. Data were obtained by calculating the ratio between *T. cruzi*-infected cells and their respective control. Statistical analysis, when applicable, was performed with the Kruskal-Wallis test with Dunn's posttest, where $***p < 0.05$.

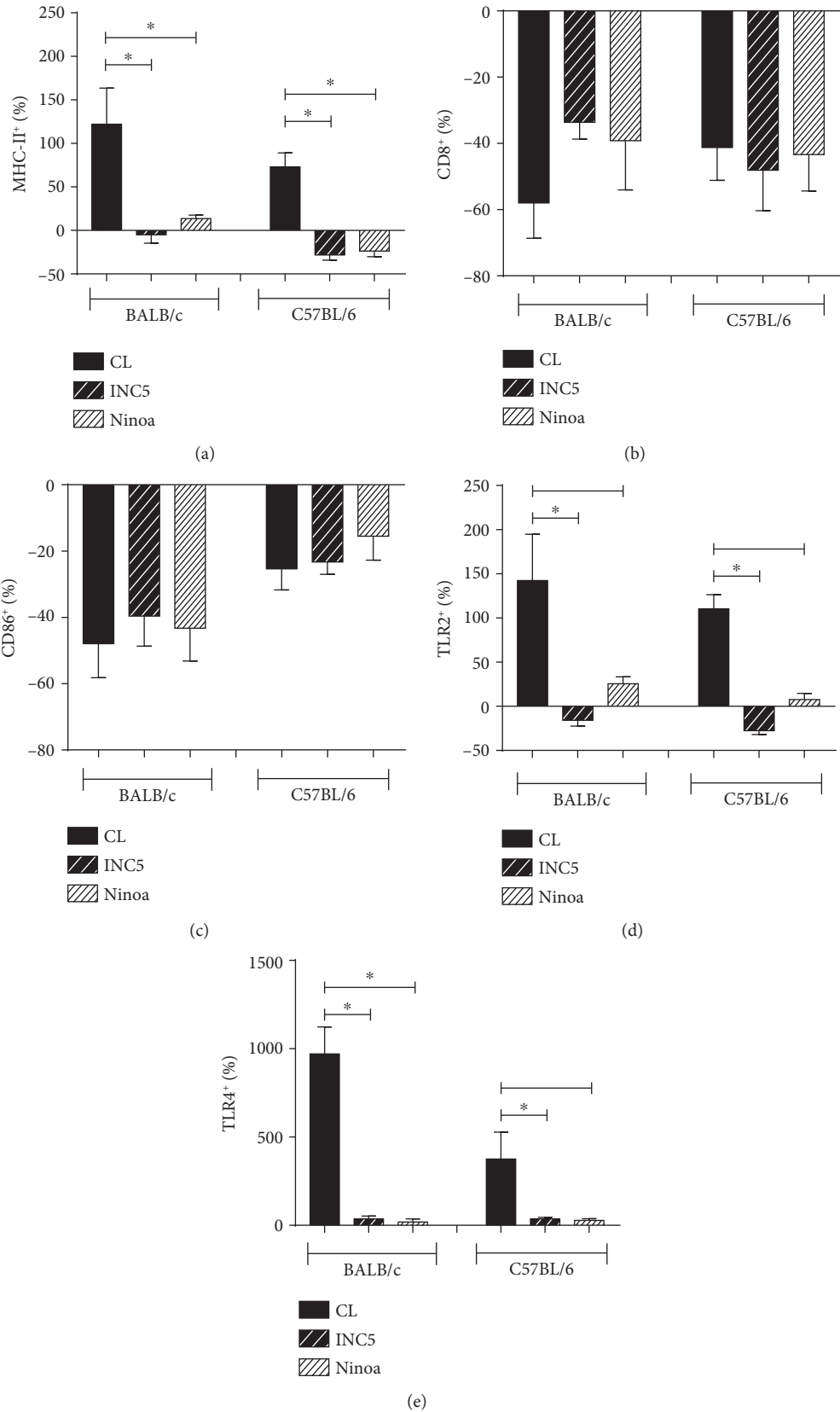


FIGURE 5: Percentage of BMDCs expressing MHC-II, costimulatory molecules, and toll-like receptors after *in vitro* *T. cruzi* infection. The expression of molecules was evaluated by flow cytometry and represented as a variation of the percentage of BMDCs expressing (a) MHC-II, (b) CD80, (c) CD86, (d) TLR2, and (e) TLR4. Statistical analysis, when applicable, was performed with the Kruskal-Wallis test with Dunn's posttest, where * $p < 0.05$.

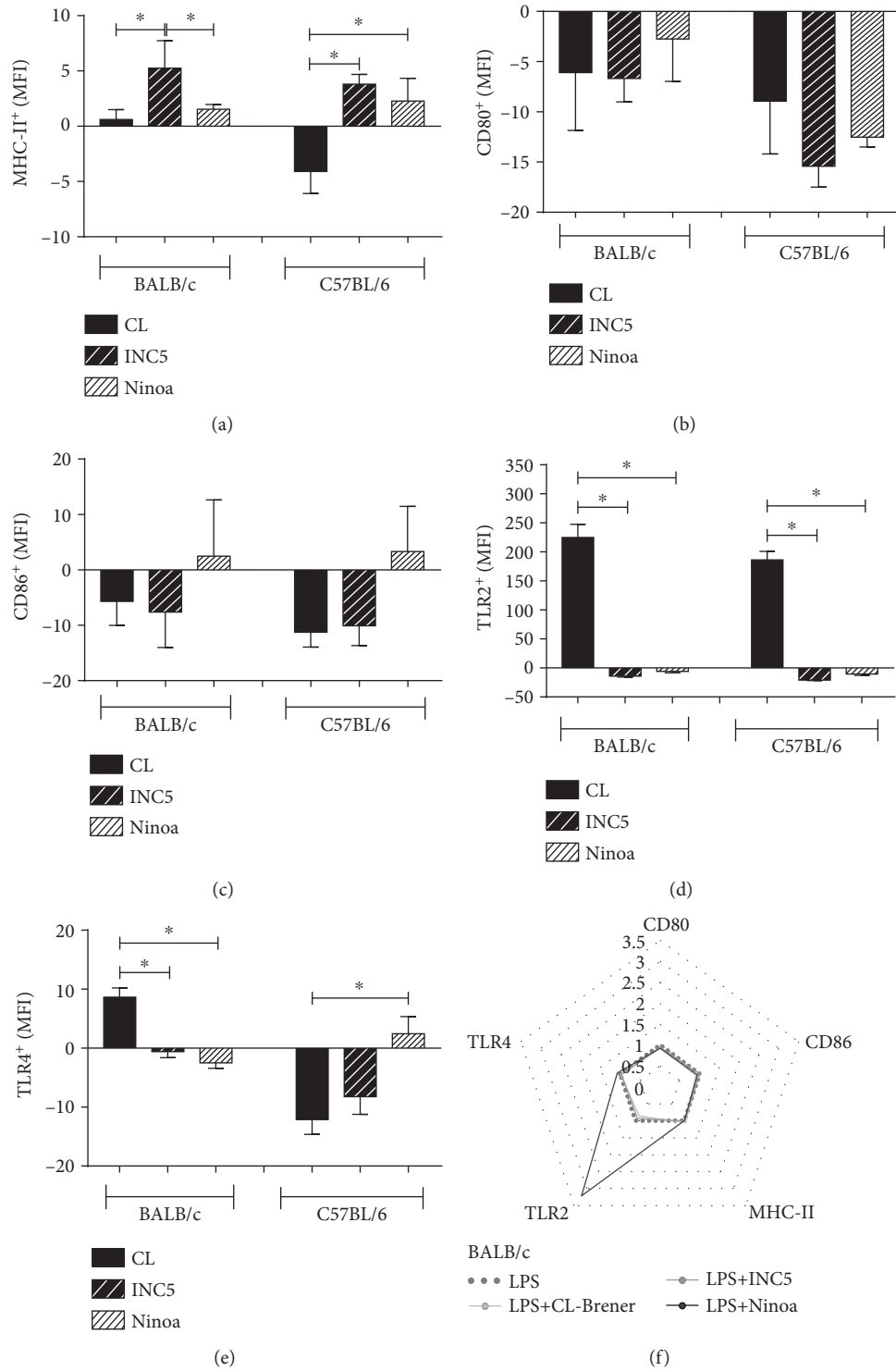


FIGURE 6: Continued.

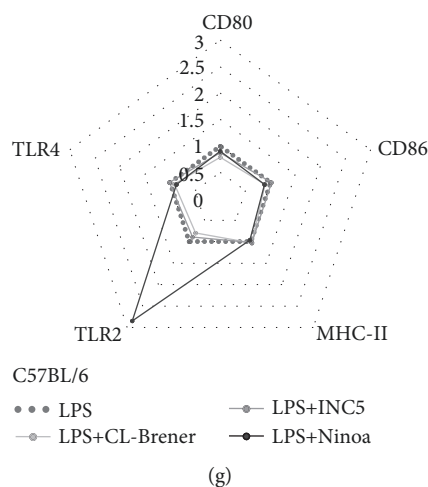


FIGURE 6: Expression of MHC-II, costimulatory molecules, and toll-like receptors in BMDCs after *in vitro* *T. cruzi* infection. The expression of molecules was evaluated by flow cytometry and represented as a variation of the mean intensity of fluorescence (a) MHC-II, (b) CD80, (c) CD86, (d) TLR2, and (e) TLR4. (f, g) Representation of the cytokine secretion pattern in BMDC culture supernatant. The lines highlight the change in cytokine levels in LPS-stimulated BMDCs and infected with different strains of *T. cruzi* (MOI 2 : 1) in relation to uninfected LPS-stimulated BMDCs. Statistical analysis, when applicable, was performed with the Kruskal-Wallis test with Dunn's posttest, where $*p < 0.05$.

parasite to be triggered [37, 60, 61]. Similar results were found in our study, where the Ninoa strain presented more modulatory behaviors compared to the other strains under similar conditions, especially when the cells were already activated. According to Gil-Jaramillo et al. [7], more virulent strains can manipulate DCs to produce more tolerogenic cytokines.

Ferreira et al. [51] described increased levels of IL-10 in C57BL/6 and BALB/c mice in the acute phase of the disease. In addition, BALB/c mice had elevated serum TGF- β levels, indicating susceptibility to the disease. The proinflammatory cytokines TNF- α , IFN- γ , IL-1 β , IL-2, IL-5, and IL-6 also showed high levels of expression during the infection period, suggesting that the balance between cytokines determines the course of infection. In DCs derived from BALB/c mice, we observed that no cytokine showed great peak expression; however, in C57BL/6, IL-10 and TNF- α were strongly stimulated by the Ninoa strain. The other cytokine levels did not change. Analyzing the serum of BALB/c animals infected with the Ninoa strain, the study conducted by Espinoza et al. demonstrated an increase in the levels of IL-10 in the acute phase, which decays and rises gradually during the course of infection. IL-12, which reached its peak in the acute phase and was maintained throughout the chronic phase, was also evaluated [17].

TLRs form a family of transmembrane proteins responsible for the recognition of molecular patterns essential for the triggering of immune responses [62–64]. Several surface molecules of *T. cruzi* are recognized by these receptors. Some molecules of trypomastigotes are recognized by TLR2 [65, 66], and other molecules present in epimastigotes are recognized by TLR4 [67]. The relationship between the recognition of *T. cruzi* by these receptors and the development of a susceptible or resistant immune response has been extensively investigated. TLR2, TLR4, TLR7, and TLR9 are impor-

tant for the development mechanisms of *T. cruzi* infection [64]. The parasitic form tested in our study for all the strains used was the metacyclic, the same as that of the natural infections in vector transmission, and we observed a better expression of TLR2 in cells infected by the CL-Brener strain belonging to TcVI in relation to the INC5 strain belonging to TcI and a better expression of TLR4 in relation to the Ninoa strain in the TcI group. Similar studies using other strains showed strains belonging to the TcI group that were able to improve TLR2 expression, whereas the decrease in TLR4 $^{+}$ was evidenced in the TcII group [6]. The increase in TLR2 can be related to the ability to evade host defense by changing the cytokine profile produced, favoring the production of TLR2-dependent IL-10, as in infections by several other microorganisms [6, 51, 59, 67, 68]. Although this strain has not been highlighted by the production of IL-10 compared to others, the TLR2 pathway may be responsible for the observed production. TLR4 can trigger the production of cytokines such as IL-12, IFN- γ , TNF- α , and nitric oxide (NO) in *T. cruzi* infections [67, 69], leading to better response. Our data show that the CL-Brener strain presents a greater number of TLR4 $^{+}$ DCs, although not showing a significant expression with respect to the cytokines of these profiles.

The ability of maturation and presentation of antigens by DCs is impaired by the presence of the parasite. This damage is due to the modulation of important molecules such as MHC, CD80, CD40, and CD86, whose levels are reduced in the presence of the parasite [6, 25, 28, 37, 38]. Only the INC5 strain induced high amounts of MHC-II. In general, this molecule is responsible for the success of antigen presentation and efficient assembly of specific immune response, including the production of antibodies [27, 30–32]. This is consistent with the data shown by Henrique et al., indicating that the most virulent strains Ninoa, INC5, and Colombian

induced high production of antibodies. The costimulatory molecules CD80 and CD86 are also related to the maturation and presentation capacity of the antigen [27, 30–32, 52]. The strains studied here presented a negative variation for CD80 and CD86 in BMDCs derived from the two mouse lineages, suggesting a difficulty of maturation of these infected cells. A similar result was observed with splenic DCs infected with the Tehuantepec strain, where the decrease in CD86 expression prevented the migration of these cells to the antigen-presenting organs [47]. This represents a good escape strategy for the host defense parasite.

The metacyclic form is the infective form of transmission of *T. cruzi*, and the first cells found after infection are DCs. However, many studies on these cells were not performed using this infective form [6]. Thus, the evaluation of our dataset allows us to observe situations that can mimic what occurs during the interaction process with the host. By using strains of *T. cruzi* and different mice, we were able to expand the observations even further and conclude that the two Mexican strains studied here were capable of modulating the response of DCs, regardless of their origin, through different pathways. The results reinforce the escape strategy of the host immune response and demonstrate the importance of investigating the mechanisms involved in this process.

Data Availability

The datasets generated during and/or analyzed during the current study are available from the corresponding author on reasonable request.

Disclosure

The funders had no role in the study design, data collection and analysis, decision to publish, or preparation of the manuscript.

Conflicts of Interest

The authors declare that they have no conflicts of interest.

Acknowledgments

The research leading to these results has received support and funding from the Conselho Nacional de Desenvolvimento Científico e Tecnológico, Fundação de Amparo à Pesquisa do Estado de Minas Gerais (FAPEMIG), Coordenação de Aperfeiçoamento de Pessoal de Nível Superior (CAPES), and Network for Infectious Disease Research.

References

- [1] C. Chagas, “Nova tripanozomíase humana: estudos sobre a morfologia e o ciclo evolutivo do *Schizotrypanum cruzi* n. gen., n. sp., agente etiológico de nova entidade morbida do homem,” *Memórias do Instituto Oswaldo Cruz*, vol. 1, no. 2, pp. 159–218, 1909.
- [2] L. E. Echeverría and C. A. Morillo, “American trypanosomiasis (Chagas disease),” *Infectious Disease Clinics of North America*, vol. 33, no. 1, pp. 119–134, 2019.
- [3] L. A. Messenger, J. D. Ramirez, M. S. Llewellyn, F. Guhl, and M. A. Miles, “Importation of hybrid human-associated *Trypanosoma cruzi* strains of southern South American origin, Colombia,” *Emerging Infectious Diseases*, vol. 22, no. 8, pp. 1452–1455, 2016.
- [4] B. Zingales, “*Trypanosoma cruzi* genetic diversity: something new for something known about Chagas disease manifestations, serodiagnosis and drug sensitivity,” *Acta Tropica*, vol. 184, pp. 38–52, 2018.
- [5] B. Zingales, S. Andrade, M. Briones et al., “A new consensus for *Trypanosoma cruzi* intraspecific nomenclature: second revision meeting recommends TcI to TcVI,” *Memórias do Instituto Oswaldo Cruz*, vol. 104, no. 7, pp. 1051–1054, 2009.
- [6] T. A. da Costa, M. V. Silva, M. T. Mendes et al., “Immunomodulation by *Trypanosoma cruzi*: toward understanding the association of dendritic cells with infecting TcI and TcII populations,” *Journal of Immunology Research*, vol. 2014, Article ID 962047, 12 pages, 2014.
- [7] N. Gil-Jaramillo, F. N. Motta, C. B. F. Favali, I. M. D. Bastos, and J. M. Santana, “Dendritic cells: a double-edged sword in immune responses during Chagas disease,” *Frontiers in Microbiology*, vol. 7, article 1076, 2016.
- [8] Z. Brener and E. Chiari, “Morphological variations observed in different strains of *Trypanosoma cruzi*,” *Revista do Instituto de Medicina Tropical de Sao Paulo*, vol. 5, pp. 220–224, 1963.
- [9] M. Cortez, M. R. Silva, I. Neira et al., “*Trypanosoma cruzi* surface molecule gp90 downregulates invasion of gastric mucosal epithelium in orally infected mice,” *Microbes and Infection*, vol. 8, no. 1, pp. 36–44, 2006.
- [10] I. Neira, F. A. Silva, M. Cortez, and N. Yoshida, “Involvement of *Trypanosoma cruzi* metacyclic trypomastigote surface molecule gp82 in adhesion to gastric mucin and invasion of epithelial cells,” *Infection and Immunity*, vol. 71, no. 1, pp. 557–561, 2003.
- [11] N. Yoshida, “*Trypanosoma cruzi* infection by oral route: how the interplay between parasite and host components modulates infectivity,” *Parasitology International*, vol. 57, no. 2, pp. 105–109, 2008.
- [12] “Recommendations from a satellite meeting,” *Memórias do Instituto Oswaldo Cruz*, vol. 94, Supplement 1, pp. 429–432, 1999.
- [13] C. I. Cura, A. M. Mejía-Jaramillo, T. Duffy et al., “*Trypanosoma cruzi* I genotypes in different geographical regions and transmission cycles based on a microsatellite motif of the intergenic spacer of spliced-leader genes,” *International Journal for Parasitology*, vol. 40, no. 14, pp. 1599–1607, 2010.
- [14] C. Herrera, M. D. Bargas, A. Fajardo et al., “Identifying four *Trypanosoma cruzi* I isolate haplotypes from different geographic regions in Colombia,” *Infection, Genetics and Evolution*, vol. 7, no. 4, pp. 535–539, 2007.
- [15] B. Zingales, M. A. Miles, D. A. Campbell et al., “The revised *Trypanosoma cruzi* subspecific nomenclature: rationale, epidemiological relevance and research applications,” *Infection, Genetics and Evolution*, vol. 12, no. 2, pp. 240–253, 2012.
- [16] C. G. Barbosa, C. Gómez-Hernández, K. Rezende-Oliveira et al., “Oral infection of mice and host cell invasion by *Trypanosoma cruzi* strains from Mexico,” *Parasitology Research*, vol. 118, no. 5, pp. 1493–1500, 2019.
- [17] B. Espinoza, T. Rico, S. Sosa et al., “Mexican *Trypanosoma cruzi* TCI Strains with Different Degrees of Virulence Induce Diverse Humoral and Cellular Immune Responses in a Murine

- Experimental Infection Model,” *Journal of Biomedicine and Biotechnology*, vol. 2010, Article ID 890672, 10 pages, 2010.
- [18] B. Espinoza, N. Solorzano-Domínguez, A. Vizcaino-Castillo, I. Martínez, A. L. Elias-López, and J. Rodríguez-Martínez, “Gastrointestinal infection with Mexican TcI *Trypanosoma cruzi* strains: different degrees of colonization and diverse immune responses,” *International Journal of Biological Sciences*, vol. 7, no. 9, pp. 1357–1370, 2011.
- [19] C. Gómez-Hernández, S. D. Pérez, K. Rezende-Oliveira et al., “Evaluation of the multispecies coalescent method to explore intra-*Trypanosoma cruzi* I relationships and genetic diversity,” *Parasitology*, vol. 146, no. 8, pp. 1063–1074, 2019.
- [20] C. Gómez-Hernández, K. Rezende-Oliveira, G. A. N. Nascentes et al., “Molecular characterization of *Trypanosoma cruzi* Mexican strains and their behavior in the mouse experimental model,” *Revista da Sociedade Brasileira de Medicina Tropical*, vol. 44, no. 6, pp. 684–690, 2011.
- [21] A. Vizcaino-Castillo, A. Jimenez-Marin, and B. Espinoza, “Exacerbated skeletal muscle inflammation and calcification in the acute phase of infection by Mexican *Trypanosoma cruzi* DTUI strain,” *BioMed Research International*, vol. 2014, Article ID 450389, 12 pages, 2014.
- [22] J. R. R. Coura and A. C. Junqueira, “Surveillance, health promotion and control of Chagas disease in the Amazon Region - medical attention in the Brazilian Amazon Region: a proposal,” *Memórias do Instituto Oswaldo Cruz*, vol. 110, no. 7, pp. 825–830, 2015.
- [23] M. S. Llewellyn, M. D. Lewis, N. Acosta et al., “*Trypanosoma cruzi* Ilc: phylogenetic and phylogeographic insights from sequence and microsatellite analysis and potential impact on emergent Chagas disease,” *PLoS Neglected Tropical Diseases*, vol. 3, no. 9, 2009.
- [24] B. A. de Noya, Z. Díaz-Bello, C. Colmenares et al., “Update on oral Chagas disease outbreaks in Venezuela: epidemiological, clinical and diagnostic approaches,” *Memórias do Instituto Oswaldo Cruz*, vol. 110, no. 3, pp. 377–386, 2015.
- [25] C. D. Alba Soto, M. E. Solana, C. V. Poncini, A. M. Pino-Martínez, V. Tekiel, and S. M. González-Cappa, “Dendritic cells devoid of IL-10 induce protective immunity against the protozoan parasite *Trypanosoma cruzi*,” *Vaccine*, vol. 28, no. 46, pp. 7407–7413, 2010.
- [26] E. J. Pearce and B. Everts, “Dendritic cell metabolism,” *Nature Reviews Immunology*, vol. 15, no. 1, pp. 18–29, 2014.
- [27] S. Hugues, “Dynamics of dendritic cell-T cell interactions: a role in T cell outcome,” *Seminars in Immunopathology*, vol. 32, no. 3, pp. 227–238, 2010.
- [28] S. P. Manickasingham, A. D. Edwards, O. Schulz, and C. Reis e Sousa, “The ability of murine dendritic cell subsets to direct T helper cell differentiation is dependent on microbial signals,” *European Journal of Immunology*, vol. 33, no. 1, pp. 101–107, 2003.
- [29] O. Takeuchi and S. Akira, “Pattern recognition receptors and inflammation,” *Cell*, vol. 140, no. 6, pp. 805–820, 2010.
- [30] J. S. Blum, P. A. Wearsch, and P. Cresswell, “Pathways of antigen processing,” *Annual Review of Immunology*, vol. 31, no. 1, pp. 443–473, 2013.
- [31] M. F. Lipscomb and B. J. Masten, “Dendritic cells: immune regulators in health and disease,” *Physiological Reviews*, vol. 82, no. 1, pp. 97–130, 2002.
- [32] B. M. O’Neill, D. Hanway, E. A. Winzeler, and F. E. Romesberg, “Coordinated functions of WSS1, PSY2 and TOF1 in the DNA damage response,” *Nucleic Acids Research*, vol. 32, no. 22, pp. 6519–6530, 2004.
- [33] R. Förster, A. Schubel, D. Breitfeld et al., “CCR7 coordinates the primary immune response by establishing functional microenvironments in secondary lymphoid organs,” *Cell*, vol. 99, no. 1, pp. 23–33, 1999.
- [34] S. R. Holdsworth and P.-Y. Y. Gan, “Cytokines: names and numbers you should care about,” *Clinical journal of the American Society of Nephrology*, vol. 10, no. 12, pp. 2243–2254, 2015.
- [35] V. Verhasselt, C. Buelens, F. Willems, D. De Groote, N. Haeflner-Cavaillon, and M. Goldman, “Bacterial lipopolysaccharide stimulates the production of cytokines and the expression of costimulatory molecules by human peripheral blood dendritic cells: evidence for a soluble CD14-dependent pathway,” *The Journal of Immunology*, vol. 158, no. 6, pp. 2919–2925, 1997.
- [36] F. R. S. Gutierrez, F. S. Mariano, C. J. F. Oliveira et al., “Regulation of *Trypanosoma cruzi*-induced myocarditis by programmed death cell receptor 1,” *Infection and Immunity*, vol. 79, no. 5, pp. 1873–1881, 2011.
- [37] C. V. Poncini, C. D. Alba Soto, E. Batalla, M. E. Solana, and S. M. González Cappa, “*Trypanosoma cruzi* induces regulatory dendritic cells in vitro,” *Infection and Immunity*, vol. 76, no. 6, pp. 2633–2641, 2008.
- [38] C. V. Poncini, J. M. Ilarregui, E. I. Batalla et al., “*Trypanosoma cruzi* Infection Imparts a Regulatory Program in Dendritic Cells and T Cells via Galectin-1-Dependent Mechanisms,” *The Journal of Immunology*, vol. 195, no. 7, pp. 3311–3324, 2015.
- [39] C. D. Alba Soto, G. A. Mirkin, M. E. Solana, and S. M. González Cappa, “*Trypanosoma cruzi* infection modulates in vivo expression of major histocompatibility complex class II molecules on antigen-presenting cells and T-cell stimulatory activity of dendritic cells in a strain-dependent manner,” *Infection and Immunity*, vol. 71, no. 3, pp. 1194–1199, 2003.
- [40] W. O. Dutra, C. A. S. Menezes, L. M. D. Magalhães, and K. J. Gollob, “Immunoregulatory networks in human Chagas disease,” *Parasite Immunology*, vol. 36, no. 8, pp. 377–387, 2014.
- [41] P. M. Nogueira, K. Ribeiro, A. C. O. Silveira et al., “Vesicles from different *Trypanosoma cruzi* strains trigger differential innate and chronic immune responses,” *Journal of Extracellular Vesicles*, vol. 4, no. 1, article 28734, 2015.
- [42] L. Planelles, M. C. Thomas, C. Marañón, M. Morell, and M. C. López, “Differential CD86 and CD40 co-stimulatory molecules and cytokine expression pattern induced by *Trypanosoma cruzi* in APCs from resistant or susceptible mice,” *Clinical and Experimental Immunology*, vol. 131, no. 1, pp. 41–47, 2003.
- [43] C. V. Poncini and S. M. González-Cappa, “Dual role of monocyte-derived dendritic cells in *Trypanosoma cruzi* infection,” *European Journal of Immunology*, vol. 47, no. 11, pp. 1936–1948, 2017.
- [44] V. M. Monteon, J. Furuzawa-Carballeda, R. Alejandro-Aguilar, A. Aranda-Fraustro, J. L. Rosales-Encina, and P. A. Reyes, “American trypanosomiasis: in situ and generalized features of parasitism and inflammation kinetics in a murine model,” *Experimental Parasitology*, vol. 83, no. 3, pp. 267–274, 1996.
- [45] R. Ruíz-Sánchez, M. P. León, V. Matta et al., “*Trypanosoma cruzi* isolates from Mexican and Guatemalan acute and chronic chagasic cardiopathy patients belong to *Trypanosoma*

- cruzi* I,” *Memórias do Instituto Oswaldo Cruz*, vol. 100, no. 3, pp. 281–283, 2005.
- [46] M. M. Teixeira and N. Yoshida, “Stage-specific surface antigens of metacyclic trypomastigotes of *Trypanosoma cruzi* identified by monoclonal antibodies,” *Molecular and Biochemical Parasitology*, vol. 18, no. 3, pp. 271–282, 1986.
- [47] D. Chaussabel, B. Pajak, V. Vercruyse et al., “Alteration of migration and maturation of dendritic cells and T-cell depletion in the course of experimental *Trypanosoma cruzi* infection,” *Laboratory Investigation*, vol. 83, no. 9, pp. 1373–1382, 2003.
- [48] S. Malaga and N. Yoshida, “Targeted reduction in expression of *Trypanosoma cruzi* surface glycoprotein gp90 increases parasite infectivity,” *Infection and Immunity*, vol. 69, no. 1, pp. 353–359, 2001.
- [49] N. Yoshida, “Molecular basis of mammalian cell invasion by *Trypanosoma cruzi*,” *Anais da Academia Brasileira de Ciências*, vol. 78, no. 1, pp. 87–111, 2006.
- [50] J. de Meis, J. Barreto de Albuquerque, D. Silva dos Santos et al., “*Trypanosoma cruzi* entrance through systemic or mucosal infection sites differentially modulates regional immune response following acute infection in mice,” *Frontiers in Immunology*, vol. 4, p. 216, 2013.
- [51] B. L. Ferreira, É. R. Ferreira, M. V. de Brito et al., “BALB/c and C57BL/6 mice cytokine responses to *Trypanosoma cruzi* infection are independent of parasite strain infectivity,” *Frontiers in Microbiology*, vol. 9, p. 553, 2018.
- [52] P. M. Henrique, T. Marques, M. V. da Silva et al., “Correlation between the virulence of *T. cruzi* strains, complement regulatory protein expression levels, and the ability to elicit lytic antibody production,” *Experimental Parasitology*, vol. 170, pp. 66–72, 2016.
- [53] B. A. Burleigh and N. W. Andrews, “Signaling and host cell invasion by *Trypanosoma cruzi*,” *Current Opinion in Microbiology*, vol. 1, no. 4, pp. 461–465, 1998.
- [54] R. A. Mortara, “*Trypanosoma cruzi*: amastigotes and trypomastigotes interact with different structures on the surface of HeLa cells,” *Experimental Parasitology*, vol. 73, no. 1, pp. 1–14, 1991.
- [55] F. Y. Maeda, T. M. Clemente, S. Macedo, C. Cortez, and N. Yoshida, “Host cell invasion and oral infection by *Trypanosoma cruzi* strains of genetic groups TcI and TcIV from chagasic patients,” *Parasites & Vectors*, vol. 9, no. 1, p. 189, 2016.
- [56] R. C. Ruiz, S. Favoreto, L. M. Dorta et al., “Infectivity of *Trypanosoma cruzi* strains is associated with differential expression of surface glycoproteins with differential Ca²⁺ signalling activity,” *Biochemical Journal*, vol. 330, no. 1, pp. 505–511, 1998.
- [57] S. C. Goncalves da Costa, K. S. Calabrese, T. Zaverucha do Valle, and P. H. Lagrange, “*Trypanosoma cruzi*: infection patterns in intact and athymic mice of susceptible and resistant genotypes,” *Histology and Histopathology*, vol. 17, no. 3, pp. 837–844, 2002.
- [58] E. Roggero, A. Perez, M. Tamae-Kakazu et al., “Differential susceptibility to acute *Trypanosoma cruzi* infection in BALB/c and C57BL/6 mice is not associated with a distinct parasite load but cytokine abnormalities,” *Clinical & Experimental Immunology*, vol. 128, no. 3, pp. 421–428, 2002.
- [59] P. S. Doyle, Y. M. Zhou, I. Hsieh, D. C. Greenbaum, J. H. McKerrow, and J. C. Engel, “The *Trypanosoma cruzi* protease cruzain mediates immune evasion,” *PLoS Pathogens*, vol. 7, no. 9, 2011.
- [60] C. A. Hunter, L. A. Ellis-Neyes, T. Slifer et al., “IL-10 is required to prevent immune hyperactivity during infection with *Trypanosoma cruzi*,” *The Journal of Immunology*, vol. 158, no. 7, pp. 3311–3316, 1997.
- [61] J. S. Silva, D. R. Twardzik, and S. G. Reed, “Regulation of *Trypanosoma cruzi* infections in vitro and in vivo by transforming growth factor beta (TGF-beta),” *The Journal of Experimental Medicine*, vol. 174, no. 3, pp. 539–545, 1991.
- [62] T. Kawai and S. Akira, “The role of pattern-recognition receptors in innate immunity: update on Toll-like receptors,” *Nature Immunology*, vol. 11, no. 5, pp. 373–384, 2010.
- [63] E. B. Kopp and R. Medzhitov, “The Toll-receptor family and control of innate immunity,” *Current opinion in immunology*, vol. 11, no. 1, pp. 13–18, 1999.
- [64] M. M. Rodrigues, A. C. Oliveira, and M. Bellio, “The immune response to *Trypanosoma cruzi*: role of toll-like receptors and perspectives for vaccine development,” *Journal of Parasitology Research*, vol. 2012, Article ID 507874, 12 pages, 2012.
- [65] I. C. Almeida and R. T. Gazzinelli, “Proinflammatory activity of glycosylphosphatidylinositol anchors derived from *Trypanosoma cruzi*: structural and functional analyses,” *Journal of Leukocyte Biology*, vol. 70, no. 4, pp. 467–477, 2001.
- [66] M. A. S. Campos, I. C. Almeida, O. Takeuchi et al., “Activation of Toll-like receptor-2 by glycosylphosphatidylinositol anchors from a protozoan parasite,” *The Journal of Immunology*, vol. 167, no. 1, pp. 416–423, 2001.
- [67] A. C. Oliveira, J. R. Peixoto, L. B. de Arruda et al., “Expression of functional TLR4 confers proinflammatory responsiveness to *Trypanosoma cruzi* glycoinositolphospholipids and higher resistance to infection with *T. cruzi*,” *The Journal of Immunology*, vol. 173, no. 9, pp. 5688–5696, 2004.
- [68] D. E. Gaddis, C. L. Maynard, C. T. Weaver, S. M. Michalek, and J. Katz, “Role of TLR2-dependent IL-10 production in the inhibition of the initial IFN- γ T cell response to *Porphyromonas gingivalis*,” *Journal of Leukocyte Biology*, vol. 93, no. 1, pp. 21–31, 2013.
- [69] C. H. Kim, L. S. Rott, I. Clark-Lewis, D. J. Campbell, L. Wu, and E. C. Butcher, “Subspecialization of Cxcr5⁺ T cells,” *Journal of Experimental Medicine*, vol. 193, no. 12, pp. 1373–1382, 2001.

Research Article

Inhibition of CD83 Alleviates Systemic Inflammation in Herpes Simplex Virus Type 1-Induced Behçet's Disease Model Mouse

S. M. Shamsul Islam,¹ Hae-Ok Byun,² Bunsun Choi ,³ and Seonghyang Sohn ^{1,2}

¹Department of Biomedical Science, Ajou University School of Medicine, Suwon 16499, Republic of Korea

²Department of Microbiology, Ajou University School of Medicine, Suwon 16499, Republic of Korea

³Institute for Medical Sciences, Ajou University School of Medicine, Suwon 16499, Republic of Korea

Correspondence should be addressed to Seonghyang Sohn; sohnsh@ajou.ac.kr

Received 16 April 2019; Revised 12 July 2019; Accepted 8 August 2019; Published 9 September 2019

Guest Editor: Renata Sesti-Costa

Copyright © 2019 S. M. Shamsul Islam et al. This is an open access article distributed under the Creative Commons Attribution License, which permits unrestricted use, distribution, and reproduction in any medium, provided the original work is properly cited.

Behçet's disease (BD) is an autoinflammatory disease that can lead to life- and sight-threatening complications. Dendritic cells (DCs) are the most potent antigen-presenting cells that can regulate multiple inflammatory pathways. The objective of this study was to investigate the association of the DC stimulatory molecule CD83 with BD. Frequencies of costimulatory molecules expressing DCs in peripheral blood leukocytes (PBL) were measured by flow cytometry (FACS). The severity of symptoms in HSV-1-induced BD symptomatic mice was also assessed. Frequencies of CD83-positive cells were significantly increased in mice exhibiting BD symptoms, compared to those in asymptomatic mice. Abatacept, a CD80/86 blocker, significantly decreased the frequencies of CD83-positive cells in a time- and dose-dependent manner. BD symptomatic mice treated with Abatacept showed gradual reduction in the severity score of symptoms. Intraperitoneal injection of CD83 siRNA significantly reduced the frequencies of CD83-positive cells in PBL and peritoneal macrophages. After CD83 siRNA injection, BD symptoms of mice were improved and disease severity was decreased. Discontinuation of CD83 siRNA deteriorated symptoms while readministration of CD83 siRNA again improved BD symptoms of mice. These results clearly indicate the involvement of CD83-expressing cells in the inflammatory symptoms of BD. Therefore, CD83 might be useful as a therapeutic target for BD.

1. Introduction

Behçet's disease (BD) is a multisystemic autoinflammatory disease with inflammatory lesion as its main clinical feature that can affect the skin, joints, eye, intestinal tract, genital area, and nervous system. The exact etiology of BD is currently unclear. However, several factors including environmental, genetic, infectious, and/or immunologic dysregulation have been suggested as possible triggering factors. Herpes simplex virus (HSV) is considered as one of the triggering factors in BD. HSV viral DNA particles have been identified in ocular fluids [1], peripheral blood leukocytes [2], saliva [3], and skin lesions [4], of BD patients. Serum anti-HSV-1 antibodies [2] have also been identified in BD patients. HSV-1-induced model mice show similar clinical manifestations, including genital ulcer, oral ulcer, skin lesions, eye lesions, arthritis, and

intestinal ulcers [5]. When evaluated in immune modulatory experiments, HSV-1-induced model mice are very similar to those of human BD disease patterns [6].

Dendritic cells (DCs) are the most potent antigen-presenting cells (APCs) that can effectively connect innate and adaptive immune systems. Due to its unique ability to induce the activation and differentiation of T lymphocytes, many investigators focus on DC-mediated immune response. DCs are involved in several autoimmune diseases, such as inflammatory bowel disease (IBD) [7], rheumatoid arthritis (RA) [8], uveitis [9], and Crohn's disease (CD) [10]. Upon antigen capture, DCs undergo a process of maturation. Mature DCs then acquire the ability to differentiate naïve T cells, B cells, and NK cells. They also express cytokines [11]. During maturation, DCs accumulate peptides and upregulate expression levels of the major histocompatibility complex (MHC) and costimulatory molecules such as CD40, CD80,

CD83, and CD86 [12]. Among costimulatory molecules, CD83 plays an important role in immune response besides its function as an activation marker [13]. HSV-1-infected DCs can lead to degradation of CD83 within 6 to 8 hours after infection [14]. They also lead to inhibition of the CD83 mRNA transport, thus significantly inhibiting DC-mediated T lymphocyte activation [15]. CD83 upregulation and selective expression, together with CD80 and CD86, suggest an important role of CD83 in immune response [16]. CD83 is a membrane integral protein [17], and soluble CD83 (sCD83) is produced by the release of cell surface CD83 molecules [18]. Elevated levels of sCD83 have been found in plasma and synovial fluids of RA patients [19, 20] and in those with hematological malignancies [21]. Although the functions of CD83 ligands (CD83L) remain controversial, it is believed that when they are stimulated with CD3 and CD28, activated T cells can express CD83L, suggesting that CD83L might function in immune response when T cells are activated in the presence of the costimulatory signal provided by CD83 APCs [22]. The specific role of CD83 in the regulation of immune response is not yet well known. However, the manipulation of the CD83 pathway has been proposed to develop therapeutics for the treatment of inflammation and autoimmune diseases [18]. Blocking CD83 function or its ligand has not yet been demonstrated in BD. Therefore, the purpose of this study was to determine whether blocking CD83 function could affect BD symptoms in a mouse model.

2. Materials and Methods

2.1. Animal Experiment. Institute of Cancer Research (ICR) (CD1) mice at 4 to 5 weeks old were infected with HSV type 1 (1×10^6 plaque-forming unit (pfu)/mL, F strain) grown in Vero cells as previously described [5]. Virus inoculation was performed twice with a 10-day interval followed by 16 weeks of observation. Mice were bred in temperature- and light-controlled conventional rooms (20–22°C, 12 h light/dark cycle). These mice had *ad libitum* access to food and water. During the experimental period, animals were closely observed and photographed. Animals were handled in accordance with a protocol approved by the Institutional Animal Care and Use Committee of Ajou University (approval number: AMC-2018-0017).

2.2. BD Symptomatic Mouse Induced by HSV-1. Virus inoculation was performed using the published procedures [5]. Briefly, earlobes of mice were scratched with a needle and inoculated with 20 μ L of 1×10^6 pfu/mL of HSV-1 (F strain) that had been grown in Vero cells. Virus inoculation was performed twice with a 10-day interval. For virus inoculation, mice were euthanized by intramuscular injection in the hind leg with Ketamine/Xylazine cocktail (15 mg/kg Ketamine and 10 mg/kg Xylazine). Several symptoms were observed in mice after HSV inoculation. The incidence of BD was 15% of HSV-inoculated mice, including oral ulcers, genital ulcers, erythema, skin pustules, skin ulcers, arthritis, diarrhea, red eye, loss of balance, and facial swelling. Oral, genital, skin ulcers, and eye symptoms were classified as

major symptoms while arthritis, intestinal ulceration, and neurological involvement were considered as minor symptoms. Mice with one or more major symptoms and one or more minor symptoms were classified as having BD. Each symptom score was one. The sum of the scores of different symptoms was used to determine the severity of BD using BD current activity from 2006 prepared by the International Society for Behçet's Disease (<http://medhealth.leeds.ac.uk/download/910/behcetdsdiseaseactivityform>). Loss of symptoms or a reduction in lesion size of more than 20% was an indicator of BD improvement. The control group was inoculated with HSV. Asymptomatic healthy mice were used as BD normal (BDN) as previously described [5].

2.3. Medication to the Mice. To normal mice, 1 or 2 mg Abatacept per day was administered for 3 consecutive days via intraperitoneal injection. To BD mice, 2 mg Abatacept per mouse for 3 times with 3-day intervals was applied. As a control group, PBS was treated to normal or BD mice. CD83 siRNA was mixed with jetPEI transfection reagent (Polyplus-transfection, Illkirch-Graffenstaden, France) and used for *in vivo* transfection. For siRNA application to mice, 0.5 or 1.0 μ mol of CD83 siRNA was dissolved in 200 μ L of 5% glucose solution, mixed with transfection reagent jetPEI, and intraperitoneally injected into normal or BD mice for 4 times with 3-day intervals. As a control, scramble siRNA was applied to normal and BD mice following the same procedure as CD83 siRNA injection. At 2 h after the final injection, mice were sacrificed. Leukocytes isolated from peripheral blood (PBL) and macrophages from the peritoneal cavity were then isolated for further analysis.

2.4. Preparation of siRNA. CD83 siRNA oligonucleotides with the following sense and antisense sequences were synthesized by Integrated DNA Technologies (Coralville, IA, USA). Synthesized sequences of CD83 siRNA were as follows: 5'-GUGCUUUUCAGUCAUCUACAAGCTA-3' and 3'-CUCACGAAAAGUCAGUAGAUGUUCGAU-5'. For injection into mice, CD83 siRNA was mixed with transfection reagent [23].

2.5. Generation of Mouse Bone Marrow-Derived DCs. Bone marrow-derived dendritic cells (BMDCs) were obtained from femurs of mice, and red blood cells (RBC) were treated with ACK solution for RBC lysis. These cells were cultured in RPMI media (Gibco, Grand Island, NY, USA) supplemented with 10% fetal bovine serum, 2 ng/mL recombinant mouse IL-4 (ProSpec, NJ, USA), and 20 ng/mL recombinant mouse GM-CSF (ProSpec, NJ, USA). The culture medium was changed at 3 and 6 days after culture. New medium and cytokines (rmIL-4 and rmGM-CSF) were added after rinsing cells. Cells were harvested for experiments on day 9.

2.6. siRNA Transfection. Bone marrow-derived cells (2.5×10^5 /well) were seeded into 6-well plates in 2 mL of culture medium and treated with cytokines (rmIL-4 and rmGM-CSF). siRNA transfections were performed using

jetPEI reagent according to the instructions of the manufacturer. Cells were transfected with 100 ng/well of CD83 siRNA (Integrated DNA Technologies, CA, USA) and scramble siRNA (Bioneer, Daejeon, Korea) at day 3 after cell seeding. siRNA treatment was three times with 3-day intervals. After the final treatment, 2 hours later, cells were harvested for further analysis.

2.7. Flow Cytometric Analysis. PBL and peritoneal macrophages of mice were washed with phosphate-buffered saline (PBS) and stained with PerCP-eFluor-labeled anti-mouse CD40, eFluor 660-labeled anti-mouse CD83, PE-Cyanine7-labeled anti-mouse CD80, and FITC-labeled anti-mouse CD86 (eBioscience, San Diego, CA, USA) at 4°C for 30 min in the dark. For identification of regulatory T cells (Treg cells), isolated PBL was stained with PE-Cyanine7-labeled anti-mouse CD4 and PE-labeled anti-mouse CD25 for 30 min at 4°C in the dark. For intranuclear detection of Foxp3, an anti-mouse Foxp3 staining kit (eBioscience, San Diego, CA, USA) was used, according to the manufacturer's instructions. Briefly, cells were fixed using Fix/Perm buffer and, after washing with 1x permeabilization buffer, were incubated with PE-Cyanine5-labeled anti-mouse Foxp3 Ab for 30 min at 4°C in the dark. Stained cells were analyzed by a FACS Aria III flow cytometer (Becton Dickinson, San Jose, CA, USA) with $\geq 10,000$ gated cells.

2.8. Measurement of Cytokine by Enzyme-Linked Immunosorbent Assay (ELISA). After each mouse was sacrificed, blood was collected from the heart and serum was analyzed using a commercial ELISA kit for the IL-17 level (R&D Systems, Minneapolis, MN, USA). ELISA was conducted according to the manufacturer's instructions. Absorbance values of samples were read at a wavelength of 450 nm using a Bio-Rad model 170-6850 microplate reader (Hercules, CA, USA). ELISA was repeated three times in duplicate wells.

2.9. Morphological Observation under Transmission Electron Microscopy (TEM). Cellular morphological changes were observed under transmission electron microscopy. Cultured DCs were fixed with Karnovsky's fixative solution for 2 h at room temperature and postfixed with osmium tetroxide for 30 min. Fixed cells were washed with cacodylate buffer, dehydrated in graded ethanol, embedded in epon mixture, and incubated at 60°C for 48 h. Epon blocs were sectioned with an ultramicrotome (Reichert-Jung, Bayreuth, Germany), stained with uranium acetate and lead citrate, and then observed under the electron microscope (Zeiss, Oberkochen, Germany).

2.10. Statistical Analysis. All data are represented as mean \pm SD. Statistical differences between experimental groups were determined by Student's *t*-test and Bonferroni correction. Statistical analysis was conducted using MedCalc® version 9.3.0.0. (MedCalc, Ostend, Belgium). Statistical significance was considered when the *p* value was less than 0.05.

3. Result

3.1. Frequencies of CD40-, CD83-, CD80-, and CD86-Expressing Cells in Normal, HSV-Infected, BD Normal (BDN), and BD Mice. Frequencies of DC-expressing costimulatory molecules CD40+, CD83+, CD80+, and CD86+ cells in PBL of mice were analyzed by FACS. Frequencies of CD83+ cells in BD mice ($n = 5$) were significantly elevated compared to those in BDN ($n = 8$) mice ($41.0 \pm 11.28\%$ vs. $25.85 \pm 7.86\%$, $p = 0.01$), HSV-infected mice ($n = 5$) ($28.56 \pm 4.59\%$, $p = 0.05$), and control mice ($n = 8$) ($29.92 \pm 8.18\%$, $p = 0.06$) (Figure 1(b)). However, frequencies of CD86+ cells in PBL of BD mice were significantly downregulated compared to those in healthy control mice ($5.18 \pm 2.11\%$ vs. $11.91 \pm 4.55\%$, $p = 0.01$) (Figure 1(d)). Frequencies of CD86+ cells were also downregulated in HSV-infected mice ($4.94 \pm 0.92\%$ vs. $11.91 \pm 4.55\%$, $p = 0.006$) and BDN mice ($6.47 \pm 3.47\%$ vs. $11.91 \pm 4.55\%$, $p = 0.01$) compared with control mice. Frequencies of CD80+ cells in BDN mice were downregulated compared to those in control mice ($50.15 \pm 7.30\%$ vs. $60.88 \pm 6.70\%$, $p = 0.008$) (Figure 1(c)). However, there was no statistically significant difference in the frequencies of CD40+ cells among groups (Figure 1(a)). Figure 1(e) shows representative histograms of CD83+ cells and CD86+ cells in normal healthy control, HSV, BDN, and BD mice (*n* indicates the number of mice used in the analysis). To know what population of PBL cells was more correlated to the expression of CD83, the population was gated and CD83+ cells were analyzed. In granulocytes, the frequencies of CD83+ cells were significantly different in BD mice compared with normal ($64.74 \pm 16.44\%$ vs. $41.86 \pm 14.84\%$, $p = 0.02$) and BDN mice ($64.74 \pm 16.44\%$ vs. $28.7 \pm 5.70\%$, $p = 0.0002$). In lymphocytes and in monocytes, the frequencies of CD83+ cells were not significantly different between BD and control groups (Fig. S1 of the Supplementary Data).

3.2. Administration of Abatacept Inhibits CD83+ Cell Frequencies in Normal Mice in a Dose- and Time-Dependent Manner and Improves BD Symptoms. Abatacept is a fusion protein of the extracellular domain of CTLA-4 and immunoglobulin Fc portion known as a CD80/86 blocker [24]. Abatacept treatment of 2 mg/mouse, once a day for 3 consecutive days, to normal mice significantly decreased frequencies of CD40+ cells ($15.26 \pm 3.77\%$ vs. $35.13 \pm 9.50\%$, $p = 0.02$), CD83+ cells ($10.46 \pm 3.25\%$ vs. $22.43 \pm 3.44\%$, $p = 0.01$), CD80+ cells ($36.66 \pm 2.74\%$ vs. $50.86 \pm 2.77\%$, $p = 0.003$), and CD86+ cells ($3.16 \pm 1.25\%$ vs. $9.26 \pm 3.23\%$, $p = 0.03$) (Figures 2(a)–2(d)) in PBL of normal mice compared to the control. CD83+ cell frequencies were also decreased after Abatacept treatment in a time-dependent manner from day 1 to day 3 ($18.63 \pm 1.76\%$ vs. $10.46 \pm 3.25\%$, $p = 0.01$) (Figure 2(e)). GC7 (N1-guanyl-1,7-diaminoheptane), an inhibitor of hypusine formation, also known as an inhibitor of CD83 [15], was used to treat normal mice to determine whether GC7 could decrease CD83+ cell frequencies. The results showed that there was no significant difference in CD83+ cell frequencies

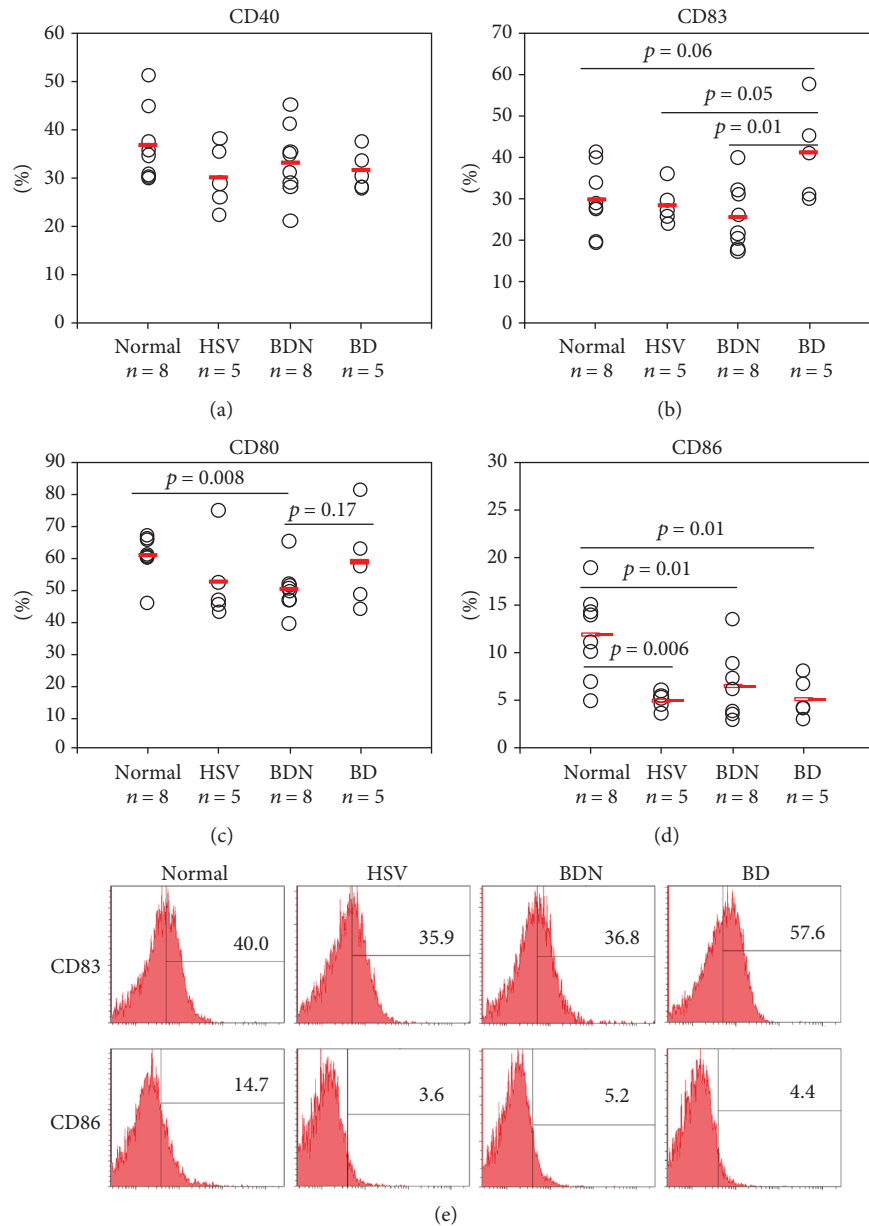


FIGURE 1: (a–d) Frequencies of DC costimulatory molecules CD40, CD83, CD80, and CD86 in the surface of peripheral blood leukocytes (PBL) were evaluated by flow cytometry analysis. (e) Representative histogram of frequencies of CD83+ and CD86+ cells in PBL. The p value was determined by Student's t -test. The number of mice used for experiments are 8 in normal, 5 in HSV-1, 8 in BDN, and 5 in BD. n indicates the number of mice in each group. Experiments were performed more than three independent times.

between before and after GC7 treatment (Fig. S2 of the Supplementary Data). Frequencies of CD40+ cells ($21.91 \pm 7.58\%$ vs. $31.64 \pm 4.11\%$, $p = 0.02$) and CD83+ cells ($28.08 \pm 10.54\%$ vs. $41.0 \pm 11.28\%$, $p = 0.06$) were significantly decreased in BD mice treated with Abatacept compared to those in nontreated BD mice (Figures 2(f) and 2(g)). However, frequencies of CD86+ cells ($7.62 \pm 0.93\%$ vs. $5.18 \pm 2.11\%$, $p = 0.05$) were increased in BD mice after treatment with Abatacept compared to those in non-treated control BD mice (Figure 2(i)). Frequencies of CD80+ cells ($67.16 \pm 8.65\%$ vs. $58.92 \pm 14.53\%$, $p = 0.22$) were not significantly changed after treatment with Abatacept (Figure 2(h)).

3.3. Frequencies of Regulatory T Cells in Abatacept-Treated BD Mice. CD4+CD25+ Foxp3+ regulatory T (Treg) cells were analyzed by flow cytometry analysis. Frequencies of CD4+ T cell in BD mice were significantly downregulated compared to those in BDN mice ($11.92 \pm 7.78\%$ vs. $22.23 \pm 7.16\%$, $p = 0.01$). They were slightly elevated after Abatacept treatment (before and after treatment: $11.92 \pm 7.78\%$ vs. $16.41 \pm 3.54\%$, $p = 0.19$) (Figure 2(m)). Frequencies of Foxp3+ cells were more downregulated in BD mice than those in BDN mice ($2.76 \pm 1.86\%$ vs. $5.06 \pm 3.20\%$, $p = 0.10$). They were marginally but not significantly increased by Abatacept treatment (before and after treatment: $2.76 \pm 1.86\%$ vs. $3.50 \pm 1.44\%$, $p = 0.42$) (Figure 2(o)). Frequencies

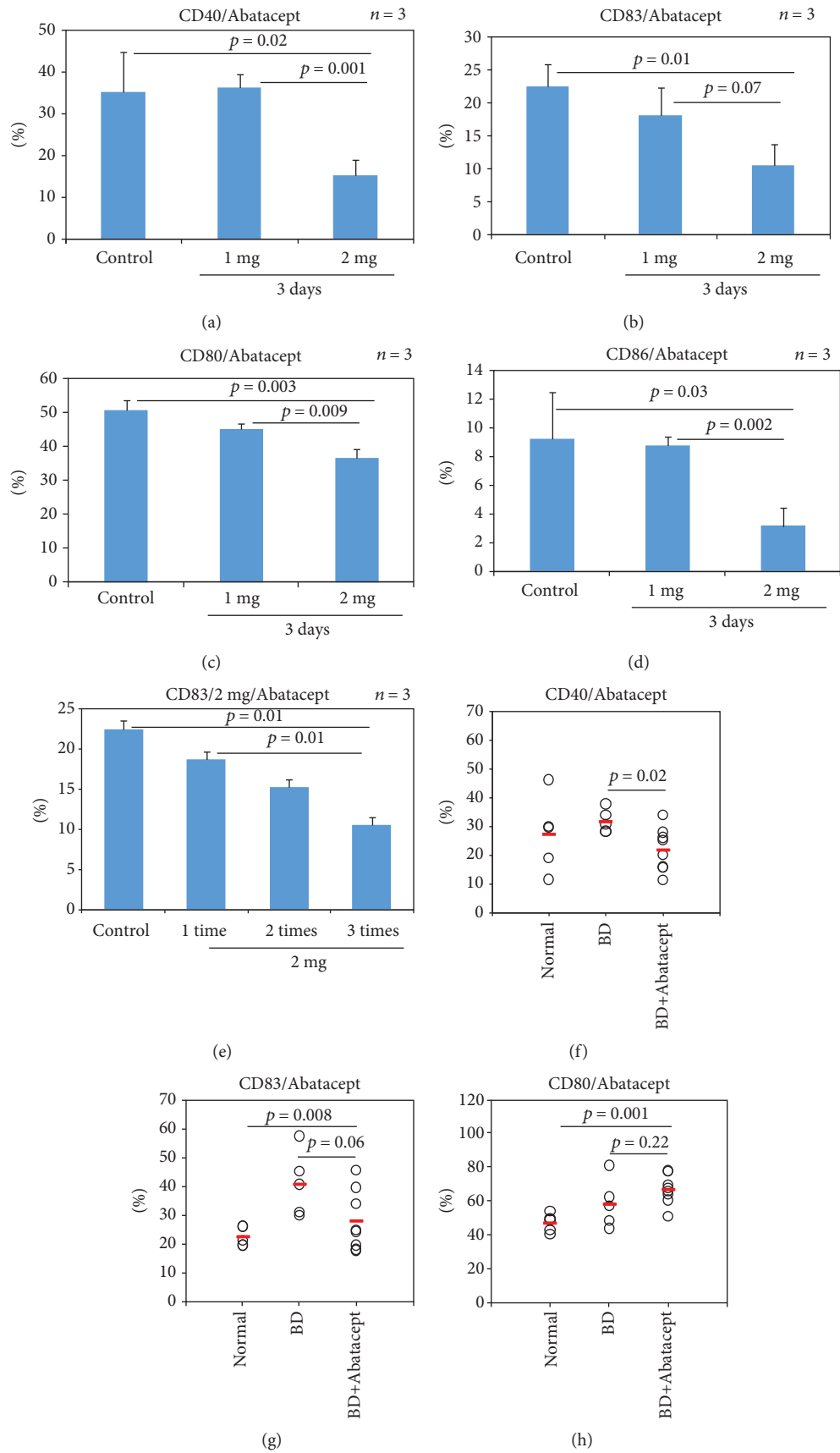


FIGURE 2: Continued.

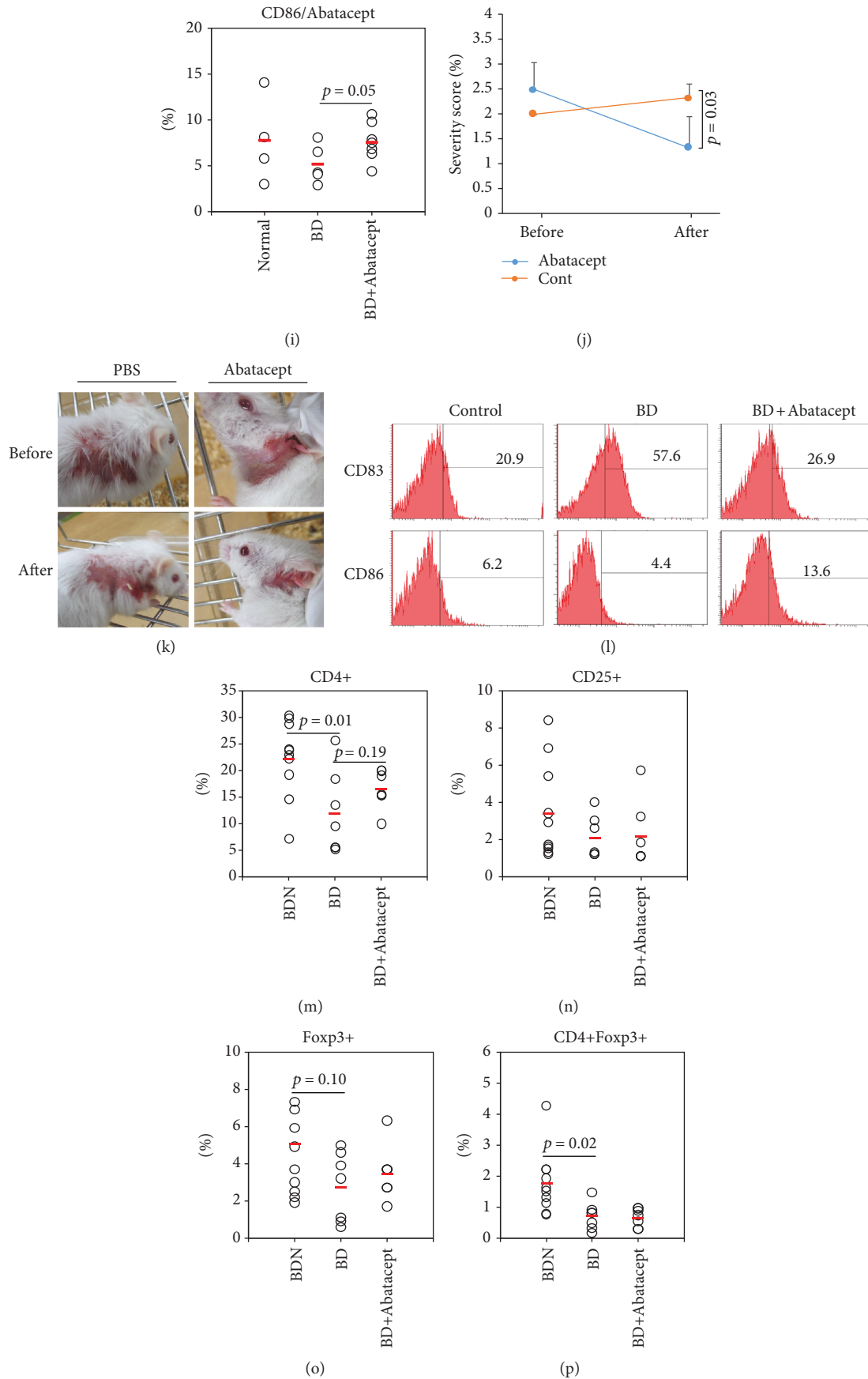


FIGURE 2: Continued.

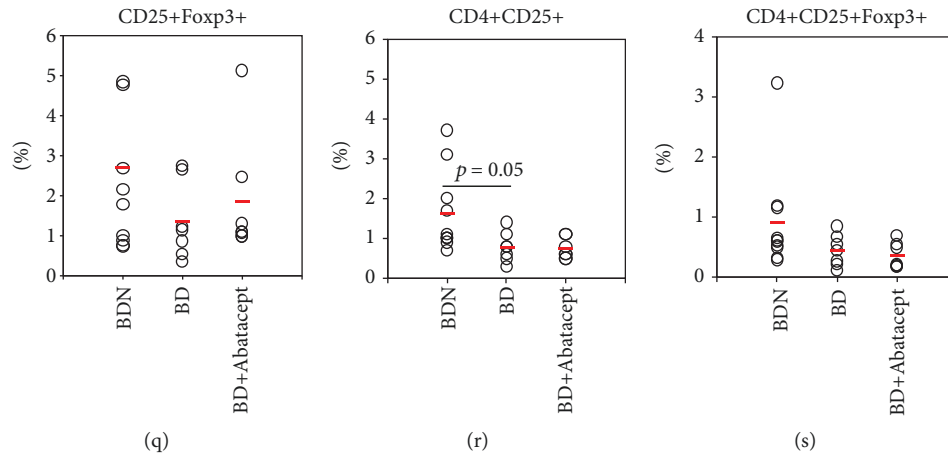


FIGURE 2: Abatacept affected the frequencies of CD83+ cells in normal and BD mice. (a–d) Frequencies of DC costimulatory molecules CD40, CD83, CD80, and CD86 in normal mice treated with Abatacept in the surface of peripheral blood leukocytes were evaluated by FACS analysis ($n = 3$ for each group). (e) Abatacept 2 mg for 1 to 3 days in normal mice was evaluated by FACS analysis ($n = 3$ for each group). (f–i) Frequencies of CD40, CD83, CD80, and CD86 in BD mice treated with Abatacept were evaluated by FACS analysis ($n = 5$ in normal, $n = 5$ in BD, and $n = 8$ in BD+Abatacept). (j, k) Abatacept treatment decreased the disease severity score and improved symptoms. (l) Representative histograms of CD83+ and CD86+ cell frequencies in PBL of BD mice treated with Abatacept. Regulatory T cells in BD mice were analyzed by FACS analysis. (m–s) Frequencies of CD4+, CD4+Foxp3+, CD4+CD25+, and CD4+CD25+Foxp3+ Treg cells in BDN, BD, and Abatacept-treated BD mice were evaluated by FACS analysis ($n = 10$ in BDN, $n = 7$ in BD, and $n = 5$ in BD+Abatacept). n indicates the number of mice used in each group. The p value was determined by Student's t -test. Experiments were performed more than three independent times.

of CD4+Foxp3+ cells were significantly decreased in BD mice compared to those in BDN mice ($0.71 \pm 0.43\%$ vs. $1.77 \pm 1.01\%$, $p = 0.02$) (Figure 2(p)). Frequencies of CD4+CD25+ cells were also lower in BD mice than those in BDN mice ($0.78 \pm 0.37\%$ vs. $1.62 \pm 1.02\%$, $p = 0.05$) (Figure 2(r)). Frequencies of CD4+CD25+Foxp3+ Treg cells were downregulated in BD mice compared to BDN mice. However, such difference was not statistically significant (Figure 2(s)).

3.4. Abatacept Treatment Decreases the Disease Severity Score and Ameliorates BD Symptoms in Mice. To determine whether Abatacept could manage BD symptoms, 2 mg Abatacept was intraperitoneally injected to BD mice 3 times with 2-day intervals and BD symptoms were traced for one week. Only PBS was injected to BD mice as control. The severity score of Abatacept-treated BD mice was significantly decreased at one week after treatment compared to that of PBS-treated BD mice ($1.33 \pm 0.62\%$ vs. $2.33 \pm 0.28\%$, $p = 0.03$) (Figure 2(j)). Figure 2(k) shows the changes of BD symptoms at 1 week after Abatacept treatment. Figure 2(l) shows representative histograms of CD83+ and CD86+ cells in normal, BD, and Abatacept-treated BD mice.

3.5. CD83 siRNA Suppresses CD83+ Cell Frequencies in Normal Mice. CD83 siRNA was used to treat normal mice to suppress the surface expression of CD83. Frequencies of CD83+ cells were measured by FACS analysis. Intraperitoneal treatment of CD83 siRNA to normal mice decreased frequencies of CD83+ cells in peritoneal macrophages ($6.74 \pm 1.62\%$ vs. $14.4 \pm 3.12\%$, $p = 0.002$) and in PBL ($24.3 \pm 3.01\%$ vs. $32.6 \pm 7.83\%$, $p = 0.06$) (Figure 3(b)) compared with the scramble siRNA treatment group.

CD83 siRNA treatment also decreased CD80+ cell frequencies in PBL ($62.18 \pm 2.40\%$ vs. $70.0 \pm 2.35\%$, $p = 0.001$) compared with the scramble siRNA treatment group (Figure 3(c)). There were no significant differences observed in CD40+ and CD86+ cells in PBL and peritoneal macrophages.

3.6. CD83 siRNA Treatment Affects BD Symptoms and Decreases the Disease Severity Score of Mice. The frequencies of CD83+ cells in BD mice treated with CD83 siRNA were measured by FACS analysis. Intraperitoneal injection of CD83 siRNA at $0.5 \mu\text{mol}/\text{mouse}$ ($12.32 \pm 5.67\%$ vs. $24.5 \pm 3.19\%$, $p = 0.006$) and $1 \mu\text{mol}/\text{mouse}$ ($8.38 \pm 4.95\%$ vs. $24.5 \pm 3.19\%$, $p = 0.0004$) to BD mice significantly decreased the frequencies of CD83+ cells in peritoneal macrophages, compared with injection with scramble siRNA (Figure 3(f)). In PBL, the $0.5 \mu\text{mol}$ - ($38.51 \pm 9.69\%$ vs. $52.22 \pm 3.07\%$, $p = 0.02$) and $1 \mu\text{mol}$ -treated groups ($24.66 \pm 16.52\%$ vs. $52.22 \pm 3.07\%$, $p = 0.01$) showed lower frequencies of CD83+ cells compared to the scramble siRNA-treated group (Figure 3(f)). Frequencies of CD40+ cells in peritoneal macrophages were downregulated in $0.5 \mu\text{mol}$ ($25.96 \pm 8.44\%$ vs. $36.07 \pm 2.67\%$, $p = 0.05$) and $1 \mu\text{mol}$ ($17.38 \pm 11.80\%$ vs. $36.07 \pm 2.67\%$, $p = 0.01$) CD83 siRNA-treated BD mice compared to those in the scramble siRNA-treated control group (Figure 3(e)). They were also decreased in PBL of the $1 \mu\text{mol}$ CD83 siRNA-treated group compared to those in the scramble siRNA-treated control ($16.85 \pm 6.30\%$ vs. $29.1 \pm 3.77\%$, $p = 0.008$) (Figure 3(e)). Frequencies of CD86+ cells in peritoneal macrophages of $1 \mu\text{mol}$ CD83 siRNA-treated BD mice were also decreased compared to those in the scramble siRNA-treated control group ($0.65 \pm 0.35\%$ vs. $1.37 \pm 0.28\%$, $p = 0.009$), although no significant differences were found in

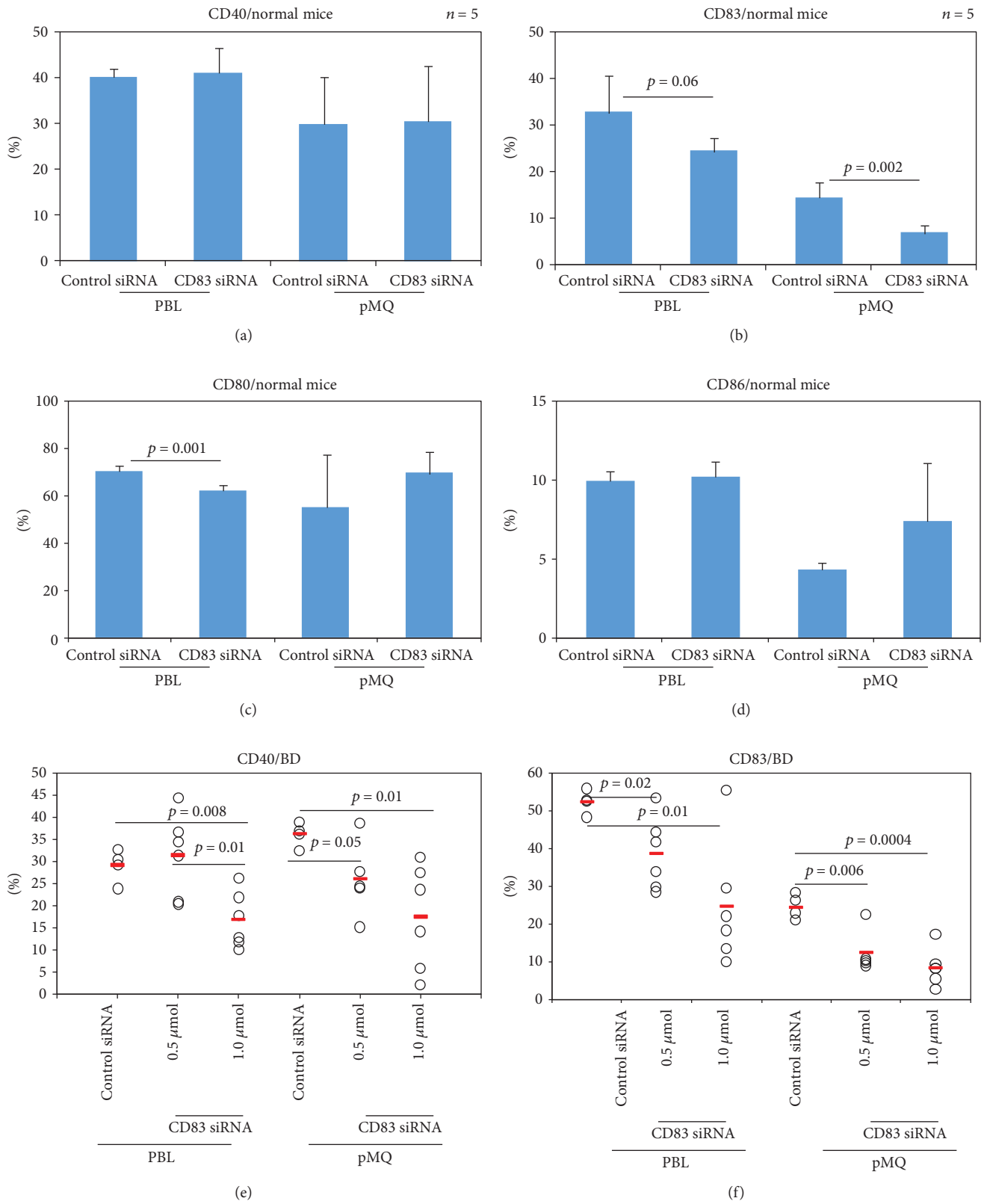


FIGURE 3: Continued.

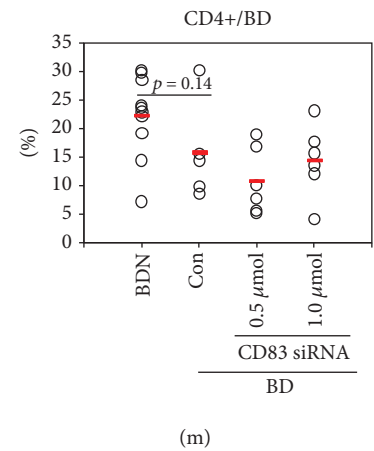
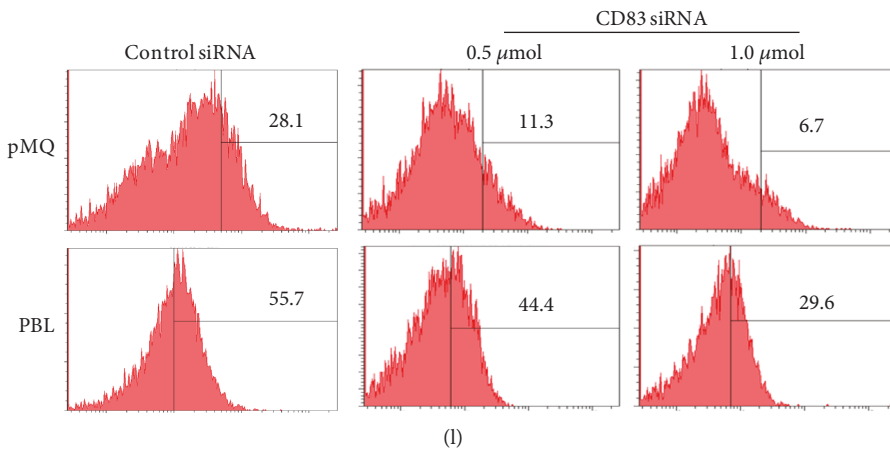
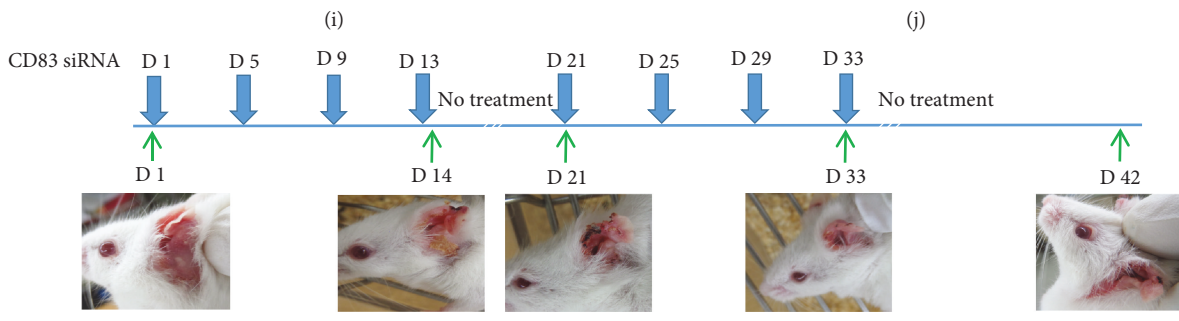
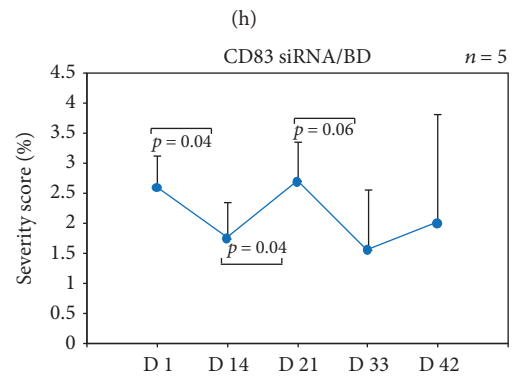
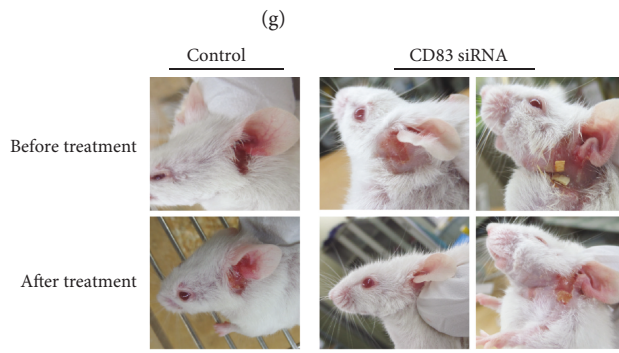
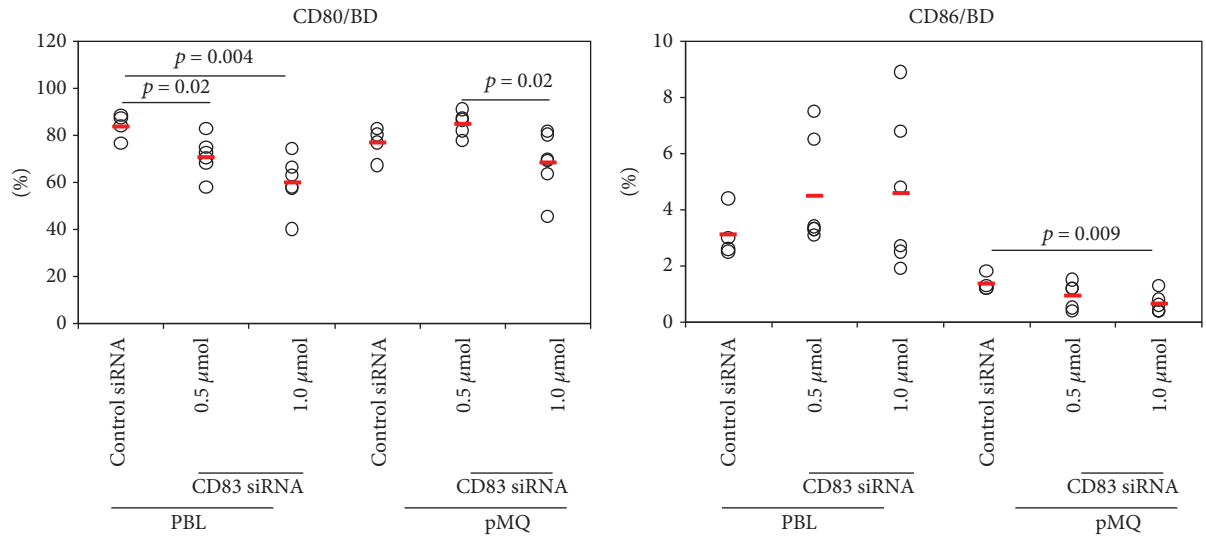


FIGURE 3: Continued.

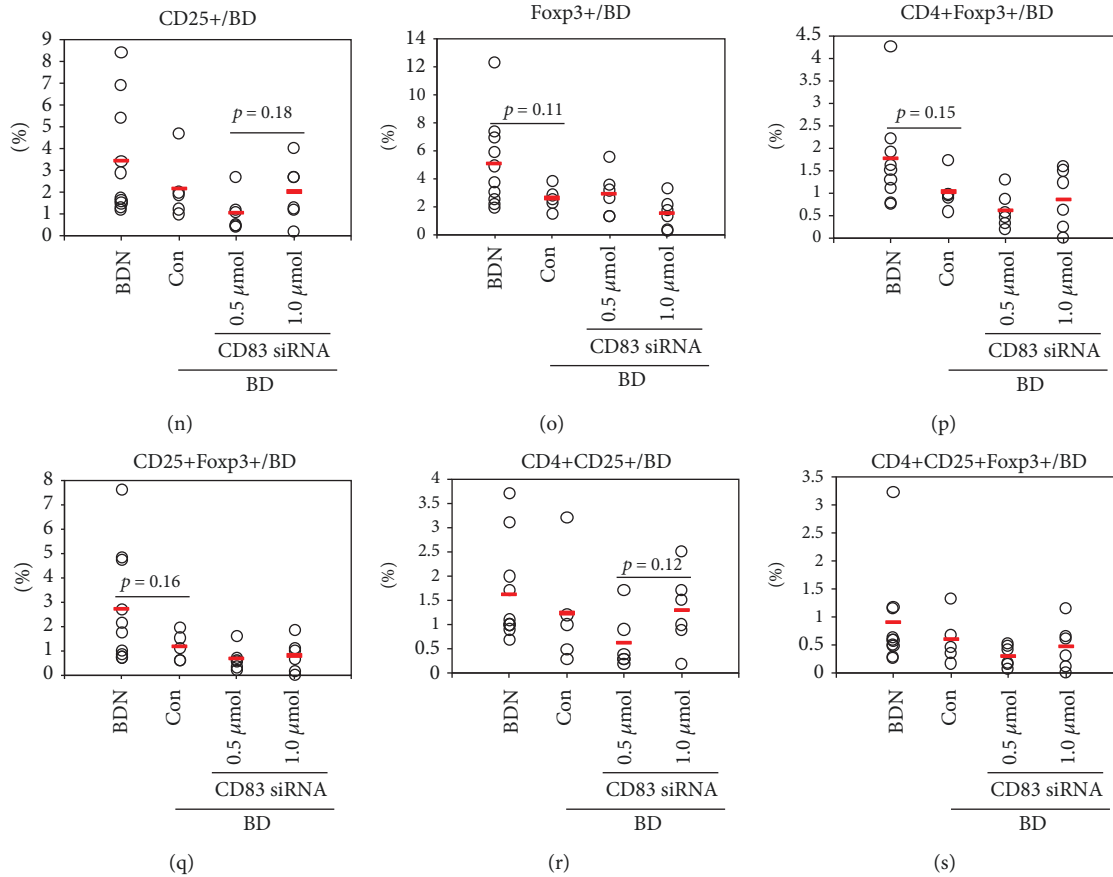


FIGURE 3: CD83 siRNA decreases the frequencies of CD83+ cells in normal mice. (a–d) Frequencies of CD40, CD83, CD80, and CD86 in the surface of peripheral blood leukocytes (PBL) and in the peritoneal macrophages of normal mice treated with CD83 siRNA were evaluated by FACS analysis ($n = 5$ in each group). (e–h) CD83 siRNA decreases frequencies of CD83 in BD mice. Frequencies of CD40, CD83, CD80, and CD86 in the surface of peripheral blood leukocytes (PBL) and in the peritoneal macrophage of BD mice treated with CD83 siRNA were evaluated by flow cytometry analysis. $n = 4$, BD symptomatic mice were used in control groups as scramble siRNA; $n = 6$, BD symptomatic mice were used in the $0.5 \mu\text{mol}$ and $1.0 \mu\text{mol}$ CD83 siRNA-treated groups. (i, j) CD83 siRNA treatment significantly decreased the severity score of BD mice and improved symptoms. (k) Treatment schedule of CD83 siRNA to BD mice. (l) Representative histogram of CD83+ cell frequencies in PBL and peritoneal macrophage of BD mice treated with CD83 siRNA. (m–s) Regulatory T cells in BD mice analyzed by FACS analysis. Frequencies of CD4+, CD4+Foxp3+, CD4+CD25+, and CD4+CD25+Foxp3+ regulatory T cells in BDN ($n = 10$), BD ($n = 5$), jetPEI-treated BD ($n = 6$), and CD83 siRNA-treated BD mice ($n = 6$) were evaluated by FACS analysis. n indicates the number of mice used in each group. The p value was determined by Student's t -test. Experiments were performed more than three independent times.

PBL (Figure 3(h)). Frequencies of CD80+ cells in PBL in the $0.5 \mu\text{mol}$ ($71.15 \pm 8.23\%$ vs. $84.1 \pm 5.29\%$, $p = 0.02$) and in the $1 \mu\text{mol}$ ($59.96 \pm 11.48\%$ vs. $84.1 \pm 5.29\%$, $p = 0.004$) CD83 siRNA-treated groups also showed downregulation compared to those in the scramble siRNA-treated control group (Figure 3(g)). In peritoneal macrophages, the $1 \mu\text{mol}$ -treated group showed lower frequencies of CD80+ cells compared to the $0.5 \mu\text{mol}$ -treated group ($68.4 \pm 13.26\%$ vs. $84.94 \pm 5.09\%$, $p = 0.02$) (Figure 3(g)). CD83 siRNA-treated BD symptomatic mice showed improved symptoms (Figure 3(i)). The disease severity score was also significantly decreased after 2 weeks (1.75 ± 0.61 vs. 2.60 ± 0.54 , $p = 0.04$) (Figure 3(j)). Discontinuation of treatment increased the disease severity score and deteriorated symptoms. Retreatment brought improvement again and decreased the disease severity score (Figure 3(j)). Figure 3(k) shows changes of BD symptoms after CD83 siRNA treatment to mice and time intervals.

Figure 3(l) shows representative histograms of CD83+ cells in BD mice treated with CD83 siRNA.

3.7. Frequencies of Regulatory T Cells in CD83 siRNA-Treated BD Mice. Frequencies of CD4+Foxp3+, CD25+Foxp3+, CD4+CD25+, and CD4+CD25+Foxp3+ Treg cells were analyzed by FACS. Frequencies of CD4+ T cells in BD mice were downregulated compared to those in BDN mice ($15.76 \pm 8.59\%$ vs. $22.23 \pm 7.16\%$, $p = 0.14$) (Figure 3(m)). Frequencies of CD4+Foxp3+ and CD25+Foxp3+ cells were slightly decreased in BD mice compared to those in BDN mice (CD4+Foxp3+: $1.04 \pm 0.39\%$ vs. $1.77 \pm 1.01\%$, $p = 0.15$; CD25+Foxp3+: $1.15 \pm 0.58\%$ vs. $2.71 \pm 2.31\%$, $p = 0.16$) (Figures 3(p) and 3(q)). Frequencies of CD4+CD25+Foxp3+ Treg cells were similar between $1 \mu\text{mol}$ CD83 siRNA-treated BD mice and BD control ($0.49 \pm 0.41\%$ vs. $0.61 \pm 0.44\%$, $p = 0.64$) (Figure 3(s)).

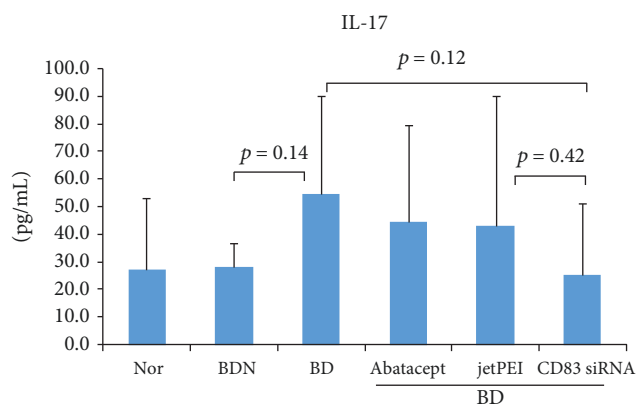


FIGURE 4: Serum interleukin 17 (IL-17) levels in BD mice after being treated with CD83 siRNA were analyzed by ELISA. Data represent two independent experiments.

3.8. CD83 siRNA Treatment Downregulates IL-17 Levels in the Plasma of BD Mice. Several studies of BD have demonstrated that a significant increase of serum IL-17 is an indicator of reactive or recurrence of infection [25, 26]. To determine whether CD83 siRNA could improve the symptoms of BD by downregulating IL-17, plasma IL-17 levels were measured in CD83 siRNA-treated BD mice by ELISA. The IL-17 level was downregulated in CD83 siRNA-treated BD symptomatic mice (25.2 ± 26.2 pg/mL) compared to that in nontreated BD mice (54.4 ± 35.3 pg/mL) ($p = 0.12$) (Figure 4). This result suggests that the inhibition of CD83 has a protective role against BD.

3.9. CD83 siRNA Suppresses CD83+ Cell Frequencies and Modulates the Morphology of Dendrites in In Vitro-Cultured Dendritic Cells. CD83 siRNA was used to treat bone marrow-derived dendritic cells to elucidate whether CD83 siRNA can suppress CD83 in *in vitro* dendritic cell cultures. Frequencies of CD83+ cells were measured by FACS analysis. CD83 siRNA significantly decreased the frequencies of CD83+ cells compared with the scramble siRNA treatment group ($71.7 \pm 3.53\%$ vs. $96.3 \pm 0.14\%$, $p = 0.01$) (Figure 5(b)). There were no significant differences observed among the groups in other costimulatory molecules (Figures 5(a), 5(c), and 5(d)). By transmission electron microscopy, dendrites of the plasma membrane in cultured dendritic cells were shown to be decreased in the CD83 siRNA-treated group when compared to those in the nontreated BD or scramble siRNA-treated BD group (Figure 5(e)). The morphology of cytoplasmic organelles was not different between the CD83 siRNA- and scramble siRNA-treated groups, except for vacuoles; CD83 siRNA-treated dendritic cells showed less vacuoles than scramble siRNA-treated cells.

4. Discussion

DCs are primary initiators and frontline cells of immune response. They are involved in the interface between innate immunity and adaptive immunity. DCs contribute to both central immunity and peripheral immunity [27]. Signals of

costimulatory molecules such as CD40, CD80, CD83, and CD86 can regulate the maturation of DCs [28]. Mitogen-activated protein kinase [29], signal transducers, and activators of transcription [30] are also involved in the maturation of DCs. Costimulatory molecules are receptors/ligands that can regulate inflammation [31]. Among those costimulatory molecules for DC maturation, CD83 is a functional molecule in the interplay between DCs and lymphocytes. CD83 is expressed as membrane-bound and soluble form (sCD83) [32]. Expression of the cell surface CD83 is upregulated upon DC activation. It is primarily used to identify the maturation or activation of DCs [33]. A significant number of CD83-expressing DCs have been observed in patients with Crohn's disease [34]. Treatment with soluble CD83 can inhibit pathological symptoms of experimental autoimmune encephalomyelitis (EAE) [35] and experimental autoimmune uveitis (EAU) [36]. In the present study, frequencies of CD83-expressing cells in the PBL surface were upregulated in BD symptomatic mice. This suggests that the elevated level of CD83 plays a pathogenic role in BD.

CD80 and CD86, also known as DC activation molecules, are stimulated via CD28 on the T cell surface. They provide T cell activation signals [37, 38]. Upregulation of CD80 and loss of constitutive properties of CD86 have been associated with the severity of disease and inflammation in humans [31]. Costimulatory interactions of CD80 and CD86 to T cells are required for the activation of autoreactive T cells and induction of arthritis [39]. Our investigation showed that in symptomatic BD mice, the proportion of CD80 was slightly increased, while the proportion of CD86 was decreased in symptomatic BD mice. It has been reported that the DC costimulatory molecule CD40 can bind to its ligand CD40L which is transiently expressed on T cells under inflammatory conditions and expressed significantly greater in ulcerative colitis and Crohn's disease [40]. We found that in BD symptomatic mice, frequencies of CD40 expressing cells were not significantly elevated.

GC7 (N1-guanyl-1,7-diaminoheptane) is an inhibitor of CD83 that interferes with CD83 surface expression and inhibits DC-mediated T cell activation by affecting the nuclear cytoplasmic translocation of CD83 mRNA [15]. However, in our study, GC7 treatment in normal mice did not show any significant difference in CD83 inhibition.

Abatacept, a recombinant fusion protein of the extracellular domain of CTLA-4 and the Fc region of human IgG1, can selectively modulate costimulatory signals CD80/CD86-CD28 for T cell activation [41, 42]. Abatacept significantly decreased CD83+ cells in a dose- and time-dependent manner in the present study. It also downregulated proportions of CD40, CD80, and CD86 in normal mice. Abatacept has been approved for use in patients with highly active rheumatoid arthritis (RA). It can improve the symptoms of RA and decrease disease activity and progression of structural damage [41, 42]. Abatacept treatment to the systemic sclerosis mouse model is effective in preventing fibrosis [43]. In our study, treatment of symptomatic BD mice with Abatacept significantly reduced the frequencies of CD83+ and CD40+ cells. We also found that Abatacept treatment to BD symptomatic mice decreased the disease severity and improved

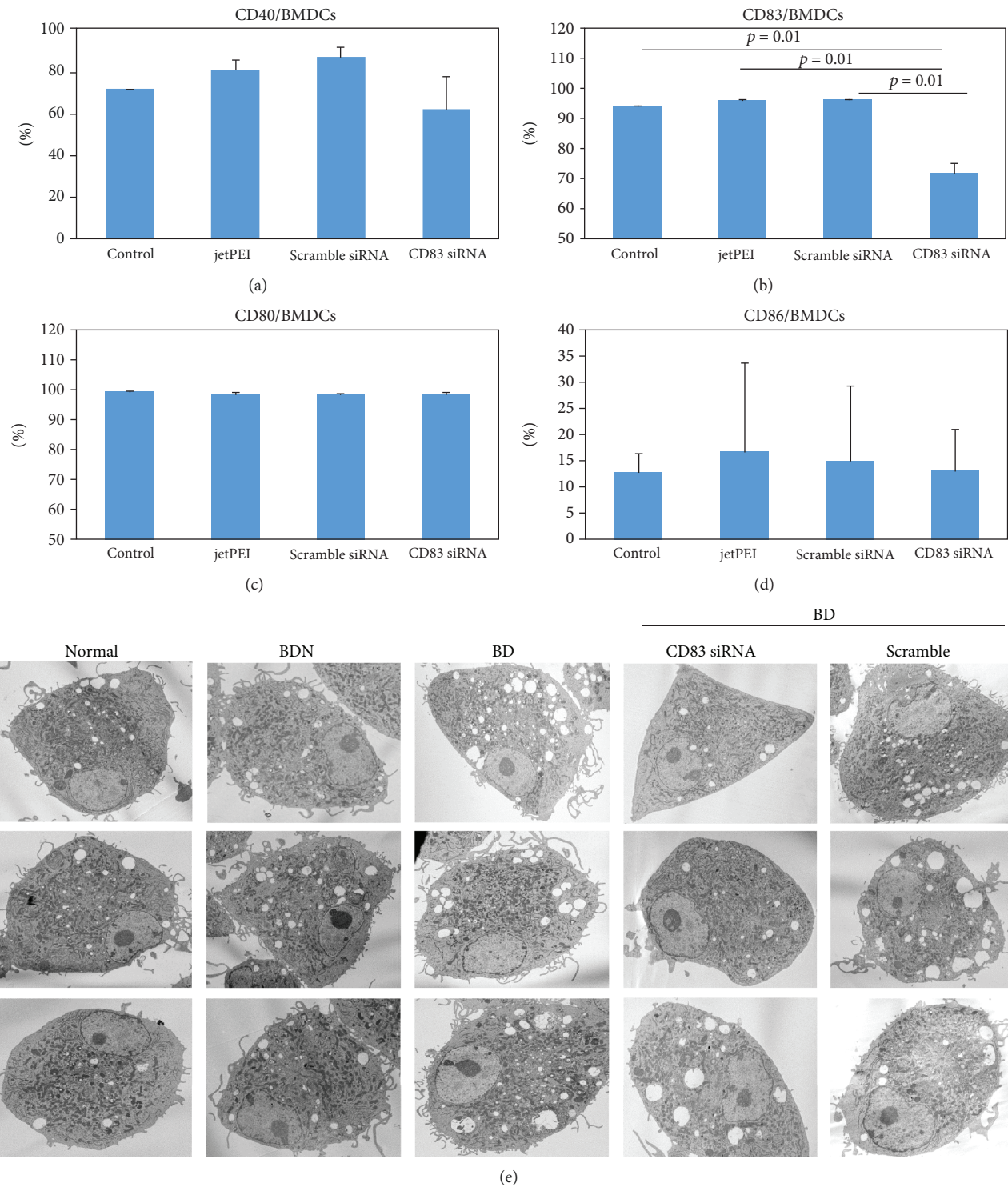


FIGURE 5: Bone marrow-derived DCs were cultured and treated with CD83 siRNA. (a–d) Frequencies of CD40-, CD83-, CD80-, and CD86-positive cells were measured by FACS analysis. (e) Morphological changes were observed under a transmission electron microscope. Data represent two independent experiments.

symptoms. Treg cells play an important role in the suppression of inflammation in autoimmune diseases. Patients with rheumatoid arthritis treated with Abatacept show increased IL-10 by producing CD4+CD25-LAG3+ Treg cells [44]. Abatacept can reduce T cell apoptosis and upregulate the proportion of Treg cells in RA patients

[45]. Increased CD4+CD25+ Treg cells are associated with improved inflammatory symptoms in BD mice [46]. In the present study, Abatacept treatment to BD mice increased the frequencies of CD4+ T cells and CD25+Foxp3+ cells compared to nontreated control. This suggests that DC costimulatory molecules are associated with BD symptoms.

It has been suggested that the inhibition of CD83 mRNA transport can be applied to develop therapeutics for autoimmune diseases [16, 47]. Preventing cell surface expression of CD83 can significantly inhibit DC-mediated T cell activation [15]. siRNA is considered to be a potent drug molecule that can silence genes associated with pathogenesis, especially in the treatment of inflammatory diseases [48, 49]. The siRNA binds to the RNA-induced silencing complex (RISC); then the passenger siRNA chain departs and initiates the process of RNA interference process, causing mRNA fragmentation and degradation [50, 51]. Injection of CD83 siRNA into normal mice significantly reduced the proportion of CD83-expressing cells in PBL and peritoneal macrophages. In addition, the frequencies of CD83+ cells in peritoneal macrophages and PBL of BD symptomatic mice treated with CD83 siRNA were significantly reduced. We also found that BD mice treated with CD83 siRNA showed reduced frequencies of CD40+ cells in peritoneal macrophages and PBL and decreased frequencies of CD80+ and CD86+ cells in peritoneal macrophages. CD4+CD25+ Treg cells can maintain self-tolerance and suppress autoimmune response and upregulation of CD4+CD25+ Treg cells in BD mice that are associated with disease improvement [46]. BD mice treated with CD83 siRNA showed a significantly reduced severity score of the disease, with improved symptoms. However, discontinuation of CD83 siRNA treatment showed deterioration of symptoms that were again improved after CD83 siRNA treatment. This clearly suggests that CD83 is a potential molecule for modulating BD symptoms. Upon activation of DCs, immature DCs can migrate to the draining lymph node and become mature antigen-presenting cells [52]. During maturation, DCs can change the surface expression of costimulatory molecules and morphology, including the expansion of dendrites and increase of lysosomes [53]. In our *in vitro* study, cultured bone marrow-derived DCs showed enhancement of dendrites in normal, BDN, and BD mice while treatment with CD83 siRNA showed less dendrite compared to nontreated BD and scramble siRNA-treated DCs. This provides evidence that CD83 plays a potent role in the maturation of DCs.

Th17 cells play an important role in autoimmunity. Expression of cytokine IL-17 is a special characteristic of Th17 cells. Increased production of IL-17 has been associated with several inflammatory disorders such as rheumatoid arthritis (RA), ankylosing spondylitis (AS), and Behçet's disease (BD) [54–56]. A significantly higher level of IL-17 has been observed in active BD patients [57, 58]. Downregulation of IL-17 is associated with the reduction of symptoms in BD mice when treated with miRNA21, IL-6 siRNA, recombinant IL-4, and N-acetyl-d-galactosamine 4-sulfate [49]. In our study, BD symptomatic mice treated with CD83 siRNA showed improved BD symptoms and downregulation of IL-17 in serum.

5. Conclusion

In summary, a high proportion of CD83+ cells in BD mice is correlated with BD symptoms. Inhibition of CD83 by treatment with CD83 siRNA to BD mice can significantly reduce

the proportions of CD83+, and that is associated with disease improvement. Discontinuation and retreatment of CD83 siRNA brought changes of symptoms. According to these data, it is clear that CD83 plays an important role in modulating BD symptoms. Our results suggest that targeting CD83 molecules can be used as a strategy to develop therapy for BD management.

Data Availability

The data used to support the findings of this study are available from the corresponding author upon request.

Conflicts of Interest

There are no conflicts of interest for any of the authors regarding the publication of this work.

Authors' Contributions

All the authors made important contributions to this article. S.S. contributed to the conception and design of the study, as well as the analysis and interpretation of the data. S.M.S.I., H.O.B., and B.C. participated in the data acquisition, analysis, and interpretation. S.S. and S.M.S.I. wrote the manuscript.

Acknowledgments

This research was supported by a grant (2017R1D1A1B03032168) of the Basic Science Research Program through the National Research Foundation of Korea (NRF) funded by the Ministry of Education, Science, and Technology. It was also supported by a grant (HI15C2483) of the Korea Health Technology R&D Project through the Korea Health Industry Development Institute (KHIDI) funded by the Ministry of Health & Welfare, Republic of Korea.

Supplementary Materials

Supplementary Figure S1: (A-C) frequencies of CD83+ cells in granulocytes, lymphocytes, and monocytes of normal ($n = 8$), HSV-1 ($n = 5$), BDN ($n = 8$), and BD mice ($n = 5$) were evaluated by FACS analysis (A-C). (D) Representative histogram of CD83+ cells in granulocytes. n indicates the number of mice used in each group. The p value was determined by Student's t -test. Supplementary Figure S2: (A-D) GC7 (N1-guanyl-1,7-diaminoheptane) was used to treat normal mice, and frequencies of CD40, CD83, CD80, and CD86 expressing cells in the PBL surface were evaluated by FACS analysis ($n = 3$ in each group). (*Supplementary Materials*)

References

- [1] F. N. Sezer, "The isolation of a virus as the cause of Behçet's diseases," *American Journal of Ophthalmology*, vol. 36, no. 3, pp. 301–315, 1953.
- [2] M. Studd, D. J. McCance, and T. Lehner, "Detection of HSV-1 DNA in patients with Behçet's syndrome and in patients with

- recurrent oral ulcers by the polymerase chain reaction," *Journal of Medical Microbiology*, vol. 34, no. 1, pp. 39–43, 1991.
- [3] S. Lee, D. Bang, Y. H. Cho, E.-S. Lee, and S. Sohn, "Polymerase chain reaction reveals herpes simplex virus DNA in saliva of patients with Behçet's disease," *Archives of Dermatological Research*, vol. 288, no. 4, pp. 179–183, 1996.
 - [4] M. I. C. H. I. K. O. TOJO, X. ZHENG, H. YANAGIHORI et al., "Detection of Herpes Virus Genomes in Skin Lesions from Patients with Behçet's Disease and Other Related Inflammatory Diseases," *Acta Dermato-Venereologica*, vol. 83, no. 2, pp. 124–127, 2003.
 - [5] S. O. H. N. Seonghyang, L. E. E. Eun-So, B. A. N. G. Dongsik, and L. E. E. Sungnack, "Behçet's disease-like symptoms induced by the Herpes simplex virus in ICR mice," *European Journal of Dermatology*, vol. 8, no. 1, pp. 21–23, 1998.
 - [6] S. Sohn, E. S. Lee, and D. Bang, "Learning from HSV-infected mice as a model of Behçet's disease," *Clinical and Experimental Rheumatology*, vol. 30, 3 Suppl 72, pp. S96–103, 2012.
 - [7] A. L. Hart, H. O. Al-Hassi, R. J. Rigby et al., "Characteristics of intestinal dendritic cells in inflammatory bowel diseases," *Gastroenterology*, vol. 129, no. 1, pp. 50–65, 2005.
 - [8] S. Khan, J. D. Greenberg, and N. Bhardwaj, "Dendritic cells as targets for therapy in rheumatoid arthritis," *Nature Reviews Rheumatology*, vol. 5, no. 10, pp. 566–571, 2009.
 - [9] M. O'Rourke, U. Fearon, C. M. Sweeney et al., "The pathogenic role of dendritic cells in non-infectious anterior uveitis," *Experimental Eye Research*, vol. 173, pp. 121–128, 2018.
 - [10] M. A. Silva, "Intestinal dendritic cells and epithelial barrier dysfunction in Crohn's disease," *Inflammatory Bowel Diseases*, vol. 15, no. 3, pp. 436–453, 2009.
 - [11] A. Tanne and N. Bhardwaj, "Chapter 9 - Dendritic Cells: General Overview and Role in Autoimmunity," in *Kelley and Firestein's Textbook of Rheumatology*, G. S. Firestein, R. C. Budd, S. E. Gabriel, I. B. McInnes, and J. R. O'Dell, Eds., pp. 126–144.e6, Elsevier, Philadelphia, PA, USA, Tenth Edition edition, 2017.
 - [12] K. Kawamura, K. Iyonaga, H. Ichiyasu, J. Nagano, M. Suga, and Y. Sasaki, "Differentiation, maturation, and survival of dendritic cells by osteopontin regulation," *Clinical and Diagnostic Laboratory Immunology*, vol. 12, no. 1, pp. 206–212, 2005.
 - [13] S. Berchtold, P. Muhl-Zurbes, C. Heufler, P. Winklehner, G. Schuler, and A. Steinkasserer, "Cloning, recombinant expression and biochemical characterization of the murine CD83 molecule which is specifically upregulated during dendritic cell maturation," *FEBS Letters*, vol. 461, no. 3, pp. 211–216, 1999.
 - [14] M. Kummer, N. M. Turza, P. Muhl-Zurbes et al., "Herpes simplex virus type 1 induces CD83 degradation in mature dendritic cells with immediate-early kinetics via the cellular proteasome," *Journal of Virology*, vol. 81, no. 12, pp. 6326–6338, 2007.
 - [15] M. Kruse, O. Rosorius, F. Krätzer et al., "Inhibition of Cd83 cell surface expression during dendritic cell maturation by interference with nuclear export of Cd83 mRNA," *The Journal of Experimental Medicine*, vol. 191, no. 9, pp. 1581–1590, 2000.
 - [16] M. Lechmann, S. Berchtold, A. Steinkasserer, and J. Hauber, "CD83 on dendritic cells: more than just a marker for maturation," *Trends in Immunology*, vol. 23, no. 6, pp. 273–275, 2002.
 - [17] I. Glezer, S. Rivest, and A. M. Xavier, "Chapter 3 - CD36, CD44, and CD83 expression and putative functions in neural tissues," in *Neural Surface Antigens*, J. Pruszk, Ed., pp. 27–40, Elsevier, Boston, 2015.
 - [18] X. Ju, P. A. Silveira, W.-H. Hsu et al., "The Analysis of CD83 Expression on Human Immune Cells Identifies a Unique CD83⁺-Activated T Cell Population," *Journal of Immunology*, vol. 197, no. 12, pp. 4613–4625, 2016.
 - [19] A.-M. Kristensen, K. Stengaard-Pedersen, M. L. Hetland et al., "Expression of soluble CD83 in plasma from early-stage rheumatoid arthritis patients is not modified by anti-TNF- α therapy," *Cytokine*, vol. 96, pp. 1–7, 2017.
 - [20] B. D. Hock, J. L. O'Donnell, K. Taylor et al., "Levels of the soluble forms of CD80, CD86, and CD83 are elevated in the synovial fluid of rheumatoid arthritis patients," *Tissue Antigens*, vol. 67, no. 1, pp. 57–60, 2006.
 - [21] B. D. Hock, L. F. Haring, A. Steinkasserer, K. G. Taylor, W. N. Patton, and J. L. McKenzie, "The soluble form of CD83 is present at elevated levels in a number of hematological malignancies," *Leukemia Research*, vol. 28, no. 3, pp. 237–241, 2004.
 - [22] N. Hirano, M. O. Butler, Z. Xia et al., "Engagement of CD83 ligand induces prolonged expansion of CD8⁺ T cells and preferential enrichment for antigen specificity," *Blood*, vol. 107, no. 4, pp. 1528–1536, 2006.
 - [23] Y. Hattori and Y. Maitani, "DNA/lipid complex incorporated with fibronectin to cell adhesion enhances transfection efficiency in prostate cancer cells and xenografts," *Biological & Pharmaceutical Bulletin*, vol. 30, no. 3, pp. 603–607, 2007.
 - [24] A. Dhirapong, G.-X. Yang, S. Nadler et al., "Therapeutic effect of cytotoxic T lymphocyte antigen 4/immunoglobulin on a murine model of primary biliary cirrhosis," *Hepatology*, vol. 57, no. 2, pp. 708–715, 2013.
 - [25] H. Shen, L. P. Xia, and J. Lu, "Elevated levels of interleukin-27 and effect on production of interferon- γ and interleukin-17 in patients with Behçet's disease," *Scandinavian Journal of Rheumatology*, vol. 42, no. 1, pp. 48–51, 2013.
 - [26] M. Ahmadi, M. Yousefi, S. Abbaspour-Aghdam et al., "Disturbed Th17/Treg balance, cytokines, and miRNAs in peripheral blood of patients with Behçet's disease," *Journal of Cellular Physiology*, vol. 234, no. 4, pp. 3985–3994, 2019.
 - [27] D. Ganguly, S. Haak, V. Sisirak, and B. Reizis, "The role of dendritic cells in autoimmunity," *Nature Reviews Immunology*, vol. 13, no. 8, pp. 566–577, 2013.
 - [28] F. Ouaz, J. Arron, Y. Zheng, Y. Choi, and A. A. Beg, "Dendritic Cell Development and Survival Require Distinct NF- κ B Subunits," *Immunity*, vol. 16, no. 2, pp. 257–270, 2002.
 - [29] L. Castiello, M. Sabatino, P. Jin et al., "Monocyte-derived DC maturation strategies and related pathways: a transcriptional view," *Cancer Immunology, Immunotherapy*, vol. 60, no. 4, pp. 457–466, 2011.
 - [30] A. S. Bharadwaj and D. K. Agrawal, "Transcription factors in the control of dendritic cell life cycle," *Immunologic Research*, vol. 37, no. 1, pp. 79–96, 2007.
 - [31] A. Nolan, H. Kobayashi, B. Naveed et al., "Differential role for CD80 and CD86 in the regulation of the innate immune response in murine polymicrobial sepsis," *PLoS ONE*, vol. 4, no. 8, p. e6600, 2009.
 - [32] B. D. Hock, M. Kato, J. L. McKenzie, and D. N. J. Hart, "A soluble form of CD83 is released from activated dendritic cells and B lymphocytes, and is detectable in normal human sera," *International Immunology*, vol. 13, no. 7, pp. 959–967, 2001.
 - [33] L. J. Zhou and T. F. Tedder, "Human blood dendritic cells selectively express CD83, a member of the immunoglobulin

- superfamily," *The Journal of Immunology*, vol. 154, no. 8, pp. 3821–3835, 1995.
- [34] P. Middel, D. Raddatz, B. Gunawan, F. Haller, and H. J. Radzun, "Increased number of mature dendritic cells in Crohn's disease: evidence for a chemokine mediated retention mechanism," *Gut*, vol. 55, no. 2, pp. 220–227, 2006.
- [35] E. Zinser, M. Lechmann, A. Golka, M. B. Lutz, and A. Steinkasserer, "Prevention and treatment of experimental autoimmune encephalomyelitis by soluble CD83," *The Journal of Experimental Medicine*, vol. 200, no. 3, pp. 345–351, 2004.
- [36] W. Lin, K. Buscher, B. Wang et al., "Soluble CD83 alleviates experimental autoimmune uveitis by inhibiting filamentous actin-dependent calcium release in dendritic cells," *Frontiers in Immunology*, vol. 9, p. 1567, 2018.
- [37] M. Thiel, M.-J. Wolfs, S. Bauer et al., "Efficiency of T-cell costimulation by CD80 and CD86 cross-linking correlates with calcium entry," *Immunology*, vol. 129, no. 1, pp. 28–40, 2010.
- [38] P. Riha and C. E. Rudd, "CD28 co-signaling in the adaptive immune response," *Self/Nonsel*, vol. 1, no. 3, pp. 231–240, 2010.
- [39] S. K. O'Neill, Y. Cao, K. M. Hamel, P. D. Doodes, G. Hutas, and A. Finnegan, "Expression of CD80/86 on B cells is essential for autoreactive T cell activation and the development of arthritis," *Journal of Immunology*, vol. 179, no. 8, pp. 5109–5116, 2007.
- [40] D. C. Baumgart, S. Thomas, I. Przesdzin et al., "Exaggerated inflammatory response of primary human myeloid dendritic cells to lipopolysaccharide in patients with inflammatory bowel disease," *Clinical and Experimental Immunology*, vol. 157, no. 3, pp. 423–436, 2009.
- [41] H. A. Blair and E. D. Deeks, "Abatacept: a review in rheumatoid arthritis," *Drugs*, vol. 77, no. 11, pp. 1221–1233, 2017.
- [42] R. Korhonen and E. Moilanen, "Abatacept, a novel CD80/86-CD28 T cell co-stimulation modulator, in the treatment of rheumatoid arthritis," *Basic & Clinical Pharmacology & Toxicology*, vol. 104, no. 4, pp. 276–284, 2009.
- [43] C. Bruni, E. Praino, Y. Allanore et al., "Use of biologics and other novel therapies for the treatment of systemic sclerosis," *Expert Review of Clinical Immunology*, vol. 13, no. 5, pp. 469–482, 2017.
- [44] S. Nakachi, S. Sumitomo, Y. Tsuchida et al., "Interleukin-10-producing LAG3⁺ regulatory T cells are associated with disease activity and abatacept treatment in rheumatoid arthritis," *Arthritis Research & Therapy*, vol. 19, no. 1, p. 97, 2017.
- [45] M. Bonelli, L. Goschl, S. Bluml et al., "Abatacept (CTLA-4Ig) treatment reduces T cell apoptosis and regulatory T cell suppression in patients with rheumatoid arthritis," *Rheumatology*, vol. 55, no. 4, pp. 710–720, 2016.
- [46] J. Shim, E. S. Lee, S. Park, D. Bang, and S. Sohn, "CD4⁺ CD25⁺ regulatory T cells ameliorate Behcet's disease-like symptoms in a mouse model," *Cytotherapy*, vol. 13, no. 7, pp. 835–847, 2011.
- [47] Y. Fujimoto and T. F. Tedder, "CD83: a regulatory molecule of the immune system with great potential for therapeutic application," *Journal of Medical and Dental Sciences*, vol. 53, no. 2, pp. 85–91, 2006.
- [48] A. A. Barba, S. Cascone, D. Caccavo et al., "Engineering approaches in siRNA delivery," *International Journal of Pharmaceutics*, vol. 525, no. 2, pp. 343–358, 2017.
- [49] S. Islam and S. Sohn, "HSV-Induced Systemic Inflammation as an Animal Model for Behçet's Disease and Therapeutic Applications," *Viruses*, vol. 10, no. 9, p. 511, 2018.
- [50] D. D. Rao, J. S. Vorhies, N. Senzer, and J. Nemunaitis, "siRNA vs. shRNA: similarities and differences," *Advanced Drug Delivery Reviews*, vol. 61, no. 9, pp. 746–759, 2009.
- [51] S. L. Ameres, J. Martinez, and R. Schroeder, "Molecular basis for target RNA recognition and cleavage by human RISC," *Cell*, vol. 130, no. 1, pp. 101–112, 2007.
- [52] P. Verdijk, P. A. van Veelen, A. H. de Ru et al., "Morphological changes during dendritic cell maturation correlate with cofilin activation and translocation to the cell membrane," *European Journal of Immunology*, vol. 34, no. 1, pp. 156–164, 2004.
- [53] J. Ji, Z. Fan, F. Zhou et al., "Improvement of DC vaccine with ALA-PDT induced immunogenic apoptotic cells for skin squamous cell carcinoma," *Oncotarget*, vol. 6, no. 19, pp. 17135–17146, 2015.
- [54] M. Ziolkowska, A. Koc, G. Luszczkiewicz et al., "High levels of IL-17 in rheumatoid arthritis patients: IL-15 triggers in vitro IL-17 production via cyclosporin A-sensitive mechanism," *The Journal of Immunology*, vol. 164, no. 5, pp. 2832–2838, 2000.
- [55] T. J. Kenna, S. I. Davidson, R. Duan et al., "Enrichment of circulating interleukin-17-secreting interleukin-23 receptor-positive γ/δ T cells in patients with active ankylosing spondylitis," *Arthritis and Rheumatism*, vol. 64, no. 5, pp. 1420–1429, 2012.
- [56] D. S. Al-Zifzaf, A. N. Mokbel, and D. M. Abdelaziz, "Interleukin-17 in Behçet's disease: relation with clinical picture and disease activity," *Egyptian Rheumatology and Rehabilitation*, vol. 42, no. 1, pp. 34–38, 2015.
- [57] W. Chi, P. Yang, X. Zhu et al., "Production of interleukin-17 in Behçet's disease is inhibited by cyclosporin A," *Molecular Vision*, vol. 16, pp. 880–886, 2010.
- [58] W. Chi, X. Zhu, P. Yang et al., "Upregulated IL-23 and IL-17 in Behçet Patients with Active Uveitis," *Investigative Ophthalmology & Visual Science*, vol. 49, no. 7, pp. 3058–3064, 2008.

Research Article

The Important Role of Dendritic Cell (DC) in iNKT-Mediated Modulation of NK Cell Function in *Chlamydia pneumoniae* Lung Infection

Lei Zhao,^{1,2} Xiaoling Gao¹,, Hong Bai¹,, Antony George Joyee,¹ Shuhe Wang,¹ Jie Yang,¹ Weiming Zhao,³ and Xi Yang^{1,3}

¹Department of Immunology, Faculty of Medicine, University of Manitoba, Winnipeg, Canada

²Institute of Basic Medical Sciences, Qilu Hospital, Shandong University, Jinan, Shandong, China

³Department of Pathogenic Biology, Shandong University School of Medicine, Jinan, Shandong, China

Correspondence should be addressed to Xi Yang; x.yang@umanitoba.ca

Received 13 December 2018; Revised 29 March 2019; Accepted 15 April 2019; Published 20 May 2019

Guest Editor: Luisa Cervantes-Barragan

Copyright © 2019 Lei Zhao et al. This is an open access article distributed under the Creative Commons Attribution License, which permits unrestricted use, distribution, and reproduction in any medium, provided the original work is properly cited.

Chlamydia pneumoniae (*Cpn*) infection causes multiple acute and chronic human diseases. The role of DCs in host defense against *Cpn* infection has been well documented. The same is true for invariant natural killer T (iNKT) cells and NK cells, but the interaction among cells is largely unknown. In this study, we investigated the influence and mechanism of iNKT cell on the differentiation and function of NK cell in *Cpn* lung infection and the role played by DCs in this process. We found that expansion of IFN- γ -producing NK cells quickly happened after the infection, but this response was altered in iNKT knockout (KO) mice. The expression of activation markers and the production of IFN- γ by different NK subsets were significantly lower in KO mice than wild-type (WT) mice. Using in vitro DC-NK coculture and in vivo adoptive transfer approaches, we further examined the role of DCs in iNKT-mediated modulation of NK cell function. We found that NK cells expressed lower levels of activation markers and produced less IFN- γ when they were cocultured with DCs from KO mice than WT mice. More importantly, we found that the adoptive transfer of DCs from the KO mice induced less NK cell activation and IFN- γ production. The results provided evidence on the modulating effect of iNKT cell on NK cell function, particularly the critical role of DCs in this modulation process. The finding suggests the complexity of cellular interactions in *Cpn* lung infection, which should be considered in designing preventive and therapeutic approaches for diseases and infections.

1. Introduction

The role of DCs in host defense against infections has been well defined. In particular, we and others have found significant interaction of iNKT/NK cells with DCs which are important for T cell response in different infection settings [1–4]. In the present study, we intended to study the modulating effect of iNKT cell on NK cell and the involvement of DCs in this process.

NK cells are an important component of the innate immune system, contributing to host resistance to microbial infection such as viruses, bacteria, and certain parasites [5–7]. Some studies have demonstrated that human and murine NK cells are highly heterogeneous populations with

multifunctional features [8, 9]. In this context, murine NK cells can be grouped into four subsets based on CD11b and CD27 expression. The CD11b^{low}CD27^{low}, CD11b^{low}CD27^{high}, CD11b^{high}CD27^{high}, and CD11b^{high}CD27^{low} NK subsets represent a continuous NK cell differentiation process [10]. Among these subsets, the CD11b^{low}CD27^{high} and CD11b^{high}CD27^{high} subsets exhibit enhanced cytokine production and higher responsiveness, while CD11b^{high}CD27^{low} NK subsets appear to be more tightly controlled due to their higher expression of inhibitory receptors [11]. The functional distinctions of NK subsets in immune responses have been discerned in several disease models [12, 13].

iNKT is an innate-like T lymphocyte sublineage that expresses NK cell markers and limited/semi-invariant T cell

repertoire that recognize lipid in the context of nonclassical MHC-I molecule CD1d [14, 15]. Functional studies on iNKT cells have suggested a significant impact of these cells on immune regulation. After activation, iNKT cells produce a broad range of cytokines and provide surface stimulatory molecules to activate NK cells, T cells, B cells, and DCs [1, 16, 17]. Some studies have shown the modulating effect of iNKT cell on NK cell in infection and noninfection settings. Injection of soluble model antigen α -galactosylceramide (α -Galcer) which is a specific agonist for iNKT cells led to NK cell activation and proliferation and production of IFN- γ in mice [18, 19]. In addition, α -Galcer-stimulated human iNKT cells also activated NK cells through an IL-2-dependent mechanism [20]. Furthermore, activated iNKT cells induced NK cell differentiation and affected NK cell education [21]. Interestingly, in infection settings, the effect of iNKT on NK cell functions appears variable in the literature [22–24]. One study showed that NK cells maintained its activity and protective function in the absence of iNKT cells during *Trypanosoma cruzi* infection [22]. Another study showed that iNKT cells suppressed IFN- γ production by NK cells following acute influenza A virus infection [23]. In contrast, we reported previously that iNKT cells promote IFN- γ production by NK cells during *C. muridarum*, a mouse strain of *Chlamydia*, infection [24]. The mixed findings suggest that the effect of iNKT cell on NK cell is likely infection specific; thus, it is important to specifically study particular pathogens.

Members of the *Chlamydia* family are obligate intracellular Gram-negative bacterial pathogens, which include several species and various serotypes. Previous studies have shown that the distinct cellular immune responses including NK/iNKT cells were induced by different species of *Chlamydia* particularly *Cpn* and *C. muridarum* (*Cm*) [25]. NK cells play a protective role in *Cm* infection [26–28], but one report showed that NK cells did not contribute to innate resistance to *Cpn* infection in a setting of T cell and B cell deficiencies [29, 30]. Notably, the kinetics and functional involvement of NK cell response in *Cpn* infection have not been well clarified. Therefore, it is important to specifically test NK cell response and the effect of iNKT cells in *Cpn* infection. In addition, we have reported that iNKT cells can modulate the phenotype, cytokine production, and function of DCs in *Cpn* infection [1, 31]. In particular, we found that iNKT cells could enhance DC IL-12p70 production in a CD40L-, IFN- γ -, and cell-cell contact-dependent manner in the coculture system. Considering the important role of DCs in modulation of NK and iNKT cell function, it is natural to study the involvement of DCs in this process.

In the present study, through depletion of NK cell in vivo and direct comparison of WT and iNKT KO mice, we examined the involvement of NK cell response in host defense against *Cpn* infection and the effect of iNKT cells on NK cell differentiation and activation during the infection. Further, we explored the mechanism by which iNKT cells modulate NK cell activation and function, particularly the involvement of DCs in this process, using in vitro DC-NK coculture and in vivo adoptive transfer approaches.

2. Materials and Methods

2.1. Mice. Female C57BL/6 mice were bred and kept under a specific pathogen-free animal facility at the University of Manitoba. Breeding pairs of $\text{J}\alpha 18^{-/-}$ gene knockout ($\text{J}\alpha 18^{-/-}$) mice which lacked invariant iNKT cells in B6 background were kindly provided by Dr. Masaru Taniguchi (RIKEN Research Center for Allergy and Immunology) and maintained at the animal care facility of the University of Manitoba. All mice used were between 6 and 12 weeks old. All experiments were conducted in accord with the guidelines of the Canadian Council on Animal Care, and the protocol was approved by the ethical committee of the University of Manitoba.

2.2. Chlamydia. *Cpn* were propagated, purified, and quantified as previously described [1]. Briefly, *Cpn* was grown in HEP-2 cells in Eagle's MEM containing 10% FBS. After 48 h culture, infected cells were harvested. Elementary bodies (EBs) were purified by discontinuous density gradient centrifugation. The purified EBs were measured by immunostaining and stored at -80°C . For mice infection, 5×10^6 inclusion-forming units (IFUs) of *Cpn* in 40 μl final volume of PBS was used to inoculate mice intranasally. The same seed stock of EBs was used throughout the study.

2.3. Antibodies. Fluorescent-labeled mAbs and corresponding isotype controls were purchased from eBioscience or BioLegend. For analysis of NK subsets by flow cytometry, anti-CD3 ϵ -PE-Cy7, anti-NK1.1-PE, anti-NK1.1-APC, anti-CD69-PE, anti-CD25-FITC, anti-CD11b-APC, anti-NK1.1-Pacific Blue, anti-CD27-FITC, and anti-CD11b-APC-Cy7 were used.

2.4. Surface Marker and Intracellular Cytokine Staining. For *in vivo* experiments, the fresh splenocytes were stained by anti-CD3 ϵ -PE-Cy7, anti-NK1.1-APC, anti-CD69-PE, and anti-CD25-FITC for CD69 and CD25 expression. NK subset staining and analysis were performed as described previously [24]. For intracellular cytokine staining, cells were stimulated with PMA (50 ng/ml) and Ionomycin (1 $\mu\text{g}/\text{ml}$) and incubated in complete RPMI 1640 medium at 37°C . After 3-hour incubation, brefeldin A was added, and cells were cultured for another 3 hours to accumulate cytokines intracellularly. Cells were subsequently washed and blocked for 10 min with anti-CD16/CD32 in FACS buffer (Dulbecco's PBS, 2% heat-inactivated FBS, 0.09% sodium azide) and then surface stained with the appropriate Abs. Cells were fixed, permeabilized, and subsequently stained with APC-anti-IFN- γ for 30 min. Stained cells were washed and analyzed using an LSR II flow cytometer. The data were subsequently analyzed with FACS express software.

2.5. Isolate DCs and Adoptive Transfer. DCs were isolated from splenocytes according to the manufacturer's instructions as described previously [1]. Briefly, spleens from either $\text{J}\alpha 18^{-/-}$ mice or C57BL/6 mice were aseptically collected at a certain time after infection and digested into single cells using 2 mg/ml collagenase D. DCs were purified using magnetic CD11c microbeads and MACS-positive

selection column (Miltenyi Biotec, Auburn, CA). The purity of the isolated CD11c⁺ cells was up to 90% based on flow cytometric analysis.

For adoptive transfer, DCs were isolated from either *Cpn*-infected $\text{J}\alpha 18^{-/-}$ mice or C57BL/6 mice, and 2×10^6 DCs in sterile PBS were adoptively transferred intravenously (i.v.) to naive C57BL/6 recipients. Twenty-four hours after adoptive transfer, the mice were intranasally inoculated with 5×10^6 IFUs of *Cpn*. The recipient mice were sacrificed at day 3 p.i., and the expression of activation markers and IFN- γ production by NK cells were measured by flow cytometry.

2.6. NK Cell Purification. Spleen cells from uninfected mice were prepared, and NK cells were isolated by negative selection using an NK cell isolation kit (Miltenyi Biotec) according to the manufacturer's instructions. NK cells (NK1.1⁺CD3e⁻) were >90% pure following separation as determined by flow cytometry.

2.7. DC and NK Cell Coculture. Purified DCs (1×10^6) from either *Cpn*-infected $\text{J}\alpha 18^{-/-}$ mice or C57BL/6 mice were cocultured with NK cells (2×10^5) isolated from uninfected C57BL/6 mice in a 96-well round bottom plate at 37°C. After 48 h, cells were collected for intracellular cytokine staining to analyze IFN- γ production by NK cells following the protocol described above. Meanwhile, concentrations of IFN- γ in the supernatants were measured by ELISA.

2.8. NK Depletion In Vivo. Mice were injected i.p. with 30 μl anti-asialo-GM1 (Wako) in 300 ml PBS to deplete NK cells *in vivo*. Control mice received appropriate normal rabbit IgG (Wako). Injections were performed 3 days prior to Chlamydia infection and repeated every 3 days to maintain depletion. The depletion of NK cells (95%) by this treatment was confirmed by flow cytometric analysis.

2.9. Statistical Analysis. Statistical analysis of the data was performed as indicated using either unpaired Student's *t*-test or one-way ANOVA (GraphPad Prism software; version 5). Values of $p < 0.05$ were considered significant.

3. Results

3.1. CD27^{high} NK Cells Expand after Respiratory Infection with *Cpn*. To test whether NK cells respond to *Cpn* infection, the percentage and the absolute number of NK cells were analyzed by flow cytometry at various time points after respiratory tract *Cpn* exposure. NK cells were identified as NK1.1⁺CD3e⁻ cells. As shown in (Figures 1(a) and 1(b)), there was a modest increase of the percentage of NK1.1-expressing cells in the spleen at day 1 after *Cpn* infection which peaked at day 3. At day 5, the percentage of NK cells started to decrease. A similar kinetic change of NK cells was also observed in the lung (Figure S1A and B). The absolute number of NK cells in the spleen also increased at day 1 and reached the peak at day 3 (Figure 1(c)). The total number of NK cells expanded about 2.5-folds in the spleen (Figure 1(c)) and 4-folds in the lung (Figure S1C) at their peak level at day 3.

It has been reported that murine NK cells can be grouped into 4 subsets based on surface CD11b and CD27 expression

[10, 11]. To explore whether the NK subsets were affected by *Cpn* infection, the pattern of NK subsets was examined. As shown in Figures 1(d) and 1(e), *Cpn* infection resulted in a significant increase of the proportion of CD27^{high} NK cells compared with uninfected mice. The frequency of both CD11b^{low}CD27^{high} and CD11b^{high}CD27^{high} NK cells was nearly doubled at day 7 p.i. The increase of CD27^{high} NK cells was accompanied by a reduction of CD11b^{high}CD27^{low} NK subset. Together, the results indicate that *Cpn* infection induces rapid expansion of NK cells, especially the CD27^{high} subsets.

3.2. NK Cells Are Activated and Produce IFN- γ after *Cpn* Infection. To determine whether NK cells are an activated phenotype in response to *Cpn* infection, we measured the expression of two early activation markers, CD69 and CD25, on NK cells in a kinetic manner. We found that *Cpn* infection rapidly increased CD69 expression on NK cells as early as day 1, peaking at day 3, with 45% NK cells in the spleen (Figures 2(a) and 2(b)) expressing this marker. The level of CD25 on splenic NK cells (Figures 2(c) and 2(d)) was also significantly elevated at day 1 and peaked at day 3 p.i. Both CD69 and CD25 gradually decreased from the peak but remained high at day 9 when the experiment was terminated. Further, intracellular cytokine staining was performed to determine IFN- γ production by NK cells following *Cpn* infection. We found that the percentage of IFN- γ -producing NK cells started to increase as early as day 1 p.i., with about 25% of NK cells stained positive for IFN- γ at day 5 p.i. (Figure 2(e)). About 5% of NK cells produced IFN- γ in uninfected control mice. The high IFN- γ production by NK cells remained during the period of the study. The results show that NK cells are activated and produce IFN- γ in response to *Cpn* infection.

3.3. NK Cell Depletion Results in Increased Susceptibility to *Cpn* Lung Infection. To further confirm the role of NK cells in host defense against *Cpn* lung infection in immune intact mice, we used anti-asialo-GM1 treatment to deplete NK cells *in vivo* and examine its effect on host susceptibility to *Cpn* infection. We found that NK-depleted mice showed greater body weight loss (Figure 3(a)) and significantly higher bacterial burden in the lung compared with control antibody-treated mice (Figure 3(b)). The depletion of NK cells in the spleen and lung was confirmed by flow cytometry (Figure S2). The result suggested that NK cells played an important protective role in host defense against *Cpn* lung infection.

3.4. iNKT Deficiency Leads to Changes of NK Cell Subset Expansion. To address the impact of iNKT cell on the expansion of NK cells during *Cpn* infection, we first measured the number of NK cells in WT and iNKT KO ($\text{J}\alpha 18^{-/-}$) mice. We found that there is no significant difference in NK cell number between these two mouse strains before and after *Cpn* infection (Figure S3). Then, we analyzed the distribution of NK subsets based on their CD27 and CD11b expression in WT and iNKT KO mice before and after *Cpn* infection. At the steady state before

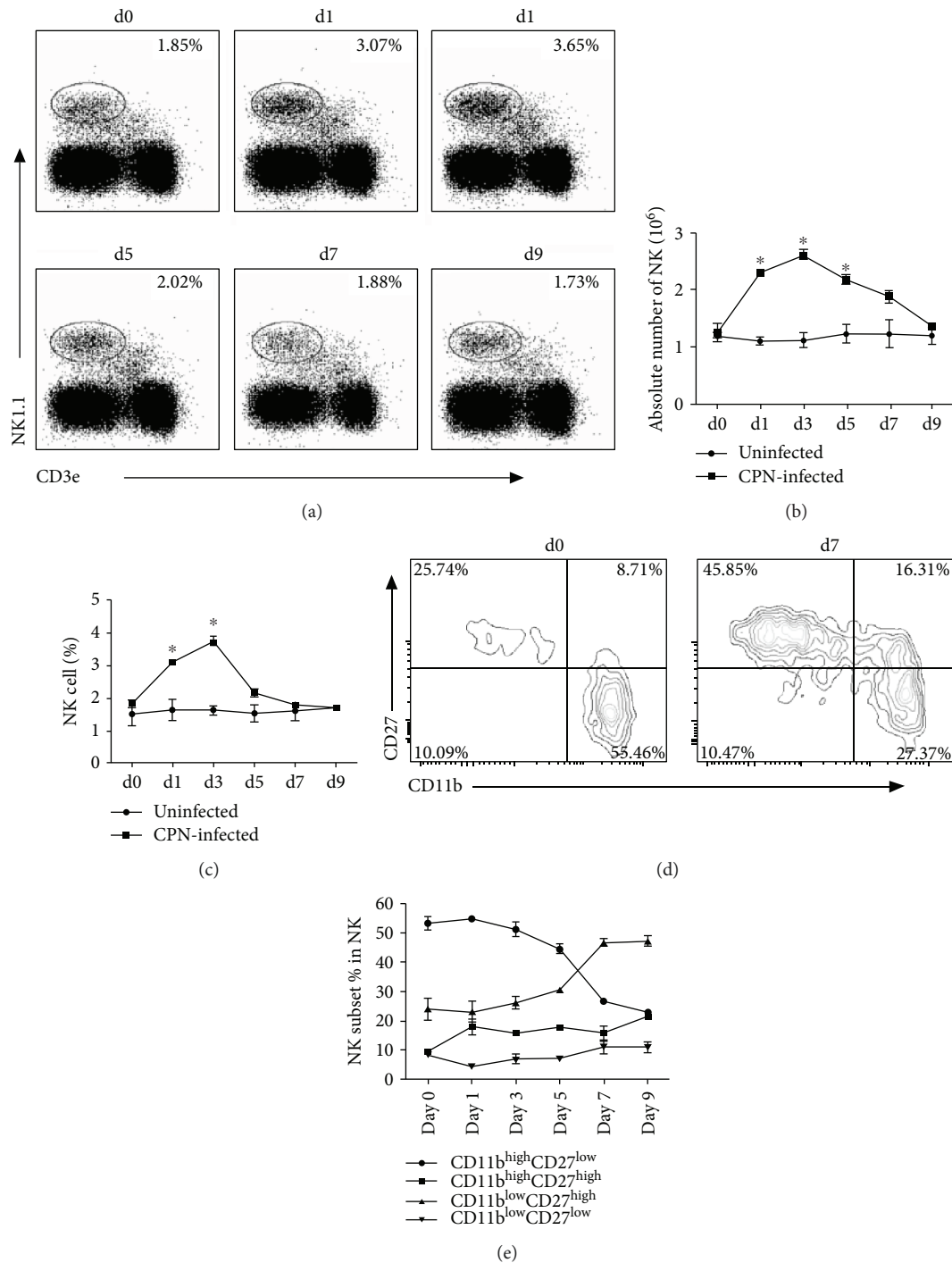


FIGURE 1: *Cpn* lung infection induces expansion of NK cell number and changes the distribution of NK subsets. Mice were infected with 5×10^6 IFUC $_{Cpn}$ intranasally and killed at specified time points. Splenocytes were stained for NK1.1 and CD3e. (a) Percentage of NK cells (NK1.1+CD3e⁻) among living lymphocytes was gated according to forward and side scatter. Representative dot plots are shown. (b) Kinetics of the percentage of NK cells. (c) Kinetics of the absolute number of NK cells per mouse spleen. (d) Based on CD11b and CD27 staining, NK cell subsets were analyzed after gating on NK1.1+CD3e⁻ cells. Representative zebra plots for CD11b⁻ and CD27-expressing NK cells before and after *Cpn* infection were shown. (e) Kinetics of the mean percentage of indicated NK cell subsets are plotted. Data are expressed as mean ($n = 4$) \pm SD and represent three independent experiments. * $p < 0.05$.

infection, the distribution of NK subsets was similar in iNKT KO and WT control mice. Following *Cpn* infection, the pattern of NK subsets was significantly altered in WT mice at day 7 p.i., showing a remarkable increase of the

CD11b^{low}CD27^{high} and CD11b^{high}CD27^{high} NK subsets (Figure 4). Notably, the increase of the CD27^{high} NK cells in iNKT KO mice was found at day 5 p.i., earlier than that shown in WT mice. Consequently, the frequency of

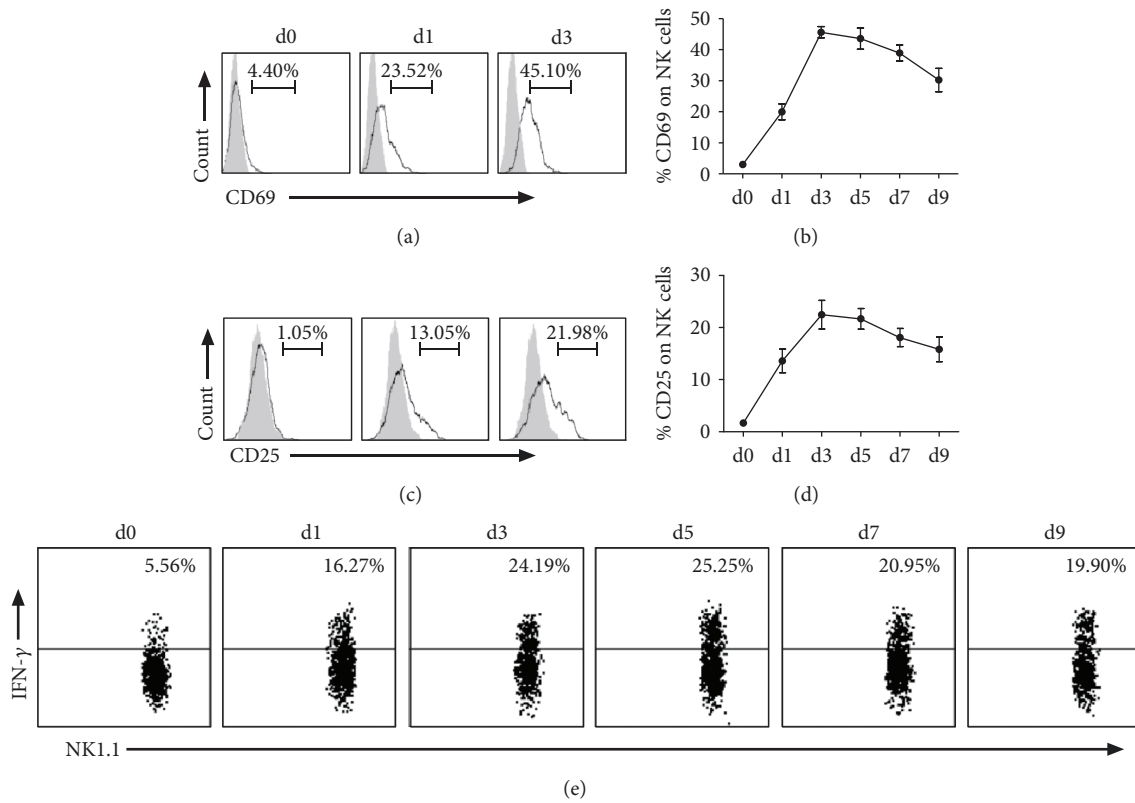


FIGURE 2: NK cells become activated and produce IFN- γ in response to *Cpn* infection. After intranasal infection by *Cpn*, mice were killed at different days, and splenocytes were stained for NK1.1, CD3e, CD25, and CD69. (a) Representative histogram of activation marker CD69 expression on NK cells at days 0, 1, and 3 p.i.: isotype control Ab staining (gray histograms) and infected mice (solid lines). (b) Kinetics of the expression of CD69 by NK cells. (c) Representative graph of the expression of activation marker CD25 on NK cells after infection: isotype control Ab staining (gray histograms) and infected mice (solid lines). (d) Kinetics of the expression of CD25 by NK cells. (e) Representative staining for intracellular IFN- γ before and after *Cpn* infection. IFN- γ production by splenic NK cells was assayed by intracellular cytokine staining on gated NK1.1+CD3e- population. The data represent one of at least three independent experiments and are shown as mean \pm SD for four mice at end time points.

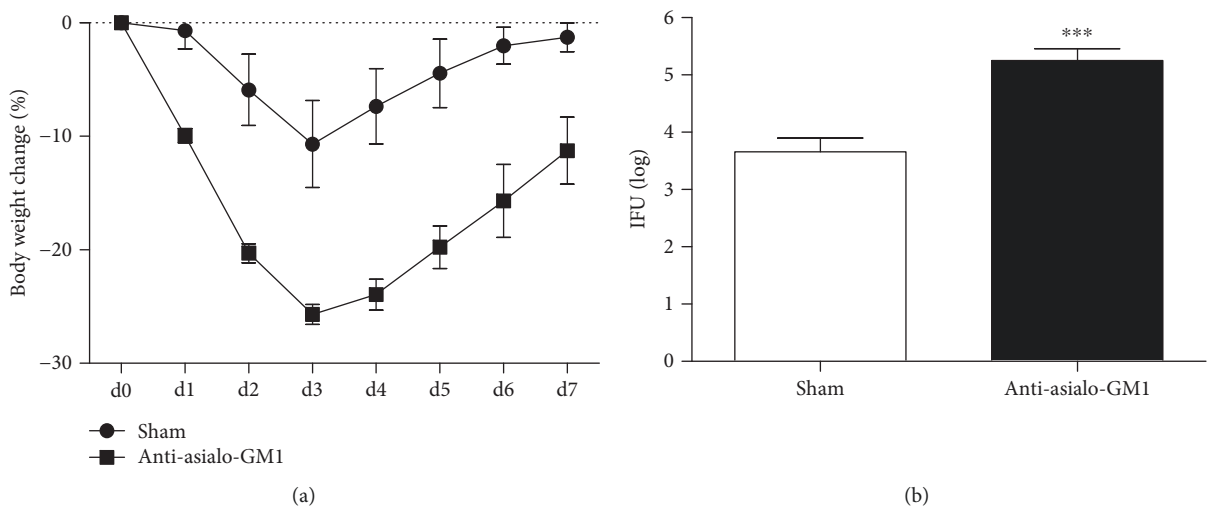


FIGURE 3: More severe disease in NK-depleted mice after *Cpn* lung infection. C57BL/6 mice were treated with anti-asialo-GM1 or control rabbit IgG during *Cpn* lung infection as described in Materials and Methods. (a) The body weight changes of the mice were monitored daily. Each time point represented the mean \pm SD of three mice. (b) Mice were sacrificed, and the lungs were collected for testing *Cpn* loads at day 7 p.i. The mean of log₁₀-transformed IFUs per lung is presented. *** $p < 0.001$.

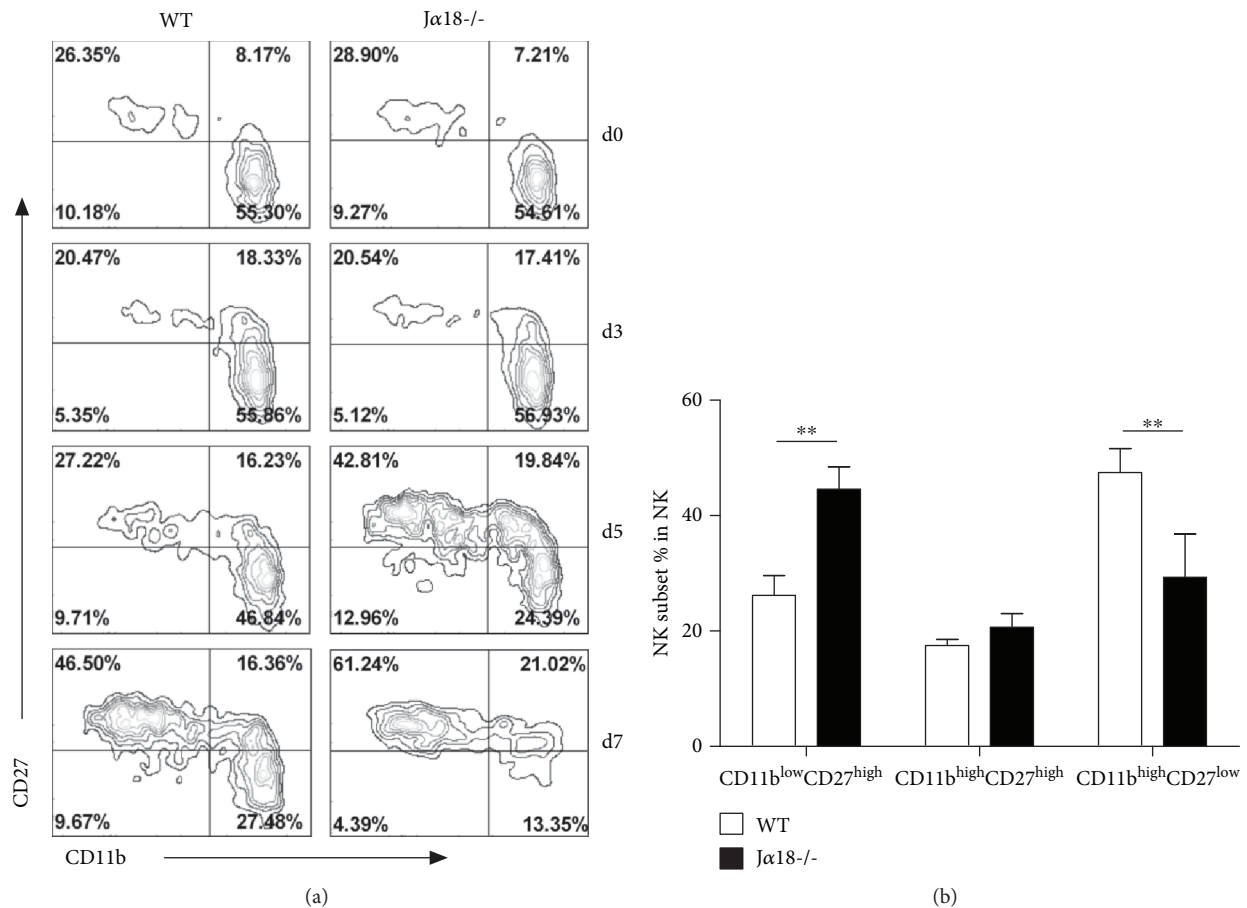


FIGURE 4: NK cells from Jα18-/- mice show altered distribution of NK subsets during *Cpn* infection. Mice were killed at different days following intranasal infection with *Cpn* EBs (5×10^6 IFUs), and the splenocytes were prepared for flow cytometry. (a) Relative distribution of CD11b- and CD27-expressing NK cells at a steady state and at specified days after infection in WT mice and Jα18-/- mice. Zebra plots were shown from at least three independent experiments. (b) The bar summarizes the relative distribution of splenic NK subsets at day 5 p.i., which are shown as mean \pm SD for four mice. ** $p < 0.01$.

CD11b^{high}CD27^{low} NK subset showed an earlier decrease in iNKT KO mice than WT control. Therefore, iNKT deficiency appeared to promote the increase of CD27^{high} NK subset in the kinetics.

3.5. iNKT Deficiency Results in Compromised NK Activation and Reduced IFN- γ Production by NK Cells following *Cpn* Infection. It has been reported that the murine CD27^{high} NK cells exhibit potent responsiveness and enhanced cytokine production, whereas the CD11b^{high}CD27^{low} subset has a higher activation threshold [11]. Therefore, the increased frequency of the CD27^{high} NK cells in Jα18-/- mice might suggest an enhanced NK function in these mice. To test this possibility, we compared the activation status and cytokine production of NK cell in the *Cpn*-infected WT and iNKT KO mice. Surprisingly, we found that the NK cells from iNKT KO mice showed much lower expression of CD69 (Figures 5(a) and 5(b)) and CD25 (Figures 5(c) and 5(d)) than WT mice at day 1 and day 3 p.i. Further analysis revealed that the levels of CD69 (Figure 5(e)) and CD25 (Figure 5(f)) expression in all the NK subsets from iNKT

KO mice were lower than that of WT mice. The data did not support the notion of higher NK activation in iNKT KO mice than WT mice although the percentage of CD27^{high} NK cells is higher in iNKT KO mice.

We further investigated the influence of iNKT cells on IFN- γ production by NK cells through intracellular cytokine staining. As shown in Figures 6(a) and 6(b), significantly less NK cells in iNKT KO mice were stained positively for IFN- γ at day 5 after *Cpn* infection, compared with those in WT mice. The percentage of IFN- γ -producing NK cells in iNKT KO mice was less than half of WT mice. IFN- γ production by NK cells partially depended on iNKT cells. Furthermore, we tested the levels of intracellular IFN- γ expression in each of the subsets to determine the functional changes in individual NK subsets. We found reduced IFN- γ production by all the three major NK subsets (Figure 6(c)), suggesting that the modulating effect of iNKT cells on IFN- γ production by NK cells was not restricted to particular NK subsets. Together, the data suggest that iNKT cells can promote the activation and IFN- γ production of NK cells following *Cpn* infection.

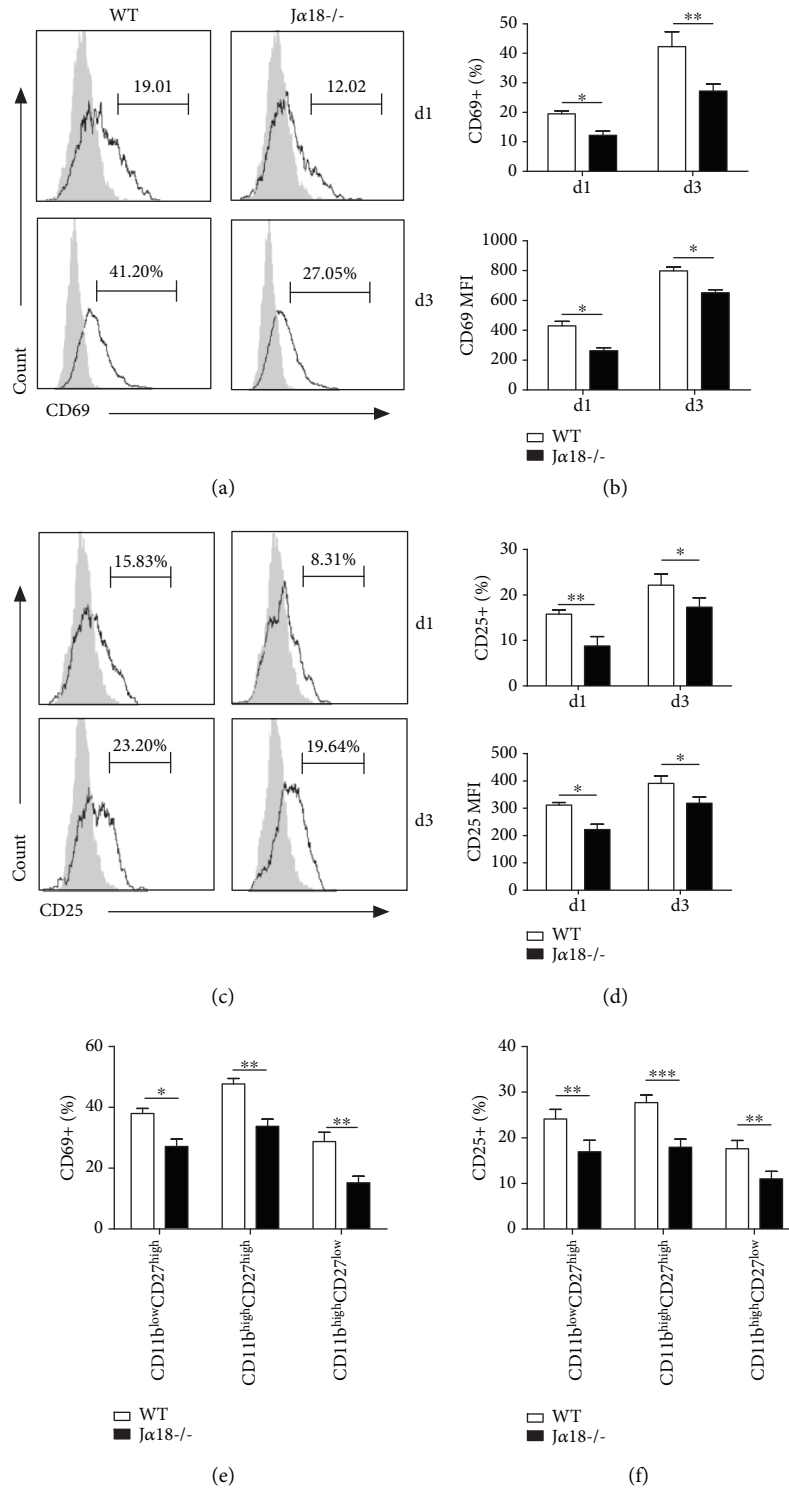


FIGURE 5: NK cells from *Ja18^{-/-}* mice show lower CD69 and CD25 expression in response to *Cpn* infection. WT and *Ja18^{-/-}* mice were intranasally infected with *Cpn* (5×10^6 IFUs) and examined at days 1 and 3 p.i. Splenocytes were prepared for flow cytometry analysis. (a) CD69 expression on NK (NK1.1+CD3e-) cells was analyzed at days 1 and 3 p.i. Representative histograms are shown. Filled gray: isotype control Ab staining; black lines: anti-CD69 Ab staining. (b) Summary of the proportion (upper) and the MFI (lower) of CD69 on NK cells. (c) Representative histograms of CD25 expression on NK cells are shown. Filled gray: isotype control Ab staining; black lines: anti-CD25 Ab staining. (d) Summary of the proportion (upper) and the MFI (lower) of CD25 on NK cells. (e) The frequency of CD69 was analyzed on the specified NK cell subsets based on CD11b and CD27 staining at day 3 p.i. (f) The frequency of CD25 was analyzed on the indicated NK cell subsets based on CD11b and CD27 staining at day 3 p.i. The results are shown as mean \pm SD of three mice in each group and are representative of three independent experiments. * $p < 0.05$ and ** $p < 0.01$.

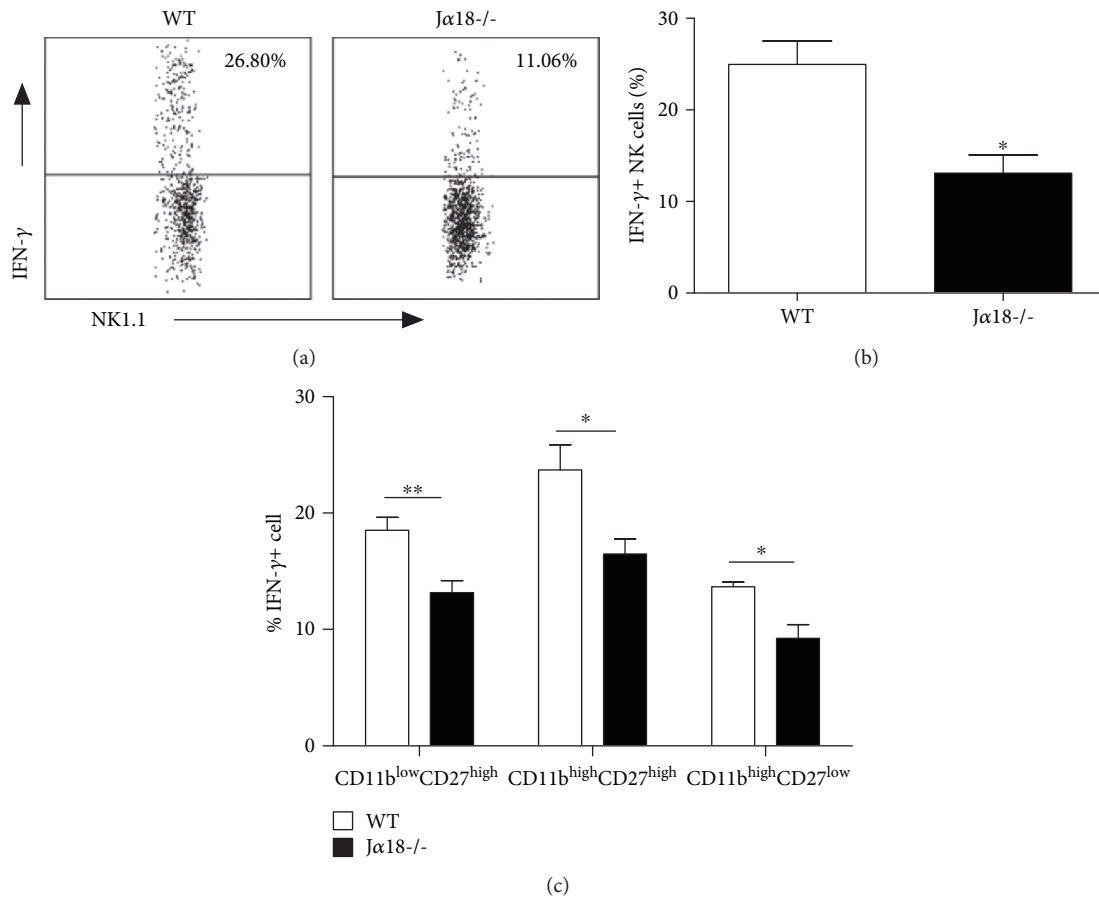


FIGURE 6: Reduced IFN- γ production by NK cells in $J\alpha 18^{-/-}$ mice following *Cpn* lung infection. Mice were intranasally infected with *Cpn* (5×10^6 IFU). At day 5 p.i., splenocytes from WT and $J\alpha 18^{-/-}$ mice were stained for NK1.1, CD3e, CD11b, CD27, and IFN- γ and analyzed by flow cytometry. (a) Representative dot plots of IFN- γ production by NK cells in WT and $J\alpha 18^{-/-}$ mice. (b) The percentage of IFN- γ -producing NK cells was summarized. (c) The frequency of IFN- γ production was analyzed on the specified NK cell subsets based on CD11b and CD27 staining. The data are shown as mean \pm SD ($n = 4$). One representative experiment of three independent experiments is shown. * $p < 0.05$.

3.6. DCs from iNKT-Deficient Mice Show Reduced Ability to Induce NK Cell Activation and IFN- γ Production. DC can prime resting NK cell both in mice [4, 32, 33] and in humans [34]. Previous studies have demonstrated a pivotal role for DC-derived IL-12 in the induction of IFN- γ -producing NK cells [35]. The level of DC maturation affected the degree of NK activation [33, 36]. Therefore, it is likely that the reduced NK cell activation and IFN- γ production in iNKT-deficient mice are a result of the altered DC function. To directly test this, DCs were isolated from *Cpn*-infected WT and iNKT KO mice and cocultured with NK cells from uninfected WT mice for 24 hours. The expression of CD69 and CD25 and production of IFN- γ by NK cells were tested by flow cytometry. As shown in Figure 7, both WT-DC and KO-DC induced enhanced CD69 and CD25 surface expression by NK cells. However, KO-DC-induced CD69 (Figures 7(a) and 7(b)) and CD25 (Figures 7(c) and 7(d)) expression of NK cells was significantly lower than that induced by WT-DC. More importantly, NK cells cocultured with KO-DC produced significantly lower levels of IFN- γ than those cocultured with WT-DC (Figures 7(e) and 7(f)). Meanwhile,

IFN- γ levels in culture supernatants were also significantly lower in KO-DC-NK coculture than in WT-DC-NK coculture (Figure 7(g)). As a control, neither DC nor NK alone produced detectable IFN- γ . To further test the role of DCs in iNKT-mediated NK response in vivo, we performed adoptive transfer experiments with DC isolated from *Cpn*-infected iNKT KO and WT mice. The activation marker expression and IFN- γ production by NK cells were examined at day 3 after *Cpn* challenge. As shown in Figure 8, significantly lower CD69 and CD25 expression and IFN- γ production by NK cells were observed in the recipients of KO-DCs than WT-DC recipients. The data suggest that DCs play a critical role in iNKT-mediated NK activation and IFN- γ production during *Cpn* infection.

4. Discussion

Our data showed a significant modulating effect of iNKT cell on NK cell activation and IFN- γ production in lung *Cpn* infection. Moreover, we found that DCs play an important role in the iNKT-mediated modulation of NK cell function.

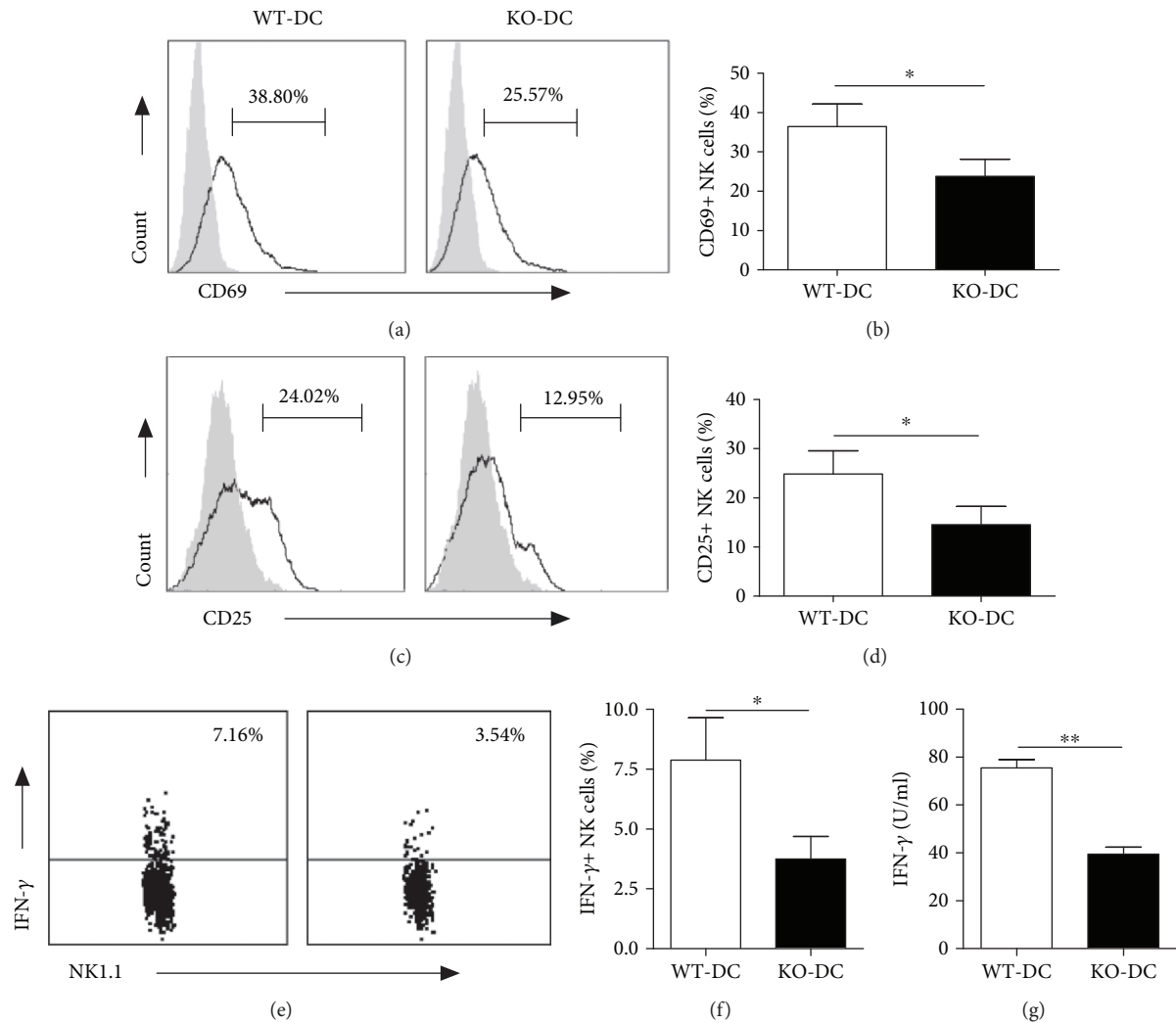


FIGURE 7: Reduced ability of DCs from *Cpn*-infected iNKT KO mice to induce activation and IFN- γ production by naïve NK cells. DCs were isolated from spleens of iNKT KO mice (KO-DC) and WT mice (WT-DC) at day 5 p.i. NK cells were enriched from the spleen of naïve mice. NK cells (2×10^5) were cocultured with DC (1×10^6) cells in a 96-well round bottom plate. After 48 h, the cells and supernatant were collected for CD69, CD25, and IFN- γ staining of the cells and ELISA measurement of IFN- γ in the supernatants, respectively. The representative histograms and dot plots for CD69 (a) and CD25 (b) expression and IFN- γ production (e) by NK cells are depicted. The percentage of CD69+ (b), CD25+ (d), and IFN- γ + (f) NK cells was summarized. (g) The concentration of IFN- γ in supernatant was examined by ELISA. The data represent one of three similar experiments and are shown as mean \pm SD. * $p < 0.05$, ** $p < 0.01$.

Specifically, we showed that respiratory *Cpn* infection induced NK cell activation and IFN- γ production with dynamic changes of NK subsets. Further comparison of NK cell response in iNKT KO and WT mice revealed a promoting role of iNKT cells in NK cell function, which was demonstrated by decreased expression of activation markers, reduced production of IFN- γ , and changes of NK subsets in iNKT KO mice. The activation and IFN- γ production by NK cells are largely influenced by iNKT cells in *Cpn* infection although it is not completely dependent on iNKT cells, suggesting a promoting role of iNKT cell on NK cell function. More interestingly, we found in a DC-NK coculture system that DCs isolated from *Cpn*-infected iNKT KO mice induced lower activation marker expression and less IFN- γ production by NK cells than those isolated from WT mice, suggesting a critical role of DCs in iNKT-mediated modulation of

NK function. We also showed in the present study that NK cells play an important protective role in host defense against *Cpn* infection. In line with this, we also found that adoptive transfer of DCs from iNKT KO mice generated less IFN- γ production by NK cells than the DCs from WT mice in vivo. Our previous studies focus on the effect of iNKT on DC function in modulating T cells [1] while the current data showed an effect of iNKT on DCs which subsequently modulate NK cell function. We have reported previously that iNKT can significantly influence DC phenotype, cytokine production, subsets, and function in the spleen and lung in chlamydial infections [1, 27, 28, 31]. The combined data from previous reports and the current study provide a mechanistic explanation for the previously reported modulating effect of iNKT on NK function [24] by showing the critical role of DCs in this modulating process. Considering our

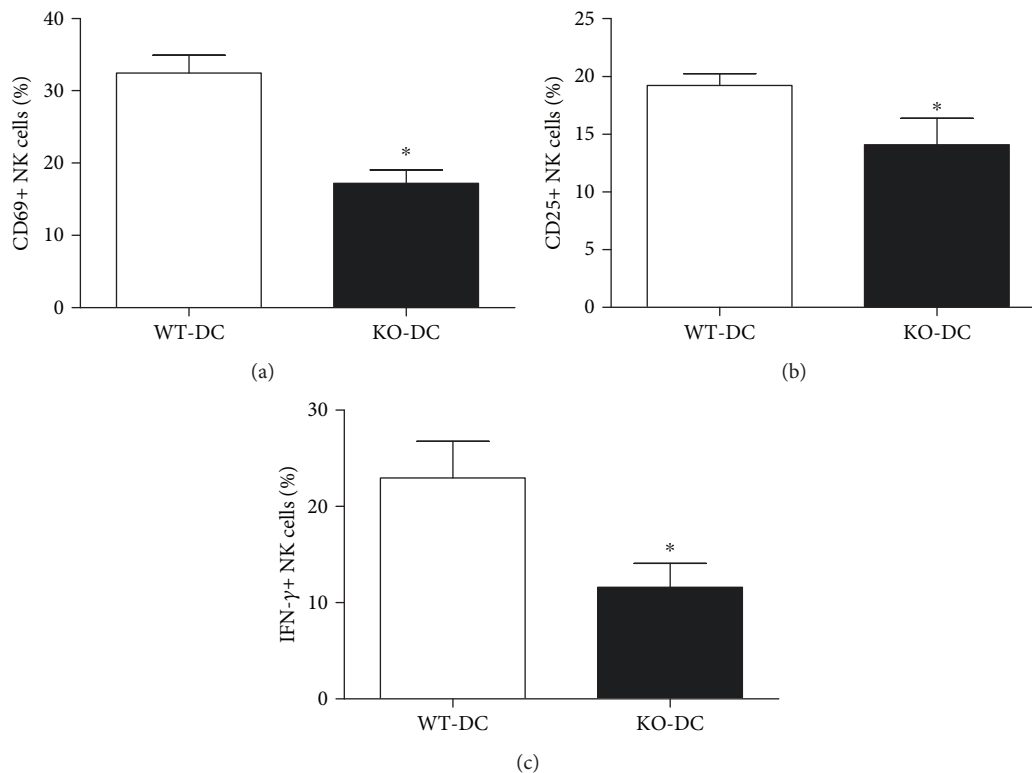


FIGURE 8: Adoptive transfer of KO-DC induces less activation and IFN- γ production by NK cells. Naive recipient mice (C57BL/6) were delivered DCs isolated from spleens of *Cpn*-infected iNKT KO mice (KO-DC) and WT mice (WT-DC). The recipient mice were sacrificed at day 3 after *Cpn* challenge. The spleen cells were collected to measure CD69 and CD25 expression and IFN- γ production by NK cells using flow cytometry. The percentage of CD69+ (a), CD25+ (b), and IFN- γ + (c) NK cells was summarized. The data represent one of three similar experiments and are shown as mean \pm SD. * $p < 0.05$.

previous report on the modulating effect of NK on DCs [27], the findings also suggest a reciprocal influence of DC and NK cells in chlamydial infection.

The study provides new data on the dynamic changes of NK cell responses in lung *Cpn* infection, showing that NK cells rapidly expanded with upregulated CD69 and CD25 expression and enhanced IFN- γ production. More interestingly, the data provided in vivo evidence of NK subset switch in response to *Cpn* infection. Distinct function of NK subsets based on CD27 and CD11b expression has been reported [12, 37, 38]. We observed that *Cpn* infection increased the percentage of CD11b^{low}CD27^{high} and CD11b^{high}CD27^{high} NK subsets so consequently reducing the proportion of CD11b^{high}CD27^{low} NK subset. It has been reported that CD27^{high} NK cells have a lower threshold for activation and produce more IFN- γ compared with CD27^{low} subset [11]. In our infection model, CD27^{high} NK cells were the major producer for IFN- γ within the whole NK population during *Cpn* infection (data not shown). The increased proportion of CD27^{high} NK cells might contribute to high levels of IFN- γ production by NK cells after *Cpn* infection. Although the exact mechanism accounting for CD27^{high} NK cell expansion remains unclear, the following possibilities are likely involved: (1) the proliferation of CD27^{high} NK cells *in situ*, (2) the migration of immature NK cells from bone marrow, and (3) the cell death or reversion of CD11b^{high}CD27^{low} NK subset.

The effect of iNKT on NK subsets was particularly interesting. It was found that the iNKT KO mice showed higher expansion of CD27^{high} NK subset than WT mice following *Cpn* infection. Considering the lower threshold of this subset for activation, one might think that the KO mice had better NK function especially IFN- γ production. However, we found that all the NK cell subsets including the CD27^{high} subset in iNKT KO mice showed lower CD69 and CD25 expression and IFN- γ production compared with the corresponding subsets in WT mice. The results suggest that the surface markers in defying the functional subsets of NK cells may not be absolute. Although CD27 expression normally suggests higher activation and IFN- γ production, the CD27^{high} NK cells, in the condition of iNKT deficiency, actually expressed lower levels of activation markers and IFN- γ than those in WT mice. Therefore, the analysis of cell subsets needs to have a combination of surface markers and cytokine patterns. Moreover, since all the three NK subsets from iNKT KO mice showed lower expression of activation markers and production of IFN- γ , the modulating effect of iNKT cells on NK cells is not restricted to a particular NK cell subset.

The results of NK-DC coculture study provide new mechanistic data on the modulating effect of iNKT on NK cells by showing the critical role of DCs in this process. Notably, we and others have shown the modulating effect of iNKT and NK cells on DC function [1, 27, 28]. In particular, we found that iNKT as well as NK cell can modulate

the function of splenic and pulmonary DCs in promoting CD4 and CD8 T cell responses [27, 28]. The present finding on the promoting effect of DCs from iNKT intact WT mice on NK cells for the production of IFN- γ suggests a loop of positive feedback in amplifying the promoting role of iNKT on type 1 T cell responses in addition to the direct promoting effect on NK effector function. The finding further supports the importance of interactions among multiple types of innate and adaptive immune cells in the expansion and restriction of the scales of inflammatory reactions for immune homeostasis.

Our data showed that NK depletion in immune intact mice led to increased *Cpn* burden in the lung (Figure 3), suggesting that NK cells are functionally involved in protection against *Cpn* lung infection. This observation might be considered inconsistent with the study using T cell- and B cell-deficient mice [29, 30]. Indeed, one report showed that RAG-1^{-/-} γ CR^{-/-} and RAG-1^{-/-} mice showed similar susceptibility to *Cpn* lung infection, suggesting a negligible role of NK cells in *Cpn* infection [30]. Another report showed that the *Cpn* load in the lung of RAG-1^{-/-} mice was not altered after eliminating NK cells using neutralizing Abs [29]. However, we think that our data are not necessarily contradictory with the previous reports. The observed discrepancy might be due to the different mice that were used in the studies: T/B cell deficient [29, 30] versus T/B intact mice in the present study. When our current study is considered with previously reported ones [29, 30], it might suggest that NK cell plays its protective role though promoting the function of other immune cells, particularly T and B cells, rather than directly controlling *Cpn* lung infection as an effector. The deficiency of T and B cells in RAG-1^{-/-} mice likely covered up this promoting function of NK cells on Th1 responses though IFN- γ production as shown in our previous study [27].

5. Conclusions

In summary, our data revealed a significant modulating effect of iNKT cell on NK cell activation and IFN- γ production in respiratory *Cpn* infection. Additionally, the results provided a mechanistic explanation for the iNKT-mediated modulation of NK cell function by showing the important role of DCs. The finding has implications on understanding the complexity of cellular networks in respiratory tract chlamydial infection, which should be considered in designing preventive and therapeutic approaches.

Data Availability

The data used to support the findings of this study are available from the corresponding author upon request.

Conflicts of Interest

The authors confirm that there are no conflicts of interest.

Acknowledgments

We are grateful to Dr. Masaru Taniguchi (RIKEN Research Center for Allergy and Immunology) for his generous gift of the $\text{J}\alpha 18$ gene knockout ($\text{J}\alpha 18^{-/-}$) mice. This work was supported by grants jointly funded by Canadian Institutes of Health Research (CIHR) to X.Y. (CCI 92213 and MOP-130423) and the National Natural Science Foundation of China (NSFC) to L.Z. (81501761) and W.Z. (30811120425). X.Y. was the Canada Research Chair in Infection and Immunity.

Supplementary Materials

Figure S1: pulmonary NK cells expand after *Cpn* lung infection. Figure S2: NK cell depletion in the spleen and lung. Figure S3: the absolute number of NK cells in WT and iNKT KO mice is similar before and after *Cpn* infection. (*Supplementary Materials*)

References

- [1] A. G. Joyee, H. Qiu, Y. Fan, S. Wang, and X. Yang, "Natural killer T cells are critical for dendritic cells to induce immunity in Chlamydial pneumonia," *American Journal of Respiratory and Critical Care Medicine*, vol. 178, no. 7, pp. 745–756, 2008.
- [2] P. Arora, A. Baena, K. O. A. Yu et al., "A single subset of dendritic cells controls the cytokine bias of natural killer T cell responses to diverse glycolipid antigens," *Immunity*, vol. 40, no. 1, pp. 105–116, 2014.
- [3] M. Lucas, W. Schachterle, K. Oberle, P. Aichele, and A. Diefenbach, "Dendritic cells prime natural killer cells by trans-presenting interleukin 15," *Immunity*, vol. 26, no. 4, pp. 503–517, 2007.
- [4] F. Gerosa, B. Baldani-Guerra, C. Nisii, V. Marchesini, G. Carra, and G. Trinchieri, "Reciprocal activating interaction between natural killer cells and dendritic cells," *The Journal of experimental medicine*, vol. 195, no. 3, pp. 327–333, 2002.
- [5] P. L. Dunn and R. J. North, "Early gamma interferon production by natural killer cells is important in defense against murine listeriosis," *Infection and Immunity*, vol. 59, no. 9, pp. 2892–2900, 1991.
- [6] M. B. Lodoen and L. L. Lanier, "Natural killer cells as an initial defense against pathogens," *Current Opinion in Immunology*, vol. 18, no. 4, pp. 391–398, 2006.
- [7] J. Loh, D. T. Chu, A. K. O'Guin, W. M. Yokoyama, and H. W. Virgin, "Natural killer cells utilize both perforin and gamma interferon to regulate murine cytomegalovirus infection in the spleen and liver," *Journal of Virology*, vol. 79, no. 1, pp. 661–667, 2005.
- [8] A. Silva, D. M. Andrews, A. G. Brooks, M. J. Smyth, and Y. Hayakawa, "Application of CD27 as a marker for distinguishing human NK cell subsets," *International Immunology*, vol. 20, no. 4, pp. 625–630, 2008.
- [9] Y. Hayakawa, N. D. Huntington, S. L. Nutt, and M. J. Smyth, "Functional subsets of mouse natural killer cells," *Immunological reviews*, vol. 214, no. 1, pp. 47–55, 2006.
- [10] L. Chiossone, J. Chaix, N. Fuseri, C. Roth, E. Vivier, and T. Walzer, "Maturation of mouse NK cells is a 4-stage developmental program," *Blood*, vol. 113, no. 22, pp. 5488–5496, 2009.

- [11] Y. Hayakawa and M. J. Smyth, "CD27 dissects mature NK cells into two subsets with distinct responsiveness and migratory capacity," *Journal of immunology*, vol. 176, no. 3, pp. 1517–1524, 2006.
- [12] M. Gao, Y. Yang, D. Li et al., "CD27 natural killer cell subsets play different roles during the pre-onset stage of experimental autoimmune encephalomyelitis," *Innate Immunity*, vol. 22, no. 6, pp. 395–404, 2016.
- [13] Z. K. Ballas, C. M. Buchta, T. R. Rosean, J. W. Heusel, and M. R. Shey, "Role of NK cell subsets in organ-specific murine melanoma metastasis," *PLoS One*, vol. 8, no. 6, p. e65599, 2013.
- [14] D. I. Godfrey, H. R. MacDonald, M. Kronenberg, M. J. Smyth, and L. V. Kaer, "NKT cells: what's in a name?," *Nature Reviews Immunology*, vol. 4, no. 3, pp. 231–237, 2004.
- [15] A. Bendelac, O. Lantz, M. E. Quimby, J. W. Yewdell, J. R. Bennink, and R. R. Brutkiewicz, "CD1 recognition by mouse NK1+ T lymphocytes," *Science*, vol. 268, no. 5212, pp. 863–865, 1995.
- [16] E. Tonti, G. Galli, C. Malzone, S. Abrignani, G. Casorati, and P. Dellabona, "NKT-cell help to B lymphocytes can occur independently of cognate interaction," *Blood*, vol. 113, no. 2, pp. 370–376, 2009.
- [17] Y. Hayakawa, K. Takeda, H. Yagita et al., "Critical contribution of IFN- γ and NK cells, but not perforin-mediated cytotoxicity, to anti-metastatic effect of α -galactosylceramide," *European Journal of Immunology*, vol. 31, no. 6, pp. 1720–1727, 2001.
- [18] G. Eberl and H. R. MacDonald, "Selective induction of NK cell proliferation and cytotoxicity by activated NKT cells," *European Journal of Immunology*, vol. 30, no. 4, pp. 985–992, 2000.
- [19] C. Carnaud, D. Lee, O. Donnars et al., "Cutting edge: cross-talk between cells of the innate immune system: NKT cells rapidly activate NK cells," *Journal of immunology*, vol. 163, no. 9, pp. 4647–4650, 1999.
- [20] L. S. Metelitsa, O. V. Naidenko, A. Kant et al., "Human NKT cells mediate antitumor cytotoxicity directly by recognizing target cell CD1d with bound ligand or indirectly by producing IL-2 to activate NK cells," *The Journal of Immunology*, vol. 167, no. 6, pp. 3114–3122, 2001.
- [21] P. Riese, S. Trittel, T. May, L. Cicin-Sain, B. J. Chambers, and C. A. Guzman, "Activated NKT cells imprint NK-cell differentiation, functionality and education," *European Journal of Immunology*, vol. 45, no. 6, pp. 1794–1807, 2015.
- [22] M. S. Duthie and S. J. Kahn, "NK cell activation and protection occur independently of natural killer T cells during Trypanosoma cruzi infection," *International Immunology*, vol. 17, no. 5, pp. 607–613, 2005.
- [23] C. Paget, S. Ivanov, J. Fontaine et al., "Potential role of invariant NKT cells in the control of pulmonary inflammation and CD8+ T cell response during acute influenza A virus H3N2 pneumonia," *Journal of Immunology*, vol. 186, no. 10, pp. 5590–5602, 2011.
- [24] L. Zhao, X. Gao, Y. Peng et al., "Differential modulating effect of natural killer (NK) T cells on interferon- γ production and cytotoxic function of NK cells and its relationship with NK subsets in Chlamydia muridarum infection," *Immunology*, vol. 134, no. 2, pp. 172–184, 2011.
- [25] A. G. Joyee, H. Qiu, S. Wang, Y. Fan, L. Bilenki, and X. Yang, "Distinct NKT cell subsets are induced by different Chlamydia species leading to differential adaptive immunity and host resistance to the infections," *The Journal of Immunology*, vol. 178, no. 2, pp. 1048–1058, 2007.
- [26] C. T. Tseng and R. G. Rank, "Role of NK cells in early host response to chlamydial genital infection," *Infection and Immunity*, vol. 66, no. 12, pp. 5867–5875, 1998.
- [27] L. Jiao, X. Gao, A. G. Joyee et al., "NK cells promote type 1 T cell immunity through modulating the function of dendritic cells during intracellular bacterial infection," *The Journal of Immunology*, vol. 187, no. 1, pp. 401–411, 2011.
- [28] S. Shekhar, Y. Peng, X. Gao et al., "NK cells modulate the lung dendritic cell-mediated Th1/Th17 immunity during intracellular bacterial infection," *European Journal of Immunology*, vol. 45, no. 10, pp. 2810–2820, 2015.
- [29] M. E. Rottenberg, A. Gigliotti Rothfuchs, D. Gigliotti et al., "Regulation and role of IFN-gamma in the innate resistance to infection with Chlamydia pneumoniae," *Journal of Immunology*, vol. 164, no. 9, pp. 4812–4818, 2000.
- [30] A. G. Rothfuchs, M. R. Kreuger, H. Wigzell, and M. E. Rottenberg, "Macrophages, CD4+ or CD8+ cells are each sufficient for protection against Chlamydia pneumoniae infection through their ability to secrete IFN-gamma," *Journal of Immunology*, vol. 172, no. 4, pp. 2407–2415, 2004.
- [31] A. G. Joyee, J. Uzonna, and X. Yang, "Invariant NKT cells preferentially modulate the function of CD8 α + dendritic cell subset in inducing type 1 immunity against infection," *The Journal of Immunology*, vol. 184, no. 4, pp. 2095–2106, 2010.
- [32] N. C. Fernandez, A. Lozier, C. Flament et al., "Dendritic cells directly trigger NK cell functions: cross-talk relevant in innate anti-tumor immune responses in vivo," *Nature Medicine*, vol. 5, no. 4, pp. 405–411, 1999.
- [33] J. Xu, A. K. Chakrabarti, J. L. Tan, L. Ge, A. Gambotto, and N. L. Vujanovic, "Essential role of the TNF-TNFR2 cognate interaction in mouse dendritic cell-natural killer cell cross-talk," *Blood*, vol. 109, no. 8, pp. 3333–3341, 2007.
- [34] G. Ferlazzo, M. L. Tsang, L. Moretta, G. Melioli, R. M. Steinman, and C. Munz, "Human dendritic cells activate resting natural killer (NK) cells and are recognized via the NKp30 receptor by activated NK cells," *The Journal of Experimental Medicine*, vol. 195, no. 3, pp. 343–351, 2002.
- [35] C. Borg, A. Jalil, D. Laderach et al., "NK cell activation by dendritic cells (DCs) requires the formation of a synapse leading to IL-12 polarization in DCs," *Blood*, vol. 104, no. 10, pp. 3267–3275, 2004.
- [36] L. Vujanovic, D. E. Szymkowski, S. Alber, S. C. Watkins, N. L. Vujanovic, and L. H. Butterfield, "Virally infected and matured human dendritic cells activate natural killer cells via cooperative activity of plasma membrane-bound TNF and IL-15," *Blood*, vol. 116, no. 4, pp. 575–583, 2010.
- [37] S. Paul, N. Kulkarni, Shilpi, and G. Lal, "Intratumoral natural killer cells show reduced effector and cytolytic properties and control the differentiation of effector Th1 cells," *Oncoimmunology*, vol. 5, no. 12, article e1235106, 2016.
- [38] K. Meinhardt, I. Kroeger, R. Bauer et al., "Identification and characterization of the specific murine NK cell subset supporting graft-versus-leukemia- and reducing graft-versus-host-effects," *Oncoimmunology*, vol. 4, no. 1, article e981483, 2015.

Research Article

The Inflammatory Response to Enterotoxigenic *E. coli* and Probiotic *E. faecium* in a Coculture Model of Porcine Intestinal Epithelial and Dendritic Cells

Henriette Loss ¹, Jörg R. Aschenbach ¹, Karsten Tedin ², Friederike Ebner,³
and Ulrike Lodemann ¹

¹Institute of Veterinary Physiology, Department of Veterinary Medicine, Freie Universität Berlin, Oertzenweg 19b, 14163 Berlin, Germany

²Institute of Microbiology and Epizootics, Department of Veterinary Medicine, Freie Universität Berlin, Robert-von-Ostertag-Str. 7-13, 14163 Berlin, Germany

³Institute of Immunology, Department of Veterinary Medicine, Freie Universität Berlin, Robert-von-Ostertag-Str. 7-13, 14163 Berlin, Germany

Correspondence should be addressed to Ulrike Lodemann; ulrike.lodemann@fu-berlin.de

Received 22 August 2018; Accepted 23 October 2018; Published 20 December 2018

Guest Editor: Renata Sesti-Costa

Copyright © 2018 Henriette Loss et al. This is an open access article distributed under the Creative Commons Attribution License, which permits unrestricted use, distribution, and reproduction in any medium, provided the original work is properly cited.

The gut epithelium constitutes an interface between the intestinal contents and the underlying gut-associated lymphoid tissue (GALT) including dendritic cells (DC). Interactions of intestinal epithelial cells (IEC) and resident DC are characterized by bidirectional crosstalk mediated by various factors, such as transforming growth factor- β (TGF- β) and thymic stromal lymphopoietin (TSLP). In the present study, we aimed (1) to model the interplay of both cell types in a porcine *in vitro* coculture consisting of IEC (cell line IPEC-J2) and monocyte-derived DC (MoDC) and (2) to assess whether immune responses to bacteria are altered because of the interplay between IPEC-J2 cells and MoDC. With regard to the latter, we focused on the inflammasome pathway. Here, we propose caspase-13 as a promising candidate for the noncanonical inflammasome activation in pigs. We conducted challenge experiments with enterotoxigenic *Escherichia coli* (ETEC) and probiotic *Enterococcus faecium* (*E. faecium*) NCIMB 10415. As potential mediators of IEC/DC interactions, TGF- β and TSLP were selected for analyses. Cocultured MoDC showed attenuated ETEC-induced inflammasome-related and proinflammatory interleukin (IL)-8 reactions compared with MoDC monocultures. Caspase-13 was more strongly expressed in IPEC-J2 cells cocultured with MoDC and upon ETEC incubation. We found that IPEC-J2 cells and MoDC were capable of releasing TSLP. The latter cells secreted greater amounts of TSLP when cocultured with IPEC-J2 cells. TGF- β was not modulated under the present experimental conditions in either cell types. We conclude that, in the presence of IPEC-J2 cells, porcine MoDC exhibited a more tolerogenic phenotype, which might be partially regulated by autocrine TSLP production. Noncanonical inflammasome signaling appeared to be modulated in IPEC-J2 cells. Our results indicate that the reciprocal interplay of the intestinal epithelium and GALT is essential for promoting balanced immune responses.

1. Introduction

Intestinal epithelial cells lining the intestinal mucosa are continuously exposed to a variety of potentially harmful antigens and build a physical interface that separates the luminal content from the host milieu [1]. In the gut, DC are found in the *lamina propria*, in the subepithelial dome region of Peyer's

patches, and in solitary lymph nodes such as the mesenteric lymph nodes [2–4]. Within the dynamic communication system between enterocytes and mucosal immune cells, IEC direct the function of resident DC by releasing immune mediators, such as the regulatory cytokine TGF- β and TSLP [5, 6]. Intestinal DC and IEC are both pivotal for maintaining normal barrier function as they support the discrimination

between inflammatory and tolerogenic immune responses [7, 8]. Therefore, functional properties of the intestinal epithelium cannot be fully understood by using *in vitro* models in which epithelial cells are solely grown as monocultures [7]. Our objective was to reconstruct the intestinal environment *in vitro* by implementing the presence of MoDC in the subepithelial compartment of a porcine jejunum epithelial cell line grown on cell culture inserts of Transwell systems.

Since luminal microbiota also participate in the crosstalk [9, 10], we hypothesized that the inflammatory response patterns of IEC and immune cells to the different types of bacteria are influenced by the mutual interplay of these cells. Therefore, a pathogenic ETEC strain frequently causing postweaning diarrhea in piglets [11, 12] and an apathogenic *E. faecium* strain were included in the study design. In pigs, the probiotic *E. faecium* NCIMB 10415, which is used as a feed additive for sows and piglets, has previously been demonstrated to exert diverse favorable effects on the immune system and performance parameters both *in vitro* [13–15] and *in vivo* [16–19], especially during the postweaning period.

We aimed to unravel variations in the inflammatory responses of IEC and DC under coculture conditions with a focus on the signaling *via* the inflammasome pathway. Nucleotide oligomerization domain (NOD)-like receptors (NLR) represent a class of intracellular pattern recognition receptors (PRR), some of which are able to form inflammasomes [20]. A well-known member of this inflammasome-forming receptor family is NLRP3 (NLR family, pyrin domain containing 3) [21]. Among other stimuli, the NLRP3 inflammasome can be activated through bacterial infection [22]. Canonical and noncanonical inflammasome activations can be distinguished with regard to the characterization of inflammasome signaling [23]. Upon canonical inflammasome activation, the effector caspase-1 leads to the production and secretion of the proinflammatory cytokines IL-1 β and IL-18 [24]. In contrast, noncanonical inflammasome activation requires species-specific inflammatory caspases other than caspase-1, particularly caspase-11 in mice [25] and caspase-4 and -5 in humans [26, 27]. Bovine caspase-13 is presumed to represent the ortholog of human caspase-4 [28]. Based on these findings, we propose that caspase-13 exerts a similar function in pigs. Noncanonical inflammasome activation has been demonstrated for various Gram-negative bacteria, such as *Vibrio cholerae*, *Escherichia coli* (*E. coli*), and *Salmonella* Typhimurium [25, 29]. Most of the inflammasome studies have been carried out in human or mouse models, but a deeper understanding of porcine inflammasome pathways is lacking. In particular, no studies exist regarding noncanonical inflammasome activation in pigs. A further hypothesis tested in the present study was that porcine caspase-13 is involved in noncanonical inflammasome activation in pigs.

2. Material and Methods

2.1. Porcine Intestinal Epithelial Cells. The cell line IPEC-J2 was used as a porcine intestinal epithelial model. The cell line was originally derived from the jejunum of a newborn piglet

and was kindly provided by Professor Dr. Anthony Blikslager (North Carolina State University, USA). Cells were cultivated as described elsewhere [15]. Medium was changed 3 times per week. Every 7 days, cells were split at a ratio of 1 : 3. Passages between 73 and 80 were included in the experiments. IPEC-J2 cells were seeded on the top surface of collagenized cell culture inserts of 12-well Transwell systems (12 mm diameter, 1.12 cm² growth surface area, 0.4 μ m pore size, Costar, Corning BV, Schiphol-Rijk, The Netherlands) at a density of 1×10^5 cells per cell culture insert. Cells were cultivated under a humidified atmosphere of 5% CO₂ at 37°C for 14 to 21 days until reaching confluency.

2.2. Generation of Monocyte-Derived Dendritic Cells. Blood was taken from conventionally reared Danbred \times Pietrain pigs (10 to 12 weeks of age) kept at the Institute of Animal Nutrition (Freie Universität Berlin, Germany) or from clinically healthy pigs at a slaughterhouse in Brandenburg, Germany. The blood sample collection procedure was conducted in accordance with the guidelines for animal welfare and was approved by the ethics committee for animal welfare, namely, “Landesamt für Gesundheit und Soziales” (LaGeSo Berlin, no. T0264/15). Blood samples were collected in 9 ml ethylenediamine tetra-acetic acid (EDTA)-coated blood tubes (S-Monovette®, SARSTEDT, Nümbrecht, Germany).

Peripheral blood mononuclear cells (PBMC) were purified by density gradient centrifugation as described by Loss et al. [30] by using Ficoll-Paque™ PLUS (1.077 g/l, GE Healthcare, Uppsala, Sweden). Monocytes were subsequently enriched by magnetic labeling based on their CD14 expression and subsequent cell sorting in a MidiMACS separator and LS separation columns (both from Miltenyi Biotec, Bergisch Gladbach, Germany). CD14⁺ monocytes were diluted in RPMI-1640 (Biochrom, Berlin, Germany) supplemented with 10% fetal calf serum (FCS, Biochrom), 100 U/ml penicillin, and 100 μ g/ml streptomycin (Sigma-Aldrich Chemie GmbH). Cells were seeded at a density of 1.44×10^6 cells/ml and 1 ml per well in 12-well cell culture plates (TPP, Faust Lab, Klettgau, Germany or Eppendorf GmbH, Hamburg, Germany). To differentiate monocytes into MoDC, cells were supplemented with recombinant porcine (rp) granulocyte-macrophage colony-stimulating factor (GM-CSF, 20 ng/ml) and rp IL-4 (50 ng/ml; both from R&D Systems, Minneapolis, MN, USA). Cells were grown at 37°C under a humidified atmosphere of 5% CO₂ for 6 days. After 3 days, cells were fed with another 1 ml of fresh differentiation medium. On day 6, adherent immature MoDC were used for the experiments. In order to ensure successful differentiation, the morphological and phenotypical features of the cells were examined by phase contrast microscopy (Leica DMI 6000 series, Leica Microsystems, Heidelberg, Germany) and flow cytometry. Flow cytometric phenotypical characterization was performed as described elsewhere [30]. Briefly, the monoclonal antibodies anti-human CD14 (clone REA599, isotype IgG1, Miltenyi Biotec), anti-pig CD16 (clone G7, isotype IgG1, Bio-Rad Laboratories GmbH, Munich, Germany), anti-pig CD1 (clone 76-7-4, isotype IgG2 α κ, SouthernBiotech, Cambridge, United Kingdom), and anti-pig swine leukocyte antigen (SLA) II (clone

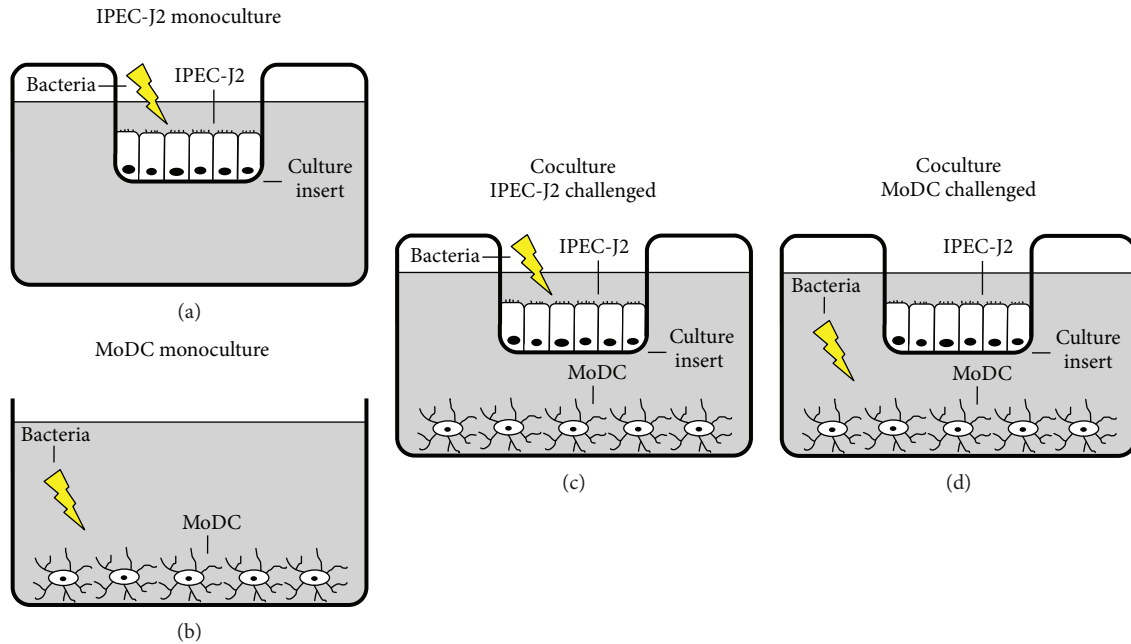


FIGURE 1: Schematic illustration of experimental design. (a) IPEC-J2 monocultures were grown as a monolayer on the top surface of Transwell cell culture inserts. Bacteria were added to the IPEC-J2 compartment. (b) MoDC monocultures were cultivated in 12-well cell culture plates. Bacteria were added to the MoDC compartment. (c)–(d) Cocultures of IPEC-J2 cells grown on Transwell inserts and adherent MoDC located in the bottom compartment. In separate approaches, bacteria were added either (c) to the IPEC-J2 compartment or (d) to the MoDC compartment. The lightning flash indicates the localization of the bacterial challenge with either *E. faecium* or ETEC.

K274.3G8, isotype IgG1, major histocompatibility complex [MHC] II, Bio-Rad Laboratories GmbH) were used. Successful differentiation was considered to have occurred when the cells showed a characteristic DC morphology and were tested as being CD14⁺ CD16⁺ CD1⁺ SLA⁺.

2.3. Bacterial Strains. Two different bacterial strains were used for the experiments: the probiotic strain *E. faecium* NCIMB 10415 (Cylactin®, DSM, Kaiseraugst, Switzerland) and enterotoxigenic *E. coli* IMT4818 (isolated from a two-week-old piglet with diarrhea, O149:K91:K88 [F4]). *E. faecium* and ETEC were grown on BHI (brain-heart infusion) and LB (Luria-Bertani) agar plates, respectively. After overnight incubation, *E. faecium* was grown in BHI broth (OXOID GmbH, Wesel, Germany) and ETEC in LB medium containing 10 g/l tryptone, 5 g/l yeast extract, and 10 g/l NaCl, at pH 7.0 (Roth, Karlsruhe, Germany). Each bacterial strain was cultivated at 37°C until the midlog phase was reached. Bacteria were then centrifuged and washed twice with cold PBS. Prior to addition to IPEC-J2 cells, bacteria were diluted in serum- and antibiotic-free IPEC-J2 cell culture medium at a concentration of approximately 10⁸ colony-forming units (CFU)/ml. For their application into the MoDC compartment, RPMI-1640 was used for the resuspension of bacterial cells to give a concentration of approximately 10⁷ CFU/ml. In order to quantify bacterial concentrations, the optical density (OD) was measured at a wavelength of 600 nm in a Helios™ Epsilon spectrophotometer (Thermo Scientific, Rockford, IL). Additionally, dilution series were made with a subsequent CFU count on LB agar plates.

2.4. Coculture Model and Experimental Design (Figure 1). In the present study, a coculture model comprising IPEC-J2 cells and porcine MoDC was utilized as illustrated in Figures 1(c) and 1(d). To this end, Transwell inserts with confluent IPEC-J2 monolayers grown on their top surface were transferred to the 12-well culture plates containing adherent MoDC on the bottom. On the day prior to the experiments, each cell type was fed with the appropriate cell culture medium. After 24 h in coculture, the cells were challenged with the aforementioned bacterial strains.

Prior to bacterial infection, FCS- and penicillin-streptomycin-supplemented media were removed from the cell cultures and replaced by serum- and antibiotic-free IPEC-J2 or MoDC cell culture medium, respectively, after the appropriate cells had been washed with the aforementioned media.

For the experiments, cells were incubated with either the probiotic *E. faecium* strain or the pathogenic ETEC strain. The number of bacteria differed depending on the cell type infected. IPEC-J2/MoDC cocultures were incubated with bacteria by adding either 1 × 10⁶ CFU per insert to the IPEC-J2 compartment of the cultures or 5.4 × 10⁴ CFU per well to the MoDC compartment (Figures 1(c) and 1(d)). The appropriateness of the applied bacterial concentrations was evaluated in preliminary experiments.

In addition to the IPEC-J2/MoDC cocultures, monocultures of IPEC-J2 cells or MoDC were also included as controls to assess the influence of cocultivation on the reactivity of each cell type (Figures 1(a) and 1(b)).

For the sake of completeness, we examined the immune responses after direct incubation with the bacterial strains

(comparison of mono- vs. coculture), as well as after indirect bacterial incubation. In these assays, we additionally assessed the inflammatory responses of cocultured IPEC-J2 cells when MoDC had been challenged and *vice versa*. Thus, an *in vivo*-like situation discriminating between the apical or basolateral occurrence of individual bacteria was simulated. The expected higher bacterial load in the lumen compared with the subepithelial space was also modeled as described above; this has to be taken into account when interpreting the results of the indirect challenge.

In order to prevent bacterial overgrowth, cells were washed with gentamicin-containing medium (150 $\mu\text{g}/\text{ml}$, Biochrom) after 2 h of bacterial incubation. The medium was then replaced with medium supplemented with gentamicin at a final concentration of 50 $\mu\text{g}/\text{ml}$. After this medium change, cells were incubated for further 4 h.

2.5. Transepithelial Electrical Resistance (TEER) Measurements. The transepithelial electrical resistance (TEER) across the IPEC-J2 monolayers was measured in the Transwell systems by using a Millicell-ERS (Electrical Resistance System, Millipore GmbH, Schwalbach, Germany). During the experiments, the TEER was measured every two hours (before bacterial addition and at 2 h, 4 h, and 6 h of incubation). TEER values were corrected against their blank control (cell-free cell culture insert with medium) and against the membrane area. For each experimental condition, three wells were used. Results are reported as [$\Omega \times \text{cm}^2$].

2.6. Real-Time Quantitative Polymerase Chain Reaction (RT-qPCR). To perform mRNA expression analyses, samples for RT-qPCR were collected 6 h after bacterial addition. MoDC and IPEC-J2 cells were washed with cold PBS, harvested by scraping, and stored in RNeasy lysis reagent (Qiagen GmbH, Hilden, Germany) at -20°C . Isolation of RNA and its quantitative and qualitative analyses were performed as described by Kern et al. [14]. Samples were used when the RNA integrity number was higher than or equal to 8. An aliquot of 100 ng total RNA was reverse-transcribed into cDNA in a Mastercycler[™] Nexus Gradient (Eppendorf GmbH) by using the iScript[™] cDNA Synthesis Kit (Bio-Rad Laboratories GmbH). All primers for RT-qPCR were synthesized by Eurofins MWG Synthesis GmbH (Ebersberg, Germany). In preliminary experiments, various reference genes were validated for each cell line by using ge-Norm[®] software. Three reference genes were selected for normalization (MoDC: TATA-binding protein [TBP], tyrosine 3-monooxygenase/tryptophan 5-monooxygenase activation protein zeta [YWHAZ], and beta-2-microglobulin [B2M]; IPEC-J2: TBP, YWHAZ, and glyceraldehyde-3-phosphate dehydrogenase [GAPDH]). Primer information regarding the target and reference genes is given in Table 1. RT-qPCR was conducted in an iCycler iQ[™] Real-Time PCR Detection System (Bio-Rad Laboratories GmbH) by using SYBR Green I detection. Samples were run in triplicate. The final volume of the reaction (20 μl) was composed of iQ SYBR Green Supermix (Bio-Rad Laboratories GmbH), primers (0.38 μl of 20 pmol/ μl each), and 5 μl cDNA. An inter-run calibration sample was used to correct for run-to-

run variations. To check for possible genomic DNA contamination, minus-reverse transcriptase controls were included in the experiments. The software iQ5 (Bio-Rad Laboratories GmbH) was utilized to calculate the relative expression of target genes by using the $\Delta\Delta\text{Ct}$ method.

2.7. Enzyme-Linked Immunosorbent Assay (ELISA). For the analysis of cytokine release from MoDC or IPEC-J2 cells, cell-free cell culture supernatants were collected 6 h after bacterial addition, centrifuged (6000 rpm for 5 min), and stored at -80°C until used. IL-1 β , IL-8, TGF- β , and TSLP concentrations were determined by using the following ELISA kits according to the manufacturer's instructions: porcine IL-1 β ELISA (Quantikine ELISA, Porcine IL-1 β /IL-1F2 Immunoassay, R&D Systems), porcine IL-8 ELISA (Invitrogen ELISA Kit, Swine IL-8, Invitrogen Life Technologies GmbH), porcine TGF- β ELISA (Quantikine ELISA, Porcine TGF- β 1 Immunoassay, R&D Systems), and porcine TSLP ELISA (Porcine TSLP ELISA kit, BlueGene, Shanghai, China). A microplate reader (EnSpire Multimode Plate Reader, Perkin Elmer, Rodgau, Germany) was employed to measure the absorbance values and to calculate the OD-specific sample concentrations from a standard curve by using a four-parameter logistic curve fit. Results are reported as (pg/ml).

2.8. Statistical Analysis. Statistical analyses and the creation of graphs were performed by using SigmaPlot 11.0 for Windows (Systat Software Inc., San Jose, CA, USA). Statistical significance of differences between the various treatment groups was assessed by two-way repeated measures analysis of variance (ANOVA) for the factors "bacteria" ("control", "*E. faecium*", and "ETEC") and "culture" ("IPEC-J2 monoculture"/"MoDC monoculture", "coculture - IPEC-J2 challenged", and "coculture - MoDC challenged"). In addition to the analysis of these two main effects, we also tested for possible interactions between the two factors. If interactions occurred, comparisons among the different treatment groups of the factor "bacteria" were made for each "culture" condition and *vice versa*. Findings were considered to be significant when $P \leq 0.05$. When overall analysis of the data of each cell type and a certain parameter (TEER, mRNA, or protein expression) showed a statistical difference between treatment groups (including interactions), the Fisher least significant difference *post hoc* test was carried out. In the figures, results are presented as means \pm standard error of the means (SEM).

3. Results

3.1. TEER. During the course of experiments, TEER values of the IPEC-J2 monolayers were measured at four time points in order to monitor the barrier integrity (Figure 2). In addition to the cocultures, TEER was also determined in corresponding IPEC-J2 monocultures. As shown in Figure 2(a), initial TEER values of the cocultures did not differ from those of IPEC-J2 monocultures before the bacterial challenge.

In IPEC-J2 monocultures, ETEC significantly reduced the TEER after 2 h ($P \leq 0.05$) (Figure 2(b)) and after 4 h ($P \leq 0.05$) of incubation (Figure 2(c)). In cocultures with

TABLE 1: Oligonucleotide primers and amplicon length of PCR products.

Gene information	Primer sequence	Amplicon length	Accession number	Reference
<i>IL1B1</i> (interleukin-1, beta 1, <i>Sus scrofa</i>)	(S) 5'- CCT CCT CCC AGG CCT TCT GT -3' (AS) 5'- GGG CCA GCC AGCA CTA GAG A -3'	178 bp		[31]
<i>IL-18</i> (interleukin-18, <i>Sus scrofa</i>)	(S) 5'- ACG ATG AAG ACC TGG AAT CG -3' (AS) 5'- GCC AGA CCT CTA GTG AGG CTA -3'	205 bp	AF191088.1	
<i>NLRP3</i> (NLR family, pyrin domain containing 3, <i>Sus scrofa</i>)	(S) 5'- AGC AGA TTC CAG TGC ATC AAA G -3' (AS) 5'- CCT GGT GAA GCG TTT GTT GAG-3'	75 bp	NM_001256770.2	[32]
<i>NLRC4</i> (NLR family, CARD domain containing 4, <i>Sus scrofa</i>)	(S) 5'- TGC TCT GAA ACA CCT TGC AT -3' (AS) 5'- GCA TAG ATT CCT GCC TCC AG -3'	92 bp	XM_013987922.1	
<i>CASP13</i> (caspase-13, apoptosis-related cysteine peptidase, <i>Sus scrofa</i>)	(S) 5'- GTG CTA CAG AAA CGC CAT GA -3' (AS) 5'- AGG GCA AAG CTT GAG GGT AT-3'	150 bp	XM_003129812.6	
<i>CASP1</i> (caspase-1, apoptosis-related cysteine peptidase, <i>Sus scrofa</i>)	(S) 5'- CTC TCC ACA GGT TCA CAA TC -3' (AS) 5'- GAA GAC GCA GGC TTA ACT GG -3'	116 bp	NM_214162	[33]
<i>ASC</i> (<i>LOC100522011</i>) (apoptosis-associated speck-like protein containing a CARD, <i>Sus scrofa</i>)	(S) 5'- CCG ACG AGC TCA AGA AGT TT -3' (AS) 5'- AGC TCA GCG CTG TAC TCC TC -3'	154 bp	XM_003124468.4	
<i>IL-8</i> (interleukin-8, <i>Sus scrofa</i>)	(S) 5'- GGC AGT TTT CCT GCT TTC T -3' (AS) 5'- CAG TGG GGT CCA CTC TCA AT -3'	154 bp	X61151	[34]
<i>TLR4</i> (toll-like receptor 4, <i>Sus scrofa</i>)	(S) 5'- AGA ACT GCA GGT GCT GGA TT -3' (AS) 5'- AGG TTT GTC TCA ACG GCA AC -3'	180 bp	AB188301	
<i>TGF-β</i> (transforming growth factor beta, <i>Sus scrofa</i>)	(S) 5'- TGA CCC GCA GAG AGG CTA TA -3' (AS) 5'- CAT GAG GAG CAG GAA GGG C -3'	164 bp	NM_214015.2	
<i>TBP</i> (TATA box binding protein, <i>Sus scrofa</i>)	(S) 5'- GAT GGA CGT TCG GTT TAG G -3' (AS) 5'- AGC AGC ACA GTA CGA GCA A -3'	124 bp	DQ178129	[35]
<i>YWHAZ</i> (tyrosine 3-monooxygenase/tryptophan 5-monooxygenase activation protein, zeta polypeptide, <i>Sus scrofa</i>)	(S) 5'- ATG CAA CCA ACA CAT CCT ATC -3' (AS) 5'- GCA TTA TTA GCG TGC TGT CTT -3'	178 bp	DQ178130	[35]
<i>B2M</i> (beta-2-microglobulin, <i>Sus scrofa</i>)	(S) 5'- AAA CGG AAA GCC AAA TTA CC -3' (AS) 5'- ATC CAC AGC GTT AGG AGT GA -3'	178 bp	DQ178123	[35]
<i>GAPDH</i> (glyceraldehyde-3-phosphate dehydrogenase, <i>Sus scrofa</i>)	(S) 5'- ACT CAC TCT TCT ACC TTT GAT GCT -3' (AS) 5'- TGT TGC TGT AGC CAA ATT CA -3'	100 bp	DQ178124	[35]

challenged IPEC-J2 cells, this ETEC effect was only present at 2 h after bacterial infection ($P \leq 0.05$) (Figure 2(b)). Bacterial infection of cocultured MoDC revealed no ETEC-induced drop of TEER of IPEC-J2 monolayers at each considered time point. Unlike ETEC, *E. faecium* treatment led to no modifications in the TEER throughout the experimental period in each experimental setup.

3.2. Expression of Inflammation-Related Genes in IPEC-J2 Cells. The mRNA expression of various inflammation-related genes was analyzed in IPEC-J2 cells (and porcine MoDC—see next section) after 6 h of bacterial stimulation. Cells were incubated with either probiotic *E. faecium* or pathogenic ETEC. Samples were obtained from cocultures or from the corresponding monocultures.

To gain insight into the potential involvement of the inflammasome pathway, IL-1 β , IL-18, and NLRP3 were selected for the analysis of the inflammasome response to

the applied bacterial strains. As shown in Figure 3(a), mRNA expression levels of IL-1 β in IPEC-J2 cells remained rather stable independent of the cultivation method (cocultures or monocultures) and the bacterial challenge. However, the IL-18 mRNA expression of IPEC-J2 cells was generally higher in the coculture setup when MoDC had been challenged compared with IPEC-J2 monocultures ($P \leq 0.05$) (Figure 3(b)). This effect was, as a trend, mainly based on greater values in cocultures challenged with ETEC. Incubation with the pathogenic ETEC strain also provoked an upregulation of NLRP3 mRNA expression in IPEC-J2 cells in comparison with the control and the *E. faecium* group ($P \leq 0.05$) (Figure 3(c)).

We hypothesized that caspase-13 would be a promising candidate targeting noncanonical inflammasome activation in pigs. As indicated in Figure 3(d), caspase-13 mRNA expression was strongly enhanced in ETEC-infected IPEC-J2 cells under either cultivation methods ($P \leq 0.05$). Notably,

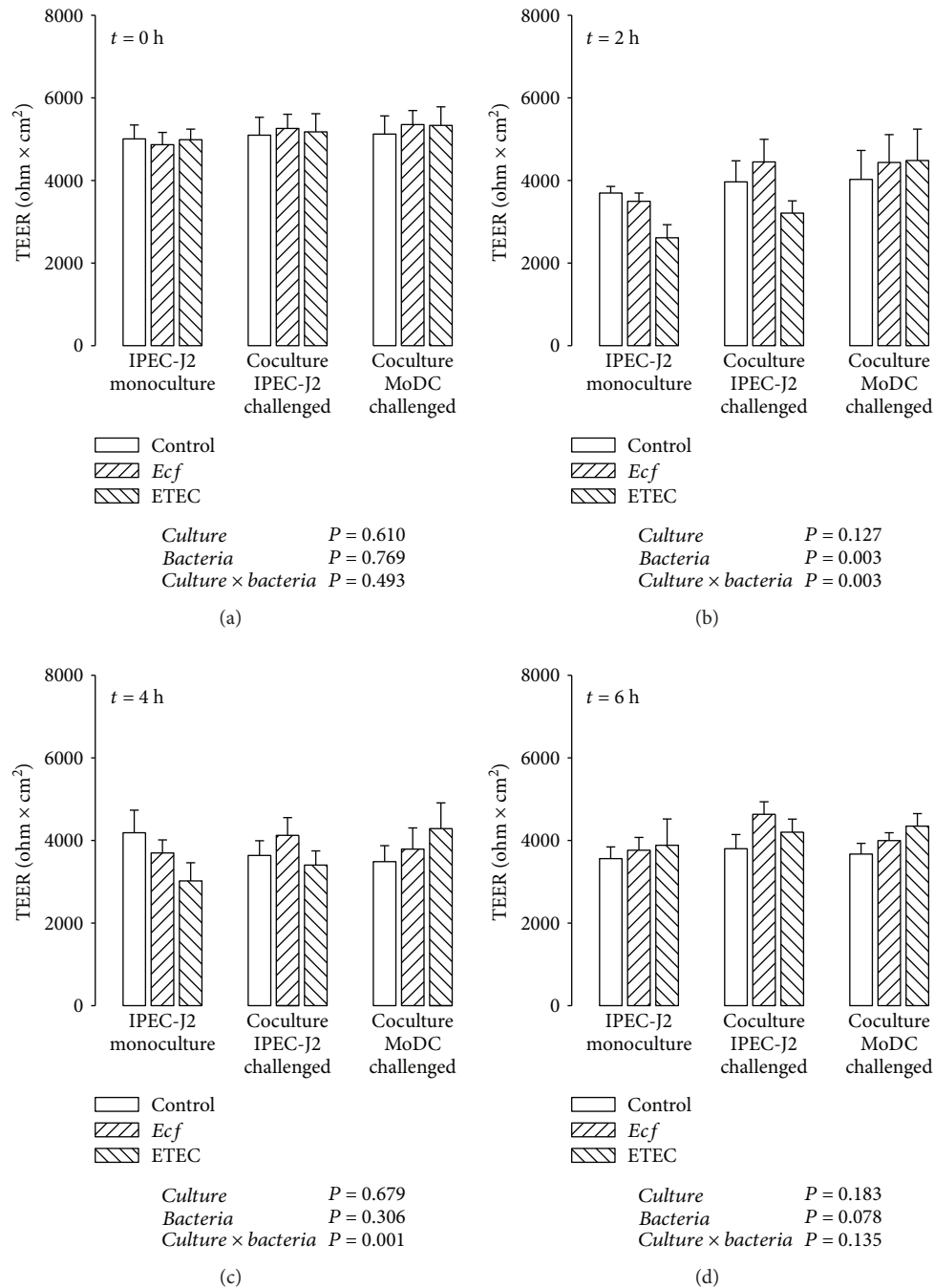


FIGURE 2: Transepithelial electrical resistance (TEER, in $\Omega \times \text{cm}^2$) of IPEC-J2 monolayers after stimulation with either *E. faecium* (*Ecf*) or ETEC. In IPEC-J2/MoDC cocultures, *Ecf* or ETEC was added either to the apical side of IPEC-J2 cells or to the MoDC compartment. In IPEC-J2 monocultures, the bacteria were added to the apical compartment. TEER values were measured at 0 h, 2 h, 4 h, and 6 h (a)-(d). Data are expressed as means \pm SEM. $N = 6$ independent experiments per bar. Results of the ANOVA are indicated below each graph. Results of *post hoc* tests are presented in Supplementary Table 1.

the observed upregulation was more evident in cocultured IPEC-J2 cells than in IPEC-J2 monocultures ($P \leq 0.05$). An interesting additional finding was that the cocultivation of IPEC-J2 with MoDC (irrespective of infection) was followed by a higher caspase-13 mRNA expression in IPEC-J2 cells ($P \leq 0.05$).

To further illuminate the noncanonical inflammasome signaling pathway in IPEC-J2 cells, we additionally included

the following genes in our analyses: inflammasome-forming NLRC4 (NLR family, CARD domain containing 4), the adapter ASC (apoptosis-associated speck-like protein containing a CARD), caspase-1, and toll-like receptor (TLR) 4 (Supplementary Tables 6 and 7). We found a lack of NLRC4 mRNA in IPEC-J2 cells (Supplementary Table 6). Whilst ASC mRNA expression was not regulated, caspase-1 mRNA expression was upregulated in cocultured IPEC-J2 cells

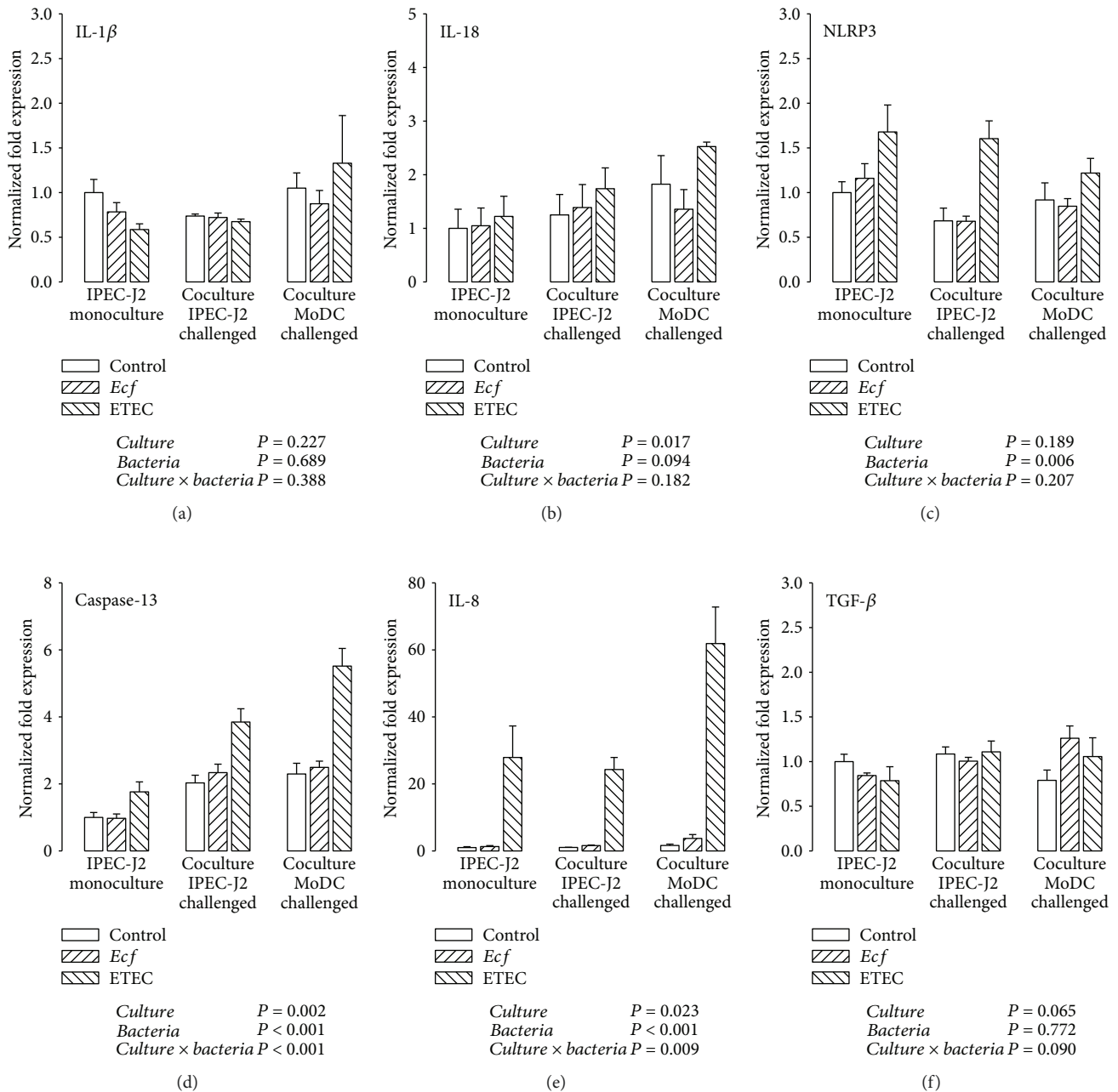


FIGURE 3: mRNA expression of (a) IL-1 β , (b) IL-18, (c) NLRP3, (d) caspase-13, (e) IL-8, and (f) TGF- β in IPEC-J2 cells after stimulation with either *E. faecium* (*Ecf*) or ETEC. In IPEC-J2/MoDC cocultures, *Ecf* or ETEC was added either to the apical side of IPEC-J2 cells or to the MoDC compartment. In IPEC-J2 monocultures, the bacteria were added to the apical compartment. Samples were taken at 6 h after addition of bacteria (means \pm SEM). $N = 4$ independent experiments per bar. Normalized fold expression was calculated by the $\Delta\Delta\text{Ct}$ method. Results of the ANOVA are indicated below each graph. Results of *post hoc* tests are presented in Supplementary Table 2.

($P \leq 0.05$). TLR4 mRNA levels were higher in the ETEC-incubated treatment groups ($P \leq 0.05$).

The mRNA expression of the proinflammatory chemokine IL-8 in IPEC-J2 cells was markedly augmented by incubation with ETEC under each culture condition ($P \leq 0.05$) (Figure 3(e)). As with caspase-13, IPEC-J2 cells from the setting in which cocultured MoDC was treated with the bacteria exhibited the largest ETEC response ($P \leq 0.05$).

In contrast, *E. faecium* treatment did not alter the mRNA expression of the considered genes within the experimental

design and showed expression levels similar to those of the unchallenged controls.

As a regulatory cytokine, we also investigated the expression of TGF- β , which was affected neither by the cultivation method nor by bacterial incubation in IPEC-J2 cells (Figure 3(f)).

3.3. Expression of Inflammation-Related Genes in Porcine MoDC. Similarly, mRNA expression was studied in porcine MoDC. Expression levels were compared between

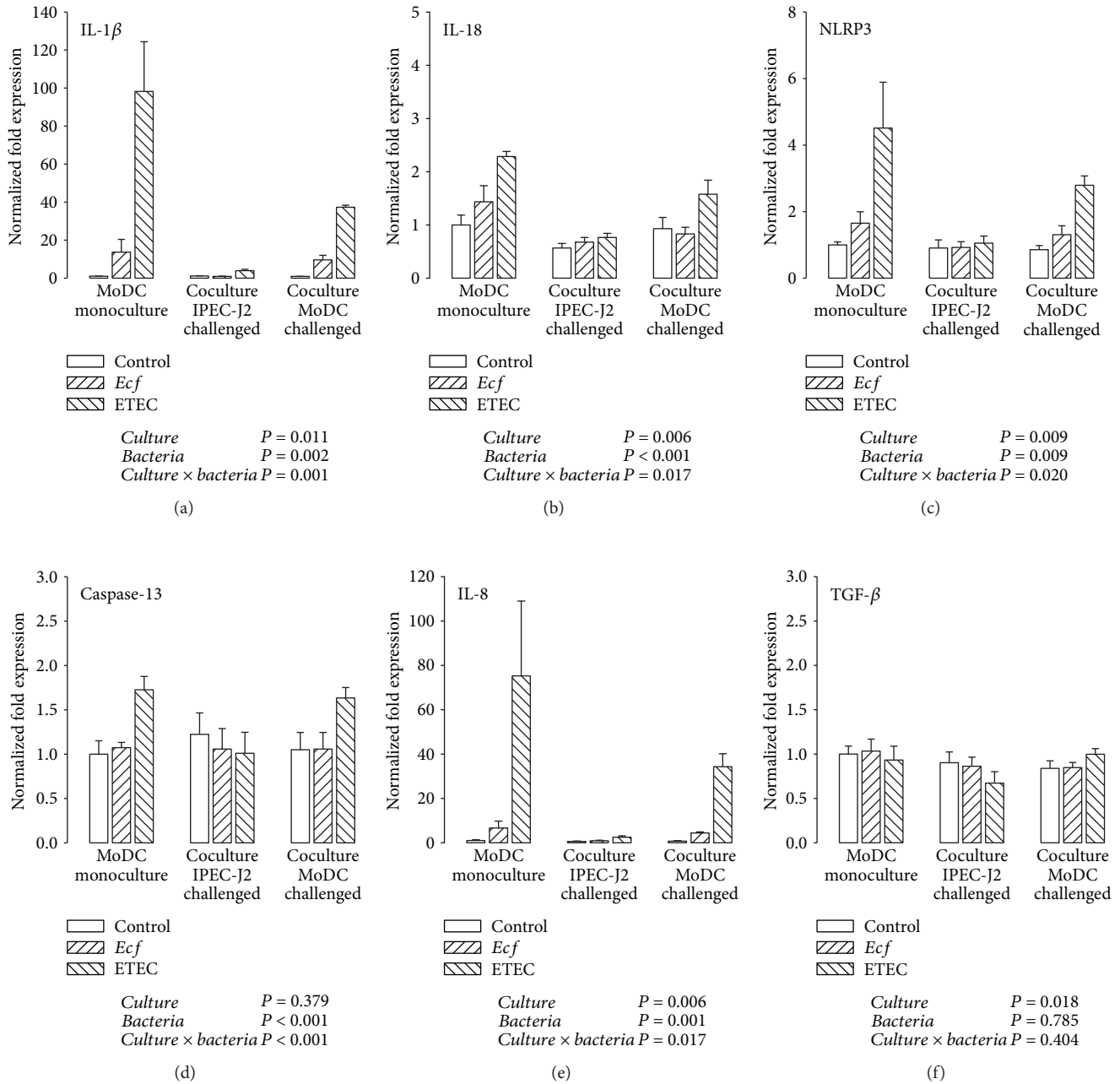


FIGURE 4: mRNA expression of (a) IL-1 β , (b) IL-18, (c) NLRP3, (d) caspase-13, (e) IL-8, and (f) TGF- β in porcine MoDC after stimulation with either *E. faecium* (*Ecf*) or ETEC. In IPEC-J2/MoDC cocultures, *Ecf* or ETEC was added either to the apical side of IPEC-J2 cells or to the MoDC compartment. In MoDC monocultures, the bacteria were added to the basolateral compartment. Samples were taken at 6 h after addition of bacteria (means \pm SEM). $N = 4$ independent experiments per bar. Normalized fold expression was calculated by the $\Delta\Delta\text{Ct}$ method. Results of the ANOVA are indicated below each graph. Results of *post hoc* tests are presented in Supplementary Table 3.

cocultured MoDC (challenged with bacteria directly or indirectly by infection of IPEC-J2 cells) and MoDC originating from monocultures.

The analysis of inflammasome-linked genes (IL-1 β , IL-18, and NLRP3) revealed an upregulation by ETEC in MoDC cultivated alone ($P \leq 0.05$) (Figures 4(a)–4(c)). To a significantly lesser extent, ETEC enhanced the mRNA expression of IL-1 β , IL-18, and NLRP3 in the challenged MoDC of the cocultures ($P \leq 0.05$). In addition, cocultured

MoDC remained relatively unaffected by the bacterial challenge of IPEC-J2 cells. Likewise, ETEC caused an enlarged caspase-13 transcription when MoDC were challenged in mono- and cocultures ($P \leq 0.05$) (Figure 4(d)). In contrast to genes associated with canonical inflammasome activation, the induced caspase-13 mRNA increase in cocultured MoDC was as great as in MoDC monocultures.

Expression patterns of IL-8 resembled those of IL-1 β and NLRP3 (Figure 4(e)). The highest response to ETEC was

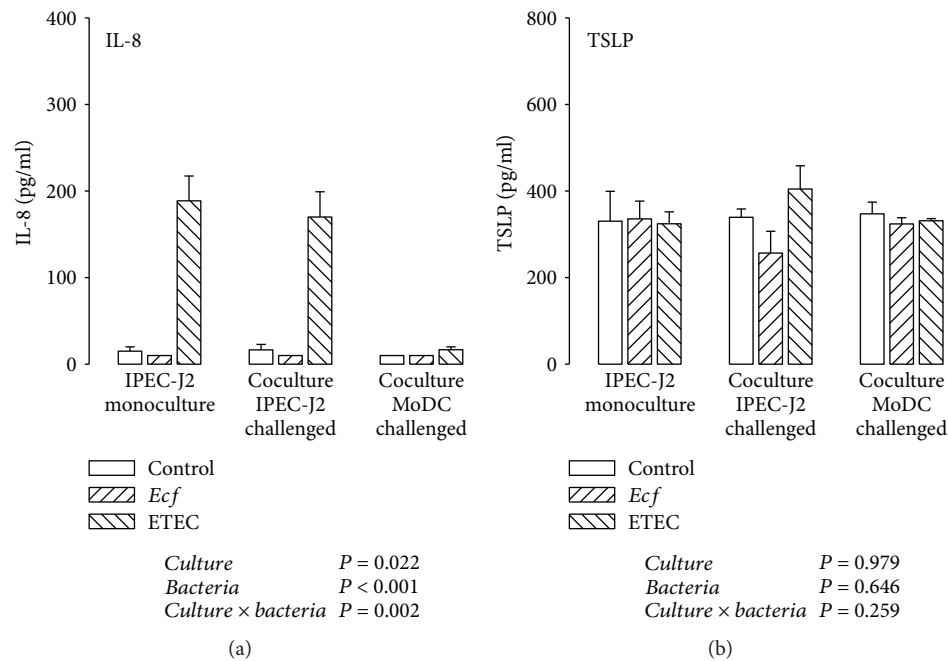


FIGURE 5: Protein expression (in pg/ml) of (a) IL-8 and (b) TSLP detected by ELISA in supernatants of IPEC-J2 cells after stimulation with either *E. faecium* (*Ecf*) or ETEC. In IPEC-J2/MoDC cocultures, *Ecf* or ETEC was added either to the apical side of IPEC-J2 cells or to the MoDC compartment. In IPEC-J2 monocultures, the bacteria were added to the apical compartment. Samples were taken at 6 h after addition of bacteria (means \pm SEM). $N = 3$ independent experiments per bar. Results of the ANOVA are indicated below each graph. Results of *post hoc* tests are presented in Supplementary Table 4.

detected in MoDC monocultures, whereas a weaker ETEC-triggered amplification of IL-8 mRNA occurred in cocultured MoDC ($P \leq 0.05$).

Exposure to the probiotic *E. faecium* strain resulted in only a slight increase of IL-18 mRNA expression in MoDC that were cultivated alone ($P \leq 0.05$) (Figure 4(b)). Similar tendencies were recognized for IL-1 β , NLRP3, and IL-8 mRNA expressions without reaching statistical significance (Figures 4(a), 4(c), and 4(e)).

Similar to that of IPEC-J2 cells, the mRNA expression of anti-inflammatory TGF- β in MoDC showed no clear effects in the context of bacterial treatment or the cultivation technique (Figure 4(f)). On average, the smallest expression level was detected in IPEC-J2/MoDC cocultures in which IPEC-J2 cells had been bacterially challenged ($P \leq 0.05$); this was attributable to a numerical ETEC-induced decrease.

3.4. Cytokine Secretion by IPEC-J2 Cells. The protein secretion of IL-8, IL-1 β , TGF- β , and TSLP into cell culture supernatants of IPEC-J2 cells and porcine MoDC (see next section) was determined by ELISA. For the analysis of the selected cytokines, samples were collected 6 h after bacterial addition.

In challenged IPEC-J2 cells of mono- and cocultures, a strong secretion of IL-8 attributable to ETEC infection could be observed ($P \leq 0.05$) (Figure 5(a)). These results corresponded with those of the qPCR analysis. Interestingly, the results after bacterial addition to the MoDC compartment varied considerably from the mRNA to the protein level.

The high upregulation of IL-8 mRNA expression could not be verified at the protein level.

IPEC-J2 cells secreted TSLP, which we proposed as being a promising candidate mediating the interactive IEC/DC crosstalk in addition to TGF- β , at levels of around 300 pg/ml, but the detected levels did not show significant variations attributable to different cultivation variants and bacterial stimulation (Figure 5(b)).

IL-1 β and TGF- β concentrations in the tested IPEC-J2 supernatant samples were mostly below the minimum detection level of the ELISA kits used (6.7 and 4.6 pg/ml, respectively; data not shown).

3.5. Cytokine Secretion by Porcine MoDC. In supernatants of mono- and cocultured MoDC, direct ETEC incubation caused an IL-1 β accumulation ($P \leq 0.05$) with a tendency of lower IL-1 β concentrations in the presence of IPEC-J2 cells (Figure 6(a)).

The IL-8 release of ETEC-infected MoDC was greater in MoDC monocultures than in cocultures with IPEC-J2 cells ($P \leq 0.05$) (Figure 6(b)). This was in agreement with results obtained at the mRNA level. Furthermore, incubation with probiotic *E. faecium* also elicited a higher IL-8 protein level in directly challenged MoDC monocultures (compared with *E. faecium* responses under the remaining culture conditions), but this was lower than the ETEC-induced increases ($P \leq 0.05$) (Figure 6(b)).

Porcine MoDC secreted low amounts of TGF- β into the respective supernatants, which tended to be increased in *E. faecium*-incubated cells ($P = 0.052$) (Figure 6(c)).

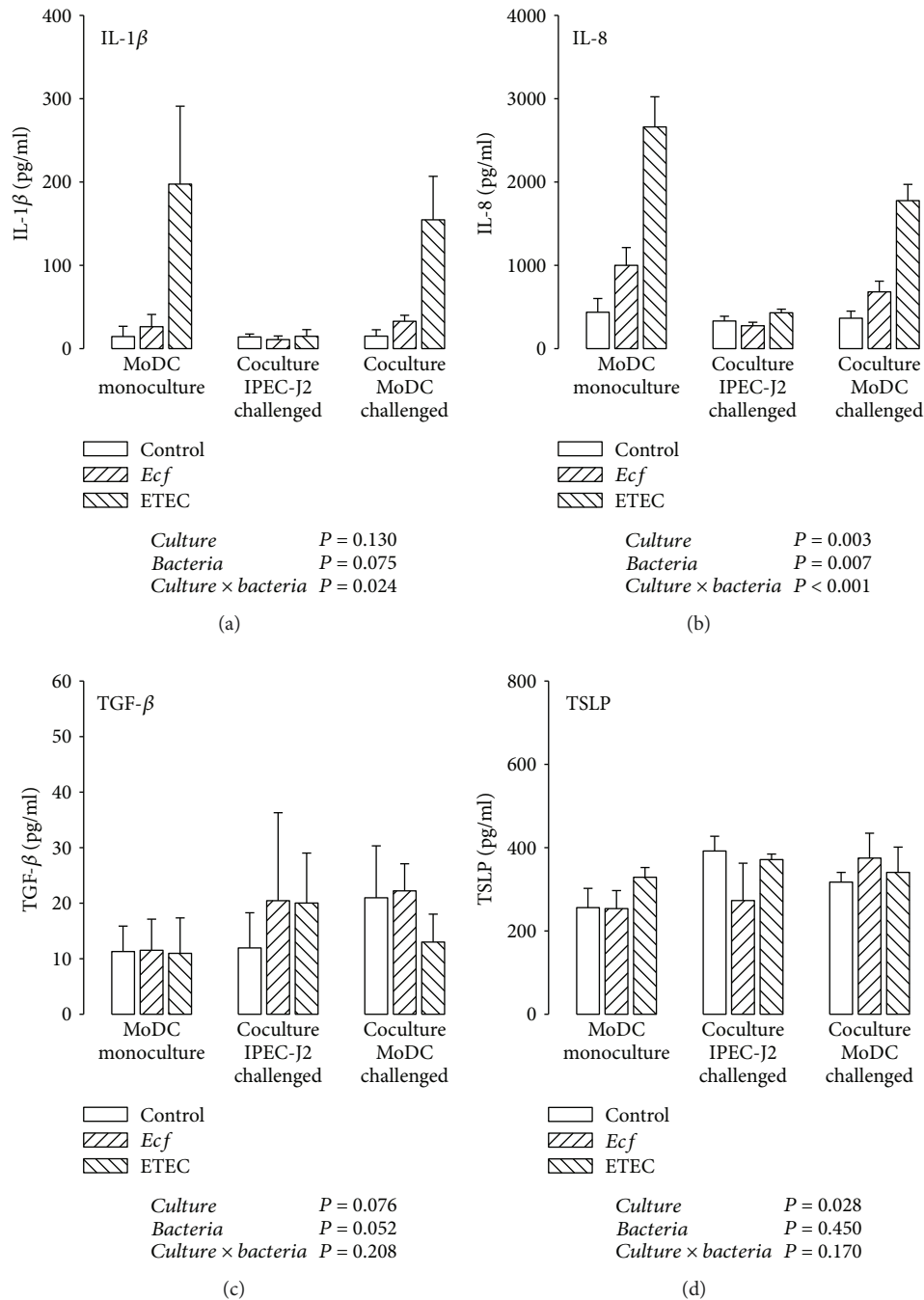


FIGURE 6: Protein expression (in pg/ml) of (a) IL-1 β , (b) IL-8, (c) TGF- β , and (d) TSLP detected by ELISA in supernatants of porcine MoDC after stimulation with either *E. faecium* (*Ecf*) or ETEC. In IPEC-J2/MoDC cocultures, *Ecf* or ETEC was added either to the apical side of IPEC-J2 cells or to the MoDC compartment. In MoDC monocultures, the bacteria were added to the basolateral compartment. Samples were taken at 6 h after addition of bacteria (means \pm SEM). $N = 3 - 4$ independent experiments per bar. Results of the ANOVA are indicated below each graph. Results of *post hoc* tests are presented in Supplementary Table 5.

Surprisingly, we also detected TSLP expression at the protein level in MoDC samples (Figure 6(d)). The quantities of MoDC-derived TSLP were comparable with those measured in IPEC-J2 cells. The supernatant of MoDC cultivated in the presence of IPEC-J2 cells contained more TSLP than that of monocultures, regardless of the bacterial treatment ($P \leq 0.05$).

4. Discussion

In the present study, the main objective was to determine whether the inflammatory response to a bacterial challenge in porcine MoDC and IPEC-J2 cells is changed by their mutual interference in an *in vitro* coculture model. As encountered enteric bacteria can be of different types, we conducted

challenge experiments with an apathogenic *E. faecium* strain and a pathogenic *E. coli* strain, the latter having disease relevance for pigs, especially in the postweaning period.

4.1. TEER. The analysis of TEER values of IPEC-J2/MoDC cocultures and their corresponding IPEC-J2 monocultures revealed that the cocultivation of IPEC-J2 cells with MoDC per se did not have an effect on the TEER of IPEC-J2 monolayers. Similar findings were achieved with human intestinal models consisting of human IEC and MoDC [36, 37].

Previous studies have shown that ETEC is capable of altering the barrier function of apically infected IPEC-J2 monolayers adversely in a dose- and time-dependent manner [15, 38–40]. In the present study, ETEC effects on the barrier integrity were predominantly detectable after 2 h of incubation. Apically challenged IPEC-J2 monocultures showed a significantly lowered TEER even after 4 h, suggesting that IPEC-J2 monocultures were slightly more sensitive to ETEC-induced impairments of the epithelial barrier function than cocultures. Surprisingly, basolateral bacterial infection had no influence on TEER at any time point. The latter might be attributable to the lower number of pathogenic bacteria added to cocultured MoDC on the basolateral side of IPEC-J2 cells resulting in a lower bacteria:IPEC-J2 cell ratio. When adding the same bacterial concentration, other research groups have shown that the basolateral infection of human IEC (cell line T84) monocultures with pathogenic bacteria, such as adherent-invasive *E. coli* [41] or *Campylobacter jejuni* [42], resulted in a considerable TEER drop, which was greater after basolateral application compared with apical application. Nonetheless, the lower number of ETEC applied to the basolateral compartment of IPEC-J2 cells in the current study induced an evident proinflammatory response (see next section).

4.2. The Inflammatory Response in IPEC-J2 Cells. In the present study, we provide evidence that inflammasome activation following a pathogenic ETEC challenge occurred in both cell types examined. In IPEC-J2 cells, this was particularly validated by an upregulation of NLRP3 mRNA expression. In addition to the main cell wall component lipopolysaccharide (LPS), other inflammasome-stimulating components of pathogenic *E. coli* include toxins, such as enterohemolysin and heat-labile enterotoxin [43, 44], or bacterial RNA [45, 46]. The role of NLRP3 in intestinal inflammation and homeostasis is controversial [47–49]. Lissner and Siegmund [50] have underlined that the outcome depends on the affected cell type. Within the epithelium, NLRP3 performs regulatory functions, e.g., by promoting enterocyte proliferation, whereas disproportionate NLRP3 activation by *lamina propria* immune cells provokes detrimental effects [50]. A protective role of the NLRP3 inflammasome in IEC has been postulated by Song-Zhao et al. [51] and Zaki et al. [52]. In a recent study, Fan et al. [53] addressed inflammasome activation in IPEC-J2 cells upon stimulation with the mycotoxin zearalenone and reported evidence supporting regulatory functions of the NLRP3 inflammasome within the gut [53].

We further studied NLRC4 mRNA expression in IPEC-J2 cells as the NLRC4 inflammasome is another well-

characterized inflammasome beyond NLRP3. We found no NLRC4 mRNA in these cells. We and others had previously reported similar findings for different porcine cells and tissues, suggesting that a functional NLRC4 gene is missing in pigs [30, 54, 55].

Whilst IEC are the main source for IL-18 being especially important for epithelial regeneration [52, 56, 57], the ability of IEC to produce IL-1 β is a matter of debate [58]. Based on our results, IL-1 β played a negligible role in IPEC-J2 cells, whereas IL-18 mRNA expression tended to follow similar expression patterns as determined for caspase-13, indicating that there might be a correlation between caspase-13 and IL-18.

Based on the assumption that caspase-13 is the porcine counterpart to murine caspase-11, the striking upregulation of caspase-13 mRNA expression in IPEC-J2 cells upon ETEC exposure suggests that ETEC could primarily trigger noncanonical inflammasome activation in IPEC-J2 cells. In addition, the caspase-13 induction as a result of the pathogenic ETEC challenge was more evident in cocultured IPEC-J2 cells than in IPEC-J2 monocultures. In human and murine IEC, Knodler et al. [59] have observed noncanonical inflammasome activation *via* caspase-4 and caspase-11, respectively, in response to enteropathogens. Recent research has assigned the murine ortholog caspase-11 guard functions within the gastrointestinal tract in inflammatory states [60–62]. For example, caspase-11-deficient mice revealed a hypersensitivity to dextran sulfate sodium-induced colitis associated with an impeded IL-18 production [60, 61], suggesting an ameliorating effect of caspase-11 during intestinal inflammation [63]. To date, it is unknown how inflammasome signaling by IEC is cross-linked with other defense mechanisms that ultimately coordinate the recruitment of neighboring immune cells [58].

Some authors have demonstrated that caspase-11 activation acts upstream of caspase-1-dependent canonical inflammasome formation [64, 65], whereas others have reported that caspase-11 forms a noncanonical inflammasome complex itself [25, 66]. Caspase-1, in contrast to caspase-4, -5, and -11, is capable of processing interleukins [67]. Analysis of caspase-1 mRNA expression in IPEC-J2 cells revealed an increase upon cocultivation, which had likewise been detected at the level of caspase-13 in IPEC-J2 cells, indicating a possible link between caspase-13 and caspase-1. Resembling results have been obtained in murine cocultures consisting of preadipocytes and muscle cells or fibroblasts, in which the mRNA expression of certain caspases (caspase-3, -7, and -9) was in some cases enhanced as an effect of coculturing [68, 69]. To our knowledge, similar investigations for caspases associated with noncanonical inflammasome signaling have not yet been carried out.

Furthermore, several authors have shown that the signaling pathway for caspase-11 activation includes TLR4 (and the TLR adapter TRIF [TIR domain containing adaptor inducing interferon- β]), which senses extracellular LPS [66, 70]. In IPEC-J2 cells, we could verify ETEC-associated upregulations of TLR4 mRNA expression, which might indicate that this signal cascade is likewise involved in porcine noncanonical inflammasome activation.

The transcriptional control differs between the caspases of different species, e.g., it has been established for murine caspase-11 but not for human caspase-4, which is constitutively expressed [71]. Summarizing the observations of the current study, it was suggested that the porcine ortholog caspase-13 responds similarly to the murine counterpart. In this respect, the verification in future studies as to whether caspase-13 constitutes the porcine equivalent to the aforementioned caspases of the noncanonical inflammasome pathway would be intriguing. Collectively, we can conclude that the DC-driven regulation of neighboring IPEC-J2 cells was mainly evidenced by caspase-13 modulation. This caspase-13 modulation might be one possible explanation for the altered TEER response observed after apical ETEC infection of IPEC-J2 mono- vs. cocultures and for the lack of a TEER response after basolateral ETEC infection of IPEC-J2 cells.

4.3. The Inflammatory Response in Porcine MoDC. Investigations into the inflammatory response in porcine MoDC revealed that MoDC from IPEC-J2/MoDC cocultures reacted more moderately to the pathogenic ETEC challenge than did monocultured MoDC; the expression of IL-1 β , IL-18, and NLRP3 was attenuated at the mRNA level and of IL-1 β , as a trend, also at the protein level. For the proinflammatory cytokine IL-8, a similar pattern was noted at both the mRNA and protein levels. In contrast to IEC, DC are known to express NLRP3 abundantly and to generate high IL-1 β levels [72]. An exaggerated production of cytokines, such as IL-1 β and IL-8, can lead to the development of intestinal pathologies linked with a disruption of the intestinal barrier, such as inflammatory bowel disease [73, 74]. Hence, our findings concerning inflammasome and IL-8 reactions support the hypothesis that IEC act beneficially to adapt the proinflammatory responsiveness of MoDC to invading enteropathogens. We propose an inflammation-restricting effect of adjacent IPEC-J2 cells on porcine MoDC in the present study. Other research groups have provided evidence that IEC are able to suppress proinflammatory responses of cocultured immune cells [37, 75]. In a human model of the intestinal epithelium, DC cultivated in direct contact with IEC were less sensitive to LPS and exhibited a reduced proinflammatory response [37].

Of note, the caspase-13 mRNA expression in MoDC did not appear to be influenced following cocultivation with IPEC-J2 cells; and the ETEC-induced caspase-13 upregulation was reduced compared with those detected in IPEC-J2 cells. We presume that the transcriptional induction of caspase-13 plays a rather minor role in porcine MoDC, at least, within our experimental design. This underlines the observation that different cell types fulfil a unique contribution to the development of immune responses, particularly in the gut [58].

The apathogenic *E. faecium* strain used in this study had only a minor impact on certain proinflammatory markers (IL-18, IL-1 β , and IL-8) in MoDC monocultures. Comparable proinflammatory responses to different *E. faecium* strains have been documented by several working groups that recorded a strain-specific and dose-dependent induction of, for example, IL-1 β , IL-8, IL-6, and tumor necrosis factor- α ,

in human DC or murine macrophages [76–79]. TGF- β was suggested to contribute to probiotic-triggered immunoregulatory mechanisms [80–82]. Accordingly, a tendency for an *E. faecium*-induced increase of TGF- β secretion by MoDC was also noted in our experiments.

4.4. Potential Mediators of Crosstalk between IPEC-J2 Cells and Porcine MoDC. As porcine MoDC revealed an attenuated inflammatory ETEC response when cocultured with IPEC-J2 cells, we aimed to look more closely at underlying IPEC-J2/MoDC interactions. In our experimental design, MoDC had no direct contact with neighboring IPEC-J2 cells. Hence, the modulation of the immune cells was assumed to occur through cell-derived humoral signals capable of crossing the filter membrane. In our analyses, we included TSLP and TGF- β , which we considered as potential mediators in this bidirectional crosstalk.

Consistent with the idea that soluble factors are likely to be responsible for the regulation of DC responses, Rimoldi et al. [8] demonstrated that human DC conditioned by supernatants of IEC displayed a downregulated IL-1 β secretion after *Salmonella* infection. In their study, IEC-derived TSLP was identified as the controlling agent [8]. Although TSLP is commonly regarded as an epithelial-derived cytokine, it has previously been detected in murine [83] and human DC [84, 85], where it was released in an autocrine manner in response to pathogenic and allergenic agents. In the present study, we observed TSLP expression by both IPEC-J2 and porcine DC. Unexpectedly, MoDC-derived TSLP appeared to contribute to an autocrine regulation under coculture conditions.

An autocrine regulation mechanism of MoDC has likewise been proposed on the basis of TGF- β secretion [37]. Butler et al. [37] observed a higher TGF- β release by human DC cocultured in direct contact with IEC; this was accompanied by weaker inflammatory reactions to pathogenic stimuli, as stated earlier. However, this effect was absent in a separated coculture setup that was more similar to our IPEC-J2/MoDC cocultures [37]. According to our results, no clear impact of cocultivation on TGF- β expression in porcine MoDC was present, either at the mRNA or at the protein level.

Since it is unclear whether IPEC-J2 cells are capable of producing TGF- β [86], we measured TGF- β at the mRNA level. We verified TGF- β mRNA expression in IPEC-J2 cells but which was, however, not regulated in the different treatment groups. Consistent with our data, Butler et al. [37] detected only very small amounts of TGF- β liberated by IEC, so that TGF- β could not be identified as a modulating IEC-derived mediator in the present experimental design.

Future studies are needed to obtain knowledge as to the extent to which results may be different when a cocultivation technique is used that allows direct contact between the cocultured cell types. Here, we provide evidence supporting a possible involvement of TSLP derived by porcine MoDC in the communication between IPEC-J2 cells and MoDC.

5. Conclusions

In the present study, we established a porcine intestinal model consisting of IPEC-J2 cells and MoDC. We

investigated inflammatory reactions to selected bacterial agents and found a more tolerogenic phenotype of MoDC cocultured with IEC. This conclusion was supported by a downregulation of inflammasome-related and other proinflammatory cytokines in comparison with MoDC cultivated alone. We further provide the first evidence that porcine caspase-13 is regulated in IPEC-J2 cells and porcine MoDC in response to bacterial infection. In IPEC-J2 cells, the possibly related noncanonical inflammasome pathway appeared to be induced not only by ETEC infection but also by the presence of MoDC. Finally, we demonstrated the ability of IPEC-J2 cells and MoDC to secrete TSLP, whereby an autocrine adaptation of cocultured MoDC was indicated. Our results suggest that the control of inflammatory responses by IEC is of critical importance to prevent unrestricted cytokine production by resident immune cells. More research is needed to unravel further the soluble factors that are implicated in IEC/DC interactions and to verify the functional aspects of porcine caspase-13 in noncanonical inflammasome signaling. We suggest the presented *in vitro* coculture model is a promising tool for studying such interactions in future.

Abbreviations

ANOVA:	Analysis of variance
ASC:	Apoptosis-associated speck-like protein containing a CARD
BHI:	Brain-heart infusion
B2M:	Beta-2-microglobulin
CFU:	Colony-forming unit
DC:	Dendritic cells
<i>E. coli</i> :	<i>Escherichia coli</i>
EDTA:	Ethylenediamine tetra-acetic acid
<i>E. faecium</i> :	<i>Enterococcus faecium</i>
ELISA:	Enzyme-linked immunosorbent assay
ETEC:	Enterotoxigenic <i>Escherichia coli</i>
FCS:	Fetal calf serum
GALT:	Gut-associated lymphoid tissue
GAPDH:	Glyceraldehyde-3-phosphate dehydrogenase
GM-CSF:	Granulocyte-macrophage colony-stimulating factor
IEC:	Intestinal epithelial cells
IL:	Interleukin
LB:	Luria-Bertani
LPS:	Lipopolysaccharide
MHC:	Major histocompatibility complex
MoDC:	Monocyte-derived DC
NLR:	NOD-like receptor
NLRC4:	NLR family, CARD domain containing 4
NLRP3:	NLR family, pyrin domain containing 3
NOD:	Nucleotide oligomerization domain
OD:	Optical density
PBMC:	Peripheral blood mononuclear cells
PBS:	Phosphate-buffered saline
PRR:	Pattern recognition receptors
rp:	Recombinant porcine
RT-qPCR:	Real-time quantitative polymerase chain reaction

SEM:	Standard error of the means
SLA:	Swine leukocyte antigen
TBP:	TATA-binding protein
TEER:	Trans epithelial electrical resistance
TGF- β :	Transforming growth factor- β
TLR:	Toll-like receptor
TSLP:	Thymic stromal lymphopietin
YWHAZ:	Tyrosine 3-monooxygenase/tryptophan 5-monooxygenase activation protein zeta.

Data Availability

The TEER, ELISA, and qPCR data used to support the findings of this study are included within the supplementary information file.

Conflicts of Interest

The authors declare that there is no conflict of interest regarding the publication of this article.

Acknowledgments

The authors thank K. Söllig whose assistance is greatly appreciated. We are grateful to P. Schwerk for technical support with the bacterial strains and J. Schulte for providing the TGF- β primers. This research was financially supported by the German Research Foundation (grant number LO 2058/1-1) and by an Elsa Neumann grant to Henriette Loss.

Supplementary Materials

In Supplementary Table 1, the results of the post hoc tests of the TEER data are presented. Supplementary Tables 2, 3, 6, and 7 show the results of the post hoc tests of the mRNA expression analyses in IPEC-J2 cells and MoDC. In the Supplementary Tables 4 and 5, those results are presented for the protein expression analyses in IPEC-J2 cells and MoDC. (*Supplementary Materials*)

References

- [1] D. C. Baumgart and A. U. Dignass, "Intestinal barrier function," *Current Opinion in Clinical Nutrition and Metabolic Care*, vol. 5, no. 6, pp. 685–694, 2002.
- [2] B. L. Kelsall and W. Strober, "Distinct populations of dendritic cells are present in the subepithelial dome and T cell regions of the murine Peyer's patch," *The Journal of Experimental Medicine*, vol. 183, no. 1, pp. 237–247, 1996.
- [3] P. Pavli, C. E. Woodhams, W. F. Doe, and D. A. Hume, "Isolation and characterization of antigen-presenting dendritic cells from the mouse intestinal lamina propria," *Immunology*, vol. 70, no. 1, pp. 40–47, 1990.
- [4] M. D. Witmer and R. M. Steinman, "The anatomy of peripheral lymphoid organs with emphasis on accessory cells: light-microscopic immunocytochemical studies of mouse spleen, lymph node, and Peyer's patch," *The American Journal of Anatomy*, vol. 170, no. 3, pp. 465–481, 1984.
- [5] I. D. Iliev, G. Matteoli, and M. Rescigno, "The yin and yang of intestinal epithelial cells in controlling dendritic cell function,"

- Journal of Experimental Medicine*, vol. 204, no. 10, pp. 2253–2257, 2007.
- [6] L. H. Zeuthen, L. N. Fink, and H. Frokiaer, “Epithelial cells prime the immune response to an array of gut-derived commensals towards a tolerogenic phenotype through distinct actions of thymic stromal lymphopoietin and transforming growth factor- β ,” *Immunology*, vol. 123, no. 2, pp. 197–208, 2008.
 - [7] M. Bermudez-Brito, J. Plaza-Díaz, L. Fontana, S. Muñoz-Quezada, and A. Gil, “*In vitro* cell and tissue models for studying host-microbe interactions: a review,” *The British Journal of Nutrition*, vol. 109, Supplement 2, pp. S27–S34, 2013.
 - [8] M. Rimoldi, M. Chieppa, V. Salucci et al., “Intestinal immune homeostasis is regulated by the crosstalk between epithelial cells and dendritic cells,” *Nature Immunology*, vol. 6, no. 5, pp. 507–514, 2005.
 - [9] A. Di Mauro, J. Neu, G. Riezzo et al., “Gastrointestinal functional development and microbiota,” *Italian Journal of Pediatrics*, vol. 39, no. 1, p. 15, 2013.
 - [10] P. Marteau, “Living drugs for gastrointestinal diseases: the case for probiotics,” *Digestive Diseases*, vol. 24, no. 1-2, pp. 137–147, 2006.
 - [11] Y. Sun and S. W. Kim, “Intestinal challenge with enterotoxigenic *Escherichia coli* in pigs, and nutritional intervention to prevent postweaning diarrhea,” *Animal Nutrition*, vol. 3, no. 4, pp. 322–330, 2017.
 - [12] J. D. Dubreuil, R. E. Isaacson, and D. M. Schifferli, “Animal enterotoxigenic *Escherichia coli*,” *EcoSal Plus*, vol. 7, no. 1, 2016.
 - [13] S. Klingspor, A. Bondzio, H. Martens et al., “*Enterococcus faecium* NCIMB 10415 modulates epithelial integrity, heat shock protein, and proinflammatory cytokine response in intestinal cells,” *Mediators of Inflammation*, vol. 2015, Article ID 304149, 11 pages, 2015.
 - [14] M. Kern, D. Günzel, J. R. Aschenbach, K. Tedin, A. Bondzio, and U. Lodemann, “Altered cytokine expression and barrier properties after *in vitro* infection of porcine epithelial cells with enterotoxigenic *Escherichia coli* and probiotic *Enterococcus faecium*,” *Mediators of Inflammation*, vol. 2017, Article ID 2748192, 13 pages, 2017.
 - [15] U. Lodemann, J. Strahlendorf, P. Schierack, S. Klingspor, J. R. Aschenbach, and H. Martens, “Effects of the probiotic *Enterococcus faecium* and pathogenic *Escherichia coli* strains in a pig and human epithelial intestinal cell model,” *Scientifica*, vol. 2015, Article ID 235184, 10 pages, 2015.
 - [16] D. Taras, W. Vahjen, M. Macha, and O. Simon, “Performance, diarrhea incidence, and occurrence of *Escherichia coli* virulence genes during long-term administration of a probiotic *Enterococcus faecium* strain to sows and piglets,” *Journal of Animal Science*, vol. 84, no. 3, pp. 608–617, 2006.
 - [17] A. Zeyner and E. Boldt, “Effects of a probiotic *Enterococcus faecium* strain supplemented from birth to weaning on diarrhoea patterns and performance of piglets,” *Journal of Animal Physiology and Animal Nutrition*, vol. 90, no. 1-2, pp. 25–31, 2006.
 - [18] L. Scharek, J. Guth, K. Reiter et al., “Influence of a probiotic *Enterococcus faecium* strain on development of the immune system of sows and piglets,” *Veterinary Immunology and Immunopathology*, vol. 105, no. 1-2, pp. 151–161, 2005.
 - [19] S. Klingspor, H. Martens, D. Çaushi, S. Twardziok, J. R. Aschenbach, and U. Lodemann, “Characterization of the effects of *Enterococcus faecium* on intestinal epithelial transport properties in piglets,” *Journal of Animal Science*, vol. 91, no. 4, pp. 1707–1718, 2013.
 - [20] J. Tschopp, F. Martinon, and K. Burns, “NALPs: a novel protein family involved in inflammation,” *Nature Reviews Molecular Cell Biology*, vol. 4, no. 2, pp. 95–104, 2003.
 - [21] D. De Nardo and E. Latz, “NLRP3 inflammasomes link inflammation and metabolic disease,” *Trends in Immunology*, vol. 32, no. 8, pp. 373–379, 2011.
 - [22] F. Bauernfeind, A. Ablasser, E. Bartok et al., “Inflammasomes: current understanding and open questions,” *Cellular and Molecular Life Sciences*, vol. 68, no. 5, pp. 765–783, 2011.
 - [23] P. Broz and D. M. Monack, “Noncanonical inflammasomes: caspase-11 activation and effector mechanisms,” *PLoS Pathogens*, vol. 9, no. 2, article e1003144, 2013.
 - [24] S. Mariathasan, K. Newton, D. M. Monack et al., “Differential activation of the inflammasome by caspase-1 adaptors ASC and Ipaf,” *Nature*, vol. 430, no. 6996, pp. 213–218, 2004.
 - [25] N. Kayagaki, S. Warming, M. Lamkanfi et al., “Non-canonical inflammasome activation targets caspase-11,” *Nature*, vol. 479, no. 7371, pp. 117–121, 2011.
 - [26] C. N. Casson, J. Yu, V. M. Reyes et al., “Human caspase-4 mediates noncanonical inflammasome activation against gram-negative bacterial pathogens,” *Proceedings of the National Academy of Sciences of the United States of America*, vol. 112, no. 21, pp. 6688–6693, 2015.
 - [27] E. Viganò, C. E. Diamond, R. Spreafico, A. Balachander, R. M. Sobota, and A. Mortellaro, “Human caspase-4 and caspase-5 regulate the one-step non-canonical inflammasome activation in monocytes,” *Nature Communications*, vol. 6, no. 1, p. 8761, 2015.
 - [28] U. Koenig, L. Eckhart, and E. Tschachler, “Evidence that caspase-13 is not a human but a bovine gene,” *Biochemical and Biophysical Research Communications*, vol. 285, no. 5, pp. 1150–1154, 2001.
 - [29] N. Kayagaki, M. T. Wong, I. B. Stowe et al., “Noncanonical inflammasome activation by intracellular LPS independent of TLR4,” *Science*, vol. 341, no. 6151, pp. 1246–1249, 2013.
 - [30] H. Loss, J. R. Aschenbach, F. Ebner, K. Tedin, and U. Lodemann, “Effects of a pathogenic ETEC strain and a probiotic *Enterococcus faecium* strain on the inflammasome response in porcine dendritic cells,” *Veterinary Immunology and Immunopathology*, vol. 203, pp. 78–87, 2018.
 - [31] C. B. Paulk, D. D. Burnett, M. D. Tokach et al., “Effect of added zinc in diets with ractopamine hydrochloride on growth performance, carcass characteristics, and ileal mucosal inflammation mRNA expression of finishing pigs,” *Journal of Animal Science*, vol. 93, no. 1, pp. 185–196, 2015.
 - [32] J. Bi, S. Song, L. Fang et al., “Porcine reproductive and respiratory syndrome virus induces IL-1 β production depending on TLR4/MyD88 pathway and NLRP3 inflammasome in primary porcine alveolar macrophages,” *Mediators of Inflammation*, vol. 2014, Article ID 403515, 14 pages, 2014.
 - [33] M. Collado-Romero, C. Arce, M. Ramírez-Boo, A. Carvajal, and J. J. Garrido, “Quantitative analysis of the immune response upon *Salmonella typhimurium* infection along the porcine intestinal gut,” *Veterinary Research*, vol. 41, no. 2, p. 23, 2010.
 - [34] T. G. Ramsay and T. J. Caperna, “Ontogeny of adipokine expression in neonatal pig adipose tissue,” *Comparative Biochemistry and Physiology Part B, Biochemistry & Molecular Biology*, vol. 152, no. 1, pp. 72–78, 2009.

- [35] T. Erkens, M. van Poucke, J. Vandesompele, K. Goossens, A. van Zeveren, and L. J. Peelman, "Development of a new set of reference genes for normalization of real-time RT-PCR data of porcine backfat and *longissimus dorsi* muscle, and evaluation with *PPARGC1A*," *BMC Biotechnology*, vol. 6, no. 1, p. 41, 2006.
- [36] M. Chalubinski, K. Wojdan, P. Gorzelak, M. Borowiec, and M. Broncel, "The effect of oxidized cholesterol on barrier functions and IL-10 mRNA expression in human intestinal epithelium co-cultured with dendritic cells in the transwell system," *Food and Chemical Toxicology*, vol. 69, pp. 289–293, 2014.
- [37] M. Butler, C. Y. Ng, D. A. van Heel et al., "Modulation of dendritic cell phenotype and function in an in vitro model of the intestinal epithelium," *European Journal of Immunology*, vol. 36, no. 4, pp. 864–874, 2006.
- [38] Z. Tian, X. Liu, R. Dai et al., "*Enterococcus faecium* HDRsEfl protects the intestinal epithelium and attenuates ETEC-induced IL-8 secretion in enterocytes," *Mediators of Inflammation*, vol. 2016, Article ID 7474306, 10 pages, 2016.
- [39] M. M. Geens and T. A. Niewold, "Preliminary characterization of the transcriptional response of the porcine intestinal cell line IPEC-J2 to enterotoxigenic *Escherichia coli*, *Escherichia coli*, and *E. coli* lipopolysaccharide," *Comparative and Functional Genomics*, vol. 2010, article 469583, 11 pages, 2010.
- [40] S. Karimi, H. Jonsson, T. Lundh, and S. Roos, "*Lactobacillus reuteri* strains protect epithelial barrier integrity of IPEC-J2 monolayers from the detrimental effect of enterotoxigenic *Escherichia coli*," *Physiological Reports*, vol. 6, no. 2, article e13514, 2018.
- [41] E. Wine, J. C. Ossa, S. D. Gray-Owen, and P. M. Sherman, "Adherent-invasive *Escherichia coli*, strain LF82 disrupts apical junctional complexes in polarized epithelia," *BMC Microbiology*, vol. 9, no. 1, p. 180, 2009.
- [42] M. L. Chen, Z. Ge, J. G. Fox, and D. B. Schauer, "Disruption of tight junctions and induction of proinflammatory cytokine responses in colonic epithelial cells by *Campylobacter jejuni*," *Infection and Immunity*, vol. 74, no. 12, pp. 6581–6589, 2006.
- [43] C. F. Brereton, C. E. Sutton, P. J. Ross et al., "*Escherichia coli* heat-labile enterotoxin promotes protective Th17 responses against infection by driving innate IL-1 and IL-23 production," *Journal of Immunology*, vol. 186, no. 10, pp. 5896–5906, 2011.
- [44] X. Zhang, Y. Cheng, Y. Xiong et al., "Enterohemorrhagic *Escherichia coli* specific enterohemolysin induced IL-1 β in human macrophages and EHEC-induced IL-1 β required activation of NLRP3 inflammasome," *PLoS One*, vol. 7, no. 11, article e50288, 2012.
- [45] T. D. Kanneganti, N. Özören, M. Body-Malapel et al., "Bacterial RNA and small antiviral compounds activate caspase-1 through cryopyrin/Nalp3," *Nature*, vol. 440, no. 7081, pp. 233–236, 2006.
- [46] T. Eigenbrod and A. H. Dalpke, "Bacterial RNA: an underestimated stimulus for innate immune responses," *Journal of Immunology*, vol. 195, no. 2, pp. 411–418, 2015.
- [47] C. Pellegrini, L. Antonioli, G. Lopez-Castejon, C. Blandizzi, and M. Fornai, "Canonical and non-canonical activation of NLRP3 inflammasome at the crossroad between immune tolerance and intestinal inflammation," *Frontiers in Immunology*, vol. 8, 2017.
- [48] M. E. Sellin, K. M. Maslowski, K. J. Maloy, and W. D. Hardt, "Inflammasomes of the intestinal epithelium," *Trends in Immunology*, vol. 36, no. 8, pp. 442–450, 2015.
- [49] V. A. K. Rathinam and F. K.-M. Chan, "Inflammasome, inflammation, and tissue homeostasis," *Trends in Molecular Medicine*, vol. 24, no. 3, pp. 304–318, 2018.
- [50] D. Lissner and B. Siegmund, "The multifaceted role of the inflammasome in inflammatory bowel diseases," *Scientific-WorldJournal*, vol. 11, pp. 1536–1547, 2011.
- [51] G. X. Song-Zhao, N. Srinivasan, J. Pott, D. Baban, G. Frankel, and K. J. Maloy, "Nlrp3 activation in the intestinal epithelium protects against a mucosal pathogen," *Mucosal Immunology*, vol. 7, no. 4, pp. 763–774, 2014.
- [52] M. H. Zaki, K. L. Boyd, P. Vogel, M. B. Kastan, M. Lamkanfi, and T. D. Kanneganti, "The NLRP3 inflammasome protects against loss of epithelial integrity and mortality during experimental colitis," *Immunity*, vol. 32, no. 3, pp. 379–391, 2010.
- [53] W. Fan, Y. Lv, S. Ren et al., "Zearalenone (ZEA)-induced intestinal inflammation is mediated by the NLRP3 inflammasome," *Chemosphere*, vol. 190, pp. 272–279, 2018.
- [54] C. Sakuma, D. Toki, H. Shinkai et al., "Pig lacks functional NLR4 and NAIP genes," *Immunogenetics*, vol. 69, no. 2, pp. 125–130, 2017.
- [55] H. D. Dawson, A. D. Smith, C. Chen, and J. F. Urban Jr, "An in-depth comparison of the porcine, murine and human inflammasomes; lessons from the porcine genome and transcriptome," *Veterinary Microbiology*, vol. 202, pp. 2–15, 2017.
- [56] J. Dupaul-Chicoine, G. Yeretssian, K. Doiron et al., "Control of intestinal homeostasis, colitis, and colitis-associated colorectal cancer by the inflammatory caspases," *Immunity*, vol. 32, no. 3, pp. 367–378, 2010.
- [57] O. J. Harrison, N. Srinivasan, J. Pott et al., "Epithelial-derived IL-18 regulates Th17 cell differentiation and Foxp3⁺ Treg cell function in the intestine," *Mucosal Immunology*, vol. 8, no. 6, pp. 1226–1236, 2015.
- [58] S. M. Crowley, B. A. Vallance, and L. A. Knodler, "Noncanonical inflammasomes: antimicrobial defense that does not play by the rules," *Cellular Microbiology*, vol. 19, no. 4, 2017.
- [59] L. A. Knodler, S. M. Crowley, H. P. Sham et al., "Noncanonical inflammasome activation of caspase-4/caspase-11 mediates epithelial defenses against enteric bacterial pathogens," *Cell Host & Microbe*, vol. 16, no. 2, pp. 249–256, 2014.
- [60] T. M. Williams, R. A. Leeth, D. E. Rothschild et al., "Caspase-11 attenuates gastrointestinal inflammation and experimental colitis pathogenesis," *American Journal of Physiology-Gastrointestinal and Liver Physiology*, vol. 308, no. 2, pp. G139–G150, 2015.
- [61] K. Oficjalska, M. Raverdeau, G. Aviello et al., "Protective role for caspase-11 during acute experimental murine colitis," *Journal of Immunology*, vol. 194, no. 3, pp. 1252–1260, 2015.
- [62] D. Demon, A. Kuchmiy, A. Fossoul, Q. Zhu, T. D. Kanneganti, and M. Lamkanfi, "Caspase-11 is expressed in the colonic mucosa and protects against dextran sodium sulfate-induced colitis," *Mucosal Immunology*, vol. 7, no. 6, pp. 1480–1491, 2014.
- [63] C. E. Diamond, H. J. Khameneh, D. Brough, and A. Mortellaro, "Novel perspectives on non-canonical inflammasome activation," *ImmunoTargets and Therapy*, vol. 4, pp. 131–141, 2015.
- [64] S. Ruhl and P. Broz, "Caspase-11 activates a canonical NLRP3 inflammasome by promoting K⁺ efflux," *European Journal of Immunology*, vol. 45, no. 10, pp. 2927–2936, 2015.

- [65] P. Broz, T. Ruby, K. Belhocine et al., "Caspase-11 increases susceptibility to Salmonella infection in the absence of caspase-1," *Nature*, vol. 490, no. 7419, pp. 288–291, 2012.
- [66] V. A. K. Rathinam, S. K. Vanaja, L. Waggoner et al., "TRIF licenses caspase-11-dependent NLRP3 inflammasome activation by gram-negative bacteria," *Cell*, vol. 150, no. 3, pp. 606–619, 2012.
- [67] J. Ding and F. Shao, "SnapShot: the noncanonical inflammasome," *Cell*, vol. 168, no. 3, pp. 544–544.e1, 2017.
- [68] S. A. Subramaniam, S. Kim, and I. Hwang, "Cell-cell communication between fibroblast and 3T3-L1 cells under co-culturing in oxidative stress condition induced by H₂O₂," *Applied Biochemistry and Biotechnology*, vol. 180, no. 4, pp. 668–681, 2016.
- [69] M. Pandurangan, D. Jeong, T. Amna, H. van Ba, and I. Hwang, "Co-culture of C2C12 and 3T3-L1 preadipocyte cells alters the gene expression of calpains, caspases and heat shock proteins," *In Vitro Cellular & Developmental Biology - Animal*, vol. 48, no. 9, pp. 577–582, 2012.
- [70] P. Gurung, R. K. S. Malireddi, P. K. Anand et al., "Toll or interleukin-1 receptor (TIR) domain-containing adaptor inducing interferon- β (TRIF)-mediated caspase-11 protease production integrates toll-like receptor 4 (TLR4) protein- and Nlrp3 inflammasome-mediated host defense against enteropathogens," *Journal of Biological Chemistry*, vol. 287, no. 41, pp. 34474–34483, 2012.
- [71] A. J. Russo, B. Behl, I. Banerjee, and V. A. K. Rathinam, "Emerging insights into noncanonical inflammasome recognition of microbes," *Journal of Molecular Biology*, vol. 430, no. 2, pp. 207–216, 2018.
- [72] J. A. Kummer, R. Broekhuizen, H. Everett et al., "Inflammasome components NALP 1 and 3 show distinct but separate expression profiles in human tissues suggesting a site-specific role in the inflammatory response," *The Journal of Histochemistry and Cytochemistry*, vol. 55, no. 5, pp. 443–452, 2007.
- [73] M. Nakamura, H. Saito, J. Kasanuki, Y. Tamura, and S. Yoshida, "Cytokine production in patients with inflammatory bowel disease," *Gut*, vol. 33, no. 7, pp. 933–7, 1992.
- [74] M. C. Grimm, S. K. Elsbury, P. Pavli, and W. F. Doe, "Interleukin 8: cells of origin in inflammatory bowel disease," *Gut*, vol. 38, no. 1, pp. 90–98, 1996.
- [75] J. Chen, C. P. Ng, D. K. Rowlands et al., "Interaction between enteric epithelial cells and Peyer's patch lymphocytes in response to Shigella lipopolysaccharide: effect on nitric oxide and IL-6 release," *World Journal of Gastroenterology*, vol. 12, no. 24, pp. 3895–3900, 2006.
- [76] N. M. Mansour, H. Heine, S. M. Abdou, M. E. Shenana, M. K. Zakaria, and A. el-Diwany, "Isolation of *Enterococcus faecium* NM113, *Enterococcus faecium* NM213 and *Lactobacillus casei* NM512 as novel probiotics with immunomodulatory properties," *Microbiology and Immunology*, vol. 58, no. 10, pp. 559–569, 2014.
- [77] H. J. Choi, M. S. Shin, S. M. Lee, and W. K. Lee, "Immunomodulatory properties of *Enterococcus faecium* JWS 833 isolated from duck intestinal tract and suppression of *Listeria monocytogenes* infection," *Microbiology and Immunology*, vol. 56, no. 9, pp. 613–620, 2012.
- [78] W. F. Li et al., "Induction of probiotic strain *Enterococcus faecium* EF1 on the production of cytokines, superoxide anion and prostaglandin E₂ in a macrophage cell line," *Pakistan Veterinary Journal*, vol. 32, no. 4, pp. 530–534, 2012.
- [79] I. Sim, K. T. Park, G. Kwon, J. H. Koh, and Y. H. Lim, "Probiotic potential of *Enterococcus faecium* isolated from chicken cecum with immunomodulating activity and promoting longevity in *Caenorhabditis elegans*," *Journal of Microbiology and Biotechnology*, vol. 28, no. 6, pp. 883–892, 2018.
- [80] Y. Huang, Y. L. Li, Q. Huang et al., "Effect of orally administered *Enterococcus faecium* EF1 on intestinal cytokines and chemokines production of suckling piglets," *Pakistan Veterinary Journal*, vol. 32, no. 1, pp. 81–84, 2012.
- [81] M. Boirivant and W. Strober, "The mechanism of action of probiotics," *Current Opinion in Gastroenterology*, vol. 23, no. 6, pp. 679–692, 2007.
- [82] W. F. Li, Y. Huang, Y. L. Li et al., "Effect of oral administration of *Enterococcus faecium* EF1 on innate immunity of sucking piglets," *Pakistan Veterinary Journal*, vol. 33, no. 1, pp. 9–13, 2013.
- [83] M. Kashyap, Y. Rochman, R. Spolski, L. Samsel, and W. J. Leonard, "Thymic stromal lymphopoietin is produced by dendritic cells," *The Journal of Immunology*, vol. 187, no. 3, pp. 1207–1211, 2011.
- [84] M. Elder, S. Webster, A. Ng, J. S. H. Gaston, and J. C. Goodall, "Human dendritic cells produce thymic stromal lymphopoietin in response to pattern recognition receptor ligation and this secretion is augmented by endoplasmic reticulum stress," *Immunology*, vol. 140, pp. 123–123, 2013.
- [85] M. J. Elder, S. J. Webster, D. L. Williams, J. S. H. Gaston, and J. C. Goodall, "TSLP production by dendritic cells is modulated by IL-1 β and components of the endoplasmic reticulum stress response," *European Journal of Immunology*, vol. 46, no. 2, pp. 455–463, 2016.
- [86] A. J. Brosnahan and D. R. Brown, "Porcine IPEC-J2 intestinal epithelial cells in microbiological investigations," *Veterinary Microbiology*, vol. 156, no. 3–4, pp. 229–237, 2012.